UNIVERSIDAD DE CONCEPCIÓN
DIRECCIÓN DE POSTGRADO
CONCEPCIÓN, CHILE

NUMERICAL SOLUTION OF STOCHASTIC DIFFERENTIAL EQUATIONS WITH MULTIPLICATIVE NOISE

Solución Numérica de Ecuaciones Diferenciales Estocásticas con Ruido Multiplicativo

Hernán Alfredo Mardones González

Tesis para optar al grado de
Doctor en Ciencias Aplicadas con mención en Ingeniería Matemática

Directores de Tesis : **Dr. Carlos Mora**, Departamento de Ingeniería Matemática,
Centro de Investigación en Ingeniería Matemática,
Universidad de Concepción, Chile

Dr. Antoine Lejay, Institut Élie Cartan de Lorraine,
Institut National de Recherche en Informatique et en Automatique,
Nancy, Grand Est,
Université de Lorraine, France

FACULTAD DE CIENCIAS FÍSICAS Y MATEMÁTICAS
DEPARTAMENTO DE INGENIERÍA MATEMÁTICA
CONCEPCIÓN - JUNIO 2017

SOLUCIÓN NUMÉRICA DE ECUACIONES DIFERENCIALES ESTOCÁSTICAS CON RUIDO MULTIPLICATIVO

Hernán Alfredo Mardones González

Directores de Tesis : **Dr. Carlos Mora**, Universidad de Concepción, Chile

Dr. Antoine Lejay, Université de Lorraine, France

Director de Programa : **Dr. Raimund Bürger**,
Departamento de Ingeniería Matemática,
Centro de Investigación en Ingeniería Matemática,
Universidad de Concepción, Chile

COMISIÓN EVALUADORA

Dr. Rolando J. Biscay Lirio, Departamento de Probabilidad y Estadística,
Centro de Investigación en Matemáticas, México

Dr. François Delarue, Laboratoire J. A. Dieudonné & Institut Universitaire de France,
Université de Nice Sophia-Antipolis, France

Dr. Juan Carlos Jiménez, Departamento de Matemática Interdisciplinaria,
Instituto de Cibernética, Matemática y Física, Cuba

Dr. Arturo Kohatsu-Higa, Department of Mathematical Sciences
Ritsumeikan University, Japan

Dr. Simon J. A. Malham, Department of Mathematics,
School of Mathematical and Computer Sciences,
Heriot-Watt University, Scotland

COMISIÓN EXAMINADORA

Dr. Gregorio Moreno, Departamento de Matemática,
Pontificia Universidad Católica de Chile, Chile

Dr. Rolando Rebolledo, Centro de Investigación y Modelamiento de Fenómenos
Aleatorios de Valparaíso, Facultad de Ingeniería,
Universidad de Valparaíso, Chile

Dra. María Soledad Torres, Centro de Investigación y Modelamiento de Fenómenos
Aleatorios de Valparaíso, Facultad de Ingeniería,
Universidad de Valparaíso, Chile

Dedicado a mis Abuelas y Abuelos

Agradecimientos

Quisiera agradecer a mi familia y todos quienes han apoyado y motivado mi trabajo y formación durante estos años. A los profesores Carlos Mora y Antoine Lejay por su tiempo y supervisión, y los especialistas que gentilmente conformaron la Comisión Evaluadora y la Comisión Examinadora. Las personas que trabajan en la Facultad de Ciencias Físicas y Matemáticas y la Universidad de Concepción, Concepción, en Chile, y en el Institut Élie Cartan de Lorraine, el equipo To Simulate and Calibrate Stochastic Processes y el Institut National de Recherche en Informatique et en Automatique, Nancy, Grand Est, en Francia, por su hospitalidad y espacio. Finalmente, al Ministerio de Educación y la Comisión Nacional de Investigación Científica y Tecnológica por las becas brindadas.

Resumen

Este trabajo de tesis doctoral estudia la solución numérica débil de ecuaciones diferenciales estocásticas (EDE) con ruido multiplicativo y sistemas de EDE hacia adelante y reversivas (EDEAR), en un contexto clásico de hipótesis y vinculadas a ecuaciones diferenciales parciales (EDP) no lineales, respectivamente. En diversos contextos interesa modelar procesos de difusión, por ello la importancia de métodos de aproximación adecuados. Examinamos casos en los cuales los métodos de integración de tipo Euler aplicados a EDE conducen a estimaciones numéricas inestables. Ejemplo de ello son las EDE con ruido multiplicativo, donde usualmente es necesario utilizar discretizaciones temporales $\Delta > 0$ muy pequeñas o bien incorporar términos implícitos en los esquemas numéricos. Abordamos la solución débil de EDE, es decir, la aproximación de valores esperados $\mathbb{E}f(X_t)$ donde $(X_t)_{t\geq 0}$ es solución de una EDE d-dimensional y $f : \mathbb{R}^d \to \mathbb{R}$ algún funcional dado. Para tal propósito, consideramos el desarrollo y análisis de esquemas asintóticamente estables casi seguramente, junto con la propiedad de preservación del signo, con orden de convergencia igual al tradicional método de Euler-Maruyama. Proponemos métodos numéricos débiles sin involucrar integrales múltiples ni términos de difusión implícitos, incluso para EDE que no contengan términos de tendencia. Basado en ello, introducimos nuevos esquemas numéricos gracias a los cuales es posible simular eficientemente el proceso estocástico X_t y así estimar $\mathbb{E}f(X_t)$ utilizando, por ejemplo, el clásico método de Monte-Carlo. Comenzamos diseñando esquemas balanceados de primer orden débil para sistemas lineales de EDE, identificando funciones de estabilización en los coeficientes de tendencia. Presentamos entonces un nuevo enfoque para el tratamiento numérico de EDE con ruido multiplicativo. Para tal efecto, abordamos el contexto de sistemas bilineales de EDE a partir de la estimación eficiente de $\|X_t\|$ mediante un nuevo esquema no lineal escalar junto con la aproximación apropiada del proceso $\hat{X}_t := X_t / \|X_t\|$. El notable desempeño de los nuevos esquemas, y su potencial reflejado para estimar EDE localmente Lipschitz y exponentes de Lyapunov, es apoyado por resultados teóricos de convergencia y estabilidad e ilustrado en diversos ejemplos numéricos. Finalmente, nos introducimos en la simulación de las ecuaciones de Navier-Stokes incompresibles mediante la solución numérica de una nueva clase de sistemas de EDEAR recientemente introducido. Comenzamos estudiando la ecuación de Burgers resolviendo un sistema acoplado de EDEAR, lo que provee una aproximación probabilística vía la fórmula de Feynman-Kac no lineal, e incorporamos quantización como variable de control para reducir la varianza en el cálculo de valores esperados. Entonces solucionamos numéricamente vórtices de Taylor-Green y flujos de Beltrami usando un novedoso algoritmo probabilístico. Mediante aproximaciones de tipo Riemann y la quantización de variables Gaussianas, estimamos esperanzas de integrales que dependen de las trayectorias de movimientos Brownianos. Nuestros resultados motivan el diseño y estudio teórico de algoritmos probabilísticos para la estimación de EDEAR y, a su vez, EDP no lineales.

Abstract

This PhD thesis work studies the weak numerical solution of stochastic differential equations (SDEs) with multiplicative noise and systems of forward-backward SDEs (FBSDEs), in a classical context of hypotheses and related to nonlinear partial differential equations (PDEs), respectively. In various contexts it is demanded to model diffusion processes, therefore the importance of adequate methods for approximation. We consider cases in which the Euler-type integrating methods applied to SDEs drive us to unstable numerical estimations. For example we have the SDEs with multiplicative noise, where usually it is needed a sufficient small discretization step $\Delta > 0$ or well to incorporate implicit terms on the numerical schemes. In particular, we deal with the weak solution of SDEs, i.e. the approximation of expected values $\mathbb{E}f\left(X_t\right)$ where $\left(X_t\right)_{t\geq 0}$ is solution of a d-dimensional SDE and $f : \mathbb{R}^d \to \mathbb{R}$ some given functional. For this purpose, we consider the development and analysis of almost sure asymptotically stable schemes, together with the sign-preserving property, with convergence order equals to the traditional Euler-Maruyama method. We propose weak numerical methods without involving multiple integrals nor implicit diffusion terms, even if the SDEs have no drift terms. Based on it, we introduce new numerical schemes that help us to efficiently simulate the stochastic process X_t and then to estimate $\mathbb{E}f\left(X_t\right)$ by using e.g. the classical Monte-Carlo method. We begin designing first-order weak balanced schemes for systems of linear SDEs, identifying stabilizing functions into the drift terms. Next we present a new approach for the numerical treatment of SDEs with multiplicative noise. For this purpose, we consider the context of bilinear systems of SDEs by means of the efficient estimation of $\|X_t\|$ by using a new scalar nonlinear scheme and the appropriate approximation of the process $\hat{X}_t := X_t / \|X_t\|$. The remarkable performance of the new numerical schemes, and their potential for the estimation of locally Lipschitz SDEs and Lyapunov exponents, is supported by theoretical results of convergence and stability and illustrated in various numerical tests. Finally, we introduce in the simulation of the incompressible Navier-Stokes equations by means of the numerical solution of a new class of FBSDEs recently introduced. We begin studying the Burgers equation by solving a coupled system of FBSDEs, providing a probabilistic approximation through the nonlinear Feynman-Kac formula, and we incorporate quantization as a control variate variable to reduce the variance in the computation of expected values. Then we numerically solve Taylor-Green vortices and Beltrami flows by using a novel probabilistic algorithm. We estimate expectations of integrals involving trajectories of Brownian motions by means of Riemann-type approximations together with the quantization of the Gaussian variables. Our results motivate the theoretical study and design of probabilistic algorithms for the estimation of FBSDEs and, at the same time, nonlinear PDEs.

Contents

List of Figures

List of Tables

This PhD thesis work was created under supervision and written by the author using the LaTex software. All the computational simulations were running on MATLAB by using pseudo-random generators, logic operators, linear algebra, calculus, graphics and software facilities coded on it.

Chapter 1

Introduction

Fortune presents gifts not according to the book
Luis De Góngora (1561-1627)

Imagine a bacterial culture through a fluid in a Petri dish. Mainly the trajectories of bacteria are governed by the drift field of the fluid. However, the viscosity induces an *erratic* movement to each *organic* bacterium. Definitively Awesome, I could observe a *real* Wiener process. So, is it possible to experiment such phenomenon with *inorganic* particles? The answer is Yes, the pollen particles are documented...

Diffusion processes have been observed at least from the XIX Century. The botanist Robert Brown observed through a microscope an unusual movement of pollen particles over a fluid, the optical developments were very relevant. Ludwig Boltzmann explained the nature of Brownian motion through the kinetic theory of gases. Some years later mathematician Louis Bachelier related the Brownian motion by studying finance. Then physicist Albert Einstein developed the basis of the Brownian motion by means of the physics of matter. In abstract form Norbert Wiener presented the mathematical description of the Brownian motion. Mathematicians called Wiener processes to such nice movements in his honour.

The probability theory initiated by Andrey Kolmogorov helps us to understand *random* phenomena. Then Kiyosi Itô constructed the theory of stochastic differential equations (SDEs for short), a notable scientific contribution to the study of diffusion processes. The connection between stochastic processes and the theory of partial differential equations (PDEs) is due to Richard Feynman and Mark Kac. We refer to such probabilistic representation of *deterministic* solutions as the Feynman-Kac formula. The seminal Euler-Maruyama method, introduced by Gisiro Maruyama as an extension of the Leonhard Euler's method, remains as the usual alternative to deal with the numerical solution of SDEs.

The Itô SDEs have been intensively studied in the specialized literature during the last decades. In different contexts and applications such stochastic models naturally appear in the description of diverse phenomena. Roughly speaking, the stochastic modeling permits us to deal with systems subject to environmental randomness. We mention, for example, diffusion processes associated to dynamical systems, physics of fluids, waves, neuroscience, finance, genetic evolution, epidemiology, diffusion

networks, machine learning and applications on turbulence, oscillators, vortices, superconductivity, social behavior, among various others phenomena. Nowadays, technological and scientific computing developments provide a notable scenario for the simulation of mathematical models, and in turn the research and design of efficient numerical methodologies to approximate such unknown exact solutions.

This Doctor of Philosophy thesis (PhD thesis) studies the weak numerical solution of SDEs driven by Brownian motion subject to multiplicative noise and the simulation of systems of forward-backward SDEs associated to nonlinear PDEs models, which provide stochastic algorithms to approximate the deterministic strong solutions.

1.1 Context

Let us consider a diffusion process governed by an adapted stochastic process $(X_t)_{t\geq 0}$ that solves the d-dimensional Itô stochastic differential equation (SDE), written in matrix notation,

$$X_t = X_0 + \int_0^t b\left(X_s\right) ds + \int_0^t \sigma\left(X_s\right) dW_s, \tag{1.1}$$

in which we have the drift coefficient $b : \mathbb{R}^d \to \mathbb{R}^d$, a diffusion term $\sigma = \left(\sigma^1 \mid \ldots \mid \sigma^m\right) : \mathbb{R}^d \to \mathbb{R}^{d\times m}$ and the m-dimensional Wiener process $W = \left(W^1, \ldots, W^m\right)^\top : \Omega \to \mathbb{R}^m$ defined on a filtered complete probability space $\left(\Omega, \mathcal{F}, (\mathcal{F}_t)_{t\geq 0}, \mathbb{P}\right)$. The Itô SDEs were introduced during the 1940s by K. Itô's seminal works [111, 112]. In this PhD thesis work we assume the standard conditions for existence and uniqueness *up to indistinguishability* of solutions

$$X = \left(X^1, \ldots, X^d\right) \in L^2_{\mathcal{F}}\left(\Omega; C\left(\left[0,T\right]; \mathbb{R}^d\right)\right)$$

for the Itô SDEs (1.1), i.e. a fixed final time $T > 0$, a given $\mathcal{F}_0$-measurable initial condition X_0 such that $\mathbb{E}\left\|X_0\right\|^2 < \infty$ and b, σ globally Lipschitz continuous functions satisfying regularity and linear growth conditions (see e.g. [9, 108, 117, 125, 138, 161, 178, 181, 191] for the classical theory). Note that these theoretical hypotheses can be relaxed to non-globally Lipschitz continuous coefficients, like one-sided and locally Lipschitz functions (see e.g. [105, 117]).

The SDE (1.1) involves the Lebesgue and Itô integrals. The dynamical behavior of X depends on the noise nature, and then the usage of appropriate numerical methods for computer simulations. The SDE is said to be subject to multiplicative noise when the diffusion term σ depends on the solution X of the equation, otherwise is referred as a SDE with additive noise. In particular situations, SDEs with multiplicative noise can be transformed into SDEs with additive noise (see [188]). The equation (1.1) is autonomous because the involved coefficients do not depend explicitly on the time. As in the deterministic context of ordinary differential equations (ODEs) an autonomous SDE can be formed from a non-autonomous system by adding the trivial equation $t = \int_0^t ds$ and taking $Y_t = (t, X_t)$ (see [13]). However, when some component X^i, for $i \in \{1, \ldots, d\}$, is explicitly integrated on time it is recommended to take its exact values instead of the approximated ones. In this PhD thesis work we focus on autonomous SDEs systems subject to multiplicative noise, otherwise an additional numerical analysis is demanded.

In general exact analytic solutions X of SDEs are unknown, then the application of numerical methodologies are demanded for their estimation. If we know the initial condition X_0, a natural way to obtain temporal approximations of the process X_t at times $t \geq 0$ corresponds to consider a time discretization $0 = t_0 < t_1 < \dots$ and calculate successive estimations $Y_n \approx X_{t_n}$ by setting $Y_0 = X_0$ and defining a recursive rule to compute Y_n for each $n \geq 0$. For simplicity, we fix an equidistant time discretization $t_j = j\Delta$, where $\Delta > 0$ and $j = 0, 1, \dots$ Hence the computational effort required to simulate $(X_{t_n})_{n\geq 0}$ intrinsically depends on the desire precision, the time discretization step $\Delta > 0$ and the computing complexity to obtain the successive approximating values of the numerical scheme Y_n.

Various approaches have been proposed to numerically estimate the solutions of Itô SDEs (see e.g. [91, 120, 121, 147, 150] for related literature). The most classical way, and usual benchmark to validate or compare alternative numerical schemes, corresponds to the Euler-Maruyama method defined recursively by

$$E_{n+1} = E_n + b\left(E_n\right)\Delta + \sigma\left(E_n\right)\left(W_{n+1} - W_n\right). \tag{1.2}$$

Here we denote $W_n = W_{t_n}$. Note that its recursive formula involves the numerical simulation of independent Gaussian random increments $W_{n+1} - W_n$. This simple and easily implementable novel approximation introduced by Maruyama (1955) [140] generalizes the Euler method for ODEs and converges strongly to the exact solution X of globally Lipschitz SDEs with order $1/2$ as $\Delta \to 0$, i.e. fixing a final integration time $T > 0$ and taking $\Delta > 0$ sufficiently small we have

$$\mathbb{E}\left\|X_{t_n} - E_n\right\| \leq K\left(T\right)\Delta^{1/2} \quad \forall t_n \in [0, T], \tag{1.3}$$

with $K\left(T\right) > 0$ not depending on the time-step. Unfortunately, the Euler-Maruyama method produces numerical instabilities and poor performances in cases in which the discretization-steps are not taken small enough. Moreover, it fails to converge in general contexts such as non-globally Lipschitz coefficients (see e.g. [101, 106]). There are alternative Euler schemes that converge in the context of non-globally Lipschitz continuous coefficients (see e.g. [25, 33, 107]).

In this PhD thesis work we are concerned with the weak numerical solution of SDEs with multiplicative noise, i.e. the estimation of expectations, or mean values,

$$\mathbb{E}f\left(X_t\right) = \int_{\Omega} f\left(X_t\left(\omega\right)\right)\mathbb{P}\left(d\omega\right)$$

where $f : \mathbb{R}^d \to \mathbb{R}$ is a given smooth functional. Except for particular situations, the laws of X are explicitly known. In this context, it is well-known that the Brownian increments $\left(W_{n+1} - W_n\right)/\sqrt{\Delta}$ can be replaced by alternative, ideally simpler and cheaper to simulate, random variables having similar moment properties (see e.g. [120]). Taking $\xi_n = \left(\xi_n^1, \dots, \xi_n^m\right)^\top : \Omega \to \mathbb{R}^m$, with $\xi_0^1, \dots, \xi_0^m, \xi_1^1, \dots$ a sequence of independent random variables such that $\mathbb{P}\left(\xi_n^k = \pm 1\right) = 1/2$, the weak Euler-Maruyama method is defined by

$$\bar{E}_{n+1} = \bar{E}_n + b\left(\bar{E}_n\right)\Delta + \sigma\left(\bar{E}_n\right)\sqrt{\Delta}\xi_n. \tag{1.4}$$

The numerical scheme $\bar{E}$ converges weakly to X with order 1, that is

$$\left|\mathbb{E}f\left(X_{t_n}\right) - \mathbb{E}f\left(\bar{E}_n\right)\right| \leq K\left(T\right)\Delta \quad \forall t_n \in [0, T], \tag{1.5}$$

for f in certain smooth class of real valued functions and sufficiently small time step $\Delta > 0$ [196, 197].

The weak numerical simulation of SDEs involves the computation of mean values $\mathbb{E}f(X_T)$, so a key point is to choice an appropriate algorithm to calculate expectations. Among various approaches, the usual way is to consider Monte-Carlo simulation. More precisely, let $T > 0$ be a final integration time and denote by $\{Y(\omega_i)\}_{i\in\{1,\dots,\mathcal{M}\}}$ a set of independent realizations of the numerical scheme Y with time-step $\Delta = T/N$, for $N \in \mathbb{N}$. Combining the Monte-Carlo method with the simulation of Y gives us the empirical mean approximation

$$\mathbb{E}f(X_T) \approx \frac{1}{\mathcal{M}} \sum_{i=1}^{\mathcal{M}} f(Y_N(\omega_i)). \tag{1.6}$$

If we consider, for example, the weak Euler-Maruyama scheme $Y = \bar{E}$ and large enough parameters $N, \mathcal{M} \in \mathbb{N}$ then the error of the estimation (1.6) is bounded by

$$\begin{aligned} \left| \mathbb{E}f(X_T) - \frac{1}{\mathcal{M}} \sum_{i=1}^{\mathcal{M}} f(Y_N(\omega_i)) \right| &\leq |\mathbb{E}f(X_T) - \mathbb{E}f(Y_N)| + \left| \mathbb{E}f(Y_N) - \frac{1}{\mathcal{M}} \sum_{i=1}^{\mathcal{M}} f(Y_N(\omega_i)) \right| \\ &\leq K(T) \left(\frac{T}{N} + \frac{1}{\sqrt{\mathcal{M}}} \right), \end{aligned} \tag{1.7}$$

with $K(T) > 0$ a constant independent of N and $\mathcal{M}$. The term T/N follows from the first-order of weak convergence of the Euler-Maruyama scheme, and the order of error $1/\sqrt{\mathcal{M}}$ of the Monte-Carlo estimation follows from the strong law of large numbers. The estimation (1.6) provides us a general methodology to deal with the weak numerical approximation of SDEs.

The numerical stability of the concerned scheme Y is of great importance. For example, the Euler-Maruyama scheme applied to the scalar linear equation

$$X_t = X_0 + \int_0^t \sigma X_s dW_s^1,$$

with diffusion parameter $\sigma > 0$, provides trajectories that blows up unless the time-step $\Delta > 0$ is small enough. Moreover the variance of X_t exponentially grows as

$$\mathbb{E}|X_t|^2 - [\mathbb{E}(X_t)]^2 = e^{\sigma\sigma^\top t}\mathbb{E}|X_0|^2 - [\mathbb{E}(X_0)]^2.$$

Then, a small enough discretization step and sufficient large quantity of trajectories need to be simulated to capture the dynamical behavior of the unknown solutions and obtain accurate Monte-Carlo estimations.

Various stability criteria have been proposed for solutions of SDEs (see e.g. [10, 118, 136]). In particular, the solution X of (1.1) is said to be almost sure ($a.s.$) exponentially stable when

$$\limsup_{t\to+\infty} \frac{1}{t} \log \|X_t\| < 0 \qquad \mathbb{P} - a.s. \tag{1.8}$$

Defining

$$\ell := \sup_{x\in\mathbb{R}^d, \|x\|\neq 0} \frac{\langle x, b(x)\rangle + \frac{1}{2}\sum_{k=1}^m \left\|\sigma^k(x)\right\|^2}{\|x\|^2} - \frac{\sum_{k=1}^m \langle x, \sigma^k(x)\rangle^2}{\|x\|^4}$$

and supposing $b(0) = \sigma(0) = 0$, by using the Itô's formula we have

$$\limsup_{t\to+\infty} \frac{1}{t} \log \|X_t\| < \ell \quad a.s$$

and so the inequality $\ell < 0$ becomes a sufficient condition to the $a.s.$ asymptotic stability of X, being the zero solution an invariant state for the SDE (see [138]). In specific cases, such as bilinear systems of SDEs, explicit $a.s.$ stability criteria can be achieved by studying the limit involved in (1.8). Naturally is expected to develop numerical schemes Y inheriting the exact asymptotic behavior. Thus, the numerical stability region of Y can be defined by studying the limit

$$\limsup_{n\to+\infty} \frac{1}{n\Delta} \log \|Y_n\|, \tag{1.9}$$

and then a desired property is to reproduce the $a.s.$ asymptotic behavior of the exact solution under similar hypotheses on the equation. The Euler-Maruyama scheme provides $a.s.$ exponentially stable results only for small enough discretization parameter $\Delta > 0$, an additional restriction on the time step recurrent through the numerical methods. The implicit numerical methods, as the backward Euler scheme

$$B_{n+1} = B_n + b(B_{n+1})\Delta + \sigma(B_n)(W_{n+1} - W_n), \tag{1.10}$$

typically have better stability properties in comparison with the explicit ones, but at cost of additional computations because B_{n+1} is recovered by the solution of an algebraic equation (see e.g. [102]). As above, we consider the weak version of the backward Euler

$$\bar{B}_{n+1} = \bar{B}_n + b\left(\bar{B}_{n+1}\right)\Delta + \sigma\left(\bar{B}_n\right)\xi_n. \tag{1.11}$$

Implicitness to the stochastic numerical methods is not only restricted to the drift coefficients. Alternative approaches such as the balanced implicit method incorporates implicit diffusion terms improving the stability properties but achieving low rate of weak convergence [148, 186].

The Itô SDEs are connected with PDEs by means of the Feynman-Kac formula (see e.g. [117]). A classical example corresponds to the heat equation

$$\begin{cases} \dfrac{\partial u}{\partial t} = \sigma\sigma^\top \Delta u & ;\ 0 \le t < T, \\ u(T,\cdot) = g, \end{cases} \tag{1.12}$$

where $u(t,x) \in \mathbb{R}$ is the temperature at position $x \in \mathbb{R}^d$ and time $t > 0$, with terminal condition $g : \mathbb{R}^d \to \mathbb{R}$ at time $T > 0$ and thermal diffusivity $\sigma > 0$. The Feynman-Kac interpretation gives the probabilistic representation

$$u(t,x) = \mathbb{E}g\left(X_T^{t,x}\right); \quad \forall (t,x) \in [0,T] \times \mathbb{R}^d, \tag{1.13}$$

where the diffusion process $\left(X^{t,x}\right)_{s\in[t,T]}$ is governed by

$$X_s^{t,x} = x + \int_t^s \sigma dW_r. \tag{1.14}$$

Here the indexes t, x recall the dependence of X on the starting position $x \in \mathbb{R}^d$ at time $t \in [0,T]$. The probabilistic representation (1.13) motivates the weak numerical solution of the SDE (1.14).

We refer to the equations (1.1) as *forward* SDEs because the equations describe the diffusion processes X going $forward$ on time (FSDEs for short). However given a terminal condition $Y_T \in L^2\left(\mathcal{F}_T, \mathbb{R}^d\right)$ an important problem corresponds to find a non-anticipating stochastic process Y_t for times $t < T$. Motivated by this situation, we study the *backward* stochastic differential equations (BSDEs), in integral form,

$$Y_t = Y_T + \int_t^T h\left(s, Y_s, Z_s\right) ds - \int_t^T Z_s dW_s. \tag{1.15}$$

Here (Y, Z) is a pair of adapted stochastic processes that solve the backward stochastic equation for a given $Y_T \in L^2\left(\mathcal{F}_T, \mathbb{R}^d\right)$. The function $h : [0, +\infty) \times \mathbb{R}^d \times \mathbb{R}^{d\times m} \to \mathbb{R}^d$ is called the generator of the BSDE. The process Z appearing in the equation is the key element that permits to find a non-anticipating stochastic process Y. We refer to [171] for a survey and detailed explanations. Additionally, see [131, 167, 168] for the classic theory of BSDEs.

Systems of FSDEs and BSDEs are called FBSDEs. More precisely, let $T > 0$ be a given final time and take a time interval $[t,T]$, $t \in [0,T)$. In general, we study stochastic processes $(X, Y, Z)_{s\in[t,T]}$ governed by systems of FBSDEs of the form

$$\begin{cases} X_s = x + \displaystyle\int_t^s b\left(r, X_r, Y_r, Z_r\right) dr + \int_t^s \sigma\left(r, X_r, Y_r\right) dW_r \\ Y_s = g\left(X_T\right) + \displaystyle\int_s^T h\left(r, X_r, Y_r, Z_r\right) dr - \int_s^T Z_r dW_r \end{cases}, \tag{1.16}$$

where $b : [0,T] \times \mathbb{R}^d \times \mathbb{R}^n \times \mathbb{R}^{n\times m} \to \mathbb{R}^d$, $\sigma : [0,T] \times \mathbb{R}^d \times \mathbb{R}^n \to \mathbb{R}^{d\times m}$, $g : \mathbb{R}^d \to \mathbb{R}^n$, $h : [0,T] \times \mathbb{R}^d \times \mathbb{R}^n \times \mathbb{R}^{n\times m} \to \mathbb{R}^n$ and $W = \left(W^1, \ldots, W^m\right)^\top : \Omega \to \mathbb{R}^m$ is a multidimensional Brownian motion on $\left(\Omega, \mathcal{F}, (\mathcal{F}_t)_{t\geq 0}, \mathbb{P}\right)$. Let us remark that an adapted solution of the FBSDEs (1.16) is defined by a triple of processes

$$(X, Y, Z) \in L^2_{\mathcal{F}}\left(\Omega; C\left([t,T]; \mathbb{R}^d\right)\right) \times L^2_{\mathcal{F}}\left(\Omega; C\left([t,T]; \mathbb{R}^n\right)\right) \times L^2_{\mathcal{F}}\left(\Omega; C\left([t,T]; \mathbb{R}^{n\times m}\right)\right)$$

such that it satisfies the FBSDEs $\mathbb{P}$-almost surely. In this PhD thesis work we deal with uniformly elliptic diffusion matrices $\sigma\sigma^\top$, i.e there exists $K > 0$ such that for each $(t, x, y) \in [0,T] \times \mathbb{R}^d \times \mathbb{R}^n$ the property

$$\zeta^\top \left[\sigma\sigma^\top\right](t, x, y)\, \zeta \geq K \|\zeta\|^2$$

holds for all $\zeta \in \mathbb{R}^d$.

The classical Feynman-Kac formula is extended by using systems of FBSDEs to obtain probabilistic representations for the solutions of nonlinear PDEs through a nonlinear Feynman-Kac formula (see e.g. [51, 131, 167]). The relation between FBSDEs and PDEs introduces probabilistic algorithms to numerically estimate deterministic solutions of PDEs, and involve the approximation of expectations taking into account stochastic processes governed by SDEs. The probabilistic algorithms can be regarded as an alternative to deterministic methods (see e.g. [74, 199]).

As in the spirit of the celebrated Feynman-Kac formula, it is deduced a probabilistic representation for the solution $u : [0,T] \times \mathbb{R}^d \to \mathbb{R}^n$ of the quasilinear PDE

$$\begin{cases} \dfrac{\partial u}{\partial t}(t,x) + \mathcal{L}(t,x,u(t,x)) + h(t,x,u(t,x), Du(t,x)\,\sigma(t,x,u(t,x))) = 0 \quad ;\ \forall (t,x) \in [0,T) \times \mathbb{R}^d, \\ u(T,x) = g(x) \quad ;\ \forall x \in \mathbb{R}^d. \end{cases} \tag{1.17}$$

Here, the differential operator $\mathcal{L}$ corresponds to the infinitesimal generator of the Itô diffusion X given by the solution of the SDE. If the system of FBSDEs admits unique adapted solutions $\left(X^{t,x}, Y^{t,x}, Z^{t,x}\right)$ on each subintervals $[t,T] \subseteq [0,T]$, indexed by t,x to recall dependence, then we have

$$Y_s^{t,x} = u\left(s, X_s^{t,x}\right), Z_s^{t,x} = Du\left(s, X_s^{t,x}\right)\sigma\left(s, X_s^{t,x}, Y_s^{t,x}\right) \quad ;\ \forall s \in [t,T].$$

The relation

$$u(t,x) = Y_t^{t,x}; \quad \forall (t,x) \in [0,T] \times \mathbb{R}^d$$

is called the nonlinear Feynman-Kac formula.

The d-dimensional Burgers equation (see Burgers (1948) [45])

$$\begin{cases} \dfrac{\partial u}{\partial t} + \dfrac{\nu^2}{2}\Delta u + (u \cdot \nabla)\, u + f = 0 \quad ;\ 0 \le t < T, \\ u(T) = g, \end{cases} \tag{1.18}$$

with external force $f : [0,T] \times \mathbb{R}^d \to \mathbb{R}^d$, terminal condition $g : \mathbb{R}^d \to \mathbb{R}^d$ and viscosity parameter $\nu > 0$, is related to the coupled system of FBSDEs

$$\forall s \in [t,T], \begin{cases} X_s^{t,x} = x + \displaystyle\int_t^s Y_r^{t,x} dr + \int_t^s \nu dW_r, \\ Y_s^{t,x} = g\left(X_T^{t,x}\right) + \displaystyle\int_s^T f\left(r, X_r^{t,x}\right) dr - \int_s^T \nu Z_r^{t,x} dW_r. \end{cases} \tag{1.19}$$

Then, we have

$$Y_s^{t,x} = u\left(s, X_s^{t,x}\right), \quad Z_s^{t,x} = Du\left(s, X_s^{t,x}\right)$$

for all $(s,x) \in [t,T] \times \mathbb{R}^d$ (see e.g. [130]).

Suppose that $u : [0,T] \times \mathbb{R}^d \to \mathbb{R}^n$ represents the vector field of a fluid over a d-dimensional space through a time interval. Since the Feynman-Kac formula, one can estimate u in specific time and position $(t,x) \in [0,T] \times \mathbb{R}^d$ by knowing the field at a particular time $u(T,\cdot) = g$. Indeed, imagine that we put a particle inside the fluid in position $x \in \mathbb{R}^d$ at time $T_j \in [t,T]$. The movement of the particle

is governed by the diffusion process X_s^{x,T_j} and its vector field is given by Y_s^{x,T_j} for each $s \in [T_j, T_{j+1}]$. To obtain $u(t,x)$ the idea is to apply backward regressions to have successive estimations of

$$u(T,\cdot), u(T_{N-1},\cdot), \ldots, u(T_1,\cdot), u(t,\cdot).$$

In order to make this, observe that

$$\begin{cases} X_{T_{j+1}} = x + \displaystyle\int_{T_j}^{T_{j+1}} b(s, X_s, Y_s)\, ds + \int_{T_j}^{T_{j+1}} \sigma(s, X_s, Y_s)\, dW_s, \\ Y_{T_j} = u\left(T_{j+1}, X_{T_{j+1}}\right) + \displaystyle\int_{T_j}^{T_{j+1}} h(s, X_s, Y_s)\, ds - \int_{T_j}^{T_{j+1}} Z_s dW_s. \end{cases}$$

Then if we have $u(T_{j+1},x) \approx \bar{u}(T_{j+1},x)$ for all $x \in \mathbb{R}^d$ we can consider, in particular, the following recursive rule to locally integrate the FBSDEs:

$$\begin{cases} \bar{X}_{T_{j+1}} = x + b\left(T_{j+1}, x, \bar{u}(T_{j+1},x)\right)(T_{j+1} - T_j) + \sigma\left(T_{j+1}, x, \bar{u}(T_{j+1},x)\right)\left(W_{T_{j+1}} - W_{T_j}\right) \\ \bar{u}(T_j,x) = \mathbb{E}\left[\bar{u}\left(T_{j+1}, \bar{X}_{T_{j+1}}\right)\right] + h\left(T_{j+1}, x, \bar{u}(T_{j+1},x)\right)(T_{j+1} - T_j). \end{cases}$$

Here, the SDE is numerically solved by means of the Euler-Maruyama method and the martingale part of the BSDE is neglected by taking conditional expectations. Following the same recursive rule we complete the sequence until the desire estimation

$$u(t,x) \approx \bar{u}(t,x) \quad \forall x \in \mathbb{R}^d.$$

The above numerical algorithm is completely probabilistic. To apply it, we only need initialize $\bar{u}(T,\cdot) = g$. We use the traditional Euler schemes to locally integrate both forward and backward SDEs in order to be as simple as possible.

We study the backward Navier-Stokes equations for incompressible fluids in $\mathbb{R}^d$, for $d \in \{2,3\}$,

$$\begin{cases} \frac{\partial u}{\partial t} + \frac{\nu^2}{2}\triangle u + (u\cdot\nabla)u + \nabla p + f = 0 \quad ; \ 0 \le t < T, \\ \nabla \cdot u = 0, \quad u(T) = g, \end{cases} \tag{1.20}$$

which is equivalent to the classical *forward* formulation by a time-reversing transformation. It was introduced by C.-L. Navier in 1822 [160] and G. G. Stokes in 1849 [193] by incorporating a pressure term and the fluid viscosity to the Euler equations due to L. Euler [79]. Here $T > 0$ is a fixed time, $\nu > 0$ is the kinematic viscosity, f is the external force field and g is a given initial divergence-free vector field. The Navier-Stokes equations describes the motion of an incompressible fluid by means of unknown fields of velocity $u(t,x) \in \mathbb{R}^d$ and pressure $p(t,x) \in \mathbb{R}$ defined for each time $t \in [0,T]$ and position $x \in \mathbb{R}^d$. The Burgers equation (1.18) can be seen as a simplified version of the incompressible Navier-Stokes equations. Under regularity assumptions and supposing a divergence-free external force field f, an approach to incorporate both the pressure term ∇p and the incompressibility condition $\nabla \cdot u = 0$ into the Burgers equation is to recover the pressure by means of the Poisson problem

$$-\triangle p = \operatorname{div}\operatorname{div}(u \otimes u),$$

where div := $\nabla\cdot$ represents the divergence operator and $\otimes$ the tensor product (see e.g. [53, 133]). Then the incompressible Navier-Stokes system is equivalent to

$$\begin{cases} \frac{\partial u}{\partial t} + \frac{\nu}{2}\triangle u + (u\cdot\nabla)\, u + \nabla\left(-\triangle\right)^{-1} \operatorname{div}\operatorname{div}\left(u\otimes u\right) + f = 0 \quad ;\ 0 \leq t < T, \\ u\left(T\right) = g. \end{cases} \tag{1.21}$$

Recently Delbaen, Qiu and Tang (2015) [76] introduced a coupled FBSDEs system (FBSDS) associated to the backward Navier-Stokes equations through the nonlinear Feynman-Kac formula $u\left(t,x\right) = Y_t^{t,x}$ and the probabilistic representation $\nabla p = \widetilde{Y}_0$, where $\widetilde{Y}$ is itself solution to a BSDE involving a Brownian motion independent from the diffusion one. The nonlocal operator $\nabla\left(-\triangle\right)^{-1}\operatorname{div}\operatorname{div}$ is represented by means of a BSDE defined on the infinite time interval $(0,\infty)$. Then, incorporating this extra BSDE to the FBSDEs representation of the Burgers equation it is obtained a stochastic representation to the unsteady Navier-Stokes equations. More precisely, we have the following new FBSDEs representation

$$\begin{cases} dX_s^{t,x} = Y_s^{t,x}ds + \sqrt{\nu}dW_s \quad ;\ s\in[t,T], \\ X_t^{t,x} = x, \\ -dY_s^{t,x} = \left[f\left(s,X_s^{t,x}\right) + \widetilde{Y}_0\left(s,X_s^{t,x}\right)\right]ds - \sqrt{\nu}Z_s^{t,x}dW_s \quad ;\ s\in[t,T], \\ Y_T^{t,x} = g\left(X_T^{t,x}\right), \\ -d\widetilde{Y}_r^{s,x} = \frac{27}{2r^3}Y_s^i\cdot Y_s^j\left(s,x+B_r\right)\left(B_r - B_{\frac{2r}{3}}\right)^i\left(B_{\frac{2r}{3}} - B_{\frac{r}{3}}\right)^j B_{\frac{r}{3}}dr - \widetilde{Z}_r^{s,x}dB_r \quad ;\ r\in(0,\infty), \\ \widetilde{Y}_\infty^{s,x} = 0, \end{cases} \tag{1.22}$$

where W and B are two independent d-dimensional standard Brownian motions. Here $\widetilde{Y}_0\left(s,X_s^{t,x}\right)$ and $Y_s\left(s,x+B_r\right)$ means $\widetilde{Y}_0^{s,X_s^{t,x}}$ and $Y_s^{s,x+B_r}$, respectively.

Following Delbaen *et al.* [76], the infinite interval $(0,\infty)$ of the probabilistic representation for the operator $\nabla\left(-\triangle\right)^{-1}\operatorname{div}\operatorname{div}$ is restricted to $\left[\frac{1}{N},N\right]$, for $N\in(1,\infty)$. Hence the incompressible velocity field u on $(T_0,T]$, with $T_0\in[0,T)$, is approximated by u^N which solves the PDE

$$\begin{cases} \frac{\partial u^N}{\partial t} + \frac{\nu}{2}\triangle u^N + \left(u^N\cdot\nabla\right)u^N + \mathbf{P}^N\left(u^N\otimes u^N\right) + f = 0 \quad ;\ T_0\leq t<T, \\ u^N\left(T\right) = g \end{cases} \tag{1.23}$$

where for $N\in(1,\infty)$ and smooth enough u^N the nonlocal operator is estimated by means of $\mathbf{P}^N$ Then, the *truncated* PDE is associated through the nonlinear Feynman-Kac formula

$$u^N\left(t,x\right) = Y_t^{t,x}; \quad \forall\left(t,x\right)\in[0,T]\times\mathbb{R}^d$$

to the following FBSDS

$$\begin{cases} dX_s^{t,x} = Y_s\left(s, X_s^{t,x}\right) ds + \sqrt{\nu} dW_s \quad ; \ s \in [t,T], \\ X_t^{t,x} = x, \\ -dY_s\left(s, X_s^{t,x}\right) = \left[f\left(s, X_s^{t,x}\right) + \mathbf{P}^N\left(Y_s \otimes Y_s\right)\left(s, X_s^{t,x}\right)\right] ds - \sqrt{\nu} Z_s^{t,x} dW_s \quad ; \ s \in [t,T], \\ Y_T\left(T,x\right) = g\left(x\right), \\ \mathbf{P}^N\left(Y_s \otimes Y_s\right)(s,x) = \mathbb{E}\int_{\frac{1}{N}}^{N} \frac{27}{2r^3} Y_s^i \cdot Y_s^j\left(s, x + B_r\right)\left(B_r - B_{\frac{2r}{3}}\right)^i \left(B_{\frac{2r}{3}} - B_{\frac{r}{3}}\right)^j B_{\frac{r}{3}} dr, \end{cases} \tag{1.24}$$

where W and B are independent d-dimensional Wiener processes and, by abuse of notation, we write $Y_s\left(t,y\right) := Y_s^{t,y}$.

Motivated by the above *forward-backward* probabilistic representations, we can simulate systems of stochastic particles governed by the FBSDS from a Lagrangian point of view. That is, imagine a fixed grid of spatial points. Over the covered spatial domain is moving a fluid at specific times. The velocity field over the discrete domain represents the velocity of fluid particles passing through the grid at each time. To be clear, the time-space domain $[0,T] \times \mathbb{R}^d$ is discretized by $\{0, h, \ldots, N \cdot h\} \times \delta \cdot \mathbb{Z}^d$, with spatial discretization parameter $\delta > 0$ and time-step $h = \frac{T}{N}$ such that the spatial step is less than the time step, that is $\delta < h$. Therefore, for all (T_j, x) belonging to the discrete time-spatial domain, we compute estimations $\bar{u}\left(T_j, x\right)$ to the velocity field $u\left(T_j, x\right) \in \mathbb{R}^n$. At this point, the nonlinear Feynman-Kac formula

$$Y = u\left(\cdot, X\right)$$

involves the simulation of diffusion processes and then our interest on the weak numerical solution of systems of FBSDEs. Various difficulties appeared in such work.

1.2 Objectives and outline

The main goal of this PhD thesis work is to provide of efficient numerical methodologies to obtain weak approximations for the solutions of Itô SDEs driven by Brownian motion and systems of FBSDEs. The design of numerical schemes for SDEs with multiplicative noise achieving the same rate of weak convergence of the traditional Euler-based methods, and guarantying the almost sure asymptotic exponential behavior and the sign-preserving ability of such exact solutions for any discretization step. The numerical treatment of systems of FBSDEs associated to nonlinear PDEs and the numerical simulation of the incompressible Navier-Stokes equations by means of probabilistic algorithms, and to study alternative Monte-Carlo methods to compute mean values in order to reduce the time for computer simulations.

We propose the development of first-order weak numerical methods for SDEs with multiplicative noise without involving stochastic implicit terms nor the computation of multiple integrals. The numerical analysis of the introduced numerical schemes and the computational implementation through a machine. The validation of dynamical behaviors and theoretical aspects on relevant test equations. We study the numerical approximation for solutions of nonlinear PDEs by means of probabilistic algorithms motivated by the numerical treatment of FBSDEs. Moreover, the computer simulation

of velocity fields governed by the demanding incompressible Navier-Stokes equations, as well as the Burgers equation, by numerically solving the associated systems of FBSDEs.

The *outline* of the PhD thesis work is as follows.

In Chapter 2 we begin by designing first-order weak balanced schemes for systems of linear SDEs with multiplicative noise, identifying stabilizing functions into the drift coefficients. As a motivational problem, we first study linear scalar SDEs and introduce sign-preserving and stable first-order weak balanced and trapezoidal schemes with explicit weights. Then we deal with bilinear systems of SDEs following two approaches to find the appropriate weight functions: through a closed heuristic formula or well by means of an optimization procedure. We test both approaches, exhibiting better performances with respect to previously reported balanced schemes.

Chapter 3 introduces the direction and norm decomposition (DND) approach for the numerical approximation of SDEs with multiplicative noise. For this purpose, we begin by presenting a new numerical scheme for nonlinear scalar SDEs. Then, we consider the context of systems of linear SDEs following the novel methodology. The DND method involves the efficient estimation of the norm process $\|X_t\|$ by using the new nonlinear scalar scheme together with the appropriate numerical solution of the direction process $\hat{X}_t := X_t / \|X_t\|$. We put special attention on the cases of well and ill-conditioned drift term matrices. Additionally, we illustrate the potential of the new numerical schemes to the approximation of locally Lipschitz SDEs and the estimation of Lyapunov exponents. The good performance of the presented numerical schemes is supported by theoretical results of convergence and stability, and illustrated by several numerical examples (see Mora and Mardones (2014)[156] for manuscript versions of the work).

Chapter 4 deals with the numerical simulation for the strong solutions of the incompressible Navier-Stokes equations by means of a novel system of FBSDEs, where a SDE component with additive noise appears (see Delbaen, Qiu and Tang (2015) [76]). Such system of SDEs involve backward SDEs which generalizes the relation between stochastic equations and PDEs by means of the nonlinear Feynman-Kac formula, which provides probabilistic representations to the strong solution of nonlinear PDEs. Following a rather practical approach, we highlight the potential of systems of FBSDEs for the numerical treatment of PDEs. We incorporate recent tools of computational implementation for the estimation of expected values by using the quantization of Gaussian random processes and reduction variance techniques.

Finally, the last Chapter is devoted to conclusions, remarks, discussions and future directions. YOU are welcome to study, research and continue, *forward* or *backward*, on whichever of the presented problems.

Chapter 2

First-order weak balanced schemes for systems of linear SDEs

The immediate ways are not always the best

We introduce some weak balanced schemes for linear systems of stochastic differential equations (SDEs) with multiplicative noise. First, we consider the test problem of linear scalar SDEs to construct sign-preserving and almost sure asymptotically stable first-order weak balanced schemes based on the addition of stabilizing functions to the drift terms. Then, we design balanced schemes for multidimensional linear SDEs achieving the first order of weak convergence, which do not involve multiple stochastic integrals. To this end, we follow two methodologies to find appropriate stabilizing weights: firstly based on a closed heuristic formula and then through an optimization procedure. Numerical experiments show a promising performance of the introduced weak balanced schemes.

2.1 Introduction

Consider the Itô SDE

$$X_t = X_0 + \int_0^t b\left(X_s\right) ds + \sum_{k=1}^{m} \int_0^t \sigma^k\left(X_s\right) dW_s^k, \tag{2.1}$$

where X_t is an adapted $\mathbb{R}^d$-valued stochastic process, the coefficients $b, \sigma^k : \mathbb{R}^d \to \mathbb{R}^d$ are smooth functions and $W^1, \ldots, W^m$ are independent standard Wiener processes (see e.g. [108, 117, 125, 138, 161, 178] for existence and uniqueness results and the general theory). For solving (2.1) in cases the diffusion terms σ^k play an essential role in the dynamics of X_t, Milstein, Platen and Schurz (1998) [148] introduced the balanced implicit method

$$\begin{aligned} Z_{n+1} &= Z_n + b\left(Z_n\right)\Delta + \sum_{k=1}^{m} \sigma^k\left(Z_n\right)\left(W_{(n+1)\Delta}^k - W_{n\Delta}^k\right) \\ &\quad + \left(c^0\left(Z_n\right)\Delta + \sum_{k=1}^{m} c^k\left(Z_n\right)\left|W_{(n+1)\Delta}^k - W_{n\Delta}^k\right|\right)\left(Z_n - Z_{n+1}\right), \end{aligned} \tag{2.2}$$

where $\Delta > 0$ and $c^0, c^1, \ldots, c^m$ are weight functions that should be appropriately chosen for each SDE. Here Z_n corresponds to a numerical approximation of X_{T_n}, for time nodes $T_n = n\Delta$.

To the best of our knowledge, the schemes of type (2.2) use the damping functions $c^1, \ldots, c^m$ to control the numerical instabilities caused by σ^k and the pathwise behavior. Hence their rate of weak convergence is equal to $1/2$, which is lower than the traditional Euler-Maruyama method (see e.g. [4, 148, 184, 186, 202]). Concrete balanced versions of the Milstein scheme have been developed only in particular cases, like $m = 1$, where the Milstein scheme does not involve multiple stochastic integrals with respect to different Brownian motions [5, 116].

We deal with the problem of constructing balanced Euler schemes having the same rate of weak converge as the Euler method. More precisely, we are interested in the development of efficient first-order balanced schemes for computing $\mathbb{E}f(X_t)$, with $f : \mathbb{R}^d \to \mathbb{R}$ smooth. This motivates us to design balanced schemes based only on c_0, without using increments of Brownian motions, and the general question of whether we can find appropriate weights c^0 such that

$$Z_{n+1} = Z_n + b(Z_n)\Delta + c^0(\Delta, Z_n)(Z_{n+1} - Z_n)\Delta + \sum_{k=1}^{m} \sigma^k(Z_n)\sqrt{\Delta}\xi_n^k \tag{2.3}$$

reproduces the long-time behavior of X_t. Here, $\xi_0^1, \xi_0^2, \ldots, \xi_0^m, \xi_1^1, \ldots$ are independent discrete random variables satisfying $\mathbb{P}\left(\xi_n^k = \pm 1\right) = 1/2$. The Section 2.2 gives a positive answer to this problem when equation (2.1) reduces to a linear scalar SDE. In this test case, we obtain an explicit expression for $c^0(\Delta, \cdot)$ that makes Z_n an almost sure asymptotically stable numerical scheme with the sign-preserving ability for all time-step $\Delta > 0$. Moreover, Section 2.2 introduces a stabilized trapezoidal scheme achieving the same dynamical properties. The Section 2.3 focuses on systems of linear SDEs. In case $b, \sigma^k : \mathbb{R}^d \to \mathbb{R}^d$ are linear, we propose an optimization procedure for identifying a suitable weight function c_0. Section 2.3 also provides a choice of c_0 based on a heuristic closed formula. Both techniques show good results in our numerical experiments, which encourages further studies of the numerical method (2.3). All proofs are deferred to Section 2.4.

2.2 Linear scalar SDE

In this section, we assume that X_t satisfies the linear scalar SDE

$$X_t = X_0 + \int_0^t \mu X_s ds + \int_0^t \lambda X_s dW_s^1, \tag{2.4}$$

where $\mu, \lambda \in \mathbb{R}$. The SDE (2.4) is a classical test equation for studying the stability properties of the numerical schemes for equation (2.1) (see e.g. [4, 99, 102]). It is well known its explicit solution

$$X_t = \exp\left(\left(\mu - \frac{\lambda^2}{2}\right)t + \lambda W_t^1\right) X_0$$

and the asymptotic stability property

$$\lim_{t \to +\infty} |X_t| = 0 \ \mathbb{P} - a.s. \Leftrightarrow 2\mu - \lambda^2 < 0.$$

2.2.1 Stabilized Euler scheme

Set $T_n = n\Delta$, with $\Delta > 0$ and $n = 0, 1, \ldots$ For all $t \in [T_n, T_{n+1}]$ we have

$$X_t = X_{T_n} + \int_{T_n}^{t} (\mu X_s + a(\Delta) X_s - a(\Delta) X_s)\, ds + \int_{T_n}^{t} \lambda X_s dW_s^1,$$

where $a(\Delta)$ is an arbitrary real number. Then

$$X_{T_{n+1}} \approx X_{T_n} + \mu X_{T_n}\Delta + a(\Delta)\left(X_{T_{n+1}} - X_{T_n}\right)\Delta + \lambda X_{T_n}\left(W_{T_{n+1}}^1 - W_{T_n}^1\right),$$

and so X_t is weakly approximated by the recursive scheme

$$Y_{n+1}^s = Y_n^s + \mu Y_n^s \Delta + a(\Delta)\left(Y_{n+1}^s - Y_n^s\right)\Delta + \lambda Y_n^s \sqrt{\Delta}\xi_n^1, \tag{2.5}$$

where, from now on, $\xi_0^1, \xi_1^1, \ldots$ is a sequence of independent random variables taking values ± 1 with probability $1/2$. In case $a(\Delta)\Delta \neq 1$, we have

$$Y_{n+1}^s = Y_n^s \left(1 + \left(\mu\Delta + \lambda\sqrt{\Delta}\xi_n^1\right) / \left(1 - a(\Delta)\Delta\right)\right).$$

Therefore, we wish to find a locally bounded function $\Delta \mapsto a(\Delta)$ such that:

P1) Y_n^s preserves *a.s.* the sign of Y_0^s for all $n \in \mathbb{N}$.

P2) Y_n^s converges almost surely to 0 as $n \to \infty$ whenever $2\mu - \lambda^2 < 0$.

We check easily that

$$\text{Property P1} \Leftrightarrow a(\Delta) \in \,]-\infty, p_1[\cup]p_2, +\infty[\,,$$

with $p_1 := \min\left\{1, 1 - |\lambda|\sqrt{\Delta} + \mu\Delta\right\}/\Delta$ and $p_2 := \max\left\{1, 1 + |\lambda|\sqrt{\Delta} + \mu\Delta\right\}/\Delta$. A close look at the mean value $\mathbb{E}\log\left(1 + \left(\mu\Delta + \lambda\sqrt{\Delta}\xi_n^1\right)/\left(1 - a(\Delta)\Delta\right)\right)$ reveals that:

Lemma 2.2.1 *Suppose that $a(\Delta)\Delta \neq 1$. Then, a necessary and sufficient condition for Property P1, together with $\lim_{n\to\infty} Y_n^s = 0$ a.s., is that*

$$a(\Delta) \in \begin{cases} \,]-\infty, p_1[\cup]p_2, p_3[& ;\ \textit{in case } \mu < 0 \\ \,]-\infty, p_1[\cup]p_2, +\infty[& ;\ \textit{when } \mu = 0 \textit{ and } \lambda \neq 0 \\ \,]p_3, p_1[\cup]p_2, +\infty[& ;\ \textit{if } \mu > 0 \end{cases},$$

where $p_3 := \left(\mu^2\Delta + 2\mu - \lambda^2\right)/(2\mu\Delta)$.

Remark 2.2.1 *The numerical scheme Y_n^s with $a(\Delta) \equiv 0$ (i.e. the Euler-Maruyama scheme) satisfies Properties P1 and P2 iff*

$$\Delta \in \begin{cases} \left]0, \left(\frac{|\lambda|-\sqrt{\lambda^2-4\mu}}{2\mu}\right)^2\right[& ; \text{ in case } \mu < 0, \\ ]0, \frac{1}{\lambda^2}[& ; \text{ in case } \mu = 0 \text{ and } \lambda \neq 0, \\ \left]0, \frac{\lambda^2-2\mu}{\mu^2}\right[& ; \text{ in case } \mu > 0 \text{ and } \lambda^2 - 4\mu < 0, \\ \left]0, \frac{\lambda^2-2\mu}{\mu^2}\right[\setminus \left\{\frac{\lambda^2}{4\mu^2}\right\} & ; \text{ in case } \mu > 0 \text{ and } \lambda^2 - 4\mu = 0, \\ \left]0, \left(\frac{|\lambda|-\sqrt{\lambda^2-4\mu}}{2\mu}\right)^2\right[\cup \left]\left(\frac{|\lambda|+\sqrt{\lambda^2-4\mu}}{2\mu}\right)^2, \frac{\lambda^2-2\mu}{\mu^2}\right[& ; \text{ in case } \mu > 0 \text{ and } \lambda^2 - 4\mu > 0. \end{cases}$$

Using Lemma 2.2.1 we deduce that we can choose

$$a(\Delta) = \begin{cases} \mu - \alpha_1(\Delta)\lambda^2 & ; \text{ if } \mu \leq 0 \\ \mu - \alpha_2(\Delta)\lambda^2 & ; \text{ if } \mu > 0 \text{ and } \Delta < 2/\mu \\ \left(1 + |\lambda|\sqrt{\Delta} + \mu\Delta\right)/\Delta + \beta & ; \text{ if } \mu > 0 \text{ and } \Delta \geq 2/\mu \end{cases}, \tag{2.6}$$

where $\beta > 0$, $1/4 < \alpha_2(\Delta) \leq 1/4 + \left(\lambda^2 - 2\mu\right)(2 - \mu\Delta)/\left(8\lambda^2\right)$ and $\alpha_1 : \mathbb{R}_+ \to \mathbb{R}$ is a bounded function satisfying $\alpha_1(\Delta) > 1/4$.

Theorem 2.2.1 *Let $2\mu - \lambda^2 < 0$. Then, Y_n^s with $a(\Delta)$ given by (2.6) satisfies Properties P1 and P2.*

Remark 2.2.2 *In order to reproduce the a.s. exponentially unstable behavior, consider the following property:*

P3) *Y_n^s doesn't converge almost surely to 0 as $n \to \infty$ whenever $2\mu - \lambda^2 \geq 0$.*

The next result characterizes $\Delta \mapsto a(\Delta)$ to guarantee the sign-preserving property and the unstable region of the balanced scheme (2.5), which follows from the proof of Lemma 2.2.1.

Lemma 2.2.2 *Suppose that $\mu \neq 0$ and $a(\Delta)\Delta \neq 1$. Then*

$$\text{Property P1 and } \lim_{n\to\infty} Y_n^s \neq 0 \text{ a.s.} \Leftrightarrow a(\Delta) \in \begin{cases}]p_2, +\infty[\cap [p_3, +\infty[& ; \text{ in case } \mu < 0 \\ ]-\infty, p_1[\cap]-\infty, p_3] & ; \text{ in case } \mu > 0 \end{cases}.$$

Up to now, we have constructed weak balanced schemes according to the underlying dynamical properties of the exact solutions of the linear scalar SDE (2.4). In order to guaranty the first order of rate of convergence, we introduce the next notation.

Notation 2.2.1 *We denote by $C_p^\ell\left(\mathbb{R}^d, \mathbb{R}\right)$ the set of all ℓ-times continuously differentiable functions from $\mathbb{R}^d$ to $\mathbb{R}$, whose partial derivatives up to order ℓ have at most polynomial growth.*

Remark 2.2.3 *Assume that X_0 has finite moments of any order, together with $2\mu - \lambda^2 < 0$. Suppose that for every $g \in C_p^4(\mathbb{R},\mathbb{R})$ there exists $K > 0$ such that $|\mathbb{E}g(X_0) - \mathbb{E}g(Y_0^s)| \leq K(1 + \mathbb{E}|X_0|^q)\,T/N$ for all $N \in \mathbb{N}$. Let $a(\Delta)$ be given by (2.6). Since $\Delta \mapsto a(\Delta)$ is a bounded function, using classical arguments (see e.g. [120, 147, 154, 184, 199]) we can deduce that there exists $N_0 \in \mathbb{N}$ such that for any $f \in C_p^4(\mathbb{R},\mathbb{R})$,*

$$|\mathbb{E}f(X_T) - \mathbb{E}f(Y_N^s)| \leq K(T)(1 + \mathbb{E}|X_0|^q)\,T/N \qquad \forall N \geq N_0, \tag{2.7}$$

where $q \geq 2$ and $T \mapsto K(T)$ is a positive increasing function. Furthermore, it follows that there exists $\epsilon \in (0,1)$ such that

$$|1 - a(\Delta)\Delta| > \epsilon \qquad \forall \Delta > 0 \tag{2.8}$$

(see Section 2.4), and so (2.7) holds for all $N \in \mathbb{N}$. This is proved by applying, for instance, Theorem 2.3.2.

Following Milstein *et al.* [148], we now illustrate the behavior of Y_n^s using (2.4) with $\mu = 0$ and $\lambda = 4$. We take $X_0 = 1$. Since $\mu \leq 0$, we choose $\alpha_1(\Delta) = 1/4 + 1/100$; its convenient to keep the weights as small as possible. Figure 2.1 displays the computation of $\mathbb{E}\sin(X_t/5)$ obtained from the sample means of $25 \cdot 10^9$ observations of: Y_n^s with $a(\Delta) = -0.26\ \lambda^2$, the fully implicit method $\tilde{Y}_{n+1} = \tilde{Y}_n / \left(1 + \lambda^2\Delta - \lambda\sqrt{\Delta}\xi_n^1\right)$ (see p. 497 of [120]), and the balanced scheme

$$\widetilde{Z}_{n+1} = \widetilde{Z}_n \left(1 + \lambda\sqrt{\Delta}\xi_n^1 + \lambda\sqrt{\Delta}\right) / \left(1 + \lambda\sqrt{\Delta}\right),$$

which is a weak version of the method developed in Section 2 of [148]. Solid lines identifies the "true" values gotten by sampling $25 \cdot 10^9$ times $\exp\left(-8t + 4W_t^1\right)$. In contrast with the incorrect performance of the Euler-Maruyama scheme when the step sizes are greater than or equal to $1/16$ (that is in concordance with Remark 2.2.1), Figure 2.1 suggests us that Y_n^s is an efficient scheme having good qualitative and convergence properties. In this numerical experiment, the accuracy of $\tilde{Z}_n$ is not good, and $\tilde{Y}_n$ decays too fast to 0 as $n \to \infty$.

2.2.2 Stabilized trapezoidal method

The trapezoidal scheme (see p. 497 of [120])

$$Z_{n+1}^T = Z_n^T + \mu\frac{Z_{n+1}^T + Z_n^T}{2}\Delta - \lambda^2\frac{Z_{n+1}^T + Z_n^T}{4}\Delta + \lambda\frac{Z_{n+1}^T + Z_n^T}{2}\sqrt{\Delta}\xi_n^1$$

has a good speed of weak convergence to the solution of (2.4), but Z_n^T fails to preserve the sign of X_0. Analysis similar to that in the above Subsection 2.2.1 shows the next theorem, which ensures the existence of $a \in \mathbb{R}$ such that

$$\begin{aligned} Y_{n+1}^T &= Y_n^T + \mu\left(Y_{n+1}^T + Y_n^T\right)\Delta/2 - \lambda^2\left(Y_{n+1}^T + Y_n^T\right)\Delta/4 \\ &\quad + \lambda\left(Y_{n+1}^T + Y_n^T\right)\sqrt{\Delta}\xi_n^1/2 + \left(Y_{n+1}^T - Y_n^T\right)a\Delta \end{aligned} \tag{2.9}$$

verifies the properties:

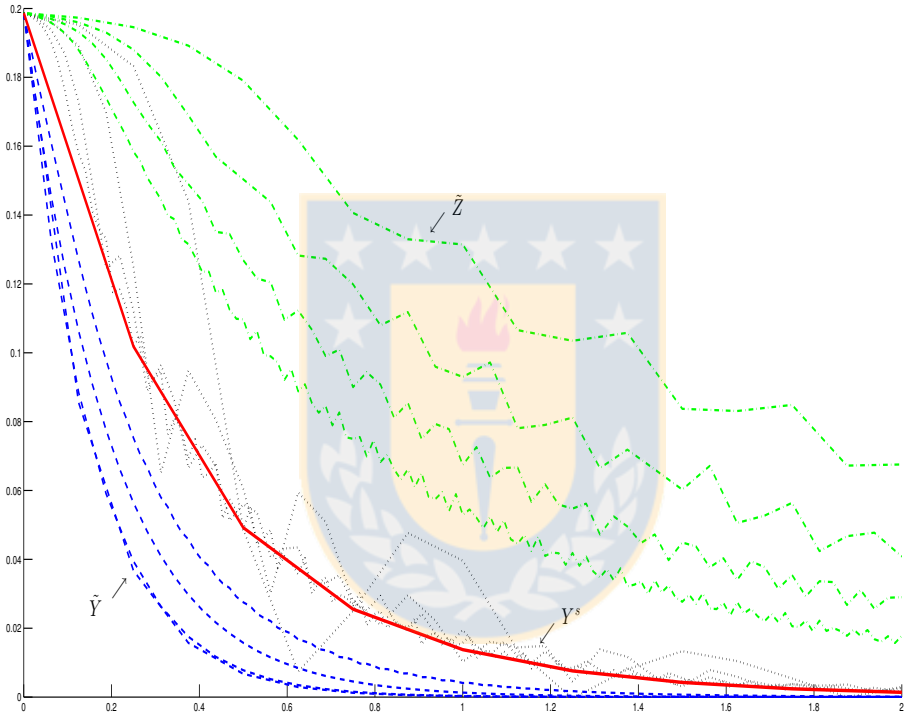

Figure 2.1: Computation of $\mathbb{E}\sin(X_t/5)$, where $t \in [0,2]$ and X_t solves (2.4) with $\mu = 0$, $\lambda = 4$ and $X_0 = 1$. Dashed line: $\tilde{Y}$, dashdot line: $\tilde{Z}$, dotted line: Y^s, and solid line: reference values. Here, Δ takes the values 1/8, 1/16, 1/32 and 1/64. As we expected, smaller Δ produce better approximations.

P1') Y_n^T has the same sign as Y_0^T *a.s.* for all $n \in \mathbb{N}$.

P2') Y_n^T converges *a.s.* to 0 as $n \to \infty$ whenever $2\mu - \lambda^2 < 0$.

Moreover, as in Remark 2.2.3 using standard arguments we can prove that Y_n^T has linear rate of weak convergence.

Theorem 2.2.2 *Let $2\mu - \lambda^2 < 0$. Consider Scheme (2.9) with $a < \mu/2 - 5\lambda^2/16$. Then Y_n^T satisfies Properties P1' and P2'. Moreover,*

$$Y_{n+1}^T = \frac{4 + \left(2\mu - \lambda^2 - 4a\right)\Delta + 2\lambda\sqrt{\Delta}\xi_n^1}{4 - \left(2\mu - \lambda^2 + 4a\right)\Delta - 2\lambda\sqrt{\Delta}\xi_n^1}\, Y_n^T.$$

In order to evaluate the sign-preserving property and the accuracy of Y_n^T, we compute $\mathbb{E}g\left(X_t\right)$ and $\mathbb{E}h\left(X_t\right)$, where $g\left(x\right) = 100\left(\pi/2 - \arctan\left(1000x + 100\right)\right)$ and $h\left(x\right) = \log\left(1 + x^2\right)$. We choose $X_0 = 1$, $\lambda = 4$, and μ takes the values -1 and 2. In Table 2.1 we compare the following schemes: Y_n^T given by (2.9) with $a = \mu/2 - 3\lambda^2/8$, the trapezoidal scheme Z_n^T, the weak balanced scheme

$$\widetilde{Z}_{n+1} = \widetilde{Z}_n\left(1 + \left(\mu\Delta + \lambda\sqrt{\Delta}\xi_1^n\right) / \left(1 - \mu\Delta/2 + |\lambda|\sqrt{\Delta}\right)\right)$$

and scheme Y_n^s given by (2.5) with $\alpha_1\left(\Delta\right) = 0.26$, $\alpha_2\left(\Delta\right) = 1/4 + 10^{-4}\left(\lambda^2 - 2\mu\right)\mu/\left(8\lambda^2\right)$ and $\beta = 0.01$. Indeed, Table 2.1 presents the errors

$$\epsilon\left(\hat{Y}\right) := \left|\mathbb{E}g\left(X_T\right) - \mathbb{E}g\left(\hat{Y}_N\right)\right| + \left|\mathbb{E}h\left(X_T\right) - \mathbb{E}h\left(\hat{Y}_N\right)\right|,$$

with $T = 1$ and $N = T/\Delta$. For each numerical method $\hat{Y}$, we estimate $\epsilon\left(\hat{Y}\right)$ by sampling $25 \cdot 10^9$ times both $\hat{Y}$ and the explicit solution $\exp\left(\left(\mu - 8\right)t + 4W_t^1\right)$. Table 2.1 shows that Y_n^T has good qualitative properties, and in addition Y_n^T inherits the good speed of weak convergence of Z_n^T. We can also observe the very good behavior of the stabilized Euler scheme Y^s.

2.3 Bilinear systems of SDEs

This section is devoted to the SDE

$$X_t = X_0 + \int_0^t BX_s\, ds + \sum_{k=1}^m \int_0^t \sigma^k X_s\, dW_s^k, \tag{2.10}$$

where $X_t \in \mathbb{R}^d$ and $B, \sigma^1, \ldots, \sigma^m$ are given real matrices of size $d \times d$. The bilinear SDEs describe dynamical features of non-linear SDEs via the linearization around their equilibrium points (see e.g. [10, 19]). The system of SDEs (2.10) also appears, for example, in the spatial discretization of stochastic partial differential equations (see e.g. [93, 114]).

		Δ				
		1/4	1/8	1/16	1/32	1/64
$\epsilon\left(Y^T\right)$	$\mu=-1$	0.1510	0.0668	0.0321	0.0172	0.0110
	$\mu=2$	0.2436	0.1638	0.1074	0.0713	0.0437
$\epsilon\left(Z^T\right)$	$\mu=-1$	77.935	9.8110	0.0706	0.0402	0.0218
	$\mu=2$	78.527	10.047	0.1983	0.1012	0.0514
$\epsilon\left(Y^s\right)$	$\mu=-1$	0.3703	0.1250	0.0545	0.0269	0.0133
	$\mu=2$	0.3633	0.0697	0.0361	0.0178	0.0088
$\epsilon\left(\widetilde{Z}\right)$	$\mu=-1$	0.9259	0.7567	0.5870	0.4353	0.3115
	$\mu=2$	1.4534	1.3128	1.1220	0.9116	0.7092

Table 2.1: Estimation of errors involved in the computation of $\mathbb{E}g\left(X_T\right)$ and $\mathbb{E}h\left(X_T\right)$ for $T=1$. Here, X_t verifies (2.4) with $X_0=1$ and $\lambda=4$.

2.3.1 Heuristic balanced scheme

We now return to (2.3). Since (2.10) is bilinear, for each $\Delta>0$ we restrict c^0 to be constant, and so (2.3) becomes

$$Z_{n+1}=Z_n+BZ_n\Delta+H\left(\Delta\right)\left(Z_{n+1}-Z_n\right)\Delta+\sum_{k=1}^{m}\sigma^kZ_n\sqrt{\Delta}\xi_n^k, \tag{2.11}$$

with $H:]0,\infty[\to\mathbb{R}^{d\times d}$ and $\Delta>0$. The rate of weak convergence of Z_n is equal to 1 provided, for instance, that $H\left(\Delta\right)$ and $\left(I-\Delta H\left(\Delta\right)\right)^{-1}$ are bounded on any interval $\Delta\in]0,a]$ (see [184]). Generalizing roughly Subsection 2.2.1 we choose

$$H\left(\Delta\right)=B-\sum_{k=1}^{m}\alpha_k\left(\Delta\right)\left(\sigma^k\right)^{\top}\sigma^k,$$

where, for example, $\alpha_k\left(\Delta\right)=0.26$. This gives the recursive scheme

$$\left(I-\Delta B+0.26\ \Delta\sum_{k=1}^{m}\left(\sigma^k\right)^{\top}\sigma^k\right)Y_{n+1}^s=Y_n^s+0.26\ \Delta\sum_{k=1}^{m}\left(\sigma^k\right)^{\top}\sigma^kY_n^s+\sum_{k=1}^{m}\sigma^kY_n^s\sqrt{\Delta}\xi_n^k, \tag{2.12}$$

which is a first-order weak balanced version of the semi-implicit Euler method.

Remark 2.3.1 *Combining (2.12) with ideas of the local linearization method (see e.g. [30, 71]) we deduce the following numerical method for (2.1):*

$$U_{n+1}=U_n+b\left(U_n\right)\Delta+\sum_{k=1}^{m}\sigma^k\left(U_n\right)\sqrt{\Delta}\xi_n^k+H\left(\Delta,U_n\right)\left(U_{n+1}-U_n\right)\Delta,$$

where $H\left(\Delta,x\right)=\nabla b\left(x\right)-\sum\limits_{k=1}^{m}\alpha_k\left(\Delta\right)\left(\nabla\sigma^k\left(x\right)\right)^{\top}\nabla\sigma^k\left(x\right)$*;* $\forall x\in\mathbb{R}^d$*, with* $\alpha_k\left(\Delta\right)=0.26$*.*

2.3.2 Optimal criterion to select weights

In case $I - \Delta H(\Delta)$ is invertible, according to (2.11) we have

$$Z_{n+1} = Z_n + (I - \Delta H(\Delta))^{-1} \left(\Delta B + \sum_{k=1}^{m} \sqrt{\Delta} \xi_n^k \sigma^k \right) Z_n, \tag{2.13}$$

where I is the $d \times d$ identity matrix. Therefore, a more general formulation of Z_n is given by

$$V_{n+1} = V_n + (I + \Delta M(\Delta)) \left(\Delta B + \sum_{k=1}^{m} \sqrt{\Delta} \xi_n^k \sigma^k \right) V_n, \tag{2.14}$$

with $M :]0, \infty[\to \mathbb{R}^{d \times d}$. In fact, taking $M(\Delta) = \left((I - \Delta H(\Delta))^{-1} - I \right) / \Delta$ we obtain (2.13) from (2.14). The following theorem provides a useful estimate of the growth rate of V_n in terms of $\mathbb{E} \log (\|A_0(\Delta, M(\Delta)) x\|)$, a quantity that we can explicitly compute in each specific situation.

Theorem 2.3.1 *Let V_n be defined recursively by (2.14). Then*

$$\lim_{n \to \infty} \frac{1}{n\Delta} \log \|V_n\| \leq \frac{1}{\Delta} \sup_{x \in \mathbb{R}^d, \|x\|=1} \mathbb{E} \log \|A_n(\Delta, M(\Delta)) x\|, \tag{2.15}$$

where $A_n(\Delta, M) = I + (I + \Delta M) \left(\Delta B + \sum_{k=1}^{m} \sqrt{\Delta} \xi_n^k \sigma^k \right)$.

Set $\ell := \sup_{x \in \mathbb{R}^d, \|x\|=1} \left(\langle x, Bx \rangle + \frac{1}{2} \sum_{k=1}^{m} \left\| \sigma^k x \right\|^2 - \sum_{k=1}^{m} \langle x, \sigma^k x \rangle^2 \right)$. Then

$$\limsup_{t \to \infty} \frac{1}{t} \log \|X_t\| \leq \ell \qquad a.s. \tag{2.16}$$

(see e.g. [102]). Fix $\Delta > 0$. We would like that for all $x \in \mathbb{R}^d$ such that $\|x\| = 1$,

$$\frac{1}{\Delta} \mathbb{E} \log \|A_0(\Delta, M(\Delta)) x\| \approx \langle x, Bx \rangle + \frac{1}{2} \sum_{k=1}^{m} \left\| \sigma^k x \right\|^2 - \sum_{k=1}^{m} \langle x, \sigma^k x \rangle^2.$$

A simpler problem is to find $M(\Delta)$ for which the upper bounds of inequalities (2.15) and (2.16) are as close as possible, and so we can expect that V_n inherits the long-time behavior of X_t. Then, we propose to take

$$M(\Delta) \in \arg\min \left\{ \left(\frac{1}{\Delta} \sup_{x \in \mathbb{R}^d, \|x\|=1} \mathbb{E} \log \|A_0(\Delta, M) x\| - \ell \right)^2 : M \in \mathcal{M} \right\}, \tag{2.17}$$

where $\mathcal{M}$ is a predefined subset $\mathbb{R}^{d \times d}$. Two examples of $\mathcal{M}$ successfully used in our numerical experiments are $\mathbb{R}^{d \times d}$ and

$$\left\{ (M_{i,j})_{1 \leq i,j \leq d} : |M_{i,j}| \leq K \text{ for all } i, j = 1, \ldots, d \right\},$$

with K large enough.

Applying the classical methodology introduced by Talay and Milstein for studying the weak convergence order (see e.g. [91, 150]) we can deduce that V_n converges weakly with order 1 whenever $\Delta \to M(\Delta)$ is locally bounded. The next theorem summarizes this result.

Theorem 2.3.2 *Consider $T > 0$ and $f \in C_p^4(\mathbb{R}^d, \mathbb{R})$. Let V_n be given by (2.14) with $\Delta = T/N$, where $N \in \mathbb{N}$. Assume that X_0 has finite moments of any order, and that for every $g \in C_p^4(\mathbb{R}^d, \mathbb{R})$,*

$$|\mathbb{E}g(X_0) - \mathbb{E}g(V_0)| \leq K\left(1 + \mathbb{E}\|X_0\|^q\right) T/N \qquad \forall N \in \mathbb{N},$$

with $K > 0$. Let $\Delta \to M(\Delta)$ be bounded on $[0, T]$. Then

$$|\mathbb{E}f(X_T) - \mathbb{E}f(V_N)| \leq K(T)\left(1 + \mathbb{E}\|X_0\|^q\right) T/N \qquad \forall N \in \mathbb{N}, \tag{2.18}$$

where $q \geq 2$ and $K(\cdot)$ is a positive increasing function.

Remark 2.3.2 *In some situations, the asymptotic behavior of the stochastic process X_t that solves (2.1) depends on the properties of the SDE obtained by linearizing (2.1) around 0 (see e.g. [10, 18, 19]). More precisely, the SDE given by*

$$Y_t = Y_0 + \int_0^t \left(\nabla b(0) Y_s + b(0)\right) ds + \sum_{k=1}^m \int_0^t \left(\nabla \sigma^k(0) Y_s + \sigma^k(0)\right) dW_s^k. \tag{2.19}$$

In these cases, we can extend the scheme given by (2.14) and (2.17) to the nonlinear SDE (2.1) as

$$V_{n+1} = V_n + (I + \Delta M(\Delta)) \left(b(V_n)\Delta + \sum_{k=1}^m \sigma^k(V_n)\sqrt{\Delta}\xi_n^k\right)$$

where now $M(\Delta)$ is described by (2.17) with $\mathcal{M}$ a predefined subset of $\mathbb{R}^{d\times d}$,

$$\ell := \sup_{x\in\mathbb{R}^d, \|x\|=1} \left(\langle x, \nabla b(0) x\rangle + \frac{1}{2}\sum_{k=1}^m \left\|\nabla \sigma^k(0) x\right\|^2 - \sum_{k=1}^m \langle x, \nabla \sigma^k(0) x\rangle^2\right)$$

and $A_0(\Delta, M) = I + (I + \Delta M)\left(\nabla b(0)\Delta + \sum_{k=1}^m \nabla \sigma^k(0)\sqrt{\Delta}\xi_0^k\right)$.

2.3.3 Numerical experiments

Exponentially stable SDE

We consider the non-commutative test equation

$$dX_t = \begin{pmatrix} \sigma_1 & 0 \\ 0 & \sigma_2 \end{pmatrix} X_t\, dW_t^1 + \begin{pmatrix} 0 & -\epsilon \\ \epsilon & 0 \end{pmatrix} X_t\, dW_t^2, \tag{2.20}$$

where $\sigma_1 = 7$, $\sigma_2 = 4$, $\epsilon = 1$ and $X_0 = (1, 2)^\top$. Since $0 < \sigma_2 < \sigma_1 < 3\sigma_2$, applying elementary calculus we get $\ell = \left(\epsilon^2 - \sigma_2^2\right)/2 < 0$, and so X_t converges exponentially fast to 0. To illustrate the performance of schemes of type (2.3), we take V_n defined by (2.14) and (2.17) with

$$\mathcal{M} = \left\{(M_{i,j})_{1\leq i,j\leq 2} : |M_{i,j}| \leq 20 \text{ for all } i, j = 1, 2\right\}.$$

Δ	1/2	1/4	1/8	1/16	1/32	1/64
$M_{1,1}(\Delta)$	−1.6099	−5.1036	−4.8804	−7.1499	−1.6758	0.9887
$M_{2,1}(\Delta)$	0.0975	0.2758	0.7667	1.0136	1.1500	0.9918
$M_{1,2}(\Delta)$	−0.0975	−0.2752	−0.8505	−0.1814	−1.0448	−1.9947
$M_{2,2}(\Delta)$	−1.3173	−5.9305	−2.6136	−2.3003	−1.7421	−1.9005
Order	−10	−19	−21	−21	−20	−19

Table 2.2: Approximate values of the weight matrix $(M_{i,j}(\Delta))_{1\leq i,j\leq 2}$ for (2.20) with $\sigma_1 = 7$, $\sigma_2 = 4$ and $\epsilon = 1$, together with the corresponding order of magnitude of the objective function minimum.

		Δ					
		1/2	1/4	1/8	1/16	1/32	1/64
$\epsilon\left(\widetilde{Y}\right)$	$T=1$	6.5497	9.4879	12.733	11.0676	0.15183	0.02365
	$T=3$	18.814	28.8744	38.9743	34.1327	0.0086188	0.00075718
$\epsilon\left(\widetilde{Z}\right)$	$T=1$	1.3395	1.1777	0.98272	0.7757	0.58279	0.42137
	$T=3$	1.0611	0.78255	0.51624	0.30475	0.1643	0.08361
$\epsilon(Y^s)$	$T=1$	1.1914	0.85936	0.49789	0.15466	0.042484	0.018271
	$T=3$	0.81853	0.38585	0.10185	0.0096884	0.0013717	0.00055511
$\epsilon(V)$	$T=1$	1.2544	0.8482	0.36579	0.11998	0.029324	0.0069274
	$T=3$	0.64867	0.16695	0.035366	0.0065051	0.00068084	0.00031002

Table 2.3: Estimation of errors involved in the computation of $\mathbb{E}\log\left(1+\|X_T\|^2\right)$ for $T=1$ and $T=3$. Here, X_t solves the equation (2.20) with $\sigma_1 = 7$, $\sigma_2 = 4$, $\epsilon = 1$ and $X_0 = (1,2)^\top$.

Table 2.2 provides four-decimal approximations of the components of $M(\Delta)$, which have been obtained by running (5^4-times) the MATLAB function `fmincon` for the initial parameters

$$\left\{(M_{i,j})_{1\leq i,j\leq 2} : M_{i,j}\in\{-2,-1,0,1,2\} \text{ for all } i,j=1,2\right\}.$$

Figure 2.2 shows the computation of $\mathbb{E}\log\left(1+\|X_t\|^2\right)$ by means of V_n (dashed line), Y_n^s (dotted line), and

$$\begin{aligned}\widetilde{Z}_{n+1} &= \widetilde{Z}_n + \begin{pmatrix}\sigma_1 & 0\\ 0 & \sigma_2\end{pmatrix}\widetilde{Z}_n\sqrt{\Delta}\xi_n^1 + \begin{pmatrix}0 & -\epsilon\\ \epsilon & 0\end{pmatrix}\widetilde{Z}_n\sqrt{\Delta}\xi_n^2\\ &\quad +\sqrt{\Delta}\begin{pmatrix}|\sigma_1|+|\epsilon| & 0\\ 0 & |\sigma_2|+|\epsilon|\end{pmatrix}\left(\widetilde{Z}_n - \widetilde{Z}_{n+1}\right)\end{aligned}$$

(dashdot line). The scheme $\widetilde{Z}_n$ is a weak version of the balanced scheme proposed in Subsection 5.2 of [184]. The reference values for $\mathbb{E}\log\left(1+\|X_t\|^2\right)$ (solid line) have been calculated by using the weak

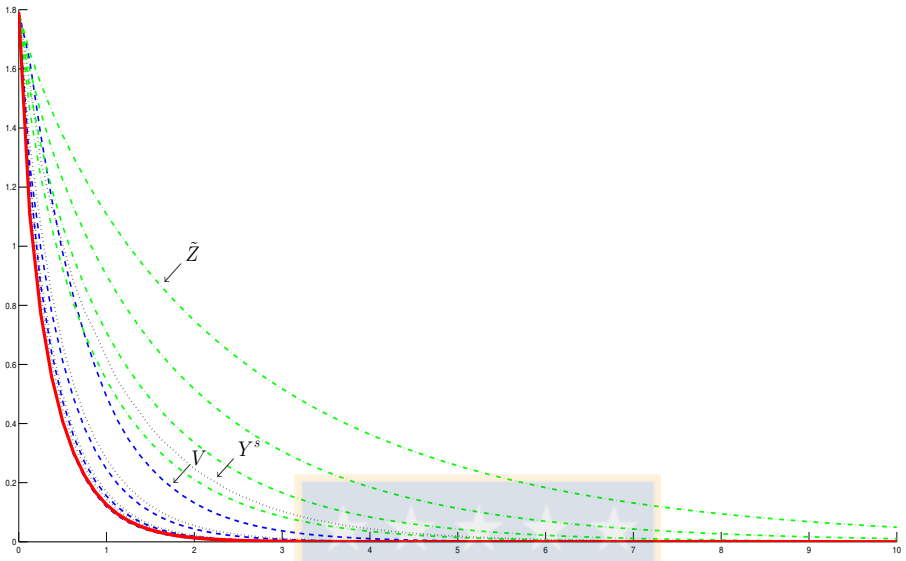

Figure 2.2: Computation of $\mathbb{E}\log\left(1+\|X_t\|^2\right)$, where $t \in [0,10]$ and X_t solves (2.20). Dashed line: V, dashdot line: $\widetilde{Z}$, dotted line: Y^s, and solid line: reference values. Here, Δ is equal to 1/8, 1/16, 1/32 and 1/64; smaller discretization steps produce better approximations.

Euler method

$$\widetilde{Y}_{n+1} = \widetilde{Y}_n + \begin{pmatrix} \sigma_1 & 0 \\ 0 & \sigma_2 \end{pmatrix} \widetilde{Y}_n \sqrt{\Delta}\xi_n^1 + \begin{pmatrix} 0 & -\epsilon \\ \epsilon & 0 \end{pmatrix} \widetilde{Y}_n \sqrt{\Delta}\xi_n^2$$

with step-size $\Delta = 2^{-13} \approx 0.000122$. Indeed, we plot the sample means obtained from 10^8 trajectories of each scheme. Furthermore, Table 2.3 provides estimates of the errors

$$\epsilon\left(\hat{Y}\right) := \left|\mathbb{E}\log\left(1+\|X_T\|^2\right) - \mathbb{E}\log\left(1+\left\|\hat{Y}_N\right\|^2\right)\right|$$

where $T = 1, 3$, $N = T/\Delta$, and $\hat{Y}$ represents the numerical methods V_n, Y_n^s, $\widetilde{Y}_n$ and $\widetilde{Z}_n$. From Table 2.3 we can see that $\widetilde{Y}_n$ blows up for $\Delta \leq 1/16$. The Figure 2.2, together with Table 2.3, illustrate that $\widetilde{Z}_n$ is stable, but presents a slow rate of weak convergence. In contrast, the performance of V_n is very good, V_n mix good stability properties with reliable approximations. The heuristic balanced scheme Y_n^s shows a very good behavior. In fact, the accuracy of Y_n^s is very similar to that of V_n for $\Delta \leq 1/16$, and Y_n^s does not involve any optimization process.

Δ	1/4	1/8	1/16	1/32	1/64	1/128
$M_{1,1}(\Delta)$	−0.6568	−0.6683	−0.6745	−0.6805	−0.6887	−0.6949
$M_{2,1}(\Delta)$	−0.2573	−0.3220	−0.3587	−0.3777	−0.3867	−0.3911
$M_{1,2}(\Delta)$	0.3123	0.3110	0.3112	0.3130	0.3165	0.3193
$M_{2,2}(\Delta)$	−0.6382	−0.6492	−0.6544	−0.6597	−0.6675	−0.6735
Order	−18	−19	−19	−20	−21	−26

Table 2.4: Approximate weight matrices $(M_{i,j}(\Delta))_{1\leq i,j\leq 2}$ for (2.21), together with the corresponding order of magnitude of the objective function minimum.

SDE with an unstable equilibrium point

We numerically solve the SDE

$$dX_t = \begin{pmatrix} 0 & b_2 \\ -b_2 & b_1 \end{pmatrix} X_t\, dt + \begin{pmatrix} \sigma_1 & 0 \\ 0 & \sigma_2 \end{pmatrix} X_t\, dW_t^1 + \begin{pmatrix} 0 & -\epsilon \\ \epsilon & 0 \end{pmatrix} X_t\, dW_t^2, \tag{2.21}$$

with $b_1 = 0.06$, $b_2 = 1$, $\sigma_1 = 0.2$, $\sigma_2 = 0.1$, $\epsilon = 0.3$ and $X_t = \left(X_t^1, X_t^2\right)^\top \in \mathbb{R}^2$. We set $X_0 = (1,-1)^\top/\sqrt{2}$. We have that 0 is an unstable equilibrium point of (2.21). Indeed, $\liminf_{t\to+\infty} \|X_t\| > 0$, because there exists $\theta \in (0,1/2)$ such that $\langle x, Bx\rangle + \frac{1}{2}\sum_{k=1}^m \left\|\sigma^k x\right\|^2 - (1+\theta)\sum_{k=1}^m \langle x, \sigma^k x\rangle^2 \geq 0$ for all $x \in \mathbb{R}^d$ such that $\|x\| = 1$ (see e.g. [8]).

We apply to (2.21) the scheme V_n given by (2.14), where $M(\Delta)$ is defined by (2.17) with

$$\mathcal{M} = \left\{(M_{i,j})_{1\leq i,j\leq 2} : |M_{i,j}| \leq 6 \text{ for all } i,j = 1,2\right\}.$$

To this end, we first compute $M(1/128)$ by proceeding as in Subsection 2.3.3 with initial parameters $M_{i,j} \in \{-1,-0.5,0,0.5,1\}$. Then, we solve the optimization problem corresponding to $\Delta = 1/64$ (resp. $\Delta = 1/32,\ldots,1/4$) by running the MATLAB code `fmincon` with initial solution $M(1/128)$ (resp. $M(1/64),\ldots,M(1/8)$) (see Table 2.4).

Figure 2.3 presents the computation of $\mathbb{E}\arctan\left(1+\left(X_t^2\right)^2\right)$ estimated by sampling 10^8 trajectories of V_n, the backward Euler scheme

$$\widetilde{Y}_{n+1} = \widetilde{Y}_n + \begin{pmatrix} 0 & b_2 \\ -b_2 & b_1 \end{pmatrix} \widetilde{Y}_{n+1}\Delta + \begin{pmatrix} \sigma_1 & 0 \\ 0 & \sigma_2 \end{pmatrix} \widetilde{Y}_n\sqrt{\Delta}\xi_n^1 + \begin{pmatrix} 0 & -\epsilon \\ \epsilon & 0 \end{pmatrix} \widetilde{Y}_n\sqrt{\Delta}\xi_n^2$$

and the balanced scheme $\widetilde{Z}_n$ defined by (2.2) with $W_{T_{n+1}}^k - W_{T_n}^k$ replaced by discrete random variables $\sqrt{\Delta}\xi_n^k$, $c^0 = -\frac{1}{2}\begin{pmatrix} 0 & b_2 \\ -b_2 & b_1 \end{pmatrix}$, $c^1 = \begin{pmatrix} \sigma_1 & 0 \\ 0 & \sigma_2 \end{pmatrix}$ and $c^2 = \begin{pmatrix} \epsilon & 0 \\ 0 & \epsilon \end{pmatrix}$ (see [4, 184]). Solid line provides the "exact" values obtained by sampling 10^8 times the weak Euler-Maruyama scheme with step-size $\Delta = 2^{-13} \approx 0.000122$. Moreover, Table 2.5 provides the errors $\epsilon\left(\hat{Y}\right) := \left|\mathbb{E}f(X_T) - \mathbb{E}f\left(\hat{Y}_N\right)\right|$, where

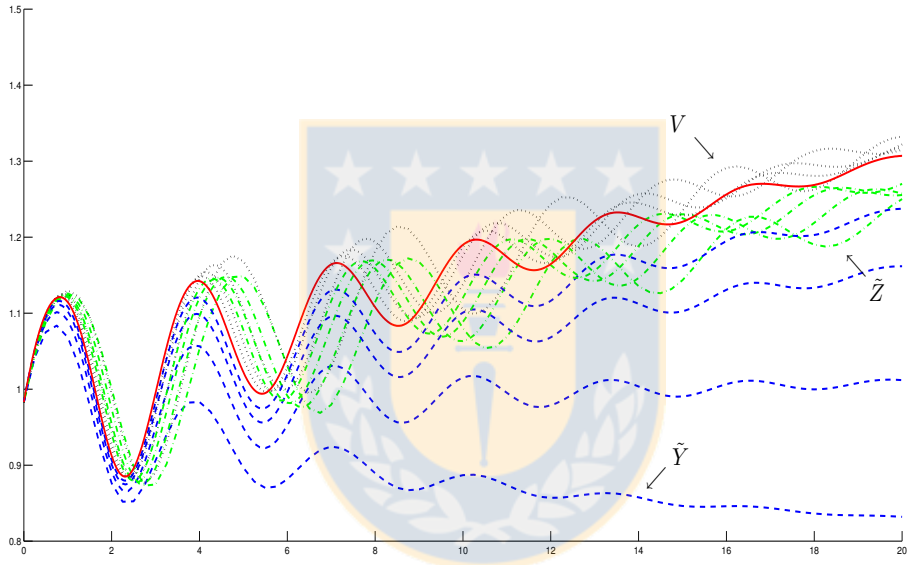

Figure 2.3: Computation of $\mathbb{E}\arctan\left(1+\left(X_t^2\right)^2\right)$, where $t \in [0, 20]$ and X_t solves (2.21). Dashed line: $\widetilde{Y}$, dashdot line: $\widetilde{Z}$, dotted line: V, and solid line: reference values. Here, Δ takes the values 1/4, 1/8, 1/16 and 1/32; smaller values of Δ produce better approximations.

$T = 10, 20$, $N = T/\Delta$, and $\hat{Y}$ stands for the schemes V_n, $\widetilde{Y}_n$ and $\widetilde{Z}_n$. Figure 2.3 and Table 2.5 show the good accuracy of the new scheme V_n. We also see that V_n and $\widetilde{Z}_n$ reply the unstable behavior of the exact solution and that $\widetilde{Y}_n$ tends to 0 in case $\Delta = 1/4$. Finally, we have checked that the performance of the heuristic scheme Y_n^s is similar to that of the backward Euler scheme $\widetilde{Y}_n$.

		Δ					
		1/4	1/8	1/16	1/32	1/64	1/128
$\epsilon\left(\widetilde{Y}\right)$	$T = 10$	0.30305	0.17473	0.089215	0.04452	0.022189	0.011144
	$T = 20$	0.47504	0.29513	0.14533	0.069623	0.033923	0.016778
$\epsilon\left(\widetilde{Z}\right)$	$T = 10$	0.10986	0.12667	0.10127	0.069549	0.044963	0.028632
	$T = 20$	0.056883	0.049722	0.051519	0.036835	0.022017	0.0127
$\epsilon(V)$	$T = 10$	0.084783	0.051834	0.014313	0.0031168	0.00055984	0.00011417
	$T = 20$	0.025462	0.0080347	0.014935	0.011232	0.0062795	0.0032123

Table 2.5: Estimation of errors involved in the computation of $\mathbb{E}\arctan\left(1 + \left(X_T^2\right)^2\right)$ for $T = 10$ and $T = 20$, where $X_t = \left(X_t^1, X_t^2\right)^\top$ solves (2.21).

2.4 Proofs

Proof 2.4.1 (Proof of Lemma 2.2.1) *We first prove that under Property P1,* $\lim_{n\to\infty} Y_n^s = 0$ *a.s. iff*

$$a(\Delta) \in \begin{cases}]-\infty, p_3[& ; \; if \;\; \mu < 0 \\ \mathbb{R} & ; \; if \;\; \mu = 0 \;\; and \;\; \lambda \neq 0 \\ ]p_3, +\infty[& ; \; if \;\; \mu > 0 \end{cases} . \tag{2.22}$$

Suppose that Property P1 holds. Applying the strong law of large numbers and the law of iterated logarithm we obtain that $Y_n^s \to 0$ *a.s. as* $n \to \infty$ *iff*

$$\mathbb{E}\log\left(1 + \left(\mu\Delta + \lambda\sqrt{\Delta}\xi_n^1\right) / \left(1 - a(\Delta)\Delta\right)\right) < 0 \tag{2.23}$$

(see e.g. Lemma 5.1 *of [99]). Since*

$$\mathbb{E}\log\left(1 + \frac{\mu\Delta + \lambda\sqrt{\Delta}\xi_n^1}{1 - a(\Delta)\Delta}\right) = \frac{1}{2}\log\left(\left(1 + \frac{\mu\Delta}{1 - a(\Delta)\Delta}\right)^2 - \frac{\lambda^2\Delta}{(1 - a(\Delta)\Delta)^2}\right),$$

inequality (2.23) *becomes* $2\mu(1 - a(\Delta)\Delta) + \mu^2\Delta - \lambda^2 < 0$, *which is equivalent to* (2.22). *This establishes our first claim.*

From the assertion of the first paragraph we get that Property P1, together with $\lim_{n\to\infty} Y_n^s = 0$ *a.s., is equivalent to (a)* $a(\Delta) \in]-\infty, \min\{p_1, p_3\}[\cup]p_2, p_3[$ *for* $\mu < 0$*; (b)* $a(\Delta) \in]-\infty, p_1[\cup]p_2, +\infty[$

for $\mu = 0$ and $\lambda \neq 0$; and $a(\Delta) \in]p_3, p_1[\cup]\max\{p_2, p_3\}, +\infty[$ for $\mu > 0$. This gives the lemma, because $p_1 < p_3$ (resp. $p_2 > p_3$) whenever $\mu < 0$ (resp. $\mu > 0$).

Proof 2.4.2 (Proof of Theorem 2.2.1) *In case $\lambda \neq 0$, using differential calculus we obtain that the function $\Delta \mapsto \left(1 - |\lambda|\sqrt{\Delta} + \mu\Delta\right)/\Delta$ attains its global minimum at $4/\lambda^2$. Then, for all $\Delta > 0$ and $\lambda \in \mathbb{R}$ we have*

$$\left(1 - |\lambda|\sqrt{\Delta} + \mu\Delta\right)/\Delta \geq \mu - \lambda^2/4. \tag{2.24}$$

First, we suppose that $\mu \leq 0$ and $\alpha_1(\Delta) > 1/4$. From (2.24) it follows that $p_1 > \mu - \alpha_1(\Delta)\lambda^2$, which implies $a(\Delta) \in]-\infty, p_1[$. Second, if $\mu > 0$ and $\Delta \geq 2/\mu$, then $a(\Delta) \in]p_2, +\infty[$. Third, assume that $\mu > 0$ and $\Delta < 2/\mu$. Since $\mu > 0$, for any $\Delta < \lambda^2/\mu^2$ we have $1 - |\lambda|\sqrt{\Delta} + \mu\Delta < 1$. Using $2\mu - \lambda^2 < 0$ we get $\lambda^2/\mu^2 > 2/\mu$, and so $p_1 = \left(1 - |\lambda|\sqrt{\Delta} + \mu\Delta\right)/\Delta$ whenever $\Delta < 2/\mu$. Applying (2.24) gives $p_1 > \mu - \alpha_2(\Delta)\lambda^2$, because $\alpha_2(\Delta) > 1/4$. On the other hand, we have $p_3 < \mu - \alpha_2(\Delta)\lambda^2$ if and only if $2\mu - \lambda^2 < \mu\Delta\left(2\mu - 4\alpha_2(\Delta)\lambda^2\right)/2$, which becomes

$$\frac{2}{\mu} > \Delta\left(1 + (4\alpha_2(\Delta) - 1)\frac{\lambda^2}{\lambda^2 - 2\mu}\right) \tag{2.25}$$

since $2\mu - \lambda^2 < 0$ and $\mu > 0$. By $2/\mu > \Delta$, (2.25) holds in case

$$\frac{2}{\mu} \geq \Delta + (4\alpha_2(\Delta) - 1)\frac{\lambda^2}{\lambda^2 - 2\mu}\frac{2}{\mu},$$

which is equivalent to $\alpha_2(\Delta) \leq 1/4 + \left(\lambda^2 - 2\mu\right)(2 - \mu\Delta)/\left(8\lambda^2\right)$. Then $p_3 < \mu - \alpha_2(\Delta)\lambda^2$, hence $a(\Delta) \in]p_3, p_1[$.

Combining Lemma 2.2.1 with the above three cases yields Properties P1 and P2.

Proof 2.4.3 (Proof of the inequality (2.8)) *If $\mu \leq 0$, then $a(\Delta) \leq \mu - \lambda^2/4 \leq 0$, and so $1 - a(\Delta)\Delta \geq 1$. Let $\mu > 0$, together with $\Delta \geq 2/\mu$. Then we have $1 - a(\Delta)\Delta = -|\lambda|\sqrt{\Delta} - \mu\Delta - \beta\Delta \leq -2$.*

Finally, suppose that $\mu > 0$ and $\Delta < 2/\mu$. Since $2\mu - \lambda^2 < 0$, there exists $\epsilon \in (0, 1)$ such that $2\mu - \lambda^2 < -2\epsilon\mu$. Hence $\mu - \lambda^2/4 < (1 - \epsilon)\mu/2 < (1 - \epsilon)/\Delta$, which implies

$$\left(\mu - \frac{1 - \epsilon}{\Delta}\right)\frac{1}{\lambda^2} < \frac{1}{4} < \alpha_2(\Delta).$$

We thus get $1 - a(\Delta)\Delta > \epsilon$.

Proof 2.4.4 (Proof of Theorem 2.2.2) *We first prove that Properties P1' and P2' hold provided that $2\mu - \lambda^2 < 0$ and*

$$a < \min\left\{1/\Delta, \mu/2 - \lambda^2/4 + \left(2 - |\lambda|\sqrt{\Delta}\right)/2\Delta\right\}. \tag{2.26}$$

From (2.26) we have $4 + \left(2\mu - \lambda^2 - 4a\right)\Delta - 2|\lambda|\sqrt{\Delta} > 0$, and so for all $\Delta > 0$,

$$4 + \left(2\mu - \lambda^2 - 4a\right)\Delta + 2\lambda\sqrt{\Delta}\xi_n^1 > 0.$$

Since $2\mu-\lambda^2<0$, $4-\left(2\mu-\lambda^2+4a\right)\Delta-2\left|\lambda\right|\sqrt{\Delta}>0$. *Hence, for any* $\Delta>0$, $4-\left(2\mu-\lambda^2+4a\right)\Delta-2\lambda\sqrt{\Delta}\xi_n^1>0$. *Therefore* Y_n^T *satisfies Property P1'. Moreover, as in the proof of Lemma 2.2.1, using the strong law of large numbers and the law of iterated logarithm we deduce that* $Y_n^T\to 0$ *a.s. as* $n\to\infty$ *iff*

$$\mathbb{E}\log\left(\frac{4+\left(2\mu-\lambda^2-4a\right)\Delta+2\lambda\sqrt{\Delta}\xi_n^1}{4-\left(2\mu-\lambda^2+4a\right)\Delta-2\lambda\sqrt{\Delta}\xi_n^1}\right)<0. \tag{2.27}$$

Inequality (2.27) *is equivalent to*

$$\left(4+\left(2\mu-\lambda^2-4a\right)\Delta\right)^2-4\lambda^2\Delta<\left(4-\left(2\mu-\lambda^2+4a\right)\Delta\right)^2-4\lambda^2\Delta,$$

which becomes $16\left(2\mu-\lambda^2\right)\Delta\left(1-a\Delta\right)<0$, *and so Property P2' holds because* $a<1/\Delta$.

Consider $\lambda=0$. *Then, the claim of the first paragraph guarantees that Properties P1' and P2' holds if* $a<\min\left\{1/\Delta,\mu/2+1/\Delta\right\}$. *Since* $2\mu-\lambda^2<0$ *we have* $\mu<0$, *and so a sufficient condition for Properties P1' and P2' is* $a<\mu/2$.

Finally, suppose that $\lambda\neq 0$ *and set* $f\left(\Delta\right)=\left(2-\left|\lambda\right|\sqrt{\Delta}\right)/2\Delta$ *for all* $\Delta>0$. *Then, we get* $f'\left(\Delta\right)=\left(\left|\lambda\right|/4-1/\sqrt{\Delta}\right)/\Delta^{3/2}$. *Note that* f *is increasing or decreasing depending on* $\sqrt{\Delta}>4/\left|\lambda\right|$ *or* $\sqrt{\Delta}<4/\left|\lambda\right|$, *respectively. Thus,* f *attains its global minimum at* $\Delta_0=16/\lambda^2$. *Since* $2\mu-\lambda^2<0$, *we have* $\mu/2-\lambda^2/4+f\left(\Delta_0\right)=\mu/2-5\lambda^2/16<0$. *Then,* $\mu/2-5\lambda^2/16\leq\min\left\{1/\Delta,\mu/2-\lambda^2/4+f\left(\Delta\right)\right\}$. *Using again the claim of the first paragraph we conclude that Properties P1' and P2' holds under* $a<\mu/2-5\lambda^2/16$.

Proof 2.4.5 (Proof of Theorem 2.3.1) *From* (2.14) *it follows that*

$$V_n=A_{n-1}\left(\Delta,M\left(\Delta\right)\right)A_{n-2}\left(\Delta,M\left(\Delta\right)\right)\cdots A_0\left(\Delta,M\left(\Delta\right)\right)V_0.$$

Since ξ_n^k *are bounded random variables,*

$$\sup_{x\in\mathbb{R}^d,\|x\|=1}\mathbb{E}\log_+\left\|A_0\left(\Delta,M\left(\Delta\right)\right)x\right\|<\infty,$$

where $\log_+\left(x\right)$ *stands for the positive part of* $\log\left(x\right)$ *for each* $x>0$. *Hence, the limit*

$$\lim_{n\to\infty}\frac{1}{n}\log\left\|V_n\right\|$$

exists whenever $V_0\neq 0$, *and only depending on* V_0. *Furthermore,*

$$\lim_{n\to\infty}\frac{1}{n}\log\left\|V_n\right\|=\int_{x\in\mathbb{R}^d,\|x\|=1}\mathbb{E}\log\left\|A_0\left(\Delta,M\left(\Delta\right)\right)x\right\|\mu\left(dx\right),$$

where μ *is a probability measure (see e.g. Theorem* 3.1 *of [62]). This gives* (2.15).

Proof 2.4.6 (Proof of Theorem 2.3.2) *Let* $q\geq 2$. *Iterating* (2.14) *we obtain*

$$V_{n+1}=V_0+\left(I+\Delta M\left(\Delta\right)\right)\left(\Delta B\sum_{k=0}^{n}V_k+\sum_{j=1}^{m}\sum_{k=0}^{n}\sqrt{\Delta}\xi_k^j\sigma^jV_k\right).$$

Since $\Delta \to M(\Delta)$ *is locally bounded,*

$$\|V_{n+1}\|^q \leq K_q(T)\left(\|V_0\|^q + \frac{1}{N}\sum_{k=0}^{n}\|V_k\|^q + m^{q-1}\sum_{j=1}^{m}\left\|\sum_{k=0}^{n}\sqrt{\Delta}\xi_k^j\sigma^j V_k\right\|^q\right),$$

where, from now on, $K_q(\cdot)$ *is a generic positive increasing function. By* ξ_k^j *is bounded, applying the Burkholder-Davis-Gundy inequality yields*

$$\mathbb{E}\|V_{n+1}\|^q \leq K_q(T)\left(\|V_0\|^q + \frac{1}{N}\sum_{k=0}^{n}\|V_k\|^q\right),$$

and so using a discrete Gronwall lemma (see e.g. [10]) we get

$$\mathbb{E}\|V_n\|^q \leq K_q(T)\,\mathbb{E}\|V_0\|^q \qquad \forall n = 0,\ldots,N. \tag{2.28}$$

According to (2.14) *we have*

$$V_{n+1} - V_n = (I + \Delta M(\Delta))\left(\Delta B + \sum_{k=1}^{m}\sqrt{\Delta}\xi_n^k\sigma^k\right)V_n. \tag{2.29}$$

Hence $\|V_{n+1} - V_n\| \leq K(T)\Delta^{1/2}\|V_n\|$, *which implies*

$$\mathbb{E}\left(\|V_{n+1} - V_n\|^q \diagup \mathcal{F}_{T_n}\right) \leq K_q(T)\Delta^{q/2}\|V_n\|^q. \tag{2.30}$$

From (2.29) *it follows*

$$\left\|\mathbb{E}\left(V_{n+1} - V_n - \left(B\Delta + \sum_{k=1}^{m}\sigma^k\left(W^k_{(n+1)\Delta} - W^k_{n\Delta}\right)\right)V_n \diagup \mathcal{F}_{n\Delta}\right)\right\|$$
$$\leq K(T)\Delta^2(1 + \|V_n\|).$$

Moreover, using (2.29) *we deduce that the second (resp., third) moments of* $V_{n+1} - V_n$ *coincide with that of* $\left(B\Delta + \sum_{k=1}^{m}\sigma^k\left(W^k_{(n+1)\Delta} - W^k_{n\Delta}\right)\right)V_n$, *except for terms of order* $\mathcal{O}(\Delta^2)\|V_n\|^2$ *(resp.,* $\mathcal{O}(\Delta^2)\|V_n\|^3$*). Here,* $\mathcal{O}(\Delta^2)$ *stands for different random functions depending on* Δ^2 *that are less than* $K(T)\Delta^2$*. Therefore, combining classical arguments [146, 196, 197] with* (2.28) *and* (2.30) *we conclude that* (2.18) *holds (see also Theorem* 14.5.2 *of [120]).*

Chapter 3

Stable numerical methods for nonlinear scalar and linear systems of SDEs

Uniqueness up to indistinguishable ability

We propose a new methodology for solving bilinear systems of stochastic differential equations (SDEs), which allows us to design first order weak numerical schemes that preserve for any step-size the almost sure exponential stability of the unknown exact solutions, under general conditions. Moreover, the new numerical methods also keep intact the possible property of being distant from the origin. To achieve our main goal, we develop a new stable method for non-linear scalar SDEs. The good performance of the new schemes is illustrated by some numerical experiments.

3.1 Introduction

This chapter addresses the numerical solution of stiff stochastic differential equations (SDEs) with multiplicative noise, namely, SDEs of the form

$$X_t = X_0 + \int_0^t b\left(X_s\right) ds + \sum_{k=1}^{m} \int_0^t \sigma^k\left(X_s\right) dW_s^k \tag{3.1}$$

whose numerical integrations by the Euler-Maruyama scheme exhibit incorrect behaviors. Here, $W^1, \ldots, W^m$ are independent real valued Wiener processes on a filtered complete probability space $\left(\Omega, \mathcal{F}, (\mathcal{F}_t)_{t\geq 0}, \mathbb{P}\right)$, X_t is an adapted $\mathbb{R}^d$-valued stochastic process, and $b, \sigma^k : \mathbb{R}^d \to \mathbb{R}^d$ are smooth. More precisely, we introduce a new methodology to design almost sure exponentially stable schemes for bilinear SDEs (i.e. b and σ^k are linear). To this end, we first develop a promising numerical method for nonlinear scalar SDEs (i.e. $d = 1$).

3.1.1 Previous works

In many cases, the semi-implicit and explicit Euler methods preserve the dynamical properties of the underlying SDEs provided that the step size $\Delta > 0$ of the discretization is small enough (see [102]).

This does not prevent that the classical Euler schemes have poor numerical performance in situations where, for example, some partial derivatives of the diffusion coefficients σ^k are not small. A simple model problem for such SDEs is

$$dX_t = \lambda X_t dW_t^1, \tag{3.2}$$

with $\lambda > 0$ (see e.g. [148, 149]); the trajectories of the Euler-Maruyama method applied to (3.2) blow up unless Δ is very small. Using (3.2) as a motivational problem, Milstein, Platen and Schurz (1998) [148] introduced the general formulation of the balanced implicit methods, a class of fully implicit schemes for (3.1) whose implementation depends on the choice of certain weights (see e.g. [4, 99, 148]). The reported balanced schemes present good asymptotic stability properties, but exhibit low speed of weak convergence (except incipient progress achieved by [155]).

Other implicit integrators for (3.1), together with their predictor-corrector versions, arise from the Itô-Taylor expansions of X_t (see e.g. [46, 47, 149, 175, 176, 182]). In particular, Kloeden and Platen (1992) [120] proposed a class of weak implicit schemes that includes, for instance, the trapezoidal method and the following scheme applied to (3.2): $\tilde{E}_{n+1} = \tilde{E}_n + \left(1 - \lambda^2\Delta + \lambda\sqrt{\Delta}\xi_n^1\right)\tilde{E}_{n+1}$, where $\xi_0^1, \xi_1^1, \ldots$ is a sequence of independent random variables taking values ± 1 with probability $1/2$. The trapezoidal method has good asymptotic stability properties, nevertheless it fails to preserve the sign of X_0 in the numerical solution of (3.2). The implicit method $\tilde{E}_n$ is almost sure asymptotically stable, but converges to 0 as $n \to \infty$ too much faster than X_t.

Numerical methods adapted to specific types of SDEs with multiplicative noise have been developed, for instance, in [6, 16, 27, 149, 153, 159]. The numerical integration of mean-square stable SDEs has been treated, for example, in [1, 30, 43, 99, 152].

3.1.2 Outline

To the best of our knowledge, this is the first time to present numerical methods for SDEs that preserve, for any step size $\Delta > 0$, the almost sure asymptotic stability of the solutions of relevant classes of SDEs (see e.g. [98, 102] and Thm. 3.5 of [184]).

Section 3.2 is devoted to (2.1) with $d = 1$. Indeed, we develop a new numerical method that, under general hypotheses, keeps intact the almost sure exponential stability of X_t (i.e. the property $\limsup_{t\to\infty} (\log |X_t|)/t < 0$) for all $\Delta > 0$, as well as the sign of X_0. This paves the way for the main objective of this chapter: to provide stable schemes for computing the mean value of $f(X_t)$, where $f : \mathbb{R}^d \to \mathbb{R}$ is smooth, and, by abuse of notation,

$$X_t = X_0 + \int_0^t BX_s ds + \sum_{k=1}^m \int_0^t \sigma^k X_s dW_s^k, \tag{3.3}$$

with $B, \sigma^1, \ldots, \sigma^m$ real matrices of dimension $d \times d$ and $X_0 \in \mathbb{R}^d \setminus \{0\}$. In addition to the fact that (3.3) is a good test problem for the numerical solution of SDEs with multiplicative noise (see e.g. [43, 100, 198]), using stable schemes for (3.3) we can design numerical methods for (2.1) via the local linearization method (see e.g. [30, 49, 71, 153, 154]). Moreover, the bilinear SDE (3.3) arises, for example, from the spatial discretization of some stochastic partial differential equations (see e.g. [1, 44]), and describes important dynamical features of non-linear SDEs by means of the linearization around their equilibrium points (see e.g. [18, 19, 198]).

Section 3.3 presents a new technique for constructing almost sure stable methods for (3.3). We take advantage of $\|X_t\|$ and $\hat{X}_t := X_t/\|X_t\|$ are described by the SDEs (3.23) and (3.21) given below. Indeed, we propose to compute $X_t = \|X_t\|\,\hat{X}_t$ by solving this coupled system of two SDEs. Essentially, we first approximate $\hat{X}_t$ by an adapted stochastic process taking values in the unit sphere that solves numerically (3.23), and then we compute $\|X_t\|$ by means of schemes that preserve the dynamical properties of (3.21). Using this idea, we obtain a set of weak numerical schemes for (3.3) that are almost sure exponentially stable under classical conditions that guarantee the almost sure exponential stability of X_t. Moreover, the new integrators for (3.3) preserve the property of being distant from 0, under general hypotheses. Sections 3.2 and 3.3 also contain numerical experiments that illustrate the very good numerical performance of the new schemes.

3.1.3 Notation

For simplicity, we consider the equidistant time discretization $T_j = j\Delta$, where $\Delta > 0$ and $j = 0, 1, \ldots$ We will use the same symbol $K(\cdot)$ (resp. K) for different positive increasing functions (resp. positive real numbers) having the common property to be independent of Δ. Similarly, q denotes generic constants greater than or equal to 2. We write $\mathcal{C}_p^{\ell}(\mathbb{R}^d, \mathbb{R})$ for the set of all ℓ-times continuously differentiable functions $f : \mathbb{R}^d \to \mathbb{R}$ such that f and all its partial derivatives of orders $1, 2, \ldots, \ell$ have at most polynomial growth.

3.2 One-dimensional SDEs

In this section, we restrict our attention to stiff scalar SDEs, that is, we focus on

$$X_t = X_0 + \int_0^t b(X_s)\,ds + \sum_{k=1}^{m} \int_0^t \sigma^k(X_s)\,dW_s^k, \tag{3.4}$$

where $X_0 \in L^2(\Omega, \mathbb{P})$ and $b, \sigma^k : \mathbb{R} \to \mathbb{R}$ are continuously differentiable functions. We suppose that (3.4) has a unique global solution (see e.g. [108, 181] for sufficient conditions).

In this section we use two general methods: the weak version of a Balanced implicit scheme applied to (3.4) (see Schurz [184], Alcock and Burrage [4])

$$\begin{aligned} B_{n+1} = B_n + b(B_n)\,\Delta + \sum_{k=1}^{m} \sigma^k(B_n)\sqrt{\Delta}\xi_n^k \\ + \left(-\frac{1}{2}\nabla b(B_n) + \sum_{k=1}^{m} \left(\left[\nabla \sigma^k(B_n)\right]_+ + \left[\nabla \sigma^k(B_n)\right]_- \right)\sqrt{\Delta} \right)(B_n - B_{n+1}), \end{aligned}$$

where $[\cdot]_+$ and $[\cdot]_-$ represent the positive semidefinite and negative semidefinite parts, respectively. Additionally, the weak version of the Tamed Euler scheme applied to (3.4) (see Hutzenthaler, Jentzen and Kloeden 2012 [107])

$$\hat{E}_{n+1} = \hat{E}_n + \frac{b\left(\hat{E}_n\right)}{1 + \left\|b\left(\hat{E}_n\right)\right\|\Delta}\Delta + \sum_{k=1}^{m} \sigma^k\left(\hat{E}_n\right)\sqrt{\Delta}\xi_n^k.$$

3.2.1 Derivation of the numerical method

We begin by assuming $b(0) = \sigma^k(0) = 0$. Then, the coefficients $\mu(x) = \begin{cases} b(x)/x & \text{if } x \neq 0 \\ b'(0) & \text{if } x = 0 \end{cases}$, and $\lambda^k(x) = \begin{cases} \sigma^k(x)/x & \text{if } x \neq 0 \\ (\sigma^k)'(0) & \text{if } x = 0 \end{cases}$, are smooth bounded functions (see Remark 3.2.3). Let $\bar{X}_n$ be an $\mathcal{F}_{T_n}$-measurable random variable such that $\bar{X}_n \approx X_{T_n}$. Since we can efficiently compute $\mu(x)$ and $\lambda^k(x)$ (see Remark 3.2.3), we locally rewrite (3.4) as

$$X_t = X_{T_n} + \int_{T_n}^t \mu(X_s) X_s ds + \sum_{k=1}^m \int_{T_n}^t \lambda^k(X_s) X_s dW_s^k \qquad \forall t \in [T_n, T_{n+1}],$$

and so the continuity of μ and λ^k leads to

$$X_t \approx \bar{X}_n + \int_{T_n}^t \mu(\bar{X}_n) X_s ds + \sum_{k=1}^m \int_{T_n}^t \lambda^k(\bar{X}_n) X_s dW_s^k \qquad \forall t \in [T_n, T_{n+1}].$$

Hence X_t, with $t \in [T_n, T_{n+1}]$, is approximated by the explicit solution of

$$Y_t = \bar{X}_n + \int_{T_n}^t \mu(\bar{X}_n) Y_s ds + \sum_{k=1}^m \int_{T_n}^t \lambda^k(\bar{X}_n) Y_s dW_s^k. \tag{3.5}$$

This gives $X_{T_{n+1}} \approx Y_{T_{n+1}}$. Replacing $W^k_{T_{n+1}} - W^k_{T_n}$ by random variables with similar laws in the closed formula of the exact solution of (3.5), we introduce the following weak approximation of $X_{T_{n+1}}$:

Scheme 3.2.1 *Suppose that $\hat{W}_0^1, \hat{W}_0^2, \ldots, \hat{W}_0^m, \hat{W}_1^1, \ldots$ are independent and identically distributed (i.i.d.) random variables with symmetric law and variance 1. Set*

$$\bar{X}_{n+1} = \exp\left(\left(\mu(\bar{X}_n) - \frac{1}{2}\sum_{k=1}^m \lambda^k(\bar{X}_n)^2\right)\Delta + \sum_{k=1}^m \lambda^k(\bar{X}_n)\sqrt{\Delta}\hat{W}_n^k\right)\bar{X}_n.$$

The Scheme 3.2.1 keeps intact the sign of the initial data. Next, we establish that $\bar{X}_n$ is almost sure exponentially stable for any $\Delta > 0$ provided that a standard condition for the almost sure exponential stability of X_t holds (see e.g. [102, 138]).

Theorem 3.2.1 *Suppose that $b(0) = 0$, $|\sigma^k(x)| \leq K|x|$ for all $x \in \mathbb{R}$, and*

$$-\lambda := \sup_{x \in \mathbb{R}, x \neq 0} \left(b(x)/x - \sum_{k=1}^m \left(\sigma^k(x)/x\right)^2/2\right) < 0. \tag{3.6}$$

Let $\left(\bar{X}_n\right)_{n \geq 0}$ be given by Scheme 3.2.1 with $\mathbb{E}\left(\bar{X}_0\right)^2 < \infty$ and $\bar{X}_0 \neq 0$ a.s. Then

$$\limsup_{n \to \infty} \frac{1}{n\Delta} \log\left|\bar{X}_n\right| \leq -\lambda \qquad \mathbb{P} - a.s. \tag{3.7}$$

Proof 3.2.1 *Deferred to Section 3.2.3.*

Remark 3.2.1 *Assume the hypotheses of Theorem 3.2.1 with* (3.6) *replaced by the existence of* $\theta > 0$ *such that* $b(x)/x - (1/2+\theta)\sum_{k=1}^{m}\left(\sigma^k(x)/x\right)^2 \geq 0$ *for all* $x \neq 0$. *Then, an analysis similar to that in the proof of Theorem 3.3.3 below shows* $\liminf_{n\to\infty}\left|\bar{X}_n\right| > 0$ *a.s.*

Scheme 3.2.1 retains important dynamical properties of the solution of (3.4), as well as achieves a high performance in our numerical tests. This motivates us to adapt $\bar{X}_n$ to the framework where $b(0), \sigma^1(0), \ldots, \sigma^m(0)$ are not necessarily equal to 0. To this end, we rewrite (3.4) in $[T_n, T_{n+1}]$ as

$$X_t = X_{T_n} + \int_{T_n}^{t}\left(\mu(X_s)X_s + b(0)\right)ds + \sum_{k=1}^{m}\int_{T_n}^{t}\left(\lambda^k(X_s)X_s + \sigma^k(0)\right)dW_s^k,$$

with $\mu(x) = \begin{cases} (b(x)-b(0))/x & \text{if } x \neq 0 \\ b'(0) & \text{if } x = 0 \end{cases}$, $\lambda^k(x) = \begin{cases} \left(\sigma^k(x)-\sigma^k(0)\right)/x & \text{if } x \neq 0 \\ \left(\sigma^k\right)'(0) & \text{if } x = 0 \end{cases}$. If $\bar{X}_n$ is an $\mathcal{F}_{T_n}$-measurable random variable approximating X_{T_n}, then

$$X_t \approx \bar{X}_n + \int_{T_n}^{t}\left(\mu\left(\bar{X}_n\right)X_s + b(0)\right)ds + \sum_{k=1}^{m}\int_{T_n}^{t}\left(\lambda^k\left(\bar{X}_n\right)X_s + \sigma^k(0)\right)dW_s^k.$$

This leads to locally approximate X_t in $[T_n, T_{n+1}]$ by the solution of

$$Y_t = \bar{X}_n + \int_{T_n}^{t}\left(\mu\left(\bar{X}_n\right)Y_s + b(0)\right)ds + \sum_{k=1}^{m}\int_{T_n}^{t}\left(\lambda^k\left(\bar{X}_n\right)Y_s + \sigma^k(0)\right)dW_s^k. \tag{3.8}$$

The explicit solution of (3.8) is

$$Y_t = \Phi_t\left(\bar{X}_n + \left(b(0) - \sum_{k=1}^{m}\lambda^k\left(\bar{X}_n\right)\sigma^k(0)\right)\int_{T_n}^{t}\Phi_s^{-1}ds + \sum_{k=1}^{m}\sigma^k(0)\int_{T_n}^{t}\Phi_s^{-1}dW_s^k\right),$$

with $\Phi_t = \exp\left(\left(\mu\left(\bar{X}_n\right) - \frac{1}{2}\sum_{k=1}^{m}\lambda^k\left(\bar{X}_n\right)^2\right)(t-T_n) + \sum_{k=1}^{m}\lambda^k\left(\bar{X}_n\right)\left(W_t^k - W_{T_n}^k\right)\right)$. Using $\Phi_s^{-1} \approx \Phi_{T_n}^{-1}$, for all $s \in [T_n, T_{n+1}]$, we get that $X_{T_{n+1}}$ is approximated by

$$\Phi_{T_{n+1}}\left(\bar{X}_n + \left(b(0) - \sum_{k=1}^{m}\lambda^k\left(\bar{X}_n\right)\sigma^k(0)\right)\Delta + \sum_{k=1}^{m}\sigma^k(0)\left(W_{T_{n+1}}^k - W_{T_n}^k\right)\right).$$

This yields the weak scheme:

Scheme 3.2.2 *Let* $\hat{W}_0^1, \hat{W}_0^2, \ldots, \hat{W}_0^m, \hat{W}_1^1, \ldots$ *be i.i.d. random variables with symmetric law and variance* 1. *Define recursively*

$$\bar{X}_{n+1} = \bar{\Phi}_{n+1}\left(\bar{X}_n + \left(b(0) - \sum_{k=1}^{m}\lambda^k\left(\bar{X}_n\right)\sigma^k(0)\right)\Delta + \sum_{k=1}^{m}\sigma^k(0)\sqrt{\Delta}\hat{W}_n^k\right),$$

where $\bar{\Phi}_{n+1} = \exp\left(\left(\mu\left(\bar{X}_n\right) - \frac{1}{2}\sum_{k=1}^{m}\lambda^k\left(\bar{X}_n\right)^2\right)\Delta + \sum_{k=1}^{m}\lambda^k\left(\bar{X}_n\right)\sqrt{\Delta}\hat{W}_n^k\right)$.

The following theorem establishes that $\bar{X}$ converges weakly to X with order $\mathcal{O}(\Delta)$ under a basic set of assumptions. In case $b(0) = \sigma^k(0) = 0$, the Scheme 3.2.2 becomes Scheme 3.2.1, and so the rate of weak convergence of Scheme 3.2.1 is equal to 1.

Theorem 3.2.2 *Let $b, \sigma^1, \ldots, \sigma^m$ be Lipschitz continuous functions belonging to $C_p^4(\mathbb{R}, \mathbb{R})$ such that $|b(x)| + |\sigma^1(x)| + \cdots + |\sigma^m(x)| \leq K(1 + |x|)$ for all $x \in \mathbb{R}$. Fix $T > 0$ and $f \in C_p^4(\mathbb{R}, \mathbb{R})$. Consider $\bar{X}_n$ as described by Scheme 3.2.2 with $\Delta = T/N$, where $N \in \mathbb{N}$. Assume that $\mathbb{E}\exp\left(r\hat{W}_n^k\right) < \infty$ for all $r > 0$, X_0 has finite moments of any order, and that for every $g \in C_p^4(\mathbb{R}, \mathbb{R})$, $\left|\mathbb{E}g(X_0) - \mathbb{E}g\left(\bar{X}_0\right)\right| \leq K(1 + \mathbb{E}|X_0|^q)\, T/N$ for all $N \in \mathbb{N}$. Then for all $N \in \mathbb{N}$,*

$$\left|\mathbb{E}f(X_T) - \mathbb{E}f\left(\bar{X}_N\right)\right| \leq K(T)(1 + \mathbb{E}|X_0|^q)\, T/N. \tag{3.9}$$

Proof 3.2.2 *Deferred to Section 3.2.3.*

Remark 3.2.2 *If $\hat{W}_n^k$ are standard Normal random variables, then $\mathbb{E}\exp\left(r\hat{W}_n^k\right) = \exp\left(r^2/2\right)$. In case $\hat{W}_n^k$ are bounded we also have $\mathbb{E}\exp\left(r\hat{W}_n^k\right) < \infty$.*

Remark 3.2.3 *Combining Leibniz's rule with Taylor's theorem we obtain that μ and λ^k are j-times differentiable whenever b and σ^k have derivatives of order $j+1$. Indeed, $\frac{d^j}{dx^j}\mu(0) = \frac{1}{j+1}\frac{d^{j+1}}{dx^{j+1}}b(0)$ and $\frac{d^j}{dx^j}\lambda^k(0) = \frac{1}{j+1}\frac{d^{j+1}}{dx^{j+1}}\sigma^k(0)$. This allows us to avoid the effect of round-off errors in the implementation of $\mu(x)$ and $\lambda^k(x)$, when x is near 0, by approximating $\mu(x)$ and $\lambda^k(x)$, with $x \approx 0$, by means of their truncated Taylor expansions around 0; a technique used successfully in our preliminary numerical experiments. Alternatively, we can interpolate μ and λ^k in a neighborhood of 0, or sometimes we can efficiently evaluate closed analytical expressions for μ and λ^k like in Subsection 3.2.2.*

3.2.2 Numerical experiments

A nonlinear SDE

Let us consider the nonlinear equation

$$X_t = 1 - \int_0^t 10\sin(10X_s)\,ds + \int_0^t 20\log\left(1+(X_s)^2\right)dW_s^1, \tag{3.10}$$

with $X_t \in \mathbb{R}$ and W^1 a real valued Wiener process. We numerically test the sign-preserving and exponential stability properties by computing the mean values of $f(X_t) = 100\left(\frac{\pi}{2} - \arctan(1000X_t + 100)\right)$ and $g(X_t) = \log\left(1+(X_t)^2\right)$. We get the reference values for $\mathbb{E}f(X_t)$ and $\mathbb{E}g(X_t)$ by averaging 10^6 observations of the weak Euler-Maruyama scheme $\bar{E}_n$ with $\Delta = 2^{-20} \approx 10^{-6}$, i.e.

$$\bar{E}_{n+1} = \bar{E}_n + b\left(\bar{E}_n\right)\Delta + \sigma^1\left(\bar{E}_n\right)\sqrt{\Delta}\xi_n^1,$$

where $b(x) = -10\sin(10x)$, $\sigma^1(x) = 20\log\left(1+x^2\right)$ and $\xi_0^1, \xi_1^1, \ldots$ are independent random variables taking the values ± 1 each with probability $1/2$.

Consider $\bar{X}_n$ described by Scheme 3.2.1 with $\hat{W}_n^k = \xi_n^k$, that is to say

$$\bar{X}_{n+1} = \bar{X}_n \exp\left(\left(\mu\left(\bar{X}_n\right) - \frac{1}{2}\lambda^1\left(\bar{X}_n\right)^2\right)\Delta + \lambda^1\left(\bar{X}_n\right)\sqrt{\Delta}\xi_n^1\right).$$

In the implementation of $\bar{X}_n$ we replace $\mu(x)$ and $\lambda^1(x)$ by

$$\mu(x) \approx \begin{cases} b(x)/x & ;\text{ if } |x| \geq \epsilon \\ b'(0) & ;\text{ if } |x| < \epsilon \end{cases} \quad \text{and } \lambda^1(x) \approx \begin{cases} \sigma^1(x)/x & ;\text{ if } |x| \geq \epsilon \\ \left(\sigma^1\right)'(0) & ;\text{ if } |x| < \epsilon \end{cases}, \tag{3.11}$$

with $\epsilon = 10^{-6}$. This avoids that the round-off errors damage the performance of $\bar{X}_n$. In preliminary calculations, we check that (3.11) essentially produces the same numerical results that the approximations obtained by using linear interpolations or Taylor approximations of $b(x)/x$ and $\sigma^1(x)/x$ when $|x| < \epsilon$.

Figures 3.1 and 3.2 compare the results obtained by Monte-Carlo estimations with 10^6 trajectories of $\bar{X}_n$, $\bar{E}_n$ and the weak Balanced scheme

$$\bar{B}_{n+1} = \bar{B}_n + b\left(\bar{B}_n\right)\Delta + \sigma^1\left(\bar{B}_n\right)\sqrt{\Delta}\xi_n^1 - \left(b'\left(\bar{B}_n\right)\Delta/2 - \left|\left(\sigma^1\right)'\left(\bar{B}_n\right)\right|\sqrt{\Delta}\right)\left(\bar{B}_n - \bar{B}_{n+1}\right)$$

(see e.g. [4, 184]). We can see in both figures that the behavior of Scheme 3.2.1 is not affected by round-off errors. For all $\Delta > 0$, $\bar{X}_n$ preserves the sign of X_0. In contrast, $\bar{B}_n$ and $\bar{E}_n$ need to use discretization steps less than or equal to $\Delta = 2^{-7}$ and $\Delta = 2^{-8}$, respectively, to guarantee the sign-preserving property of the initial condition (see Figure 3.1). Figure 3.2 shows the estimations of $\mathbb{E}g(X_t)$ when $\Delta = 2^{-6}, 2^{-7}$ and 2^{-8}. As we expected, the numerical schemes gives us better results as $\Delta > 0$ decreases.

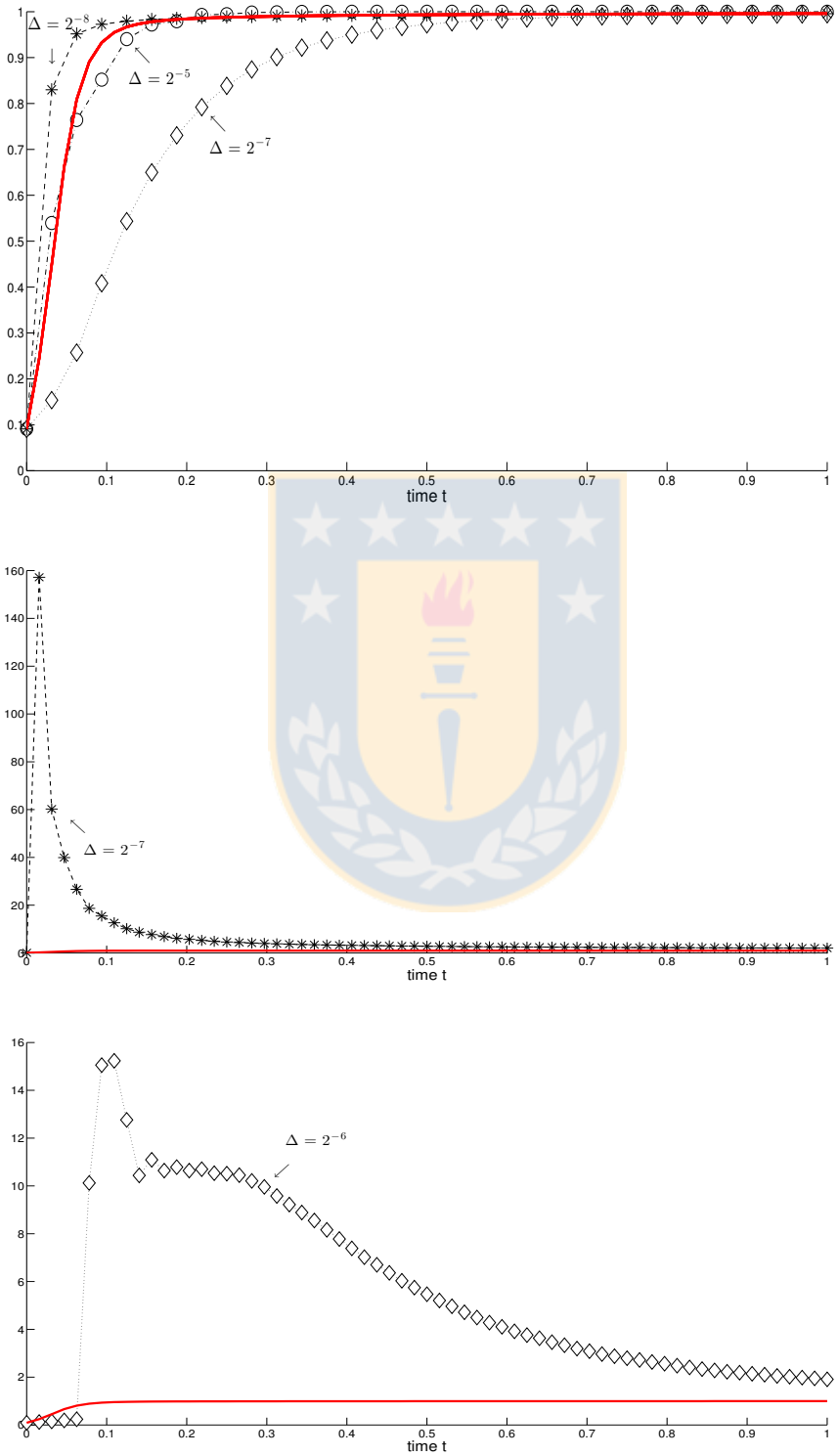

Figure 3.1: Approximation of $\mathbb{E}f(X_t) = \mathbb{E}100(\pi/2 - \arctan(1000X_t + 100))$, where $t \in [0,1]$ and X_t satisfies (3.10). The "true" values are plotted with a solid line. The schemes $\bar{X}_n$, $\bar{E}_n$ and $\bar{B}_n$ are represented by circles, stars and diamonds, respectively.

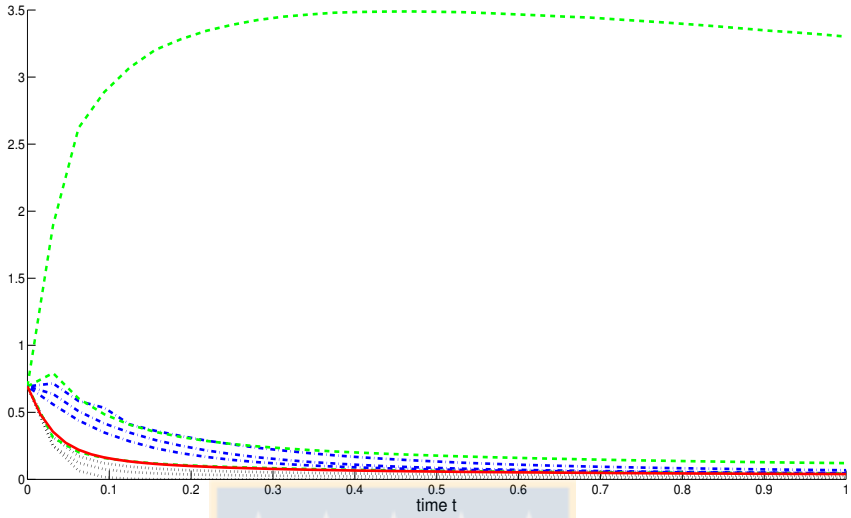

Figure 3.2: Computation of $\mathbb{E}g(X_t) = \mathbb{E}\log\left(1+(X_t)^2\right)$, where $t \in [0,1]$ and X_t satisfies (3.10). The "true" values are plotted with a solid line. The schemes $\bar{X}_n$, $\bar{E}_n$ and $\bar{B}_n$ are represented by black-dotted, green-dashed and blue-dashdot lines, respectively.

Locally Lipschitz SDE

We illustrate the behavior of Scheme 3.2.1 by means of the locally Lipschitz SDE

$$X_t = X_0 + \int_0^t \left(aX_s - b(X_s)^3\right) ds + \int_0^t \sigma X_s dW_s^1, \tag{3.12}$$

where b, σ are positive real numbers and $a \in \mathbb{R}$. This scalar cubic SDE is known as the stochastic Ginzburg-Landau equation, and constitutes a classical test equation in the theory of stochastic bifurcation (see e.g. [10, 19, 77, 104]). Let $\xi_0^1, \xi_1^1, \ldots$ be independent random variables taking the values ± 1 each with probability $1/2$. Then, we numerically solve (3.12) using five schemes: $\bar{X}_n$ given by Scheme 3.2.1 with $\hat{W}_n^1$ replaced by ξ_n^1, the backward Euler method

$$\bar{E}_{n+1} = \bar{E}_n + \left(a\bar{E}_{n+1} - b\left(\bar{E}_{n+1}\right)^3\right)\Delta + \sigma\bar{E}_n\sqrt{\Delta}\xi_n^1,$$

the weak version of the Balanced scheme proposed by Schurz (2005) [184] (see also Alcock and Burrage (2006) [4])

$$B_{n+1} = B_n + \left(aB_n - b(B_n)^3\right)\Delta + \sigma B_n\sqrt{\Delta}\xi_n^1 + \left(-\frac{1}{2}\left(a - 3b(B_n)^2\right)\Delta + \sigma\sqrt{\Delta}\right)(B_n - B_{n+1}),$$

$$\begin{cases} \tilde{Z}_{n+1/2}^s = \tilde{Z}_n^s \exp\left(\left(a - \sigma^2/2\right)\Delta + \sigma\sqrt{\Delta}\xi_n^1\right) \\ \tilde{Z}_{n+1}^s = \tilde{Z}_{n+1/2}^s \left(1 - b\Delta\left(\tilde{Z}_{n+1/2}^s\right)^2/2\right) / \left(1 + b\Delta\left(\tilde{Z}_{n+1/2}^s\right)^2/2\right) \end{cases}$$

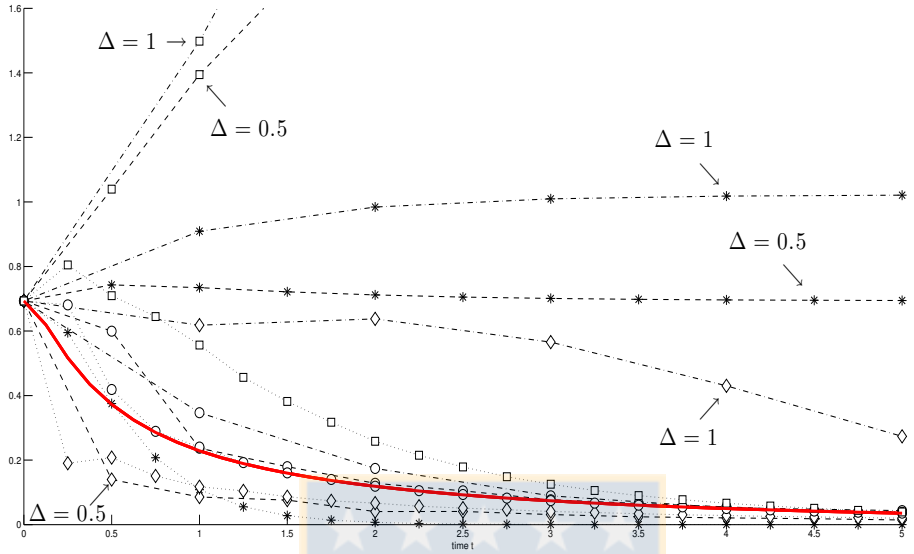

Figure 3.3: Computation of $\mathbb{E}\log\left(1+(X_t)^2\right)$, where $t\in[0,5]$ and X_t satisfies (3.12) with $a=b=1$, $\sigma=2$ and $X_0=1$. The "true" values are plotted with a solid line. The circles, stars, diamonds and squares stand for the schemes $\bar{X}_n$, $\bar{E}_n$, $\tilde{Z}_n^s$ and $\hat{E}_n$, respectively. The step sizes 1, 0.5 and 0.25 are represented by dashdot, dashed and dotted lines, respectively.

and

$$\hat{E}_{n+1}=\hat{E}_n+\left(a\hat{E}_n-b\left(\hat{E}_n\right)^3\right)\Delta/\left(1+\Delta\left|a\hat{E}_n-b\left(\hat{E}_n\right)^3\right|\right)+\sigma\hat{E}_n\sqrt{\Delta}\xi_n^1.$$

It is worth pointing out that $\bar{E}_n$ entails the solution of a nonlinear equation at each step, the scheme $\tilde{Z}_n^s$ is a weak version of the splitting-step algorithm for (3.12) introduced by Subsection 4.2 of [159], and that $\hat{E}_n$ is a weak version of the tamed Euler method proposed by Hutzenthaler, Jentzen and Kloeden (2012) [107].

Figures 3.3, 3.4 and Table 3.1 show the features of the computation of $\mathbb{E}\log\left(1+(X_t)^2\right)$ obtained from the sample means of 10^8 observations of Scheme 3.2.1, $\bar{E}_n$, B_n, $\tilde{Z}_n^s$ and $\hat{E}_n$. The solid lines identify the "true" values gotten by sampling 10^8 times $\bar{E}_n$ with $\Delta=2^{-11}\approx 0,000488$. The lengths of all the 99% confidence intervals are at least of order 10^{-3}, they have been estimated following [120].

First, we take $a=b=1$, $\sigma=2$ and $X_0=1$, which is the motivating example of [102]. Since $b(x)/x-\left(\sigma^1(x)/x\right)^2/2\leq -1$, $\limsup_{t\to\infty}\frac{1}{t}\log|X_t|\leq -1$ $a.s.$ From [102] we have that the Euler-Maruyama scheme applied to (3.12) blows up, with positive probability, at a geometric rate. In preliminary numerical experiments, we have seen that $\bar{E}_n$, $\tilde{Z}_n^s$ and $\hat{E}_n$ fail to preserve the sign of X_0 for $\Delta=1$ and $\Delta=0.5$ (even $\Delta=0.25$ for $\hat{E}_n$). To this end, we have computed $10\mathbb{E}\left(\pi/2-\arctan\left(10^3X_t+10^2\right)\right)$. Figure 3.3 presents the numerical solution of $\mathbb{E}\log\left(1+(X_t)^2\right)$,

where $t \in [0,5]$, using the step sizes $\Delta = 0.25, 0.5, 1$. It suggests us that Scheme 3.2.1 replicate very well the long time behavior of X_t, even for $\Delta = 1$. Moreover, we can see that the accuracy of $\bar{X}_n$ is very good, even for large step sizes; Scheme 3.2.1 achieves significantly lower errors than $\tilde{Z}_n^s$ and $\hat{E}_n$, which are methods adapted to the characteristics of (3.12).

Second, we choose $a = 6$, $b = 9$, $\sigma = 3$ and $X_0 = 1$. Then $\sup_{x\in\mathbb{R}, x\neq 0}\left(a - bx^2 - \sigma^2/2\right) > 0$, and so the condition (3.6) does not hold. In this case, (3.12) has three invariant forward Markov measures (see e.g. [10]). Calculating $10\mathbb{E}\left(\pi/2 - \arctan\left(10^3 X_t + 10^2\right)\right)$ we observe that $\bar{E}_n$ (resp. $\tilde{Z}_n^s$ and $\hat{E}_n$) can take negative values when $\Delta \geq 1/8$ (resp. $\Delta \geq 1/16$). Figure 3.4 displays the numerical approximation of $\mathbb{E}\log\left(1 + (X_t)^2\right)$ by means of Scheme 3.2.1 and $\bar{E}_n$ with step sizes $\Delta = 0.25$ and $\Delta = 0.0625$, as well as by using $\tilde{Z}_n^s$ and $\hat{E}_n$ with $\Delta = 0.0625$. Moreover, Table 3.1 shows errors made in the weak numerical integration of (3.12), where the reference value of $\mathbb{E}\log\left(1 + (X_{10})^2\right)$ was obtained by sampling 10^8 times $\bar{E}_n$ with $\Delta = 2^{-11}$. In this test problem, the new scheme $\bar{X}_n$ again provides very good approximations of $\mathbb{E}f(X_t)$, even for large values of Δ.

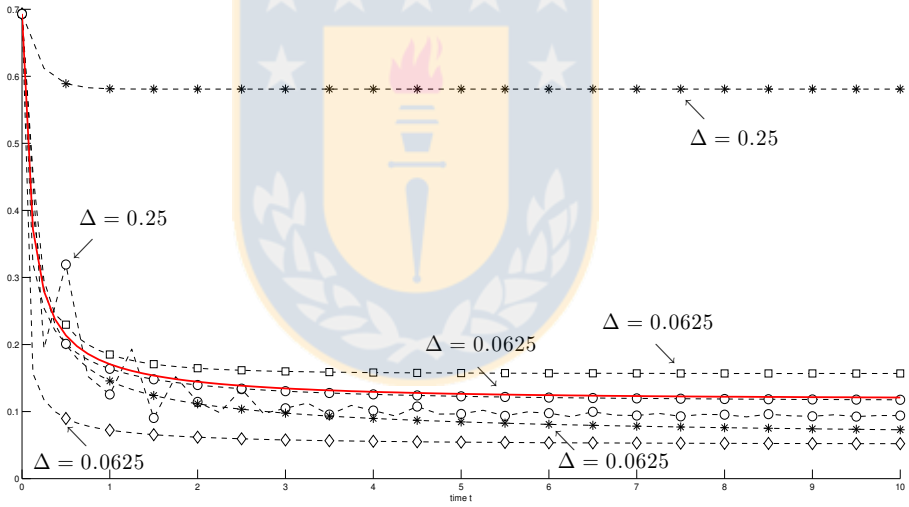

Figure 3.4: Computation of $\mathbb{E}\log\left(1 + (X_t)^2\right)$, where $t \in [0,10]$ and X_t solves (3.12) with $a = 6$, $b = 9$, $\sigma = 3$ and $X_0 = 1$. The "true" values are plotted with a solid line. The circles, stars, diamonds and squares represent the schemes $\bar{X}_n$, $\bar{E}_n$, $\tilde{Z}_n^s$ and $\hat{E}_n$, respectively. The step sizes 0.25 and 0.0625 are denoted by dashed and dotted lines, respectively.

Finally, we select $a = 9$, $b = 1$ and $\sigma = 4$. In the deterministic context, $\sigma = 0$, when $a > 0$ and $b = 1$ the system (3.12) has two stable points $\pm\sqrt{a}$ and the zero solution becomes an unstable steady state (see [104]).

We have tested alternative numerical schemes proposed to the stochastic Ginzburg-Landau equation [28, 50, 101, 183, 185]. Our numerical tests lead to step-size reduction to guarantee the sign-preserving and stability properties of the exact solution. Moreover, we have observed low rate of weak

$\boldsymbol{\Delta}$	$\left\vert \mathbb{E}\boldsymbol{f}\left(\boldsymbol{X_T}\right) - \mathbb{E}\boldsymbol{f}\left(\bar{\boldsymbol{E}}_{\boldsymbol{T/\Delta}}\right)\right\vert$	$\left\vert \mathbb{E}\boldsymbol{f}\left(\boldsymbol{X_T}\right) - \mathbb{E}\boldsymbol{f}\left(\tilde{\boldsymbol{Z}}^{\boldsymbol{s}}_{\boldsymbol{T/\Delta}}\right)\right\vert$	$\left\vert \mathbb{E}\boldsymbol{f}\left(\boldsymbol{X_T}\right) - \mathbb{E}\boldsymbol{f}\left(\hat{\boldsymbol{E}}_{\boldsymbol{T/\Delta}}\right)\right\vert$	$\left\vert \mathbb{E}\boldsymbol{f}\left(\boldsymbol{X_T}\right) - \mathbb{E}\boldsymbol{f}\left(\bar{\boldsymbol{X}}_{\boldsymbol{T/\Delta}}\right)\right\vert$
1	0.51106	29.0077	20.8951	0.074617
1/2	0.51504	26.1167	25.6113	0.05854
1/4	0.45996	21.5922	14.0218	0.026918
1/8	0.0089311	4.1708	0.56664	0.0078809
$\mathbf{2^{-4}}$	0.048116	0.068864	0.035861	0.003364
$\mathbf{2^{-5}}$	0.015164	0.041187	0.005734	0.0029212
$\mathbf{2^{-6}}$	0.0056366	0.022123	0.0048193	0.0017523
$\mathbf{2^{-7}}$	0.0023573	0.011367	0.0024914	0.00095535

Table 3.1: Estimation of errors involved in the computation of $\mathbb{E}f\left(X_T\right)$ for $T = 10$ and $f\left(x\right) = \log\left(1+x^2\right)$. Here, X_t verifies (3.12) with $a = 6$, $b = 9$, $\sigma = 3$ and $X_0 = 1$.

convergence.

3.2.3 Proofs

Proof of Theorem 3.2.1

From the formulation of Scheme 3.2.1 we have

$$\log\left\vert \bar{X}_{n+1}\right\vert = \log\left\vert \bar{X}_0\right\vert + \sum_{j=0}^{n}\left(\frac{b\left(\bar{X}_j\right)}{\bar{X}_j} - \frac{1}{2}\sum_{k=1}^{m}\left(\frac{\sigma^k\left(\bar{X}_j\right)}{\bar{X}_j}\right)^2\right)\Delta + S_n,$$

with $S_n = \sum_{j=0}^{n}\sum_{k=1}^{m}\sigma^k\left(\bar{X}_j\right)/\bar{X}_j\ \sqrt{\Delta}\hat{W}_j^k$. Using (3.6) yields

$$\frac{1}{n+1}\log\left\vert \bar{X}_{n+1}\right\vert \leq \frac{1}{n+1}\log\left\vert \bar{X}_0\right\vert - \lambda\Delta + \frac{1}{n+1}S_n. \tag{3.13}$$

By $\left\vert \sigma^k\left(x\right)\right\vert \leq K\left\vert x\right\vert$ for all $x \in \mathbb{R}$, we get $\mathbb{E}\left(\sum_{k=1}^{m}\sigma^k\left(\bar{X}_j\right)/\bar{X}_j\ \sqrt{\Delta}\hat{W}_j^k\right)^2 \leq K\Delta$, and so

$$\sum_{j=0}^{\infty}\frac{1}{\left(j+1\right)^2}\mathbb{E}\left(\sum_{k=1}^{m}\frac{\sigma^k\left(\bar{X}_j\right)}{\bar{X}_j}\sqrt{\Delta}\hat{W}_j^k\right)^2 < \infty.$$

Since $\mathbb{E}\left(\sum_{k=1}^{m}\frac{\sigma^k\left(\bar{X}_j\right)}{\bar{X}_j}\sqrt{\Delta}\hat{W}_j^k \middle/ \sigma\left(\bar{X}_0, \hat{W}_0^1, \ldots, \hat{W}_0^m, \ldots, \hat{W}_{j-1}^1, \ldots, \hat{W}_{j-1}^m\right)\right) = 0$, applying a generalized law of large numbers we deduce that $S_n/\left(n+1\right) \to_{n\to\infty} 0$ *a.s.* (see p. 243 of [81]). Then, letting $n \to \infty$ in (3.13) we obtain (3.7).

Proof of Theorem 3.2.2

To shorten notation, for any $n \geq 0$ we set

$$f_n := \left(\mu\left(\bar{X}_n\right) - \frac{1}{2}\sum_{k=1}^{m}\lambda^k\left(\bar{X}_n\right)^2\right)\Delta + \sum_{k=1}^{m}\lambda^k\left(\bar{X}_n\right)\sqrt{\Delta}\hat{W}_n^k$$

and $g_n := \left(b\left(0\right) - \sum_{k=1}^{m}\lambda^k\left(\bar{X}_n\right)\sigma^k\left(0\right)\right)\Delta + \sum_{k=1}^{m}\sigma^k\left(0\right)\sqrt{\Delta}\hat{W}_n^k$. Then

$$\bar{X}_{n+1} = \exp\left(f_n\right)\left(\bar{X}_n + g_n\right) = \bar{X}_n + \left(e^{f_n} - 1 - f_n\right)\bar{X}_n + \left(e^{f_n} - 1\right)g_n + f_n\bar{X}_n + g_n,$$

and hence

$$\bar{X}_{n+1} = \bar{X}_0 + \sum_{k=0}^{n}\left(e^{f_k} - 1 - f_k\right)\bar{X}_k + \sum_{k=0}^{n}\left(e^{f_k} - 1\right)g_k + \sum_{k=0}^{n}\left(f_k\bar{X}_k + g_k\right).$$

Let $q \geq 2$. By $\left|\exp\left(x\right) - \sum_{j=0}^{k-1}x^j/\left(j!\right)\right| \leq \left|x\right|^k\exp\left(\left|x\right|\right)$, using Hölder's inequality yields

$$\begin{aligned}
\left|\bar{X}_{n+1}\right|^q \quad \leq \quad & K\left|\bar{X}_0\right|^q + K\left(n+1\right)^{q-1}\left(\sum_{k=0}^{n}\left|f_k\right|^{2q}e^{q\left|f_k\right|}\left|\bar{X}_k\right|^q + \sum_{k=0}^{n}\left|f_k\right|^q\left|g_k\right|^q e^{q\left|f_k\right|}\right) \\
& + K\left(n+1\right)^{q-1}\sum_{k=0}^{n}\Delta^q\left|\mu\left(\bar{X}_k\right) - \frac{1}{2}\sum_{j=1}^{m}\lambda^j\left(\bar{X}_k\right)^2\right|^q\left|\bar{X}_k\right|^q \\
& + K\left(n+1\right)^{q-1}\sum_{k=0}^{n}\Delta^q\left|b\left(0\right) - \sum_{j=1}^{m}\lambda^j\left(\bar{X}_k\right)\sigma^j\left(0\right)\right|^q \\
& + K\Delta^{q/2}\sum_{j=1}^{m}\left|\sum_{k=0}^{n}\left(\lambda^j\left(\bar{X}_k\right)\bar{X}_k + \sigma^j\left(0\right)\right)\hat{W}_k^j\right|^q. \qquad (3.14)
\end{aligned}$$

For any $t > 0$,

$$\mathbb{E}\exp\left(t\left|\hat{W}_k^j\right|\right) \leq \mathbb{E}\exp\left(t\hat{W}_k^j\right) + \mathbb{E}\exp\left(-t\hat{W}_k^j\right) < \infty, \qquad (3.15)$$

and so for all $\ell \in \mathbb{N}$,

$$\mathbb{E}\left(\left|\hat{W}_k^j\right|^\ell\right) < \ell!\,\mathbb{E}\exp\left(\left|\hat{W}_k^j\right|\right) < \infty. \qquad (3.16)$$

Since μ and λ^k are bounded functions, we use (3.15), (3.16) and the Burkholder-Davis-Gundy inequality to obtain from (3.14) that

$$\mathbb{E}\left|\bar{X}_{n+1}\right|^q \leq K\mathbb{E}\left|\bar{X}_0\right|^q + K\left(T\right) + K\left(T\right)\Delta\sum_{k=0}^{n}\mathbb{E}\left|\bar{X}_k\right|^q,$$

with $n = 0, \ldots, N-1$. Applying a discrete Gronwall lemma (see e.g. [10]) we deduce that for all $n = 0, \ldots, N$,

$$\mathbb{E}\left|\bar{X}_n\right|^q \leq K(T)\left(1 + \mathbb{E}\left|\bar{X}_0\right|^q\right). \tag{3.17}$$

Consider again $q \geq 2$. Using

$$\left|\bar{X}_{n+1} - \bar{X}_n\right| \leq \left|e^{f_n} - 1\right|\left|\bar{X}_n\right| + e^{f_n}|g_n| \leq |f_n|\exp(|f_n|)\left|\bar{X}_n\right| + \exp(f_n)|g_n|,$$

together with (3.15) and (3.16), we get

$$\mathbb{E}\left(\left|\bar{X}_{n+1} - \bar{X}_n\right|^q \diagup \mathcal{F}_{T_n}\right) \leq K(T)\,\Delta^{q/2}\left(1 + \left|\bar{X}_n\right|^q\right). \tag{3.18}$$

Here, we assume without loss of generality that $\hat{W}_n^1, \ldots \hat{W}_n^m$ are $\mathcal{F}_{T_{n+1}}$-measurable and independent of $\mathcal{F}_{T_n}$.

Since $\left|\bar{X}_{n+1} - \left(1 + f_n + f_n^2/2 + f_n^3/6\right)\left(\bar{X}_n + g_n\right)\right| \leq |f_n|^4 \exp(|f_n|)\left|\bar{X}_n + g_n\right|$,

$$\begin{aligned}
\bar{X}_{n+1} \;=\; & \bar{X}_n + \sqrt{\Delta}\sum_{k=1}^m \left(\lambda^k\left(\bar{X}_n\right)\bar{X}_n + \sigma^k(0)\right)\hat{W}_n^k \\
& + \Delta\bar{X}_n\left(\mu\left(\bar{X}_n\right) - \frac{1}{2}\sum_{k=1}^m \lambda^k\left(\bar{X}_n\right)^2 + \frac{1}{2}\left(\sum_{k=1}^m \lambda^k\left(\bar{X}_n\right)\hat{W}_n^k\right)^2\right) \\
& + \Delta\left(b(0) - \sum_{k=1}^m \lambda^k\left(\bar{X}_n\right)\sigma^k(0) + \sum_{j,k=1}^m \sigma^j(0)\,\lambda^k\left(\bar{X}_n\right)\hat{W}_n^j\hat{W}_n^k\right) \\
& + \Delta^{3/2}\bar{X}_n\left(\mu\left(\bar{X}_n\right) - \frac{1}{2}\sum_{k=1}^m \lambda^k\left(\bar{X}_n\right)^2\right)\sum_{k=1}^m \lambda^k\left(\bar{X}_n\right)\hat{W}_n^k \\
& + \Delta^{3/2}\bar{X}_n\left(\sum_{k=1}^m \lambda^k\left(\bar{X}_n\right)\hat{W}_n^k\right)^3/6 \\
& + \Delta^{3/2}\left(\mu\left(\bar{X}_n\right) - \frac{1}{2}\sum_{k=1}^m \lambda^k\left(\bar{X}_n\right)^2 + \frac{1}{2}\left(\sum_{k=1}^m \lambda^k\left(\bar{X}_n\right)\hat{W}_n^k\right)^2\right)\sum_{k=1}^m \sigma^k(0)\,\hat{W}_n^k \\
& + \Delta^{3/2}\left(b(0) - \sum_{k=1}^m \lambda^k\left(\bar{X}_n\right)\sigma^k(0)\right)\sum_{k=1}^m \lambda^k\left(\bar{X}_n\right)\hat{W}_n^k + \mathcal{R}_n\left(\Delta, \bar{X}_n\right),
\end{aligned}$$

where $\left|\mathcal{R}_n\left(\Delta, \bar{X}_n\right)\right| \leq |f_n|^4 \exp(|f_n|)\left|\bar{X}_n + g_n\right| + K(T)\,\Delta^2\left(1 + \left|\bar{X}_n\right|\right)$. This gives

$$\begin{aligned}
&\left|\mathbb{E}\left(\left(\bar{X}_{n+1} - \bar{X}_n\right)^\ell - \left(b\left(\bar{X}_n\right)\Delta + \sum_{k=1}^m \sigma^k\left(\bar{X}_n\right)\left(W_{\Delta(n+1)}^k - W_{\Delta n}^k\right)\right)^\ell \diagup \mathcal{F}_{T_n}\right)\right| \\
&\leq K(T)\,\Delta^2\left(1 + \left|\bar{X}_n\right|^q\right)
\end{aligned} \tag{3.19}$$

provided that $\ell = 1, 2, 3$.

From (3.17), (3.18) and (3.19) we obtain (3.9). To this end, we can apply the classical methodology introduced by Milstein [146] and Talay [196, 197], or we can directly use Theorem 9.1 of [147] (see also Theorem 14.5.2 of [120]).

3.3 Systems of linear SDEs

This section is devoted to the SDE

$$X_t = X_0 + \int_0^t BX_s \, ds + \sum_{k=1}^{m} \int_0^t \sigma^k X_s \, dW_s^k, \tag{3.20}$$

where $B, \sigma^1, \ldots, \sigma^m \in \mathbb{R}^{d\times d}$. Without loss of generality we suppose $X_0 \neq 0$ *a.s.*, and so, almost surely, $X_t \neq 0$ for all $t > 0$ (see e.g. [102, 138]).

3.3.1 General methodology

We divide the numerical solution of (3.20) into the computations of $\|X_t\|$ and $\hat{X}_t := X_t / \|X_t\|$, leading to solve the coupled system formed by (3.21) and (3.24), given below.

Applying Itô's formula to $X_{t\wedge\tau_j}/\sqrt{\left\|X_{t\wedge\tau_j}\right\|^2}$ we get after a long calculation that

$$\hat{X}_{t\wedge\tau_j} = \hat{X}_0 + \int_0^{t\wedge\tau_j} B\left(\hat{X}_s\right)\hat{X}_s \, ds + \sum_{k=1}^{m} \int_0^{t\wedge\tau_j} \left(\sigma^k - \left\langle \hat{X}_s, \sigma^k \hat{X}_s \right\rangle\right) \hat{X}_s \, dW_s^k,$$

where $\tau_j := \inf\{t > 0 : \|X_t\| < 1/j\}$ and, by abuse of notation,

$$B(x) = B - \langle x, Bx\rangle + \sum_{k=1}^{m} \left(\frac{3}{2}\left\langle x, \sigma^k x\right\rangle^2 - \left\langle x, \sigma^k x\right\rangle \sigma^k - \frac{1}{2}\left\|\sigma^k x\right\|^2 \right) \qquad \forall x \in \mathbb{R}^d.$$

Since almost surely X_t will never reach the origin, $\tau_j \longrightarrow_{j\to\infty} \infty$ *a.s.*, and so taking limit as $j \to \infty$ gives

$$\hat{X}_t = \hat{X}_0 + \int_0^t B\left(\hat{X}_s\right)\hat{X}_s \, ds + \sum_{k=1}^{m} \int_0^t \left(\sigma^k - \left\langle \hat{X}_s, \sigma^k \hat{X}_s \right\rangle\right) \hat{X}_s \, dW_s^k. \tag{3.21}$$

We propose to compute $\hat{X}_{T_n}$ by numerically solving (3.21). Here, $T_n = n\Delta$ with $\Delta > 0$ and $n \in \mathbb{Z}_+$. To this end, we can approximate $\hat{X}_t$ in $[T_n, T_{n+1}]$ by

$$Z_t = \tilde{X}_n + \int_{T_n}^t B\left(\hat{Y}_n\right) Z_s \, ds + \sum_{k=1}^{m} \int_{T_n}^t \left(\sigma^k - \left\langle \hat{Y}_n, \sigma^k \hat{Y}_n \right\rangle\right) Z_s \, dW_s^k, \tag{3.22}$$

where $\tilde{X}_n$ and $\hat{Y}_n$ are $\mathcal{F}_{T_n}$-measurable random variables of norm 1 such that $\tilde{X}_n \approx \hat{X}_{T_n}$ and $\hat{Y}_n \approx \hat{X}_s$ for all $s \in [T_n, T_{n+1}]$. Numerically integrating (3.22) by using, for instance, the Euler-Maruyama

method we obtain $\bar{Z}_{n+1} \approx Z_{T_{n+1}}$. Since $\left\|\hat{X}_{T_{n+1}}\right\| = 1$, we expect that $\left\|\bar{Z}_{n+1}\right\| \approx 1$ in many situations. Hence, we can improve the performance of the numerical schemes applied to (3.21) by projecting on the unit sphere at each discretization step; a projection procedure used with success in the numerical solution of the non-linear Schödinger equations (see e.g. [153, 173]). This gives $\bar{Z}_{n+1}/\left\|\bar{Z}_{n+1}\right\| \approx \hat{X}_{T_{n+1}}$ (see Remark 3.3.1 below).

In order to handle $\|X_t\|$, applying Itô's formula to $\sqrt{\left\|X_{t\wedge\tau_j}\right\|^2}$ we deduce that

$$\begin{aligned}\|X_t\| = \|X_0\| &+ \int_0^t \left(\frac{\langle X_s, BX_s\rangle + \frac{1}{2}\sum_{k=1}^m \left\|\sigma^k X_s\right\|^2}{\|X_s\|} - \frac{1}{2}\sum_{k=1}^m \frac{\langle X_s, \sigma^k X_s\rangle^2}{\|X_s\|^3} \right) ds \\ &+ \sum_{k=1}^m \int_0^t \frac{\langle X_s, \sigma^k X_s\rangle}{\|X_s\|}\, dW_s^k. \end{aligned} \tag{3.23}$$

A close look at Scheme 3.2.1 leads us to rewrite (3.23) as

$$\begin{aligned}\|X_t\| = \|X_0\| &+ \int_0^t \left(\langle \hat{X}_s, B\hat{X}_s\rangle + \frac{1}{2}\sum_{k=1}^m \left(\left\|\sigma^k \hat{X}_s\right\|^2 - \langle \hat{X}_s, \sigma^k \hat{X}_s\rangle^2 \right) \right) \|X_s\|\, ds \\ &+ \sum_{k=1}^m \int_0^t \langle \hat{X}_s, \sigma^k \hat{X}_s\rangle \|X_s\|\, dW_s^k. \end{aligned} \tag{3.24}$$

Since $\langle \hat{X}_s, B\hat{X}_s\rangle + \sum_{k=1}^m \left(\left\|\sigma^k \hat{X}_s\right\|^2 - \langle \hat{X}_s, \sigma^k \hat{X}_s\rangle^2 \right)/2$ and $\langle \hat{X}_s, \sigma^k \hat{X}_s\rangle$ are smooth functions of $\hat{X}_s$, $\|X_t\|$ is well approximated on $[T_n, T_{n+1}]$ by the solution of

$$\begin{aligned}\eta_t = \bar{\eta}_n &+ \int_{T_n}^t \left(\langle \hat{Y}_n, B\hat{Y}_n\rangle + \frac{1}{2}\sum_{k=1}^m \left(\left\|\sigma^k \hat{Y}_n\right\|^2 - \langle \hat{Y}_n, \sigma^k \hat{Y}_n\rangle^2 \right) \right) \eta_s\, ds \\ &+ \sum_{k=1}^m \int_{T_n}^t \langle \hat{Y}_n, \sigma^k \hat{Y}_n\rangle \eta_s\, dW_s^k \end{aligned} \tag{3.25}$$

with $\bar{\eta}_n \approx \|X_{T_n}\|$ and $\hat{Y}_n \approx \hat{X}_s$. Let $\hat{W}_0^1, \ldots, \hat{W}_0^m, \hat{W}_1^1, \ldots$ be i.i.d. random variables with symmetric law and variance 1. Replacing $W_{T_{n+1}}^k - W_{T_n}^k$ by $\sqrt{\Delta}\hat{W}_n^k$ in the explicit solution of the linear scalar SDE (3.25) we obtain $\bar{\eta}_{n+1} \approx \left\|X_{T_{n+1}}\right\|$, where $\bar{\eta}_{n+1}$ is given by the recursive formula

$$\begin{aligned}\bar{\eta}_{n+1} = \bar{\eta}_n \exp\Bigg(\Bigg(\langle \hat{Y}_n, B\hat{Y}_n\rangle + \frac{1}{2}\sum_{k=1}^m \left\|\sigma^k \hat{Y}_n\right\|^2 - \sum_{k=1}^m \langle \hat{Y}_n, \sigma^k \hat{Y}_n\rangle^2 \Bigg) \Delta \\ + \sum_{k=1}^m \langle \hat{Y}_n, \sigma^k \hat{Y}_n\rangle \sqrt{\Delta}\hat{W}_n^k \Bigg). \end{aligned} \tag{3.26}$$

The simplest selection $\hat{Y}_n = \tilde{X}_n$ yields the following numerical method for (3.20):

Scheme 3.3.1 *Define recursively* $\bar{X}_{n+1} = \begin{cases} \bar{Z}_{n+1}/\left\|\bar{Z}_{n+1}\right\| & ;\ if\ \bar{Z}_{n+1} \neq 0 \\ \bar{X}_n & ;\ if\ \bar{Z}_{n+1} = 0 \end{cases}$, *where*

$$\bar{Z}_{n+1} = \bar{X}_n + B\left(\bar{X}_n\right)\bar{X}_n\Delta + \sum_{k=1}^{m}\left(\sigma^k - \left\langle \bar{X}_n, \sigma^k \bar{X}_n \right\rangle\right)\bar{X}_n\sqrt{\Delta}\hat{W}_n^k \tag{3.27}$$

with $\hat{W}_0^1, \hat{W}_0^2, \ldots, \hat{W}_0^m, \hat{W}_1^1, \ldots$ *i.i.d. symmetric random variables having variance* 1. *The stochastic process* $\bar{\eta}_{n+1}$ *is given by* (3.26) *with* $\hat{Y}_n = \bar{X}_n$.

From (3.26) it follows that $\bar{\eta}_n > 0$ for all $n \in \mathbb{N}$, whenever $\bar{\eta}_0 > 0$. We next establish that $\bar{\eta}_n\bar{X}_n$ approximates X_{T_n} with rate of weak convergence equal to 1.

Theorem 3.3.1 *Consider* $T > 0$ *and* $f \in C_p^4\left(\mathbb{R}^d, \mathbb{R}\right)$. *Let* $\bar{\eta}_n\bar{X}_n$ *be described by Scheme 3.3.1 with* $\Delta = T/N$, *where* $N \in \mathbb{N}$. *Assume that* $\hat{W}_n^k$ *are bounded random variables,* X_0 *has finite moments of any order, and that for every* $g \in C_p^4\left(\mathbb{R}^d, \mathbb{R}\right)$, $\left|\mathbb{E}g\left(X_0\right) - \mathbb{E}g\left(\bar{\eta}_0\bar{X}_0\right)\right| \leq K\left(1 + \mathbb{E}\left\|X_0\right\|^q\right)T/N$ *whenever* $N \in \mathbb{N}$. *Then*

$$\left|\mathbb{E}f\left(X_T\right) - \mathbb{E}f\left(\bar{\eta}_N\bar{X}_N\right)\right| \leq K\left(T\right)\left(1 + \mathbb{E}\left\|X_0\right\|^q\right)T/N \qquad \forall N \in \mathbb{N}. \tag{3.28}$$

Proof 3.3.1 *Deferred to Section 3.3.5.*

Scheme 3.3.1 reproduces very well the behavior of $\|X_t\|$. In fact, Theorem 3.3.2 below asserts that for all $\Delta > 0$, Scheme 3.3.1 converges exponentially fast to 0 under a classical condition for $\limsup_{t\to\infty}\left(\log\|X_t\|\right)/t < 0$ (see e.g. [102, 138]). Moreover, Theorem 3.3.3 establishes that Scheme 3.3.1 is away from 0 for any step-size in a case where 0 is an unstable equilibrium point of (3.20) (see e.g. [8]).

Theorem 3.3.2 *Consider Scheme 3.3.1 with* $\mathbb{E}\left(\bar{\eta}_0\right)^2 < \infty$ *and* $\bar{\eta}_0 > 0$. *Assume that*

$$-\lambda := \sup_{x\in\mathbb{R}^d, \|x\|=1}\left(\langle x, Bx\rangle + \sum_{k=1}^{m}\left(\frac{1}{2}\left\|\sigma^k x\right\|^2 - \langle x, \sigma^k x\rangle^2\right)\right) < 0. \tag{3.29}$$

Then $\limsup_{n\to\infty}\frac{1}{n\Delta}\log\left(\bar{\eta}_n\right) \leq -\lambda\ \ \mathbb{P}$-*a.s.*

Proof 3.3.2 *Deferred to Section 3.3.5.*

Theorem 3.3.3 *Let* $\bar{\eta}_n$ *be described by Scheme 3.3.1 with* $\mathbb{E}\left(\bar{\eta}_0\right)^2 < \infty$ *and* $\bar{\eta}_0 > 0$. *Suppose that there exists* $\theta > 0$ *such that*

$$\langle x, Bx\rangle + \frac{1}{2}\sum_{k=1}^{m}\left\|\sigma^k x\right\|^2 - (1+\theta)\sum_{k=1}^{m}\langle x, \sigma^k x\rangle^2 \geq 0 \qquad \forall\left\|x\right\| = 1. \tag{3.30}$$

Then $\liminf_{n\to\infty}\bar{\eta}_n > 0$ *a.s.*

Proof 3.3.3 *Deferred to Section 3.3.5.*

Remark 3.3.1 *Consider Scheme 3.3.1. From* $\bar{Z}_{n+1} \approx \hat{X}_{T_{n+1}}$ *we have* $\left\|\bar{Z}_{n+1}\right\| \approx 1$*, and so we can expect that* $\left\|\bar{Z}_{n+1}\right\|$ *is not close to* 0*. This motivates the approximation* $\bar{Z}_{n+1}/\left\|\bar{Z}_{n+1}\right\| \approx \hat{X}_{T_{n+1}}$*, which efficiently reproduces the unit-norm property of* $\hat{X}_{T_{n+1}}$ *and is seldom influenced by the effect of round-off errors. First,* $\left\|\bar{Z}_{n+1}\right\|$ *may take small values only for certain special combinations of* $\bar{X}_n$ *and* Δ*. For example,* $\bar{Z}_{n+1} \approx 0$ *implies* $\left\langle \bar{X}_n, \bar{Z}_{n+1}\right\rangle \approx 0$*, and hence* $\sum_{k=1}^{m}\left(\left\|\sigma^k \bar{X}_n\right\|^2 - \left\langle \bar{X}_n, \sigma^k \bar{X}_n\right\rangle^2\right) \approx 2/\Delta$*. Second, suppose, for instance, that* $\hat{W}_n^k$ *is distributed uniformly on* $\left[-\sqrt{3}, \sqrt{3}\right]$*. Then, using* $\left\|\bar{X}_n\right\| = 1$ *we deduce that* $\left\|\bar{Z}_{n+1}\right\|$ *is uniformly bounded from below by a positive constant whenever* Δ *is small enough. According to Theorem 3.3.4 below we have that* $\bar{Z}_{n+1} \neq 0$ *a.s. for all* $\Delta > 0$*. Moreover, the proof of Theorem 3.3.4 suggests us that the special cases where* $\left\|\bar{Z}_{n+1}\right\| \approx 0$ *happen with quite small probability. In these situations, we can implement Scheme 3.3.1 by using a preconditioner like* $\bar{X}_{n+1} = \left(\bar{Z}_{n+1}/\left\|\bar{Z}_{n+1}\right\|_\infty\right)/\left\|\bar{Z}_{n+1}/\left\|\bar{Z}_{n+1}\right\|_\infty\right\|$*, or by setting* $\bar{X}_{n+1} = \bar{X}_n$ *in the worst case.*

Theorem 3.3.4 *Adopt the framework of Scheme 3.3.1. Let the distribution of* $\hat{W}_n^k$ *be absolutely continuous with respect to the Lebesgue measure. Then for all* $n \geq 0$*,* $\bar{Z}_n \neq 0$ *a.s.*

Proof 3.3.4 *Deferred to Section 3.3.5.*

3.3.2 Numerical experiments: well-conditioned drift matrix

A first bilinear test

We study the performance of Scheme 3.3.1 applied to the following test problem [26, 43]:

$$X_t = X_0 + \int_0^t \begin{pmatrix} b & 0 \\ 0 & b \end{pmatrix} X_s \, ds + \int_0^t \begin{pmatrix} \sigma & 0 \\ 0 & \sigma \end{pmatrix} X_s \, dW_s^1 + \int_0^t \begin{pmatrix} 0 & -\epsilon \\ \epsilon & 0 \end{pmatrix} X_s \, dW_s^2, \tag{3.31}$$

where $X_t = \left(X_t^1, X_t^2\right)^\top \in \mathbb{R}^2$, $b = -2$, $\sigma = \epsilon = 4$ and $X_0 = (1,2)^\top$. In order to avoid variance problems, we calculate $\mathbb{E}\arctan\left(1 + \left(X_t^1\right)^2\right)$, whose "true" values (solid line) have been obtained by sampling 10^8 times the explicit solution of (3.31). Since $-\lambda = -2 < 0$, the test equation (3.31) is almost sure exponentially stable.

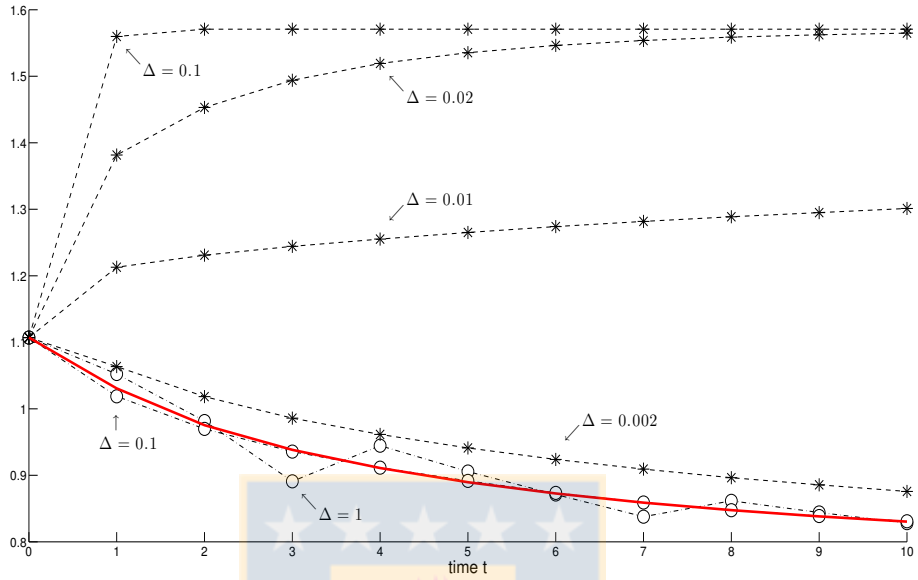

Figure 3.5: Computation of $\mathbb{E}\arctan\left(1+\left(X_t^1\right)^2\right)$, where X_t solves (3.31). The true values are plotted with a solid line. The circles (resp. stars) represent the approximations of $\mathbb{E}\arctan\left(1+\left(X_t^1\right)^2\right)$, with $t=0,1,\ldots,10$, given by Scheme 3.3.1 (resp. the backward Euler method $\bar{E}_n$).

First, we consider $\bar{\eta}_n\bar{X}_n$ defined by Scheme 3.3.1 with $\hat{W}_n^k=\xi_n^k$, where $\xi_0^1,\xi_0^2,\ldots,\xi_0^m$, $\xi_1^1,\ldots$ are independent random variables taking values ±1 with probability $1/2$. In Figure 3.5 we compare the computation of $\mathbb{E}\arctan\left(1+\left(X_t^1\right)^2\right)$ by using $\bar{\eta}_n\bar{X}_n$ (represented by circles) with that produced by the backward Euler method

$$\bar{E}_{n+1}=\bar{E}_n+B\bar{E}_{n+1}\Delta+\sum_{k=1}^{m}\sigma^k\bar{E}_n\sqrt{\Delta}\xi_n^k. \tag{3.32}$$

All the sample sizes are equal to 10^6. Figure 3.5 shows the very good qualitative behavior of Scheme 3.3.1 in the numerical solution of (3.31), which is in good agreement with Theorem 3.3.2. We can observe that the first coordinate of $\bar{\eta}_n\bar{X}_n$ decays to 0 with the same speed that the true solution, even for large step-sizes. In contrast, the trajectories of $\bar{E}_n$ blow up when $\Delta=0.1$ and $\Delta=0.02$. Moreover, $\bar{\eta}_n\bar{X}_n$ achieves an excellent accuracy in cases $\Delta=1$ and $\Delta=0.1$.

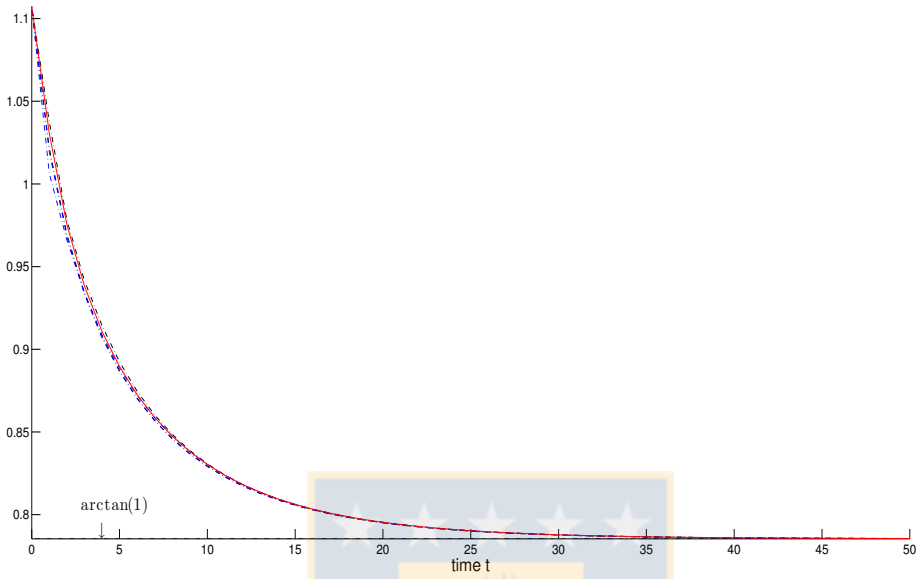

Figure 3.6: Long time computation of $\mathbb{E}\arctan\left(1+\left(X_t^1\right)^2\right)$ by sampling 10^8 times the Scheme 3.3.1 with $\Delta = 1/8, 1$ and $\hat{W}_n^2$ distributed according to the normal and uniform laws. Here, X_t satisfies (3.31). The very good accuracy of Scheme 3.3.1 makes difficult to distinguish between the four simulations (dashdot lines) and the true values (solid line).

Second, we discuss the effect of round-off errors on Scheme 3.3.1 applied to (3.31). Using simple algebraic transformations we get

$$\left\|\bar{Z}_{n+1}\right\|^2 = \left(1-\epsilon^2\Delta/2\right)^2 + \epsilon^2\Delta\left(\hat{W}_n^2\right)^2. \tag{3.33}$$

If $\hat{W}_n^2 = \xi_n^2$, then $\left\|\bar{Z}_{n+1}\right\|^2 = 1+\epsilon^4\Delta^2/4$, and so we can calculate $\bar{Z}_{n+1}/\left\|\bar{Z}_{n+1}\right\|$ without problems. From (3.33) it follows that $\bar{Z}_{n+1} \approx 0$ if and only if $\Delta \approx 2/\epsilon^2$ and $\hat{W}_n^2 \approx 0$. The latter happens with a extremely low probability in case $\hat{W}_n^2$ is uniformly distributed on $\left[-\sqrt{3},\sqrt{3}\right]$. In fact, Figure 3.6 illustrates the very good behavior of Scheme 3.3.1 with $\Delta = 2/\epsilon^2 = 1/8$ in the long-time computation of $\mathbb{E}\arctan\left(1+\left(X_t^1\right)^2\right)$ when $\hat{W}_n^2$ is uniformly distributed on $\left[-\sqrt{3},\sqrt{3}\right]$; our implementation of Scheme 3.3.1 does not take any precaution against $\bar{Z}_{n+1} \approx 0$. If $\hat{W}_n^2$ is obtained by means of a normal pseudorandom number generator, then $\hat{W}_n^2$ is equal to 0 with small probability, and hence the performance of Scheme 3.3.1 is not affected when $\Delta = 2/\epsilon^2$, as we can see in Figure 3.6.

Third, Figure 3.7 addresses the numerical solution of (3.31) with $b = -2$ replaced by $b = 0.5$. We can check that (3.31) satisfies the assumptions of Theorem 3.3.3 whenever $b > 0$. Furthermore, it follows from the proofs of Theorem 12 of [8] and Theorem 3.3.3 that the norms of X_t and $\bar{\eta}_n\bar{X}_n$ converge almost surely to $+\infty$ in this case. Figure 3.7 shows that Scheme 3.3.1 reproduces very well the divergent behavior of X_t.

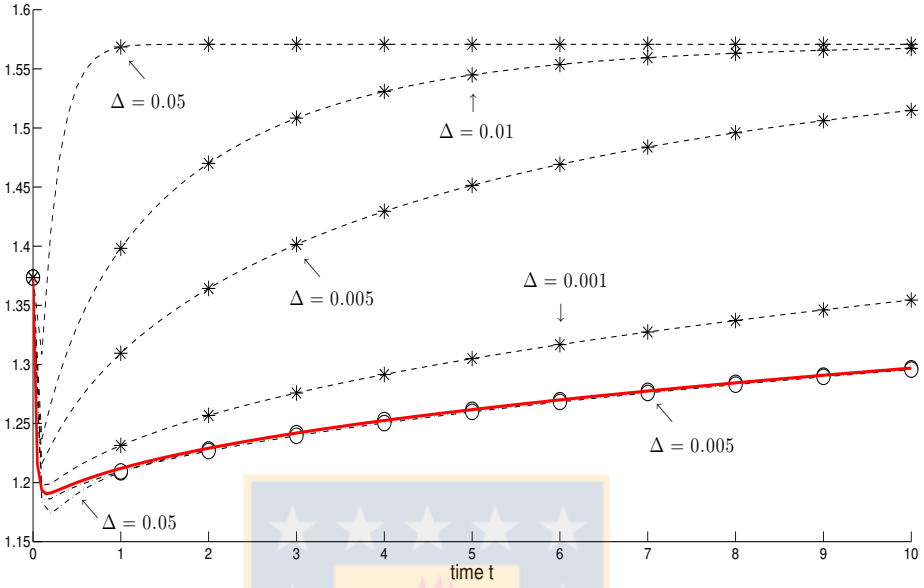

Figure 3.7: Computation of $\mathbb{E}\arctan\left(1+\left(X_t^2\right)^2\right)$, where X_t solves (3.31) with $b = 0.5$. The true values are plotted with a solid line. Scheme 3.3.1, resp. the backward Euler method $\bar{E}_n$, is represented by circles, resp. stars. For each scheme, 10^8 samples have been used.

An unstable bilinear system

Let us introduce the second order SDE

$$dX_t = \begin{pmatrix} 0 & 1 \\ -1 & -2\zeta \end{pmatrix} X_t \, dt + \begin{pmatrix} 0 & 0 \\ -\sigma & 0 \end{pmatrix} X_t \, dW_t^1, \tag{3.34}$$

where $\zeta \in \mathbb{R}$, $\sigma > 0$ and $X_0 \neq 0$ (see e.g. [11, 19, 20, 109, 110, 124]). Applying a result due to Khas'minskii (1967) [119], Kozin and Prodromou (1971) [124] studied the exact stability region of (3.34) in terms of the parameters $\left(\zeta, \sigma^2\right)$ where the Lyapunov exponent is positive or negative by using numerical integration. In particular it was proved that if $\sigma > 0$ and $\zeta \leq 0$ then system (3.34) is almost surely exponentially unstable, i.e. the biggest Lyapunov exponent $\ell := \lim_{t\to\infty} \frac{1}{t} \log \|X_t\|$ is strictly positive independent of how small is the value of $\sigma > 0$ (see [19, 124] and references therein). Further, Imkeller and Lederer [109, 110] obtained an integral representation of the top Lyapunov exponent and then they gave a explicit formula in terms of hypergeometric functions. If $\sigma = 0$, that is the deterministic case, using (3.29) we have that system (3.34) is *a.s.* exponentially stable for all $\zeta > 0$. Further, given $\zeta > 0$ it is possible to destabilize (3.34) by choosing a large enough noise intensity $\sigma > 0$ (see p. 46 in [110]). A more general form of the system (3.34) was studied in [20].

We consider the numerical estimation of expectations $\mathbb{E}f\left(X_t\right)$ and $\mathbb{E}g\left(X_t\right)$; where $X_t = \left(X_t^1, X_t^2\right)^\top$, by averaging 10^6 realizations of $\bar{\eta}_n \bar{X}_n$ defined by Scheme 3.3.1 with $\hat{W}_n^k = \xi_n^k$, and the backward Euler

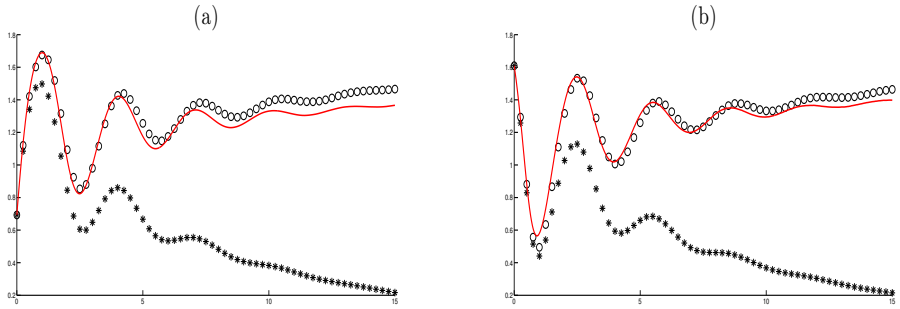

Figure 3.8: Approximations of $\mathbb{E}f(X_t)$; $t \in [0,15]$, obtained by $\bar{\eta}_n \bar{X}_n$ (circles) and $\bar{E}_n$ (stars) using $\Delta = 1/4$. Here, X_t solves (3.34) with $\zeta = 0.062$, $\sigma^2 = 0.5$ and $X_0 = (1,2)^\top$. The true values are plotted with a solid line. (a) $f(x) = \log\left(1 + x_1^2\right)$; (b) $f(x) = \log\left(1 + x_2^2\right)$.

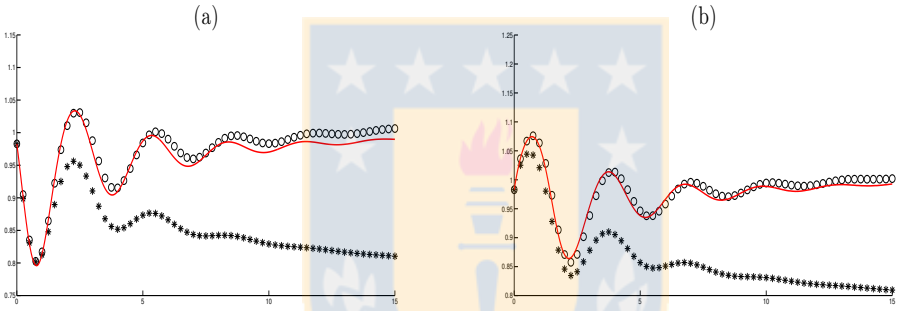

Figure 3.9: Estimations of $\mathbb{E}g(X_t)$; $t \in [0,15]$, obtained by $\bar{\eta}_n \bar{X}_n$ (circles) and $\bar{E}_n$ (stars) using $\Delta = 1/4$. Here, X_t solves (3.34) with $\zeta = 0.062$, $\sigma^2 = 0.5$ and $X_0 = (1,-1)^\top/\sqrt{2}$. The true values are plotted with a solid line. (a) $g(x) = \arctan\left(1 + x_1^2\right)$; (b) $g(x) = \arctan\left(1 + x_2^2\right)$.

scheme $\bar{E}_n$ given by (3.32). As in [124] we choose $\sigma^2 = 0.5$ and $\zeta = 0.062$. Thus, from Theorem 5 of [110] we have $\ell = 0.1347$ and so (3.34) is *a.s.* exponentially unstable. The "true" values were obtained by means of 10^6 sample paths of $\bar{E}_n$ with time-step $\Delta = 2^{-14}$. Figures 3.8 and 3.9 show the performance of $\bar{\eta}_n \bar{X}_n$ and $\bar{E}_n$ in the approximation of $\mathbb{E}f(X_t)$ and $\mathbb{E}g(X_t)$ for $t \in [0,15]$ and $\Delta = 1/4$. In both cases we can observe that Scheme 3.3.1 replies the desired unstable behavior. In turns, the backward Euler scheme exhibits wrong stable results.

Lyapunov exponents

We illustrate the potential of Scheme 3.3.1 to compute Lyapunov exponents of bilinear SDEs (3.20) (see e.g. [10, 198, 92] for classical theoretical and numerical references). To this end, we deal with the approximation of $\ell(X_0) := \lim_{t\to\infty} \frac{1}{t} \log \|X_t\|$, where

$$X_t = X_0 + \int_0^t \begin{pmatrix} a - \frac{\sigma^2}{2} & 0 \\ 0 & b - \frac{\sigma^2}{2} \end{pmatrix} X_s \, ds + \int_0^t \sigma \begin{pmatrix} 0 & -1 \\ 1 & 0 \end{pmatrix} X_s \, dW_s^1, \tag{3.35}$$

Δ	0.1	0.05	0.01	0.002	0.001	0.0001
$\sigma = 10,\ \ell = -0.48875$						
$\hat{\ell}_N(\Delta)$	30.09701	26.77603	−3.71372	−0.57889	−0.48503	−0.48811
$\tilde{\ell}_N(\Delta)$	−0.52693	−0.50851	−0.49928	−0.49132	−0.48930	−0.48937
$\sigma = 20,\ \ell = -0.49719$						
$\hat{\ell}_N(\Delta)$	86.56572	114.26780	93.37706	−9.63927	−2.96739	−0.48334
$\tilde{\ell}_N(\Delta)$	−0.55164	−0.51945	−0.50120	−0.49883	−0.49798	−0.49703

Table 3.2: Computed values for a final integration time $T = N\Delta = 500$ of the Lyapunov exponent ℓ for (3.35) with $a = 1$, $b = -2$, $X_0 = \left(1/\sqrt{2}, 1/\sqrt{2}\right)^\top$ and different diffusion parameters σ.

with $a, b \in \mathbb{R}$, $\sigma > 0$ and $X_0 \neq 0$. In this well-known test problem [17, 120, 198], $\ell(X_0)$ does not depend on the initial condition X_0, and further

$$\ell = \frac{a+b}{2} + \frac{a-b}{2} \frac{\int_0^{2\pi} \cos(2\theta) \exp\left(\frac{a-b}{2\sigma^2}\cos(2\theta)\right) d\theta}{\int_0^{2\pi} \exp\left(\frac{a-b}{2\sigma^2}\cos(2\theta)\right) d\theta}. \tag{3.36}$$

Following [198] we take $a = 1$ and $b = -2$. Since $\ell(X_0) = \ell(X_0/\|X_0\|)$ for bilinear SDEs (3.20), there is no loss of generality in assuming $\|X_0\| = 1$ and we choose $X_0 = \left(1/\sqrt{2}, 1/\sqrt{2}\right)^\top$.

In case B is well-conditioned, we can approximate the Lyapunov exponent ℓ by

$$\tilde{\ell}_N(\Delta) := \frac{1}{N\Delta} \log\left\|\bar{\eta}_N \bar{X}_N\right\| = \frac{1}{N\Delta} \sum_{n=0}^{N-1} \log\left(\frac{\left\|\bar{\eta}_{n+1}\bar{X}_{n+1}\right\|}{\left\|\bar{\eta}_n \bar{X}_n\right\|}\right),$$

where $\bar{\eta}_n \bar{X}_n$ is given by Scheme 3.3.1 and $N \in \mathbb{N}$ is sufficiently large. From (3.26) we have $\tilde{\ell}_N(\Delta) = \frac{1}{N\Delta}\sum_{n=0}^{N-1} \mathcal{L}_n\left(\bar{X}_n\right)$, with

$$\mathcal{L}_n(x) = \left(\langle x, Bx\rangle + \frac{1}{2}\sum_{k=1}^m \left\|\sigma^k x\right\|^2 - \sum_{k=1}^m \langle x, \sigma^k x\rangle^2\right)\Delta + \sum_{k=1}^m \langle x, \sigma^k x\rangle \sqrt{\Delta}\hat{W}_n^k \qquad \forall x \in \mathbb{R}^2.$$

For concreteness, we consider $\hat{W}_n^k$ uniformly distributed on $\left[-\sqrt{3}, \sqrt{3}\right]$. Then

$$\tilde{\ell}_{n+1}(\Delta) = \tilde{\ell}_n(\Delta)\left(1 - \frac{1}{n+1}\right) + \frac{\mathcal{L}_n\left(\bar{X}_n\right)}{(n+1)\Delta}.$$

In order to evaluate the performance of $\tilde{\ell}_n$, we also compute ℓ by means of the algorithm $\hat{\ell}_n$ introduced in pp. 1155 and 1156 of [198].

Table 3.2 compares the average of 20 realizations of both $\tilde{\ell}_N(\Delta)$ and $\hat{\ell}_N(\Delta)$ applied to (3.35) with $\sigma = 10$ and $\sigma = 20$. We have actually computed $\frac{1}{500}\log(\|X_{500}\|)$ since we choose $N = 500/\Delta$. Numerically integrating (3.36) we obtain the reference value $\ell = -0.48875$ for $\sigma = 10$, as well as that $\ell = -0.49719$ whenever $\sigma = 20$. Table 3.2 shows the very good accuracy of $\tilde{\ell}_N$. In case $\sigma = 10$, the

relative error $\left|\tilde{\ell}_N(0.1) - \ell\right| / |\ell|$ is equal to 0.0781, and so $\tilde{\ell}_N(\Delta)$ provides a good approximation of ℓ even when $\Delta = 0.1$. If we increase the noise intensity to $\sigma = 20$, then $\left|\tilde{\ell}_N(0.05) - \ell\right| / |\ell| = 0.0448$. In contrast, $\hat{\ell}_N(0.001)$ produces the value -2.96739.

3.3.3 Weak exponential schemes for bilinear SDEs

This subsection focuses on (3.20) with drift matrix B ill-conditioned. We return to (3.21) and (3.24). If the matrix B has very different eigenvalues, then we should carefully approximate the term $\langle \hat{X}_s, B\hat{X}_s \rangle$ in (3.24). This leads us to the problem of finding good candidates for the random variable $\hat{Y}_n$ involved in (3.22) and (3.26). Using, for instance, the midpoint rule we can select $\hat{Y}_n = \exp(B\Delta/2)\bar{X}_n / \left\|\exp(B\Delta/2)\bar{X}_n\right\|$. Then, applying to (3.22) the Euler-exponential method introduced in [153] we obtain the following almost sure exponentially stable scheme.

Scheme 3.3.2 *Let $\hat{W}_0^1, \ldots, \hat{W}_0^m, \hat{W}_1^1, \ldots$ be i.i.d. random variables with symmetric law and variance equal to 1. Set* $\bar{X}_{n+1} = \begin{cases} \bar{V}_{n+1} / \left\|\bar{V}_{n+1}\right\| & ; \text{if } \bar{V}_{n+1} \neq 0 \\ \bar{X}_n & ; \text{if } \bar{V}_{n+1} = 0 \end{cases}$, *where $n \geq 0$,*

$$\bar{V}_{n+1} = \exp\left(B\left(\bar{Y}_n\right)\Delta\right)\left(\bar{X}_n + \sum_{k=1}^{m}\left(\sigma^k - \left\langle \bar{Y}_n, \sigma^k \bar{Y}_n \right\rangle\right)\bar{X}_n\sqrt{\Delta}\hat{W}_n^k\right)$$

and $\bar{Y}_n = \exp(B\Delta/2)\bar{X}_n / \left\|\exp(B\Delta/2)\bar{X}_n\right\|$. Define recursively $\bar{\eta}_{n+1}$ by (3.26) with $\hat{Y}_n = \bar{Y}_n$.

An alternative to $\bar{V}_n$ arises from solving (3.22) by the backward Euler method.

We next develop a different strategy, which has yielded promising results in our numerical experiments. Consider again equations (3.21) and (3.24). Suppose that $\bar{X}_n$ and $\bar{\rho}_n$ are $\mathcal{F}_{T_n}$-measurable random variables such that $\bar{X}_n \approx \hat{X}_{T_n}$, $\left\|\bar{X}_n\right\| = 1$, and $\bar{\rho}_n \approx \|X_{T_n}\|$. We define $Y_n(t)$ to be the solution of the ordinary differential equation

$$Y_n(t) = \bar{\rho}_n \bar{X}_n + \int_{T_n}^{t} BY_n(s)\, ds \qquad \forall t \in [T_n, T_{n+1}],$$

that is, $Y_n(t) = \exp(B(t - T_n))\,\bar{\rho}_n\bar{X}_n$. Since $\hat{Y}_n(t) := Y_n(t) / \|Y_n(t)\|$ satisfies

$$\hat{Y}_n(t) = \bar{X}_n + \int_{T_n}^{t}\left(B - \left\langle \hat{Y}_n(s), B\hat{Y}_n(s)\right\rangle\right)\hat{Y}_n(s)\, ds,$$

from (3.21) we obtain that for any $t \in [T_n, T_{n+1}]$,

$$\hat{X}_t \approx \hat{Y}_n(t) + \int_{T_n}^{t}\Psi\left(\hat{X}_s\right)\hat{X}_s ds + \sum_{k=1}^{m}\int_{T_n}^{t}\left(\sigma^k - \left\langle \hat{X}_s, \sigma^k\hat{X}_s\right\rangle\right)\hat{X}_s dW_s^k,$$

where $\Psi(x) = \sum_{k=1}^{m}\left(3\left\langle x, \sigma^k x\right\rangle^2/2 - \left\langle x, \sigma^k x\right\rangle\sigma^k - \left\|\sigma^k x\right\|^2/2\right)$, for each $x \in \mathbb{R}^d$. Hence

$$\hat{X}_t \approx \hat{Y}_n(t) + \int_{T_n}^{t}\Psi\left(\bar{X}_n\right)\hat{X}_s ds + \sum_{k=1}^{m}\int_{T_n}^{t}\left(\sigma^k - \left\langle \bar{X}_n, \sigma^k\bar{X}_n\right\rangle\right)\hat{X}_s dW_s^k.$$

In the spirit of the Euler-exponential schemes introduced by [153], we make the approximation $\hat{X}_t \approx \tilde{X}_t$, with

$$\tilde{X}_t = \hat{Y}_n(t) + \int_{T_n}^{t} \Psi\left(\bar{X}_n\right) \tilde{X}_s ds + \sum_{k=1}^{m} \int_{T_n}^{t} \left(\sigma^k - \left\langle \bar{X}_n, \sigma^k \bar{X}_n \right\rangle\right) \bar{X}_n dW_s^k. \tag{3.37}$$

Using (3.24) and $\|Y_n(t)\| = \bar{\rho}_n + \int_{T_n}^{t} \langle \hat{Y}_n(s), B\hat{Y}_n(s)\rangle \|Y_n(s)\| ds$ we can assert that $\|X_t\|$ is approximated by ρ_t, where $t \in [T_n, T_{n+1}]$ and

$$\begin{aligned} \rho_t &= \|Y_n(t)\| + \int_{T_n}^{t} \left(\sum_{k=1}^{m} \left(\left\| \sigma^k \bar{X}_n \right\|^2 /2 - \langle \bar{X}_n, \sigma^k \bar{X}_n \rangle^2 /2 \right) \right) \rho_s \, ds \\ &\quad + \sum_{k=1}^{m} \int_{T_n}^{t} \langle \bar{X}_n, \sigma^k \bar{X}_n \rangle \, \rho_s \, dW_s^k. \end{aligned} \tag{3.38}$$

Approximating the explicit solution of (3.38) we get $\rho_{T_{n+1}} \approx \bar{\rho}_{n+1}$, where

$$\bar{\rho}_{n+1} = \bar{\rho}_n \left\| \tilde{Y}_n \right\| \exp\left(\sum_{k=1}^{m} \left(\left\| \sigma^k \bar{X}_n \right\|^2 /2 - \langle \bar{X}_n, \sigma^k \bar{X}_n \rangle^2 \right) \Delta + \sum_{k=1}^{m} \langle \bar{X}_n, \sigma^k \bar{X}_n \rangle \sqrt{\Delta} \hat{W}_n^k \right) \tag{3.39}$$

with $\tilde{Y}_n = \exp(B\Delta) \bar{X}_n$.

Relations (3.37) and (3.39) are an alternative to (3.26) and (3.22). For instance, we derive the following numerical method by combining the property $\hat{Y}_n(T_{n+1}) = \tilde{Y}_n / \left\| \tilde{Y}_n \right\|$ with an approximation of the explicit solution of (3.37) obtained using arguments similar to that in [153].

Scheme 3.3.3 *Define recursively* $\bar{X}_{n+1} = \begin{cases} U_{n+1} / \|U_{n+1}\| & ; \text{ if } U_{n+1} \neq 0 \\ \bar{X}_n & ; \text{ if } U_{n+1} = 0 \end{cases}$, *where*

$$U_{n+1} = \exp\left(\Psi\left(\bar{X}_n\right) \Delta\right) \left(\tilde{Y}_n / \left\| \tilde{Y}_n \right\| + \sum_{k=1}^{m} \left(\sigma^k - \langle \bar{X}_n, \sigma^k \bar{X}_n \rangle \right) \bar{X}_n \sqrt{\Delta} \hat{W}_n^k \right) \tag{3.40}$$

for any $n \in \mathbb{Z}_+$. *Here* $\tilde{Y}_n = \exp(B\Delta) \bar{X}_n$ *and* $\hat{W}_0^1, \ldots, \hat{W}_0^m, \hat{W}_1^1, \ldots$ *are i.i.d. symmetric random variables having variance* 1. *Let* $(\bar{\rho}_n)_{n \geq 0}$ *be given by the recursive formula* (3.39).

Under the condition (3.41) given below, Higham, Mao and Yuan (2007) [102] proved that the backward Euler method applied to (3.20) is almost sure exponentially stable in case the step-size of discretization is small enough. Next, we establish the almost sure exponential stability of Scheme 3.3.3 for any $\Delta > 0$ provided that (3.41) holds.

Theorem 3.3.5 *Consider the Scheme 3.3.3 with* $\bar{\rho}_0 > 0$ *and* $\mathbb{E}(\bar{\rho}_0)^2 < \infty$. *Suppose that*

$$-\tilde{\lambda} := \sup_{x \in \mathbb{R}^d, \|x\|=1} \langle x, Bx \rangle + \sup_{x \in \mathbb{R}^d \|x\|=1} \sum_{k=1}^{m} \left(\left\| \sigma^k x \right\|^2 /2 - \langle x, \sigma^k x \rangle^2 \right) < 0. \tag{3.41}$$

Then $\limsup_{n \to \infty} \frac{1}{n\Delta} \log(\bar{\rho}_n) \leq -\tilde{\lambda} \ \ \mathbb{P} - a.s.$

Proof 3.3.5 *Deferred to Section 3.3.5.*

Using the relation (3.59) given in the proof of Theorem 3.3.5, we prove the following result in much the same way as Theorem 3.3.3.

Theorem 3.3.6 *Adopt the framework of Scheme 3.3.3. Suppose that* $\mathbb{E}\left(\bar{\rho}_0\right)^2 < \infty$, $\bar{\rho}_0 > 0$, *and that there exists* $\theta > 0$ *for which*

$$\inf_{\|y\|=1} \langle y, By\rangle + \frac{1}{2}\sum_{k=1}^{m}\left\|\sigma^k x\right\|^2 - (1+\theta)\sum_{k=1}^{m}\langle x, \sigma^k x\rangle^2 \geq 0 \qquad \forall \|x\| = 1.$$

Then $\liminf_{n\to\infty} \bar{\rho}_n > 0$ *a.s.*

Analysis similar to that in the proof of Theorem 3.3.4 shows that $\bar{U}_n \neq 0$ *a.s.* whenever the distribution of $\hat{W}_n^k$ is absolutely continuous with respect to the Lebesgue measure. As in Scheme 3.3.1, the performance of Scheme 3.3.3 is rarely affected by round-off errors. For example, we have $\|U_{n+1}\|^2 = \exp\left(-\frac{1}{2}\epsilon^2\Delta\right)\left(1+\epsilon^2\Delta\left(\hat{W}_n^2\right)^2\right)$ when we apply Scheme 3.3.3 to (3.31), and hence we can compute $U_{n+1}/\|U_{n+1}\|$ without taking precautions against $U_{n+1} \approx 0$ unless Δ is very large. Next, we assert that the rate of weak convergence of Scheme 3.3.3 is equal to 1 in case $\hat{W}_n^k$ is bounded.

Theorem 3.3.7 *Assume that* $T > 0$, $f \in C_p^4\left(\mathbb{R}^d, \mathbb{R}\right)$ *and that* X_0 *has finite moments of any order. Consider* $\bar{\rho}_n\bar{X}_n$ *defined by Scheme 3.3.3 with* $\Delta = T/N$, *where* $N \in \mathbb{N}$. *Let* $\hat{W}_n^k$ *be a bounded random variable. Given any* $g \in C_p^4\left(\mathbb{R}^d, \mathbb{R}\right)$ *suppose that* $\left|\mathbb{E}g\left(X_0\right) - \mathbb{E}g\left(\bar{\rho}_0\bar{X}_0\right)\right| \leq K\left(1+\mathbb{E}\left\|X_0\right\|^q\right)T/N$ *for all* $N \in \mathbb{N}$. *Then*

$$\left|\mathbb{E}f\left(X_T\right) - \mathbb{E}f\left(\bar{\rho}_N\bar{X}_N\right)\right| \leq K\left(T\right)\left(1+\mathbb{E}\left\|X_0\right\|^q\right)T/N \qquad \forall N \in \mathbb{N}. \tag{3.42}$$

Proof 3.3.6 *Deferred to Section 3.3.5.*

Remark 3.3.2 *Applying the Euler approximation to* (3.37) *we get:*

Scheme 3.3.4 *Let* $\hat{W}_0^1, \hat{W}_0^2, \ldots, \hat{W}_0^m, \hat{W}_1^1, \ldots$ *be i.i.d. symmetric random variables having variance* 1. *Define recursively* $\bar{X}_{n+1} = \begin{cases} V_{n+1}/\left\|V_{n+1}\right\| & ;\ \text{if } V_{n+1} \neq 0 \\ \bar{X}_n & ;\ \text{if } V_{n+1} = 0 \end{cases}$, *with*

$$V_{n+1} = \tilde{Y}_n/\left\|\tilde{Y}_n\right\| + \Psi\left(\bar{X}_n\right)\bar{X}_n\Delta + \sum_{k=1}^{m}\left(\sigma^k - \langle\bar{X}_n, \sigma^k\bar{X}_n\rangle\right)\bar{X}_n\sqrt{\Delta}\hat{W}_n^k,$$

where $n \in \mathbb{Z}_+$ *and* $\tilde{Y}_n = \exp\left(B\Delta\right)\bar{X}_n$. *Furthermore,* $\left(\bar{\rho}_n\right)_{n\geq 0}$ *is described by* (3.39).

3.3.4 Numerical experiments: ill-conditioned drift

This subsection addresses the bilinear test (3.31), but with more general drift coefficient B.

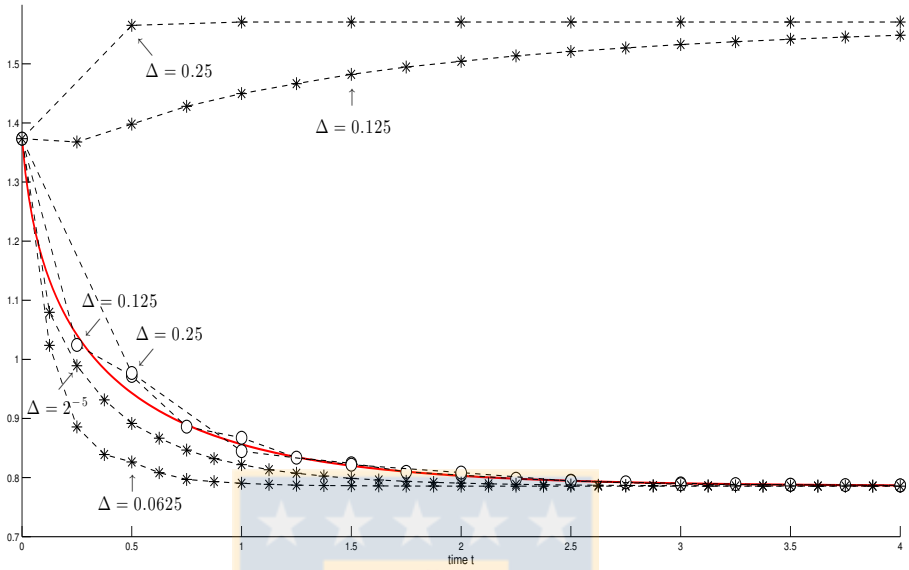

Figure 3.10: Computation of $\mathbb{E}\arctan\left(1+\left(X_t^2\right)^2\right)$, where $t \in [0,4]$ and X_t solves (3.43) with $b_1 = -100$, $b_2 = 2$, $\sigma = 4$, $\epsilon = 1$ and $X_0 = (1,2)^\top$. The true values are plotted with a solid line. The circles and stars represent the approximations obtained by Scheme 3.3.3 and $\bar{E}_n$ respectively

Diagonal matrix B

We deal with the numerical solution of the SDE

$$X_t = X_0 + \int_0^t \begin{pmatrix} b_1 & 0 \\ 0 & b_2 \end{pmatrix} X_s \, ds + \int_0^t \begin{pmatrix} \sigma & 0 \\ 0 & \sigma \end{pmatrix} X_s \, dW_s^1 + \int_0^t \begin{pmatrix} 0 & -\epsilon \\ \epsilon & 0 \end{pmatrix} X_s \, dW_s^2, \tag{3.43}$$

with $\sigma = 4$, $\epsilon = 1$ and $X_0 = (1,2)^\top$. In order to study cases where B is ill-conditioned, we take $b_1 = -100$ and $b_2 = 2$. Since $-\tilde{\lambda} = \max\{b_1, b_2\} + \left(\epsilon^2 - \sigma^2\right)/2 = -11/2$, X_t converges exponentially fast to 0 as t tends to infinity.

As in Subsection 3.3.2, we compute expectations of the bounded process $\arctan\left(1+\left(X_t^2\right)^2\right)$, where $X_t = \left(X_t^1, X_t^2\right)$. The reference values for $\mathbb{E}\arctan\left(1+\left(X_t^2\right)^2\right)$ have been obtained by sampling 10^8 times the Euler-Maruyama scheme

$$E_{n+1} = E_n + BE_n\Delta + \sum_{k=1}^{m} \sigma^k E_n \sqrt{\Delta}\xi_n^k$$

with step-size $\Delta = 2^{-14} \approx 0.0000610$. Here, $\xi_0^1, \xi_0^2, \ldots, \xi_0^m, \xi_1^1, \ldots$ are independent random variables taking values ± 1 with probability $1/2$. In Figure 3.10 the "true" values are plotted with a solid line.

Δ	Backward Euler	Scheme 3.3.1	Scheme 3.3.2	Scheme 3.3.3	Scheme 3.3.4
1/2	–	0.15767	0.16262	0.11463	0.097492
1/4	0.62209	0.15767	0.039728	0.033856	0.033187
1/8	0.45494	0.15767	0.055127	0.028848	0.027073
1/16	0.1167	0.15767	0.031429	0.00092922	0.00001519
1/32	0.051448	0.15765	0.02738	0.0034819	0.0030137
1/64	0.022656	0.057997	0.022279	0.0013437	0.001135
$\mathbf{2^{-7}}$	0.010789	0.015613	0.016977	0.0007307	0.00065061
$\mathbf{2^{-8}}$	0.0052678	0.0061579	0.011165	0.00037132	0.00034013
$\mathbf{2^{-9}}$	0.0031195	0.0032785	0.0059087	0.00034469	0.0003577
$\mathbf{2^{-10}}$	0.001551	0.001571	0.0032079	0.00017328	0.00017914
$\mathbf{2^{-11}}$	0.00045271	0.00044898	0.001994	0.00023427	0.0002315
$\mathbf{2^{-12}}$	0.00031327	0.00030817	0.00092728	0.000029582	0.000028237

Table 3.3: Absolute errors $\left|\mathbb{E}f\left(X_T\right) - \mathbb{E}f\left(Y_{T/\Delta}\right)\right|$ involved in the computation of $\mathbb{E}f\left(X_T\right)$, where X_t verifies the equation (3.43), $T = 0.5$ and $f\left(x_1, x_2\right) = \arctan\left(1 + \left(x_2\right)^2\right)$.

Moreover, the circles (resp. stars) represent the estimated values of $\mathbb{E}\arctan\left(1 + \left(X_t^2\right)^2\right)$ produced by averaging over 10^6 observations of Scheme 3.3.3 with $\hat{W}_n^k = \xi_n^k$ (resp. the backward Euler method $\bar{E}_n$ given by (3.32). Figure 3.10 shows that the second coordinate of $\bar{E}_n$ does not converge to 0 when $\Delta = 0.25, 0.125$, and it goes too fast to 0 for $\Delta = 0.0625$. On the contrary, Scheme 3.3.3 is very accurate, even with $\Delta = 0.25$.

Table 3.3 presents the errors produced at time $T = 0.5$ by the backward Euler and the new numerical methods. We assign the weak error $\varepsilon\left(Y, \Delta\right) := \left|\mathbb{E}f\left(X_T\right) - \mathbb{E}f\left(Y_{T/\Delta}\right)\right|$ to every scheme Y with step-size Δ, where $f\left(x_1, x_2\right) = \arctan\left(1 + \left(x_2\right)^2\right)$. Table 3.3 compares estimates of $\varepsilon\left(Y, \Delta\right)$ obtained by sampling 10^6 times the backward Euler method $\bar{E}_n$ and Schemes 3.3.1, ... , 3.3.4, each of them with $\hat{W}_n^k = \xi_n^k$. The length of all the 99%-confidence intervals are at least of order 10^{-3} (see e.g. [120]). Table 3.3 shows that the values of $\varepsilon\left(\textit{Scheme } 3.3.3, \Delta\right)$ and $\varepsilon\left(\textit{Scheme } 3.3.4, \Delta\right)$ are quite similar. We can also see that Schemes 3.3.3 and 3.3.4 are very accurate. Moreover, the second coordinate given by Scheme 3.3.1 decays too fast to 0 when $\Delta \geq 1/32$. Finally, Scheme 3.3.2 has exponentially stable trajectories, but tends to 0 slightly more slowly than the reference solution.

Non-normal matrix B

Let us consider the test problem

$$dX_t = \begin{pmatrix} b & \beta \\ 0 & b \end{pmatrix} X_t \, dt + \begin{pmatrix} \sigma & 0 \\ 0 & \sigma \end{pmatrix} X_t \, dW_t^1 + \begin{pmatrix} 0 & \epsilon \\ -\epsilon & 0 \end{pmatrix} X_t \, dW_t^2, \tag{3.44}$$

$\boldsymbol{\Delta}$	**1/2**	**1/4**	**1/8**	**1/16**	**1/32**	**1/64**	**1/128**
$\sigma = 0,\ T = 6,\ f(x_1, x_2) = x_1,\ g(x_1, x_2) = x_2$							
$\bar{\boldsymbol{E}}$	3.678	2.2215	1.3374	0.72102	0.37507	0.19127	0.09612
$\bar{\boldsymbol{\rho}}\bar{\boldsymbol{X}}$	0.68916	0.84471	0.50458	0.20551	0.083903	0.038641	0.017797
$\sigma = 3/2,\ T = 6,\ f(x_1, x_2) = \log\left(1 + x_1^2\right),\ g(x_1, x_2) = \log\left(1 + x_2^2\right)$							
$\bar{\boldsymbol{E}}$	2.8724	0.95405	0.70717	0.38121	0.20104	0.10199	0.051117
$\bar{\boldsymbol{\rho}}\bar{\boldsymbol{X}}$	0.30013	0.34581	0.23995	0.20972	0.098283	0.049348	0.024578
$\sigma = 3,\ T = 4,\ f(x_1, x_2) = \log\left(1 + x_1^2\right),\ g(x_1, x_2) = \log\left(1 + x_2^2\right)$							
$\bar{\boldsymbol{E}}$	10.873	6.92	1.5617	0.6615	0.30483	0.14916	0.071085
$\bar{\boldsymbol{\rho}}\bar{\boldsymbol{X}}$	0.35669	0.41193	0.19277	0.16472	0.078604	0.038411	0.019084

Table 3.4: Estimated values of $\max\{|\mathbb{E}f(X_{n\Delta}) - \mathbb{E}f(Y_n)| + |\mathbb{E}g(X_{n\Delta}) - \mathbb{E}g(Y_n)| : n = 0, \ldots, T/\Delta\}$, where X_t solves (3.44) and Y_n stands for $\bar{E}_n$ and Scheme 3.3.3.

with $X_0 = (-6, 4)^\top$, $b = -2$, $\beta = 10$ and $\epsilon = 1/\sqrt[4]{\beta}$. Moreover, we choose σ equal to 0, 3/2 and 3. In case $\sigma = 0$, equation (3.44) reduces to a mean-square asymptotically stable SDE of the type studied in [44, 100]. Since (3.44) is *a.s.* exponentially stable whenever $-\tilde{\lambda} = b + |\beta|/2 + \left(\epsilon^2 - \sigma^2\right)/2 < 0$ (see e.g. [102]), we can ensure that (3.44) with $\sigma = 3$ is *a.s.* exponentially stable. An analysis similar to that in the proof of Theorem 2.2 of [44] shows that (3.44) is mean-square asymptotically stable if and only if $\epsilon^2/3 - 2b - \sigma^2$ is greater than $\frac{1}{3}\sqrt[3]{8\epsilon^6 + 27\beta^2\epsilon^2 + 3\sqrt{48\epsilon^8\beta^2 + 81\beta^4\epsilon^4}} + \frac{4}{3}\epsilon^4/\sqrt[3]{8\epsilon^6 + 27\beta^2\epsilon^2 + 3\sqrt{48\epsilon^8\beta^2 + 81\beta^4\epsilon^4}}$. Hence, (3.44) is mean-square "unstable" for $\sigma = 3/2, 3$.

Table 3.4 compares the errors arising from averaging 10^8 samples of both Scheme 3.3.3 with $\hat{W}_n^k = \xi_n^k$ and the backward Euler scheme $\bar{E}_n$ given by (3.32). The final integration times $T > 0$ are large enough in order to guarantee that X_T is very small with high probability. The "true" values have been calculated by sampling 10^8 paths of $\bar{E}_n$ with $\Delta = 2^{-14}$. In Table 3.4 we can observe that Scheme 3.3.3 approximates well X_t, even for large step sizes Δ. As we illustrate in Figure 3.11, the good performance of Scheme 3.3.3 is due to its ability to approximate very well the transient behavior that X_t has before reaching the equilibrium point (see e.g. [44, 100]).

3.3.5 Proofs

Proof of Theorem 3.3.1

We first establish that for an arbitrary $q \geq 2$,

$$\mathbb{E}\left\|\bar{\eta}_n \bar{X}_n\right\|^q \leq K(T)\,\mathbb{E}\left|\bar{\eta}_0\right|^q \qquad \forall n = 0, \ldots, N. \tag{3.45}$$

To shorten notation, we set $\lambda^k\left(\bar{X}_n\right) = \left\langle \bar{X}_n, \sigma^k \bar{X}_n \right\rangle$ and

$$\mu\left(\bar{X}_n\right) = \left\langle \bar{X}_n, B\bar{X}_n \right\rangle + \sum_{k=1}^{m} \left(\left\|\sigma^k \bar{X}_n\right\|^2 - \left\langle \bar{X}_n, \sigma^k \bar{X}_n \right\rangle^2 \right)/2.$$

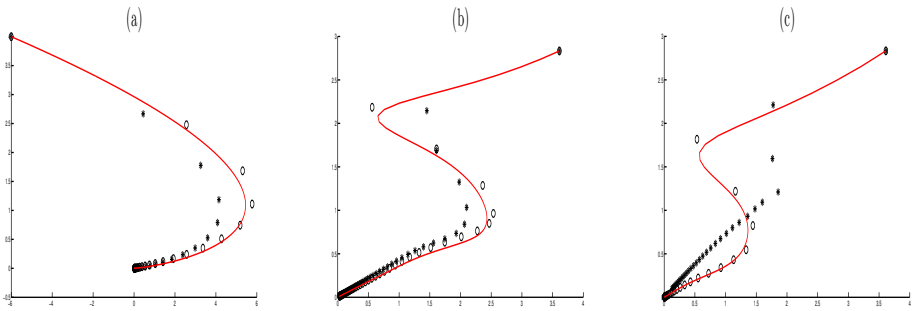

Figure 3.11: Estimated values of $(\mathbb{E}f(X_t), \mathbb{E}g(X_t))$ obtained by Scheme 3.3.3 (circles) and the backward Euler scheme $\bar{E}_n$ (stars). Here X_t solves (3.44) and the true values are plotted with a solid red line. (a) $\Delta = 1/4$, $\sigma = 0$, $f(x) = x_1$, $g(x) = x_2$; (b) $\Delta = 1/8$, $\sigma = 3/2$, $f(x) = \log\left(1 + x_1^2\right)$, $g(x) = \log\left(1 + x_2^2\right)$; and (c) $\Delta = 1/8$, $\sigma = 3$, $f(x) = \log\left(1 + x_1^2\right)$, $g(x) = \log\left(1 + x_2^2\right)$.

Similar to the proof of (3.17), we rewrite $\bar{\eta}_{n+1}$ as $\exp(h_n)\bar{\eta}_n$, and so

$$\bar{\eta}_{n+1} = \bar{\eta}_n + (\exp(h_n) - 1 - h_n)\bar{\eta}_n + h_n\bar{\eta}_n,$$

with $h_n := \left(\mu\left(\bar{X}_n\right) - \frac{1}{2}\sum_{k=1}^m \lambda^k\left(\bar{X}_n\right)^2\right)\Delta + \sum_{k=1}^m \lambda^k\left(\bar{X}_n\right)\sqrt{\Delta}\hat{W}_n^k$. Thus

$$\bar{\eta}_{n+1} = \bar{\eta}_0 + \sum_{k=0}^n (\exp(h_k) - 1 - h_k)\bar{\eta}_k + \sum_{k=0}^n h_k\bar{\eta}_k.$$

Using $|\exp(h_k) - 1 - h_k| \le |h_k|^2 \exp(|h_k|)$ we obtain

$$\begin{aligned}|\bar{\eta}_{n+1}|^q \le & K|\bar{\eta}_0|^q + K(n+1)^{q-1}\sum_{k=0}^n |h_k|^{2q} e^{q|h_k|}|\bar{\eta}_k|^q + K\Delta^{q/2}\sum_{j=1}^m \left|\sum_{k=0}^n \lambda^j\left(\bar{X}_k\right)\bar{\eta}_k\hat{W}_k^j\right|^q \\ & + K(n+1)^{q-1}\sum_{k=0}^n \Delta^q\left|\mu\left(\bar{X}_k\right) - \frac{1}{2}\sum_{j=1}^m \lambda^j\left(\bar{X}_k\right)^2\right|^q |\bar{\eta}_k|^q. \end{aligned} \tag{3.46}$$

For any $k \in \mathbb{Z}_+$, $\left|\mu\left(\bar{X}_k\right)\right| \le K$ and $\left|\lambda^j\left(\bar{X}_k\right)\right| \le K$, because $\left\|\bar{X}_k\right\| = 1$. We also have that $\hat{W}_0^1$ is a bounded random variable. Then, applying the Burkholder-Davis-Gundy inequality we deduce from (3.46) that

$$\mathbb{E}|\bar{\eta}_{n+1}|^q \le K\mathbb{E}|\bar{\eta}_0|^q + K(T)\Delta\sum_{k=0}^n \mathbb{E}|\bar{\eta}_k|^q$$

for all $n = 0, \ldots, N-1$. A discrete Gronwall lemma (see e.g. [10]) now leads to (3.45).

We proceed to find a truncated asymptotic expansion of $\bar{\eta}_{n+1}\bar{X}_{n+1}$ as Δ goes to 0. In what follows, we use the same symbol $\mathcal{O}(\cdot)$ for different random functions from $\left[0, T^2\right]$ to $\mathbb{R}$ or $\mathbb{R}^{d\times d}$ such that $\|\mathcal{O}(s)\| \le K(T)s$. Since

$$\left|\exp(x) - \left(1 + x + x^2/2 + x^3/6\right)\right| \le x^4\exp(|x|),$$

$$\begin{aligned}\bar{\eta}_{n+1} &= \bar{\eta}_n\left(1+\left(\mu\left(\bar{X}_n\right)-\frac{1}{2}\sum_{k=1}^{m}\lambda^k\left(\bar{X}_n\right)^2\right)\Delta+\sum_{k=1}^{m}\lambda^k\left(\bar{X}_n\right)\hat{W}_n^k\sqrt{\Delta}\right) \\ &+\bar{\eta}_n\left(\mu\left(\bar{X}_n\right)-\frac{1}{2}\sum_{j=1}^{m}\lambda^j\left(\bar{X}_n\right)^2\right)\left(\sum_{k=1}^{m}\lambda^k\left(\bar{X}_n\right)\hat{W}_n^k\right)\Delta^{3/2} \\ &+\frac{\bar{\eta}_n}{2}\left(\sum_{k=1}^{m}\lambda^k\left(\bar{X}_n\right)\hat{W}_n^k\right)^2\Delta+\frac{\bar{\eta}_n}{6}\left(\sum_{k=1}^{m}\lambda^k\left(\bar{X}_n\right)\hat{W}_n^k\right)^3\Delta^{3/2}+\bar{\eta}_n\mathcal{O}\left(\Delta^2\right).\end{aligned} \tag{3.47}$$

Multiplying the right hand sides of (3.27) and (3.47) yields

$$\begin{aligned}\bar{\eta}_{n+1}\bar{Z}_{n+1} &= \left(1+B\Delta+\sum_{k=1}^{m}\sigma^k\hat{W}_n^k\sqrt{\Delta}\right)\bar{\eta}_n\bar{X}_n+\Gamma_n\Delta^{3/2}\bar{\eta}_n\bar{X}_n \\ &+\Delta\sum_{k=1}^{m}\left(\sigma^k-\lambda^k\left(\bar{X}_n\right)/2\right)\lambda^k\left(\bar{X}_n\right)\left(\left(\hat{W}_n^k\right)^2-1\right)\bar{\eta}_n\bar{X}_n \\ &+\Delta\sum_{k\neq j}\left(\sigma^j-\lambda^j\left(\bar{X}_n\right)/2\right)\lambda^k\left(\bar{X}_n\right)\hat{W}_n^j\hat{W}_n^k\,\bar{\eta}_n\bar{X}_n+\mathcal{O}\left(\Delta^2\right)\bar{\eta}_n\bar{X}_n,\end{aligned} \tag{3.48}$$

where Γ_n is a random matrix such that $\|\Gamma_n\|\leq K$ and $\mathbb{E}\left(\Gamma_n\diagup\mathcal{F}_{T_n}\right)=0$; throughout the proof, we assume without loss of generality that $\hat{W}_n^1,\ldots\hat{W}_n^m$ are $\mathcal{F}_{T_{n+1}}$-measurable and independent of $\mathcal{F}_{T_n}$. Indeed,

$$\begin{aligned}\Gamma_n &= \left(B+\frac{1}{2}\sum_{k=1}^{m}\lambda^k\left(\bar{X}_n\right)^2-\sum_{k=1}^{m}\lambda^k\left(\bar{X}_n\right)\sigma^k\right)\sum_{j=1}^{m}\lambda^j\left(\bar{X}_n\right)\hat{W}_n^j \\ &+\frac{1}{6}\left(\sum_{k=1}^{m}\lambda^k\left(\bar{X}_n\right)\hat{W}_n^k\right)^3+\left(\mu\left(\bar{X}_n\right)-\frac{1}{2}\sum_{k=1}^{m}\lambda^k\left(\bar{X}_n\right)^2\right)\sum_{k=1}^{m}\left(\sigma^k-\lambda^k\left(\bar{X}_n\right)\right)\hat{W}_n^k.\end{aligned}$$

From (3.27) we have

$$\begin{aligned}\left\|\bar{Z}_{n+1}\right\|^2 &= 1+\Delta\sum_{k=1}^{m}\left(\lambda^k\left(\bar{X}_n\right)^2-\left\|\sigma^k\bar{X}_n\right\|^2\right)\left(1-\left(\hat{W}_n^k\right)^2\right) \\ &+\Delta\sum_{k\neq j}\left(\left\langle\sigma^k\bar{X}_n,\sigma^j\bar{X}_n\right\rangle-\lambda^j\left(\bar{X}_n\right)\lambda^k\left(\bar{X}_n\right)\right)\hat{W}_n^k\hat{W}_n^j \\ &+2\Delta^{3/2}\sum_{k=1}^{m}\left\langle B\left(\bar{X}_n\right)\bar{X}_n,\sigma^k\bar{X}_n-\lambda^k\left(\bar{X}_n\right)\bar{X}_n\right\rangle\hat{W}_n^k+\mathcal{O}\left(\Delta^2\right).\end{aligned} \tag{3.49}$$

Hence, there exists $\Delta_0>0$ such that $\left|1-\left\|\bar{Z}_{n+1}\right\|^2\right|\leq 1/2$ for all $\Delta\leq\Delta_0$, because $\left|\hat{W}_n^k\right|\leq K$. Using the power series expansion of $x\mapsto(1+x)^{-1/2}$ we get

$$\frac{1}{\|z\|}=1+\frac{1}{2}\left(1-\|z\|^2\right)+\left(1-\|z\|^2\right)^2\sum_{k=2}^{\infty}\frac{(2k)!}{(k!)^2\,4^k}\left(1-\|z\|^2\right)^{k-2}$$

whenever $\left|1-\|z\|^2\right|<1$. This, together with (3.49), implies that for all $\Delta\leq\Delta_0$,

$$\begin{aligned}1/\left\|\bar{Z}_{n+1}\right\| &= 1+\frac{\Delta}{2}\sum_{k=1}^{m}\left(\lambda^k\left(\bar{X}_n\right)^2-\left\|\sigma^k\bar{X}_n\right\|^2\right)\left(\left(\hat{W}_n^k\right)^2-1\right) \\ &\quad -\frac{\Delta}{2}\sum_{k\neq j}\left(\left\langle\sigma^k\bar{X}_n,\sigma^j\bar{X}_n\right\rangle-\lambda^j\left(\bar{X}_n\right)\lambda^k\left(\bar{X}_n\right)\right)\hat{W}_n^k\hat{W}_n^j \\ &\quad -\Delta^{3/2}\sum_{k=1}^{m}\left\langle B\left(\bar{X}_n\right)\bar{X}_n,\sigma^k\bar{X}_n-\lambda^k\left(\bar{X}_n\right)\bar{X}_n\right\rangle\hat{W}_n^k+\mathcal{O}\left(\Delta^2\right).\end{aligned} \tag{3.50}$$

Combining (3.48) with (3.50) gives

$$\begin{aligned}\bar{\eta}_{n+1}\bar{X}_{n+1} &= \left(1+B\Delta+\sum_{k=1}^{m}\sigma^k\hat{W}_n^k\sqrt{\Delta}\right)\bar{\eta}_n\bar{X}_n+\tilde{\Gamma}_n\Delta^{3/2}\bar{\eta}_n\bar{X}_n \\ &\quad +\Delta\sum_{k=1}^{m}\left(\lambda^k\left(\bar{X}_n\right)\sigma^k-\left\|\sigma^k\bar{X}_n\right\|^2/2\right)\left(\left(\hat{W}_n^k\right)^2-1\right)\bar{\eta}_n\bar{X}_n \\ &\quad +\Delta\sum_{k\neq j}\left(\lambda^k\left(\bar{X}_n\right)\sigma^j-\left\langle\sigma^k\bar{X}_n,\sigma^j\bar{X}_n\right\rangle/2\right)\hat{W}_n^j\hat{W}_n^k\ \bar{\eta}_n\bar{X}_n+\mathcal{O}\left(\Delta^2\right)\bar{\eta}_n\bar{X}_n,\end{aligned} \tag{3.51}$$

where $\Delta\leq\Delta_0$ and $\tilde{\Gamma}_n$ is a random matrix satisfying $\left\|\tilde{\Gamma}_n\right\|\leq K$ and $\mathbb{E}\left(\tilde{\Gamma}_n\diagup\mathcal{F}_{T_n}\right)=0$.

By (3.45), it is sufficient to prove that (3.28) holds for all $N\geq T/\Delta_0$. Then, from now we suppose $\Delta\leq\Delta_0$. Looking at (3.51) we easily see that $\left\|\bar{\eta}_{n+1}\bar{X}_{n+1}-\bar{\eta}_n\bar{X}_n\right\|\leq K\left(T\right)\Delta^{1/2}\left\|\bar{\eta}_n\bar{X}_n\right\|$, and so

$$\mathbb{E}\left(\left\|\bar{\eta}_{n+1}\bar{X}_{n+1}-\bar{\eta}_n\bar{X}_n\right\|^q\diagup\mathcal{F}_{T_n}\right)\leq K\left(T\right)\Delta^{q/2}\left(1+\left\|\bar{\eta}_n\bar{X}_n\right\|^q\right). \tag{3.52}$$

Moreover, (3.51) leads to

$$\begin{aligned}&\left\|\mathbb{E}\left(\bar{\eta}_{n+1}\bar{X}_{n+1}-\bar{\eta}_n\bar{X}_n-\left(B\Delta+\sum_{k=1}^{m}\sigma^k\left(W_{T_{n+1}}^k-W_{T_n}^k\right)\right)\bar{\eta}_n\bar{X}_n\diagup\mathcal{F}_{T_n}\right)\right\| \\ \leq\ & K\left(T\right)\Delta^2\left(1+\left\|\bar{\eta}_n\bar{X}_n\right\|\right).\end{aligned}$$

Using again (3.51) we deduce that, up to terms of order $\mathcal{O}\left(\Delta^2\right)\left\|\bar{\eta}_n\bar{X}_n\right\|^q$, the second and third moments of $\bar{\eta}_{n+1}\bar{X}_{n+1}-\bar{\eta}_n\bar{X}_n$ coincide with that of

$$B\bar{\eta}_n\bar{X}_n\Delta+\sum_{k=1}^{m}\sigma^k\bar{\eta}_n\bar{X}_n\hat{W}_n^k\sqrt{\Delta},$$

and then with that of $\left(B\Delta+\sum_{k=1}^{m}\sigma^k\left(W_{T_{n+1}}^k-W_{T_n}^k\right)\right)\bar{\eta}_n\bar{X}_n$. Therefore, combining classical arguments [146, 196, 197] with (3.45) and (3.52) we can assert that (3.28) holds for all $T/N\leq\Delta_0$ (see also Theorem 14.5.2 of [120]).

Proof of Theorem 3.3.2

Using (3.26) yields

$$\log\left(\bar{\eta}_{n+1}\right) = \log\left(\bar{\eta}_0\right) + \sum_{j=0}^{n}\left(\langle \bar{X}_j, B\bar{X}_j\rangle + \frac{1}{2}\sum_{k=1}^{m}\left\|\sigma^k\bar{X}_j\right\|^2 - \sum_{k=1}^{m}\langle \bar{X}_j, \sigma^k\bar{X}_j\rangle^2\right)\Delta + S_n, \tag{3.53}$$

where $S_n = \sum_{j=0}^{n}\sum_{k=1}^{m}\langle \bar{X}_j, \sigma^k\bar{X}_j\rangle\sqrt{\Delta}\hat{W}_j^k$. Then, (3.29) leads to

$$\frac{1}{n+1}\log\left(\bar{\eta}_{n+1}\right) \leq \frac{1}{n+1}\log\left(\bar{\eta}_0\right) + \frac{1}{n+1}S_n - \lambda\Delta. \tag{3.54}$$

Since

$$\mathbb{E}\left(\sum_{k=1}^{m}\langle \bar{X}_j, \sigma^k\bar{X}_j\rangle\sqrt{\Delta}\hat{W}_j^k\right)^2 \leq \mathbb{E}\left(\sum_{k=1}^{m}\left\|\sigma^k\right\|\left\|\bar{X}_j\right\|^2\sqrt{\Delta}\left|\hat{W}_j^k\right|\right)^2 \leq K\Delta,$$

applying a generalized law of large numbers, as in the proof of Theorem 3.2.1, we obtain that $S_n/\left(n+1\right) \to 0$ *a.s.* From (3.54) it follows that

$$\limsup_{n\to\infty}\frac{1}{n+1}\log\left(\bar{\eta}_{n+1}\right) \leq -\lambda\Delta \qquad a.s.$$

Proof of Theorem 3.3.3

We return to the proof of Theorem 3.3.2. By (3.30), it follows from (3.53) that

$$\log\left(\bar{\eta}_{n+1}\right) \geq \log\left(\bar{\eta}_0\right) + \theta A_n + S_n, \tag{3.55}$$

where $A_n = \sum_{j=0}^{n}\sum_{k=1}^{m}\langle \bar{X}_j, \sigma^k\bar{X}_j\rangle^2\Delta$. Since S_n is a square integrable martingale with quadratic variation process A_n, S_n converges *a.s.* on $\{A_\infty < \infty\}$ to a finite random variable η (see Section 2.6.1 of [70]). Therefore $\liminf_{n\to\infty}\log\left(\bar{\eta}_n\right) \geq \log\left(\bar{\eta}_0\right) + \theta A_\infty + \eta$ almost surely on $\{A_\infty < \infty\}$, and so $\liminf_{n\to\infty}\bar{\eta}_n > 0$ *a.s.* on the event $\{A_\infty < \infty\}$.

Applying the strong law of large numbers for martingales (see Section 2.6.1 of [70]) we obtain that $S_n/A_n \longrightarrow_{n\to\infty} 0$ *a.s.* on $\{A_\infty = \infty\}$. Hence (3.55) yields $\liminf_{n\to\infty}\log\left(\bar{\eta}_n\right)/A_n \geq \theta$ *a.s.* on $\{A_\infty = \infty\}$, which implies

$$\liminf_{n\to\infty}\bar{\eta}_n = +\infty \qquad a.s.\text{ on }\left\{A_\infty = \infty\right\}.$$

Proof of Theorem 3.3.4

Let $n \in \mathbb{Z}_+$. Suppose that there exist $x \in \mathbb{R}^n$ satisfying $\|x\| = 1$ and an event A having positive probability such that

$$x + B\left(x\right)x\Delta + \sum_{k=1}^{m}\left(\sigma^k - \left\langle x, \sigma^k x\right\rangle\right)x\sqrt{\Delta}\hat{W}_n^k\left(\omega\right) = 0 \qquad \forall\omega \in A. \tag{3.56}$$

Fix $\omega_0 \in A$. By (3.56),

$$\sum_{k=1}^{m} \left(\sigma^k - \left\langle x, \sigma^k x \right\rangle\right) x \left(\hat{W}_n^k(\omega) - \hat{W}_n^k(\omega_0)\right) = 0 \qquad \forall \omega \in A. \tag{3.57}$$

Since $\left\{\left(\hat{W}_n^1(\omega) - \hat{W}_n^1(\omega_0), \ldots, \hat{W}_n^m(\omega) - \hat{W}_n^m(\omega_0)\right)^\top : \omega \in A\right\}$ has positive Lebesgue measure, this subset contains a basis of $\mathbb{R}^m$. Then, (3.57) leads to $\sigma^k x - \langle x, \sigma^k x\rangle\, x = 0$. Therefore, x is an eigenvector of all σ^k, and so (3.56) becomes

$$x + \Delta\left(Bx - \langle x, Bx\rangle\, x\right) = 0. \tag{3.58}$$

Hence x is an eigenvector of B, which yields $Bx - \langle x, Bx\rangle\, x = 0$. From (3.58) it follows that $x = 0$, contrary to $\|x\| = 1$. Thus, we have obtained that $x + B(x)\, x\Delta + \sum_{k=1}^{m}\left(\sigma^k - \left\langle x, \sigma^k x\right\rangle\right) x\sqrt{\Delta}\hat{W}_n^k \neq 0$ *a.s.* whenever $\|x\| = 1$. Finally, using regular conditional distributions we deduce that $\bar{Z}_{n+1} \neq 0$ *a.s.*

Proof of Theorem 3.3.5

From (3.39) we have

$$\log(\bar{\rho}_{n+1}) = \log(\bar{\rho}_0) + \sum_{j=0}^{n}\left(\log\left\|e^{B\Delta}\bar{X}_j\right\| + \sum_{k=1}^{m}\left(\frac{1}{2}\left\|\sigma^k\bar{X}_j\right\|^2 - \langle\bar{X}_j, \sigma^k\bar{X}_j\rangle^2\right)\Delta\right) + S_n,$$

where $S_n = \sum_{j=0}^{n}\sum_{k=1}^{m}\langle\bar{X}_j, \sigma^k\bar{X}_j\rangle\sqrt{\Delta}\hat{W}_j^k$. Set $Y_j(t) := \exp(B(t - T_j))\,\bar{X}_j$. Since $dY_j(t)/dt = BY_j(t)$, combining $\left\|\bar{X}_j\right\| = 1$ with the fundamental theorem of calculus yields

$$\log\|Y_j(t)\| = \int_{T_j}^{t}\langle Y_j(s)/\|Y_j(s)\|, BY_j(s)/\|Y_j(s)\|\rangle ds,$$

and so

$$\begin{aligned}\log(\bar{\rho}_{n+1}) &= \log(\bar{\rho}_0) + S_n \\ &+ \sum_{j=0}^{n}\left(\int_{T_j}^{T_{j+1}}\langle\frac{Y_j(s)}{\|Y_j(s)\|}, B\frac{Y_j(s)}{\|Y_j(s)\|}\rangle ds + \sum_{k=1}^{m}\left(\frac{1}{2}\left\|\sigma^k\bar{X}_j\right\|^2 - \langle\bar{X}_j, \sigma^k\bar{X}_j\rangle^2\right)\Delta\right).\end{aligned} \tag{3.59}$$

Combining (3.41) and (3.59) we obtain

$$\log(\bar{\rho}_{n+1}) \leq \log(\bar{\rho}_0) - (n+1)\,\Delta\tilde{\lambda} + S_n.$$

As in the proof of Theorems 3.2.1 and 3.3.2, a generalized law of large numbers gives $S_n/(n+1) \to 0$ *a.s.*, and the theorem follows.

Proof of Theorem 3.3.7

Set $Y_n(t) = \exp(B(t-T_n))\bar{X}_n$ and $\hat{Y}_n(t) := Y_n(t)/\|Y_n(t)\|$. Then

$$\|Y_n(t)\| = 1 + \int_{T_n}^{t} \langle \hat{Y}_n(s), B\hat{Y}_n(s)\rangle \|Y_n(s)\|\, ds.$$

Hence $\left\|\tilde{Y}_n\right\| = \exp\left(\int_{T_n}^{T_{n+1}} \left\langle \hat{Y}_n(s), B\hat{Y}_n(s)\right\rangle ds\right)$, and so $\bar{\rho}_{n+1} = \exp(h_n)\bar{\rho}_n$, where

$$h_n = \left(\tilde{\mu}(\bar{X}_n) - \frac{1}{2}\sum_{k=1}^{m}\lambda^k(\bar{X}_n)^2\right)\Delta + \sum_{k=1}^{m}\lambda^k(\bar{X}_n)\sqrt{\Delta}\hat{W}_n^k,$$

with $\tilde{\mu}(\bar{X}_n) = \frac{1}{\Delta}\int_{T_n}^{T_{n+1}}\left\langle \hat{Y}_n(s), B\hat{Y}_n(s)\right\rangle ds + \sum_{k=1}^{m}\left(\left\|\sigma^k\bar{X}_n\right\|^2 - \left\langle \bar{X}_n, \sigma^k\bar{X}_n\right\rangle^2\right)/2$ and $\lambda^k(\bar{X}_n) = \left\langle \bar{X}_n, \sigma^k\bar{X}_n\right\rangle$. We can now proceed as in the first part of the proof of Theorem 3.3.1 to deduce that for any $q \geq 2$, $\mathbb{E}|\bar{\rho}_n|^q \leq K(T)\,\mathbb{E}|\bar{\rho}_0|^q$ whenever $n = 0, \ldots, N$, and that

$$\begin{aligned}
\bar{\rho}_{n+1} &= \bar{\rho}_n\left(1 + \left(\tilde{\mu}(\bar{X}_n) - \frac{1}{2}\sum_{k=1}^{m}\lambda^k(\bar{X}_n)^2\right)\Delta + \sum_{k=1}^{m}\lambda^k(\bar{X}_n)\hat{W}_n^k\sqrt{\Delta}\right) \\
&+\bar{\rho}_n\left(\tilde{\mu}(\bar{X}_n) - \frac{1}{2}\sum_{j=1}^{m}\lambda^j(\bar{X}_n)^2\right)\left(\sum_{k=1}^{m}\lambda^k(\bar{X}_n)\hat{W}_n^k\right)\Delta^{3/2} \\
&+\frac{\bar{\rho}_n}{2}\left(\sum_{k=1}^{m}\lambda^k(\bar{X}_n)\hat{W}_n^k\right)^2\Delta + \frac{\bar{\rho}_n}{6}\left(\sum_{k=1}^{m}\lambda^k(\bar{X}_n)\hat{W}_n^k\right)^3\Delta^{3/2} + \bar{\rho}_n\mathcal{O}(\Delta^2).
\end{aligned} \tag{3.60}$$

Here and subsequently, $\mathcal{O}(\cdot)$ denotes generic random functions from $[0, T^2]$ to $\mathbb{R}$ or $\mathbb{R}^{d\times d}$ satisfying $\|\mathcal{O}(s)\| \leq K(T)\,s$.

Since $\hat{Y}_n(t) = \bar{X}_n + \int_{T_n}^{t}\left(B - \left\langle \hat{Y}_n(s), B\hat{Y}_n(s)\right\rangle\right)\hat{Y}_n(s)\,ds$, for all $t \in [T_n, T_{n+1}]$ we have $\hat{Y}_n(t) = \bar{X}_n + \left(B - \langle \bar{X}_n, B\bar{X}_n\rangle\right)\bar{X}_n(t-T_n) + \mathcal{O}\left((t-T_n)^2\right)\bar{X}_n$. Therefore, (3.60) still holds with $\tilde{\mu}(\bar{X}_n)$ replaced by

$$\mu(\bar{X}_n) = \left\langle \bar{X}_n, B\bar{X}_n\right\rangle + \sum_{k=1}^{m}\left(\left\|\sigma^k\bar{X}_n\right\|^2 - \left\langle \bar{X}_n, \sigma^k\bar{X}_n\right\rangle^2\right)/2.$$

Moreover, $\tilde{Y}_n/\left\|\tilde{Y}_n\right\| = \bar{X}_n + \left(B - \langle \bar{X}_n, B\bar{X}_n\rangle\right)\bar{X}_n\Delta + \mathcal{O}(\Delta^2)\bar{X}_n$. From (3.40) it follows that

$$\begin{aligned}
U_{n+1} = \left(I + \Psi(\bar{X}_n)\Delta + \mathcal{O}(\Delta^2)\right)\Big(&\bar{X}_n + \left(B - \langle \bar{X}_n, B\bar{X}_n\rangle\right)\bar{X}_n\Delta \\
&+ \sum_{k=1}^{m}\left(\sigma^k - \langle \bar{X}_n, \sigma^k\bar{X}_n\rangle\right)\bar{X}_n\hat{W}_n^k\sqrt{\Delta} + \mathcal{O}(\Delta^2)\bar{X}_n\Big),
\end{aligned}$$

which implies

$$U_{n+1} = \bar{Z}_{n+1} + \Psi(\bar{X}_n)\sum_{k=1}^{m}\left(\sigma^k - \langle \bar{X}_n, \sigma^k\bar{X}_n\rangle\right)\bar{X}_n\hat{W}_n^k\Delta^{3/2} + \mathcal{O}(\Delta^2)\bar{X}_n,$$

where $\bar{Z}_{n+1}$ is defined as in (3.27). We are now in position to complete the proof by using an analysis similar to that in the second part of the proof of Theorem 3.3.1.

Chapter 4

A forward-backward probabilistic algorithm for the incompressible Navier-Stokes equations

Expectations are conditioned by talking about dreams

We study forward-backward stochastic differential equations (FBSDEs) and, especially, their role as probabilistic representations for deterministic solutions of partial differential equations (PDEs). The *forward* stochastic differential equations (SDEs) appear as diffusion components in systems of FBSDEs. The drift and diffusion terms of the SDEs depend on the processes (Y, Z) that solve the *backward* SDEs (BSDEs) and, in turn, the terminal condition and the drift coefficient of the BSDEs involve the solution X of the SDEs. The FBSDEs systems are connected with PDEs through the nonlinear Feynman-Kac formula, which provides a forward-backward stochastic algorithm for the PDEs by numerically solving the concerned FBSDEs. Recently Delbaen, Qiu and Tang (2015) [76] introduced a probabilistic approach to study the incompressible Navier-Stokes equations in two and three space dimensions by means of a new type of systems of FBSDEs. Essentially Delbaen *et al.* incorporate the pressure term and the incompressibility condition to the Burgers equation, seems as simplified Navier-Stokes equations, by means of additional BSDEs defined on an infinite time interval. The authors propose a numerical algorithm to approximate strong solutions of the incompressible Navier-Stokes equations in the whole Cartesian space by truncating the time interval of the extra BSDEs in the novel FBSDEs representation. Motivated by their work, we deal with the computational simulation of the incompressible Navier-Stokes equations by means of the numerical treatment of the proposed FBSDEs system. We begin by replying some experiments in the case of the Burgers equation by the numerical solution of FBSDEs as proposed in the works of Delarue and Menozzi [73, 74]. Then we test the performance of the novel probabilistic approach by means of the numerical simulation of two-dimensional Taylor-Green vortices and a Beltrami flow in three spatial dimensions, both exhibiting spatially periodic explicit solutions.

4.1 Introduction

An important interest to discover, study and understand natural phenomena have been a constant challenge through our existence. Addressed by Sciences as essential pillar in the recent evolution, we have managed to significantly learn from Nature. A captivating and complex problem corresponds to the fluid dynamics. From Physics and Mathematics the system of Navier-Stokes equations allows us to model the movement of fluids, which was introduced by Navier (1822) [160] and Stokes (1849) [193] incorporating a pressure term and viscosity to the Euler equations (see Euler (1757) [79]).

We study the numerical simulation of the Navier-Stokes equations for incompressible fluids in $\mathbb{R}^d$

$$\begin{cases} \dfrac{\partial u}{\partial t} + (u \cdot \nabla)\, u = \nu \Delta u - \nabla p + f & ;\ 0 < t \leq T, \\ \nabla \cdot u = 0, \quad u\,(0, \cdot) = g, \end{cases} \tag{4.1}$$

for spatial dimensions $d \in \{2, 3\}$, given $g\,(x)$ an initial divergence-free vector field on $\mathbb{R}^d$, $f\,(t, x)$ the external force field and kinematic viscosity parameter $\nu > 0$, until a final time $T > 0$. The system of equations (4.1) describes the motion of an incompressible fluid by means of unknown fields of velocity $u\,(t, x) \in \mathbb{R}^d$ and pressure $p\,(t, x) \in \mathbb{R}$ defined for each position $x \in \mathbb{R}^d$ and time $t \in [0, T]$, and involving a nonlinear convective term $(u \cdot \nabla)\, u$, the diffusion term $\nu \Delta u$, the pressure term ∇p and the incompressibility condition $\nabla \cdot u = 0$ (see e.g. Chorin and Marsden (1979) [61]). Although its deduction goes back to the nineteenth century, there are still open problems concerned to it (see Fefferman (2000) [80]). Nonetheless it is usual to find works that deal with fluid dynamics by using the Navier-Stokes equations (Ocean modelling, atmosphere of Earth, gas dynamics, flow around vehicles, weather prediction, dynamic of storms, air pollution, blood circulation, etc.), or simplifications such as the Burgers equation or the Boussinesq equations (see e.g. [134, 162, 192]). By its way, the Lagrangian modeling approach appears as an alternative to the Navier-Stokes equations for the study of turbulent flows (see e.g. [34, 177]).

Stochastic processes and deterministic solutions of PDEs are related, for example through the Feynman-Kac formula [82, 115] or well by means of branching processes [96, 141, 203] to obtain probabilistic representations for the unknown solutions. Nowadays probabilistic representations for solutions of deterministic models are active and important research fields in probability theory. It bring us the possibility to develop known results by using probabilistic arguments as well as to obtain new mathematical properties and interpretations to mathematical models. Additionally they incorporate new methodologies for computational simulations, because the original solutions are rewritten in terms of expected values of certain functionals depending on stochastic processes. There are various probabilistic approaches that deal with specific PDEs [2, 3, 14, 31, 32, 53, 57, 63, 73, 74, 84, 113, 126, 174, 179, 180, 189, 190, 194, 204, 206]. In general, probabilistic representations incorporating the boundary conditions of PDEs present additional challenges. In particular, we are awake of some stochastic approaches related to the incompressible Navier-Stokes equations (see Benachour, Roynette and Vallois (2001) [23], Bouchard and Menozzi (2009) [38], Constantin and Iyer (2011) [64], Milstein and Tretyakov (2012) [151]).

There exists a huge literature about Navier-Stokes equations and during the last years have been proposed probabilistic methodologies to deal with it. One of the first approaches involving stochastic processes corresponds to the seminal Chorin's random vortex method by considering the Navier-Stokes

equations in vorticity form (see [57, 58, 59, 60] and additionally [190]). The vortex method is connected with stochastic particle systems (see e.g. [142, 143, 144]). The two-dimensional incompressible Navier-Stokes equations in vorticity form belongs to a class of McKean-Vlasov equations which admits a probabilistic interpretation in terms of stochastic particle systems (see e.g. [36, 37, 195, 200]). In the three-dimensional context, a stochastic particle approximation was introduced by associating a generalized nonlinear diffusion of the McKean-Vlasov type with the solution of a vortex equation (see [85]). Moreover, the branching processes gives us another way to study PDEs (see McKean (1975) [141]). Meanwhile, the stochastic cascades approach introduced by Le Jan and Sznitman (1997) [126] essentially studies a nonlinear integral equation whose solution coincides with the Fourier transform of the vector Laplacian of the velocity field. Then, this new equation is interpreted in terms of a branching process and a composition rule through its associated random tree (see additionally [29, 163, 179, 204]). This approach appears in the study of nonlinear parabolic PDEs too (see e.g. [31, 180]).

The systems of FBSDEs associated to the incompressible Navier-Stokes equations is a novel approach (see Cruzeiro and Shamarova [68, 69]). Recently Delbaen, Qiu and Tang (2015) [76] introduced a new class of coupled FBSDEs associated to the incompressible Navier-Stokes equations in the whole space. Delbaen *et al.* proved the existence and uniqueness of local solutions and, additionally, existence and uniqueness of global solutions in specific cases. Auxiliary results are presented to the Burgers equation. Since their probabilistic representation involves a BSDE defined on an infinite time interval, it is deduced an approximated solution to the incompressible Navier-Stokes equations by truncating the infinite time interval associated to the proposed FBSDEs system. Their approach is connected to stochastic Lagrangian particle systems (see e.g. Constantin and Iyer (2008) [63] and Zhang (2010) [206]). Following a classical methodology to the treatment of FBSDEs [73, 74], the authors in [76] propose a numerical algorithm to the simulation of the incompressible Navier-Stokes equations in the whole Cartesian space.

In general probabilistic representations linked to deterministic PDEs are more studied from a theoretical point of view, there are not many works concerning to their computational implementation and numerical approximation of PDEs (see e.g. Acebrón, Rodríguez-Rozas and Spigler (2010) [3], Bossy (2005) [32], Chorin (1973) [57], Henry-Labordère, Tan and Touzi (2014) [97], Ramirez (2006) [179]). Such approaches take into consideration expected values of specific stochastic processes needed to estimate to obtain numerical approximations. An usual way to compute mean values is the Monte-Carlo method, at cost of to simulate repeatedly independent and identically distributed (i.i.d.) random variables. Alternatively, there exists the quantization method for which is necessary to know certain optimal parameters to guarantee an appropriate order of approximation in terms of the spatial dimension $d = 1, 2, 3, \ldots$ In particular, the numerical treatment of FBSDEs considers the computation of conditional expectations involving Gaussian processes in whose case the optimal quantization parameters are known (see Corlay, Pagès and Printems [66]). Regarding to the computational effort, when $d = 1$ is convenient the quantization method. In case $d = 2$ they have the same estimation order. Nonetheless if $d = 3$ the Monte-Carlo method seems to be suitable. In this last situation, it is necessary to incorporate variance reduction techniques because the simulation of a large number of samples for each expected values, i.e. for each discretization node in the associated temporal-spatial grid. Some of the variance reduction alternatives are control variate and the stratification method.

This chapter is organized as follows. In Section 4.2 we recall the link between Itô SDEs and PDEs through the celebrated Feynman-Kac formula. We motivate the introduction of BSDEs and

then we focus on FBSDEs to specify their role as probabilistic representations of PDEs by means of the nonlinear Feynman-Kac formula. Section 4.3 introduces the context of numerical schemes for FBSDEs by means of a methodology due to Delarue and Menozzi [73, 74]. We consider the numerical approximation to the Burgers equation and, additionally, we incorporate variance reduction techniques to deal with the estimation of conditional expectations (see e.g. Corlay and Pagès (2015) [65]). In Section 4.4 we study a probabilistic algorithm recently introduced by Delbaen, Qiu and Tang (2015) [76] to the numerical simulation of the incompressible Navier-Stokes equations. We numerically solve a two-dimensional Taylor-Green vortex flow and a Beltrami flow in three spatial dimensions by simulating the novel Delbaen *et al.* system of FBSDEs.

4.1.1 Notations

Let $\left(\Omega, \mathcal{F}, \{\mathcal{F}_t\}_{t\geq 0}, \mathbb{P}\right)$ be a filtered complete probability space. For each $d \in \mathbb{Z}_+$ and $q \geq 1$ consider the space $L^q\left(\mathcal{F}_t, \mathbb{R}^d\right) := \left\{\xi : \Omega \to \mathbb{R}^d : \xi \text{ a } \mathcal{F}_t\text{-measurable and } \mathbb{E}\left\|\xi\right\|^q < \infty\right\}$. For $k \in \mathbb{N}$, $\alpha \in (0,1)$ and $l \in \mathbb{Z}_+$ denote by $C_c^\infty\left(\mathbb{R}^d, \mathbb{R}^l\right)$ the $\mathbb{R}^d$-valued set of infinitely differentiable with support compact functions on $\mathbb{R}^l$ and $C^{k,\alpha}\left(\mathbb{R}^d, \mathbb{R}^l\right)$, or simplified as $C^{k,\alpha}$, the Hölder space of functions $\phi : \mathbb{R}^d \to \mathbb{R}^l$ having continuous derivatives up to order k and such that the k-order partial derivatives are Hölder continuous with exponent α. The space $C^{k,\alpha}$ is equipped with norm

$$\left\|\phi\right\|_{C^{k,\alpha}} := \sup_{x\in\mathbb{R}^d}\left\|\phi\left(x\right)\right\| + \sum_{|\beta|=1}^{k}\sup_{x\in\mathbb{R}^d}\left\|D^\beta\phi\left(x\right)\right\| + \sum_{|\beta|=k}\sup_{x,y\in\mathbb{R}^d, x\neq y}\frac{\left\|D^\beta\phi\left(x\right) - D^\beta\phi\left(y\right)\right\|}{\left\|x-y\right\|^\alpha},$$

where the multi-index notation is considered. Given $T > 0$ and $t \in [0,T)$ we take $C\left(\left[t,T\right]; C^{k,\alpha}\right)$ the space of continuous functions $\phi : [t,T] \to C^{k,\alpha}$ equipped with the norm

$$\left\|\phi\right\|_{C\left([t,T];C^{k,\alpha}\right)} := \sup_{s\in[t,T]}\left\|\phi\left(s\right)\right\|_{C^{k,\alpha}},$$

and $C_b^{2+\alpha}\left(\mathbb{R}^d\right)$, $\alpha \in (0,1)$, the space of all bounded twice differentiable functions on $\mathbb{R}^d$ being α-Hölder continuous. Let $L^2_{\mathcal{F}}\left(\Omega; C\left(\left[t,T\right]; \mathbb{R}^{n\times m}\right)\right)$ be the set of all $\{\mathcal{F}_t\}_{t\geq 0}$-progressively measurable continuous processes X taking values in $\mathbb{R}^{n\times m}$, such that $\mathbb{E}\sup_{s\in[t,T]}\left\|X_s\right\|^2 < \infty$. Finally, for $m \in \mathbb{N}$ and $q \in [1,\infty)$ denote by $L^q\left(\mathbb{R}^l\right)$ and $H^{m,q}\left(\mathbb{R}^l\right)$ the usual $\mathbb{R}^l$-valued Lebesgue and Sobolev spaces on $\mathbb{R}^d$. By abuse of notation we refer to L^q, $H^{m,q}$, or simply by H^m when $q = 2$. Moreover, denote by $H^{m,q}_\sigma$ the completion of the set $\left\{\phi \in C_c^\infty\left(\mathbb{R}^d, \mathbb{R}^l\right) : \nabla\cdot\phi = 0\right\}$ under the norm

$$\left\|\phi\right\|_{m,q} := \left(\left\|\phi\right\|_{L^q}^q + \sum_{|\alpha|=1}^{m}\left\|D^\alpha\phi\right\|_{L^q}^q\right)^{1/q}.$$

4.2 Probabilistic representations for PDEs

In this section we recall some classic results and notions concerning to the probabilistic representation for solutions of PDEs by means of the celebrated Feynman-Kac formula and its generalization through FBSDEs.

4.2.1 Feynman-Kac formula

The Feynman-Kac formula due to Feynman (1948) [82] and Kac (1949) [115] provides a link between Itô SDEs and deterministic PDEs. More precisely, fix a final time $T > 0$ and let $(X_s)_{s\in[0,T]}$ be an adapted solution of the SDE

$$X_s = X_0 + \int_0^s b\left(r, X_r\right) dr + \int_0^s \sigma\left(r, X_r\right) dW_r,$$

where $X_0 \in L^2\left(\mathcal{F}_0, \mathbb{R}^d\right)$, $b = \left(b^1, \ldots, b^d\right)^\top : [0,\infty)\times\mathbb{R}^d \to \mathbb{R}^d$, $\sigma = \left(\sigma^1 \mid \ldots \mid \sigma^m\right) : [0,\infty)\times\mathbb{R}^d \to \mathbb{R}^{d\times m}$ and $W = \left(W^1, \ldots, W^m\right)^\top$ a m-dimensional Brownian motion defined on $\left(\Omega, \mathcal{F}, \left(\mathcal{F}_t\right)_{t\geq 0}, \mathbb{P}\right)$. As usual, for each $t \in [0,T)$ and $x \in \mathbb{R}^d$ the process $\left(X_s^{t,x}\right)_{s\in[t,T]}$ denote the solution of

$$X_s^{t,x} = x + \int_t^s b\left(r, X_r^{t,x}\right) dr + \int_t^s \sigma\left(r, X_r^{t,x}\right) dW_r.$$

Define the second-order differential operator $\mathcal{L}$ by

$$\mathcal{L}v\left(t,x\right) := \frac{1}{2}\sum_{i,j=1}^{d}\left(\sigma\sigma^\top\right)^{i,j}\left(t,x\right)\frac{\partial^2 v}{\partial x_i \partial x_j}\left(t,x\right) + \sum_{i=1}^{d} b^i\left(t,x\right)\frac{\partial v}{\partial x_i}\left(t,x\right)$$

for $v : [0,\infty)\times\mathbb{R}^d \to \mathbb{R}$ smooth enough. Consider the solution $u : [0,T]\times\mathbb{R}^d \to \mathbb{R}$ of the Cauchy problem

$$\begin{cases} \dfrac{\partial u}{\partial t}\left(t,x\right) + \mathcal{L}u\left(t,x\right) + c\left(t,x\right)u\left(t,x\right) + f\left(t,x\right) = 0 \quad ; \ \forall\left(t,x\right) \in [0,T)\times\mathbb{R}^d, \\ u\left(T,x\right) = g\left(x\right) \quad ; \ \forall x \in \mathbb{R}^d, \end{cases}$$

where $c, f : [0,\infty)\times\mathbb{R}^d \to \mathbb{R}$ and $g : \mathbb{R}^d \to \mathbb{R}$. Then, for every $(t,x) \in [0,T]\times\mathbb{R}^d$ the Feynman-Kac formula gives the stochastic representation

$$\begin{aligned} u\left(t,x\right) &= \mathbb{E}^{t,x}\left[\exp\left\{\int_t^T c\left(r,X_r\right)dr\right\} g\left(X_T\right) + \int_t^T \exp\left\{\int_t^s c\left(r,X_r\right)dr\right\} f\left(s,X_s\right)ds\right] \qquad (4.2) \\ &= \mathbb{E}\left[\exp\left\{\int_t^T c\left(r,X_r^{t,x}\right)dr\right\} g\left(X_T^{t,x}\right) + \int_t^T \exp\left\{\int_t^s c\left(r,X_r^{t,x}\right)dr\right\} f\left(s,X_s^{t,x}\right)ds\right], \end{aligned}$$

where $\mathbb{E}^{t,x} := \mathbb{E}\left(\cdot \diagup X_t = x\right)$ means the conditional expectation given the event $\{\omega \in \Omega : X_t\left(\omega\right) = x\} \in \mathcal{F}_t$ (see e.g. Karatzas and Shreve (1988) [117] for hypotheses about functions b, σ, c, f and g). Therefore, from Feynman-Kac formula (4.2) we have that the solution u of the Cauchy problem evaluated at (x,t) can be obtained by computing the expectation of certain functional depending on the process $\left(X_s^{t,x}\right)_{s\in[t,T]}$.

4.2.2 Backward stochastic differential equations

Let us look at the Itô SDE

$$dX_s = b\left(X_s\right) ds + \sum_{k=1}^{m} \sigma^k\left(X_s\right) dW_s^k,$$

or in matrix notation

$$dX_s = b\left(X_s\right) ds + \sigma\left(X_s\right) dW_s, \tag{4.3}$$

where $b : \mathbb{R}^d \to \mathbb{R}^d$, $\sigma : \mathbb{R}^d \to \mathbb{R}^{d\times m}$ are smooth functions and $W = \left(W^1, \ldots, W^m\right)^\top$ is a m-dimensional standard Brownian motion on the filtered complete probability space $\left(\Omega, \mathcal{F}, \{\mathcal{F}_t\}_{t\geq 0}, \mathbb{P}\right)$. Taking an initial condition $X_0 \in L^2\left(\mathcal{F}_0, \mathbb{R}^d\right)$ it is possible to find an adapted $\mathbb{R}^d$-valued stochastic process $(X_t)_{t\geq 0}$ that solves the equation (4.3). On another hand, fixing $T > 0$ and given a terminal condition $X_T \in L^2\left(\mathcal{F}_T, \mathbb{R}^d\right)$ a different problem corresponds to find an $\mathcal{F}_t$-measurable process X_t at time $t < T$. As it was pointed out by Peng (2010) [171], from the SDE (4.3) we have

$$X_t = X_T - \int_t^T b\left(X_s\right) ds - \int_t^T \sigma\left(X_s\right) dW_s, \tag{4.4}$$

and so, in general, X_t is $\mathcal{F}_T$-measurable and thus $b\left(X_s\right)$ and $\sigma\left(X_s\right)$ are not $\mathcal{F}_s$-measurable, i.e. anticipating processes. Then the Itô integral becomes invalid and the key point corresponds to guarantee $X_t \in L^2\left(\mathcal{F}_t, \mathbb{R}^d\right)$. Motivated by this situation, Pardoux and Peng (1990) [168] introduced the backward stochastic differential equation (BSDE)

$$dY_s = -h\left(s, Y_s, Z_s\right) ds + Z_s dW_s \quad ; \; s \in [0, T],$$

or in integral form

$$Y_t = Y_T + \int_t^T h\left(s, Y_s, Z_s\right) ds - \int_t^T Z_s dW_s. \tag{4.5}$$

Here (Y, Z) is a pair of adapted processes that solve (4.5) for a given $Y_T \in L^2\left(\mathcal{F}_T, \mathbb{R}^d\right)$. The function $h : [0, \infty) \times \mathbb{R}^d \times \mathbb{R}^{d\times m} \to \mathbb{R}^d$ is called the generator of the backward equation. The process Z appearing in the BSDE (4.5) is the key element that permits to find a non-anticipating process Y. We refer to [171] for a survey and detailed explanations. Additionally, see [131, 167, 168] for the classic theory of BSDEs.

4.2.3 Forward-backward stochastic differential equations

Since their introduction and development during the early 1990s, the theory of backward stochastic differential equations (BSDEs) initiated by Pardoux and Peng (1990) [168] has incorporated novel probabilistic notions and new results with various applications (see e.g. Pardoux and Peng (1992) [167], Peng (2010) [171]). The BSDEs together with SDEs constitute systems of forward-backward stochastic differential equations (FBSDEs) that are connected with deterministic PDEs through the nonlinear Feynman-Kac formula, generalizing the classical Feynman-Kac formula (see e.g. Antonelli (1993) [7], Ma and Yong (1999) [131], Lejay (2004) [127], Cheridito *et al.* (2007) [51]).

The connection between branching processes and differential equations gives us another way to study PDEs by means of stochastic processes (see McKean (1975) [141], Le Jan and Sznitman (1997) [126]). Recently Henry-Labordère, Tan and Touzi (2014) [97] presented a new approach that use branching processes to solve decoupled systems of FBSDEs associated to semi-linear parabolic PDEs. Following [97], it is possible to directly solve FBSDEs by means of branching processes, generalizing the relation between PDEs and stochastic equations through the notion of viscosity solutions of path dependent PDEs, even in non-Markovian context. Quasi-linear parabolic PDEs involve coupled FBSDEs, hence it is necessary to extend the approach introduced by [97] to more general contexts.

Let $T > 0$ be fixed and take a time interval $[t,T]$, $t \in [0,T)$. We study stochastic processes $(X,Y,Z)_{s\in[t,T]}$ governed by the FBSDEs system

$$\begin{cases} X_s = x + \displaystyle\int_t^s b\left(r, X_r, Y_r, Z_r\right) dr + \int_t^s \sigma\left(r, X_r, Y_r\right) dW_r \\ Y_s = g\left(X_T\right) + \displaystyle\int_s^T h\left(r, X_r, Y_r, Z_r\right) dr - \int_s^T Z_r dW_r \end{cases}, \tag{4.6}$$

where $b : [0,T] \times \mathbb{R}^d \times \mathbb{R}^n \times \mathbb{R}^{n\times m} \to \mathbb{R}^d$, $\sigma : [0,T] \times \mathbb{R}^d \times \mathbb{R}^n \to \mathbb{R}^{d\times m}$, $g : \mathbb{R}^d \to \mathbb{R}^n$, $h : [0,T] \times \mathbb{R}^d \times \mathbb{R}^n \times \mathbb{R}^{n\times m} \to \mathbb{R}^n$ and $W = \left(W^1, \ldots, W^m\right)^\top$ is a m-dimensional Brownian motion defined on $\left(\Omega, \mathcal{F}, (\mathcal{F}_t)_{t\geq 0}, \mathbb{P}\right)$. The BSDEs in the system (4.6) depends on the diffusion process X that solves the *forward* SDEs. When the coefficients of the diffusion process X do not depend on Y nor Z, the system (4.6) is referred as decoupled FBSDEs. Otherwise we have coupled FBSDEs. Let us remark that an adapted solution of the FBSDEs (4.6) is defined by a triple of processes

$$(X,Y,Z) \in L^2_{\mathcal{F}}\left(\Omega; C\left(\left[t,T\right]; \mathbb{R}^d\right)\right) \times L^2_{\mathcal{F}}\left(\Omega; C\left(\left[t,T\right]; \mathbb{R}^n\right)\right) \times L^2_{\mathcal{F}}\left(\Omega; C\left(\left[t,T\right]; \mathbb{R}^{n\times m}\right)\right)$$

such that it satisfies (4.6) $\mathbb{P}$-almost surely. From now on, we denote $\left(X^{t,x}, Y^{t,x}, Z^{t,x}\right)$ to recall the dependence on the parameters $t \in [0,T)$ and $x \in \mathbb{R}^d$ (see e.g. Ma and Yong (1999) [131]). We refer to [72, 167] for the classic theory of FBSDEs.

As in the spirit of the classical Feynman-Kac formula, it is possible to obtain a probabilistic representation for the solution $u : [0,T] \times \mathbb{R}^d \to \mathbb{R}^n$ of the quasilinear PDE

$$\begin{cases} \dfrac{\partial u}{\partial t}(t,x) + \mathcal{L}\left(t,x,u\left(t,x\right)\right) + h\left(t,x,u\left(t,x\right), Du\left(t,x\right)\sigma\left(t,x,u\left(t,x\right)\right)\right) = 0 \quad ; \ \forall (t,x) \in [0,T) \times \mathbb{R}^d, \\ u\left(T,x\right) = g\left(x\right) \quad ; \ \forall x \in \mathbb{R}^d, \end{cases} \tag{4.7}$$

where $Du\left(t,x\right) = \left(\frac{\partial u^i}{\partial x_j}\left(t,x\right)\right)_{i,j}$; for $i \in \{1,\ldots,n\}, j \in \{1,\ldots,d\}$, and

$$\mathcal{L}\left(t,x,u\right) := \begin{pmatrix} L\left(t,x,u,Du^1,D^2u^1\right) \\ \vdots \\ L\left(t,x,u,Du^n,D^2u^n\right) \end{pmatrix}, \tag{4.8}$$

with $Du^k = \left(\frac{\partial u^k}{\partial x_1}, \ldots, \frac{\partial u^k}{\partial x_d}\right)^\top$, $D^2u^k = \left(\frac{\partial^2 u^k}{\partial x_i \partial x_j}\right)_{i,j}$ and

$$L\left(t,x,u,p,Q\right) := \frac{1}{2}\operatorname{tr}\left\{\sigma\sigma^\top\left(t,x,u\right)Q\right\} + \left\langle b\left(t,x,u,Du\sigma\left(t,x,u\right)\right),p\right\rangle, \tag{4.9}$$

for $p \in \mathbb{R}^d$ and $Q \in \mathbb{S}_+^d$; the set of $d \times d$ real valued symmetric non-negative (definite) matrices, that is $Q = Q^\top$ and $x^\top Qx = \langle x, Qx\rangle \geq 0$ for all $x \in \mathbb{R}^d$. More precisely, if the FBSDEs (4.6) admits unique adapted solutions $\left(X^{t,x}, Y^{t,x}, Z^{t,x}\right)$ on each subintervals $[t,T] \subseteq [0,T]$ then we have

$$Y_s^{t,x} = u\left(s, X_s^{t,x}\right), Z_s^{t,x} = Du\left(s, X_s^{t,x}\right)\sigma\left(s, X_s^{t,x}, Y_s^{t,x}\right) \quad ; \ \forall\left(s,x\right) \in [t,T] \times \mathbb{R}^d.$$

Therefore, the function $u\left(t,x\right) := Y_t^{t,x}$ is a viscosity solution to the associated PDE (4.7). The relation

$$u\left(t,x\right) = Y_t^{t,x} \quad \forall\left(t,x\right) \in [0,T] \times \mathbb{R}^d$$

is called the nonlinear Feynman-Kac formula (see, additionally, Crandall, Hitoshi and Lions (1992) [67], Delarue and Menozzi (2006) [73]). From now on, it is assumed that $\sigma\sigma^\top$ is uniformly elliptic, i.e. there exists $\lambda > 0$ such that for each $(t,x,u) \in [0,T] \times \mathbb{R}^d \times \mathbb{R}^n$ we have

$$\left\langle \zeta, \left[\sigma\sigma^\top\right]\left(t,x,u\right)\zeta\right\rangle \geq \lambda\left\|\zeta\right\|^2; \quad \forall \zeta \in \mathbb{R}^d.$$

In particular, when $h\left(t,x,y,z\right) = c\left(t,x\right)y + f\left(t,x\right)$ and $n = 1$ the BSDEs in (4.6) has explicit solution

$$\begin{aligned} Y_s^{t,x} = {} & \exp\left\{\int_s^T c\left(r, X_r^{t,x}\right)dr\right\} g\left(X_T^{t,x}\right) + \int_s^T \exp\left\{\int_s^r c\left(\theta, X_\theta^{t,x}\right)d\theta\right\} f\left(r, X_r^{t,x}\right)dr \\ & - \int_s^T \exp\left\{\int_s^r c\left(\theta, X_\theta^{t,x}\right)d\theta\right\} Z_r^{t,x} dW_r \end{aligned}$$

and the solution $u : [0,T] \times \mathbb{R}^d \to \mathbb{R}$ of the concerned equation (4.7) can be expressed as $u\left(t,x\right) = Y_t^{t,x} = \mathbb{E}^{t,x}\left(Y_t^{t,x}\right)$, that is

$$u\left(t,x\right) = \mathbb{E}\left[\exp\left\{\int_t^T c\left(r, X_r^{t,x}\right)dr\right\} g\left(X_T^{t,x}\right) + \int_t^T \exp\left\{\int_t^s c\left(r, X_r^{t,x}\right)dr\right\} f\left(s, X_s^{t,x}\right)ds\right], \tag{4.10}$$

which corresponds to the classical Feynman-Kac formula (4.2) (see e.g. Pardoux and Tang (1999) [169], Pardoux and Peng (1992) [167], Mao (1995) [137], Pardoux (1998) [166]).

As application, in case of the d-dimensional Burgers equation (see Burgers (1948) [45])

$$\begin{cases} \dfrac{\partial u}{\partial t} + \left(u \cdot \nabla\right)u + \dfrac{\nu}{2}\Delta u + f = 0 \quad ; \ 0 \leq t < T, \\ \quad u\left(T\right) = g, \end{cases} \tag{4.11}$$

where $f : [0,T] \times \mathbb{R}^d \to \mathbb{R}^d$, $g : \mathbb{R}^d \to \mathbb{R}^d$ and $\nu > 0$, we can associate the coupled FBSDEs

$$\forall s \in [t,T], \begin{cases} X_s^{t,x} = x + \displaystyle\int_t^s Y_r^{t,x} dr + \int_t^s \sqrt{\nu} dW_r, \\ Y_s^{t,x} = g\left(X_T^{t,x}\right) + \displaystyle\int_s^T f\left(r, X_r^{t,x}\right) dr - \int_s^T \sqrt{\nu} Z_r^{t,x} dW_r. \end{cases} \tag{4.12}$$

Then, we have $Y_s^{t,x} = u\left(s, X_s^{t,x}\right)$ and $Z_s^{t,x} = Du\left(s, X_s^{t,x}\right)$ for all $(s,x) \in [t,T] \times \mathbb{R}^d$ (see Theorem 4.1 in Ma, Protter and Yong (1994) [130]). Alternatively, the Burgers equation (4.11) admits a decoupled FBSDEs representation

$$\forall s \in [t,T], \begin{cases} X_s^{t,x} = x + \displaystyle\int_t^s \sqrt{\nu} dW_r, \\ Y_s^{t,x} = g\left(X_T^{t,x}\right) + \displaystyle\int_s^T \left[f\left(r, X_r^{t,x}\right) + \frac{1}{\sqrt{\nu}} Z_r^{t,x} Y_r^{t,x}\right] dr - \int_s^T \sqrt{\nu} Z_r^{t,x} dW_r. \end{cases} \tag{4.13}$$

Note that to approximate the solution component $Y^{t,x}$ of the coupled FBSDE (4.12) it is not necessary to estimate the process $Z^{t,x}$. This is an advantage in comparison to the decoupled representation (4.13) when we only are interested in the estimation of the process $Y_s^{x,t}$ without information about $Z_s^{x,t}$.

4.3 Numerical schemes for FBSDEs

In this section we follow a probabilistic approach introduced by Delarue and Menozzi (2006) [73], and improved in Delarue and Menozzi (2008) [74], to study the numerical approximation of solutions (X, Y, Z) of FBSDEs (4.6). Numerical schemes for FBSDEs is a recent field of research, we refer to Ma, Protter and Yong (1994) [130], Douglas, Ma and Protter (1996) [78], Chevance (1997) [52], Ma, Protter, San Martín and Torres (2002) [129], Ma and Zhang (2002) [132], Bally and Pagès (2003) [15], Zhang (2004) [205], Bouchard and Touzi (2004) [39], Gobet, Lemor and Warin (2005) [89], Zhao, Chen and Peng (2006) [207], Bender and Zhang (2008) [24], Peng and Xu (2011) [172], Henry-Labordère, Tan and Touzi (2014) [97], for additional literature and methodologies in such theory.

We are interested in FBSDEs (4.6) whose drift terms b and h are independent of the diffusion coefficient Z of their BSDEs. More precisely, FBSDEs of the form

$$\forall s \in [t,T], \begin{cases} X_s = x + \displaystyle\int_t^s b\left(r, X_r, Y_r\right) dr + \int_t^s \sigma\left(r, X_r, Y_r\right) dW_r, \\ Y_s = g\left(X_T\right) + \displaystyle\int_s^T h\left(r, X_r, Y_r\right) dr - \int_s^T Z_r dW_r. \end{cases} \tag{4.14}$$

As usual, we can remove the martingale part of the BSDEs by taking the conditional expectation $\mathbb{E}\left(\cdot \diagup X_t = x\right)$ and so the dependance of Y on the process Z. Thus we focus on the numerical solution of the process Y and, because the nonlinear Feynman-Kac formula, the estimation of the strong solution u of the related PDE (4.7) by means of the probabilistic numerical algorithm.

Given an integer $N \geq 1$, consider a regular mesh of $[0,T]$ with time-step $h := T/N$, i.e. we set $t_k := k \cdot h$; $\forall k \in \{0,\ldots,N\}$, and the infinite Cartesian grid $\mathcal{C}_\delta := \delta \cdot \mathbb{Z}^d$ of spatial-step $\delta > 0$. Moreover, Π_δ stands for the projection mapping on the grid $\mathcal{C}_\delta$ defined by

$$\Pi_\delta(x) := \arg\min\{\|x - \bar{x}\| : \bar{x} \in \mathcal{C}_\delta\} \qquad \forall x \in \mathbb{R}^d.$$

Supposing an α-Hölder continuous function $F : \mathbb{R}^d \to \mathbb{R}^d$, observe that

$$\|F(x) - F(\Pi_\delta(x))\| \leq K \|x - \Pi_\delta(x)\|^\alpha \leq K\delta^\alpha.$$

For each $k \in \{0,\ldots,N-1\}$, we denote $\Delta W_k = W_{t_{k+1}} - W_{t_k}$ and refer as $q(\Delta W_k) = \sqrt{h} q\left(\frac{\Delta W_k}{\sqrt{\Delta}}\right)$ to the optimal quantization of the underlying Gaussian variable $\Delta W_k/\sqrt{\Delta}$ (see Subsection 4.3.1 below).

We consider the following numerical scheme $\bar{u}$ that approximates the processes Y involved in the FBSDEs (4.14) (see Delarue and Menozzi (2006) [73]):

Algorithm 4.3.1 *Let $T > 0$. Fix $h = T/N$, with $N \geq 1$, and $\delta > 0$ such that $\delta \in]0,h[$. Then*

$$\bar{u}(T,x) \quad = \quad g(x) \quad \forall x \in \mathcal{C}_\delta.$$

Moreover, $\forall k \in \{0,\ldots,N-1\}$, $\forall x \in \mathcal{C}_\delta$, define recursively

$$\begin{aligned} \mathcal{T}(t_k,x) &= b(t_{k+1},x,\bar{u}(t_{k+1},x)) \cdot h + \sigma(t_{k+1},x,\bar{u}(t_{k+1},x))\, q(\Delta W_k), \\ \bar{u}(t_k,x) &= \mathbb{E}[\bar{u}(t_{k+1},\Pi_\delta(x+\mathcal{T}(t_k,x)))] + h(t_{k+1},x,\bar{u}(t_{k+1},x)) \cdot h. \end{aligned}$$

Usually, numerical schemes for FBSDEs involve a backward regression to compute the estimations of the processes (X,Y,Z) (see [97] for a different approach using branching processes). The process $\mathcal{T}(t_k,x)$ corresponds to the Euler-Maruyama scheme applied to the SDEs component when not considering the quantization of the Brownian increment (see [145]). In general situations we can incorporate the numerical schemes introduced in the previous chapters to deal with the approximation of the SDEs involved in the system of FBSDEs (4.14). The discretization parameters of time $h > 0$ and space $\delta > 0$ are sufficient small and they must verify $\delta < h$ to take into account the local influence of the drift b in the approximations $\mathcal{T}(t_k,x)$. Obviously we cannot deal with infinite-space grids and so, usually, it is necessary to incorporate a truncation procedure, where it is convenient to have solutions vanishing at infinity, or to consider spatially-periodic solutions. In this PhD thesis work we deal with the numerical estimation of space-periodic Navier-Stokes equations. The projection operator onto the grid Π_δ incorporates an extra source of error and affects the order of convergence of the numerical algorithms, which can be improved, e.g., using linear interpolation but at cost of higher computational effort. Moreover, the quantization of the underlying Gaussian variables $q(\Delta W_k)$ become a more efficient method to deal with the expectation approximations, instead of the classical Monte-Carlo procedure. All this elements are intrinsically bounded to the computational effort of the Algorithm 4.3.1 (see Section 4 of [73] for details and its convergence).

4.3.1 Estimation of conditional expectations

Let $(\Omega, \mathcal{A}, \mathbb{P})$ be a probability space. Suppose that $U : (\Omega, \mathcal{A}, \mathbb{P}) \to \mathbb{R}^m$ is a square integrable random variable and $F : \mathbb{R}^m \to \mathbb{R}^d$ is uniformly α-Hölder continuous, $\alpha \in (0, 1]$, such that $F(U) \in L^2\left(\mathcal{A}, \mathbb{R}^d\right)$. The usual way to estimate expectations is by means of the Monte-Carlo approximation

$$\mathbb{E}[F(U)] \approx \frac{1}{\mathcal{M}} \sum_{i=1}^{\mathcal{M}} F\left(U^{(i)}\right), \tag{4.15}$$

where $U^{(i)}$ are $\mathcal{M}$ independent realizations of the underlying random variable U. From now on, the averages are computed in a component-wise manner. It is well-known that the error of approximation by the Monte-Carlo method (4.15) depends on $\mathcal{M}^{-1/2}$ as $\mathcal{M}$ tends to infinity.

Alternatively, we can use the quantization method to estimate mean values. Indeed, let $q(U)$ be a quantizer of U, i.e. an approximation of U by a discrete random variable $q(U)$ taking values in a finite set $\Gamma = \{v_1, \ldots, v_M\} \subset \mathbb{R}^m$. Suppose that

$$q(U) = \sum_{i=1}^{M} v_i \mathbf{1}_{C_i}(U)$$

where $C = \{C_1, \ldots, C_M\}$ is a partition of $\mathbb{R}^m$ associated to Γ be means of $v_i \in C_i$ for all $i \in \{1, \ldots, M\}$. Then we have

$$\mathbb{E}[F(U)] \approx \mathbb{E}[F(q(U))] = \sum_{i=1}^{M} \mathbb{P}(U \in C_i) \cdot F(v_i). \tag{4.16}$$

Since F is α-Hölder continuous, applying the Jensen's inequality the estimation error is bounded by

$$\|\mathbb{E}[F(U)] - \mathbb{E}[F(q(U))]\| \leq K\left(\mathbb{E}\left[\|U - q(U)\|^2\right]\right)^{\alpha/2},$$

where the quantization error in the L^2-norm (to the power 2) is given by

$$\|U - q(U)\|_2^2 = \sum_{i=1}^{M} \mathbb{E}\mathbf{1}_{C_i}(U) \|U - v_i\|^2.$$

Thus, the key point is to provide convenient sets Γ and C such that the quadratic quantization error is optimal.

We deal the context of m-dimensional Brownian increments $\Delta W_k = \sqrt{h}\xi$, where $\xi \sim \mathcal{N}(0; I_m)$, and so the optimal quantization of the Normal distribution $\mathcal{N}(0; I_m)$. In such situation, it is known that the L^2-optimal M-quantizer of the $\mathcal{N}(0; I_m)$ distribution is obtained by means of Voronoï M-quantizers (see Graf and Luschgy (2000) [90], Pagès and Printems (2003) [164], Corlay, Pagès and Printems (2005) [66], Corlay and Pagès (2015) [65] for details on optimal quantization). Thus, considering

$$q(\Delta W_k) = \sqrt{h} q\left(\frac{1}{\sqrt{h}} \Delta W_k\right),$$

with $q\left(\frac{1}{\sqrt{h}}\Delta W_k\right)$ the L^2-optimal M-quantizer of the $\mathcal{N}(0;I_m)$ distribution, we have

$$\left(\mathbb{E}\left[\left\|\Delta W_k - q\left(\Delta W_k\right)\right\|^2\right]\right)^{1/2} \leq K(m)\, h^{1/2} M^{-1/m} \tag{4.17}$$

with $K(m) > 0$ only depending on the dimension m of the Gaussian process (see [73]). Then, we obtain that the error of the quantization method (4.16) depends on $M^{-\alpha/m}$ as M tends to infinity.

Additionally, we use quantization as control variate variable to reduce the variance of the Monte Carlo estimation. More precisely, we make

$$\mathbb{E}\left[F(U)\right] \approx \mathbb{E}\left[F\left(q(U)\right)\right] + \frac{1}{\mathcal{M}}\sum_{i=1}^{\mathcal{M}}\left[F\left(U^{(i)}\right) - F\left(q\left(U^{(i)}\right)\right)\right]. \tag{4.18}$$

In general, we obtain an error of estimation in terms of $\sqrt{\mathrm{Var}\left[F(U) - F\left(q(U)\right)\right]}/\sqrt{\mathcal{M}}$. In case of Gaussian variables, the error of the estimation (4.18) is then $\mathcal{M}^{-1/2}M^{-\alpha/m}$, that reduces the error of the Monte-Carlo method (4.15) and the quantization approach (4.16). We refer to Glasserman (2003) [88], Fishman (2005) [83], Pagès and Printems (2005) [165], Lejay and Reutenauer (2012) [128], Corlay and Pagès (2015) [65] for reduction variance techniques.

As especial case, let $U^1,\ldots,U^m$ be m independent and identically distributed square integrable random variables $U^k : (\Omega,\mathcal{A},\mathbb{P}) \to \mathbb{R}^d$ and $F : \left(\mathbb{R}^d\right)^m \to \mathbb{R}^d$ a α-Hölder continuous function such that $F\left(U^1,\ldots,U^m\right)$ belongs to $L^2\left(\mathcal{A},\mathbb{R}^d\right)$. Then, since $U^1,\ldots,U^m$ are independent we have

$$\begin{aligned}\mathbb{E}\left[F\left(U^1,\ldots,U^m\right)\right] &\approx \mathbb{E}\left[F\left(q\left(U^1\right),\ldots,q\left(U^m\right)\right)\right]\\ &= \sum_{i_1,\ldots,i_m=1}^{M}\mathbb{P}\left(U^1\in C_{i_1}\right)\cdots\mathbb{P}\left(U^m\in C_{i_m}\right)F\left(v_{i_1},\ldots,v_{i_m}\right)\end{aligned}$$

In case $U^k = \Delta W_k = \sqrt{h}\xi^k$, with $\xi^k \sim \mathcal{N}(0;I_d)$, we obtain

$$\left\|\mathbb{E}\left[F\left(U^1,\ldots,U^m\right)\right] - \mathbb{E}\left[F\left(q\left(U^1\right),\ldots,q\left(U^m\right)\right)\right]\right\| \leq K h^{\alpha/2} M^{-\alpha/d}.$$

Moreover, we can use quantization as a control variate variable, i.e.

$$\begin{aligned}\mathbb{E}\left[F\left(U^1,\ldots,U^m\right)\right] &\approx \mathbb{E}\left[F\left(q\left(U^1\right),\ldots,q\left(U^m\right)\right)\right]\\ &\quad + \frac{1}{\mathcal{M}^m}\sum_{i=1}^{\mathcal{M}^m}\left[F\left(\left(U^1\right)^{(i)},\ldots,\left(U^m\right)^{(i)}\right) - F\left(q\left(\left(U^1\right)^{(i)}\right),\ldots,q\left(\left(U^m\right)^{(i)}\right)\right)\right].\end{aligned}$$

Therefore, the estimation error depends on $\left(\mathcal{M}^m\right)^{-1/2} M^{-\alpha/d}$.

4.3.2 Burgers equation

We study the numerical approximation to the strong solution of the d-dimensional Burgers equation

$$\begin{cases}\dfrac{\partial u}{\partial t}(t,x) - \left((u\cdot\nabla)\,u\right)(t,x) + \dfrac{\epsilon^2}{2}\Delta u(t,x) = 0 \quad ;\ (t,x)\in[0,T[\times\mathbb{R}^d,\\ \quad u(T,x) = H(x) \quad ;\ x\in\mathbb{R}^d,\end{cases} \tag{4.19}$$

with $\epsilon > 0$, $H \in C_b^{2+\alpha}\left(\mathbb{R}^d\right)$; $\alpha \in (0,1)$, and $u = (u_1, \ldots, u_d)^\top : [0,T] \times \mathbb{R}^d \to \mathbb{R}^d$ (see e.g. Bossy, Fezoui and Piperno (1997) [37], Bossy and Jourdain (2002) [35], Delarue and Menozzi (2006) [73], Delarue and Menozzi (2008) [74]). To this end we use the probabilistic representation $u(t,x) = Y_t^{t,x}$, where $\left(Y_s^{t,x}\right)_{s\in[t,T]}$ satisfies the coupled FBSDEs

$$\begin{cases} X_s^{t,x} = x - \displaystyle\int_t^s Y_r^{t,x} dr + \int_t^s \epsilon dW_r, \\ Y_s^{t,x} = H\left(X_T^{t,x}\right) - \displaystyle\int_s^T \epsilon Z_r^{t,x} dW_r, \end{cases} \tag{4.20}$$

where W is a d-dimensional Brownian motion. We reply some numerical experiments appearing in [73, 74] by incorporating quantization as control variate variable to compute the conditional expectations.

In order to numerically approximate the solution u of (4.19) we apply the Algorithm 4.3.1 to the FBSDEs representation (4.20), i.e. we consider the following scheme:

Algorithm 4.3.2 *Define*

$$\bar{u}(T,x) = H(x) \quad \forall x \in \mathcal{C}_\delta.$$

Then, consider $\forall k \in \{0,\ldots,N-1\}$, $\forall x \in \mathcal{C}_\delta$,

$$\bar{u}(t_k,x) = \mathbb{E}\left[\bar{u}\left(t_{k+1}, \Pi_\delta\left(x - \bar{u}(t_{k+1},x)\cdot h + \epsilon q(\Delta W_k)\right)\right)\right].$$

We test the effect on Algorithm 4.3.2 when the quantization technique is replaced by the Monte-Carlo method to estimate the expectations, i.e. the following scheme:

Algorithm 4.3.3 *Define*

$$\bar{u}(T,x) = H(x) \quad \forall x \in \mathcal{C}_\delta.$$

Then, $\forall k \in \{0,\ldots,N-1\}$, $\forall x \in \mathcal{C}_\delta$, *consider*

$$\bar{u}(t_k,x) = \frac{1}{\mathcal{M}} \sum_{m=1}^{\mathcal{M}} \bar{u}\left(t_{k+1}, \Pi_\delta\left(x - \bar{u}(t_{k+1},x)\cdot h + \epsilon \Delta W_k^{(m)}\right)\right).$$

Although the convergence of the Algorithm 4.3.2 involves the optimal quantization of the underlying Gaussian variables ΔW_k, motivated by Pagès and Printems (2005) [165] (additionally Corlay and Pagès (2015) [65]) we modify the above algorithm by considering quantization as a control variate variable to compute the mean values. More precisely, we introduce the following numerical scheme

Algorithm 4.3.4 *For all* $x \in \mathcal{C}_\delta$, *define*

$$\bar{u}(T,x) = H(x).$$

Then $\forall k \in \{0,\ldots,N-1\}$, $\forall x \in \mathcal{C}_\delta$,

$$\begin{aligned} \bar{u}(t_k,x) &= \mathbb{E}\left[\bar{u}\left(t_{k+1}, \Pi_\delta\left(x - \bar{u}(t_{k+1},x)\cdot h + \epsilon q(\Delta W_k)\right)\right)\right] \\ &\quad + \frac{1}{\mathcal{M}} \sum_{m=1}^{\mathcal{M}} \bar{u}\left(t_{k+1}, \Pi_\delta\left(x - \bar{u}(t_{k+1},x)\cdot h + \epsilon \Delta W_k^{(m)}\right)\right) \\ &\quad - \frac{1}{\mathcal{M}} \sum_{m=1}^{\mathcal{M}} \bar{u}\left(t_{k+1}, \Pi_\delta\left(x - \bar{u}(t_{k+1},x)\cdot h + \epsilon q\left(\Delta W_k^{(m)}\right)\right)\right). \end{aligned}$$

Here $\Delta W_k^{(m)}$*;* $1 \leq m \leq \mathcal{M}$*, are* $\mathcal{M}$ *independent realizations of* ΔW_k*.*

First, we consider the one-dimensional Burgers equation (4.19), i.e. when $d = 1$. The explicit solution is given by

$$u(t,x) = \frac{\mathbb{E}\left[H\left(x + \epsilon B_{T-t}\right)\phi\left(x + \epsilon B_{T-t}\right)\right]}{\mathbb{E}\left[\phi\left(x + \epsilon B_{T-t}\right)\right]} \quad \forall\,(t,x) \in [0,T] \times \mathbb{R}, \tag{4.21}$$

where B is a standard Brownian motion and

$$\phi(y) = \exp\left(-\epsilon^{-2}\int_0^y H(u)\,du\right) \quad \forall y \in \mathbb{R}.$$

As in [73], we take $H(x) = \sin(2\pi x)$, $T = 1$, $h = 0.01$, $\delta = 10^{-3}$ and $\epsilon = 0.15$. Thus, from (4.21) we have a spatially 1-periodic exact solution u. Figure 4.1 summarizes the results obtained to the one-dimensional Burgers equation. The data of the optimal quantizers $q\left(\Delta B_k/\sqrt{\Delta}\right)$ have been obtained from Corlay, Pagès and Printems (2005) [66]. As we expected, the Algorithm 4.3.3 produces worse results than Algorithm 4.3.2. In turns, Algorithm 4.3.4 produces similar results as Algorithm 4.3.2 but reduces the computational effort required.

Now, we deal with the 2-dimensional context. The explicit solution is known when $H = \nabla H_0$, where H_0 is a real-valued function. More precisely, the explicit solution is

$$u(t,x) = \frac{\mathbb{E}\left[\nabla H_0\left(x + \epsilon B_{T-t}\right)\exp\left(-\epsilon^{-2}H_0\left(x + \epsilon B_{T-t}\right)\right)\right]}{\mathbb{E}\left[\exp\left(-\epsilon^{-2}H_0\left(x + \epsilon B_{T-t}\right)\right)\right]} \quad \forall\,(t,x) \in [0,T] \times \mathbb{R}. \tag{4.22}$$

As in [74], we choose a spatially periodic $H_0(x) = \prod_{i=1,2}\sin^2(\pi x_i)$, $T = 3/8$, $h = 2.5 \times 10^{-2}$, $\delta = 0.01$ and $\epsilon^2 = 0.4$. In Figure 4.2 we observe that the Algorithm 4.3.4 reduces the quantization errors to the estimation of conditional expectations of the Algorithm 4.3.2 and so it improves the resulting approximation errors. The Algorithm 4.3.4 has point-wise errors at most of 0.06879, reducing the value 0.09481 in case of the Algorithm 4.3.2.

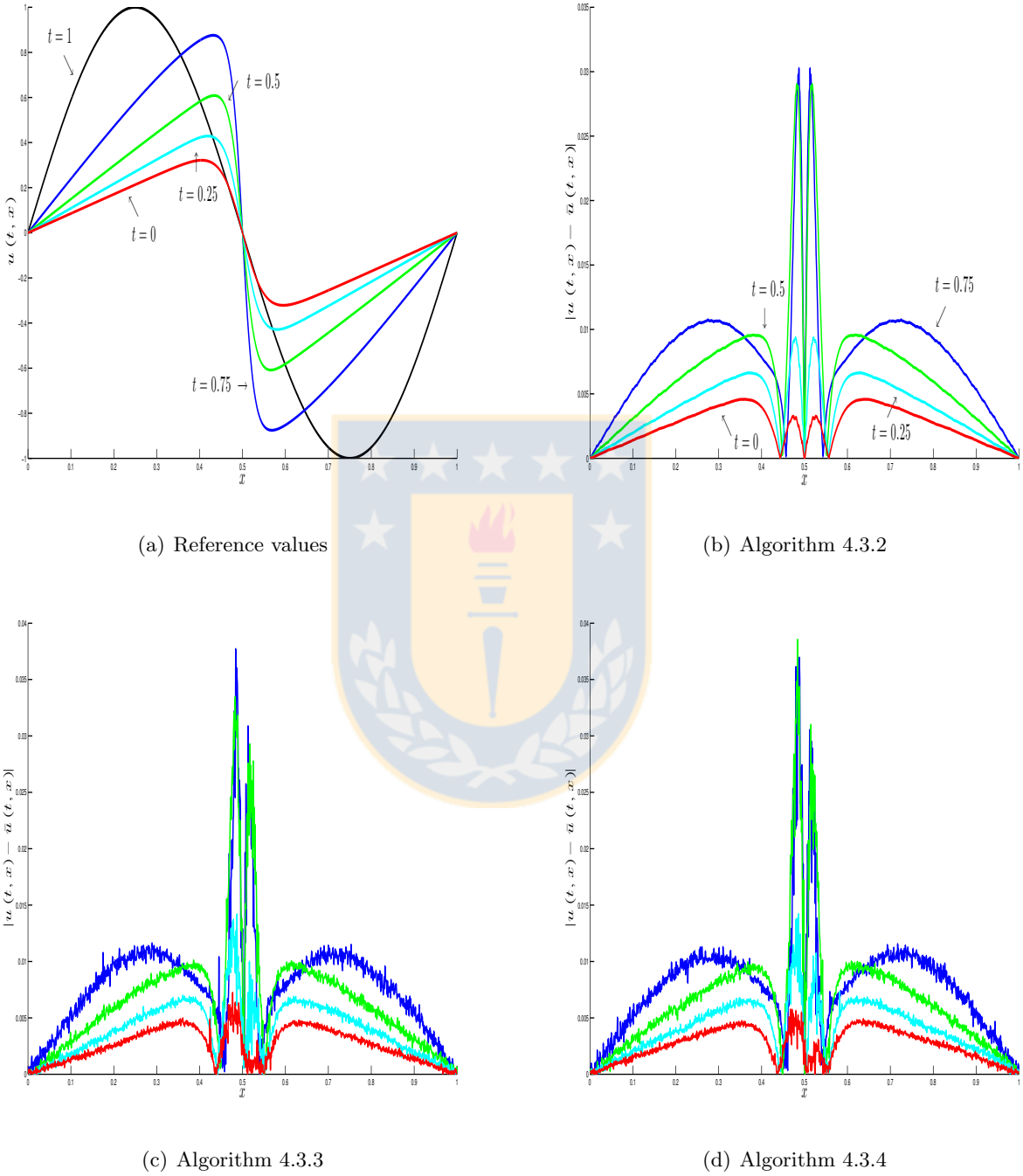

(a) Reference values

(b) Algorithm 4.3.2

(c) Algorithm 4.3.3

(d) Algorithm 4.3.4

Figure 4.1: Reference values and absolute point-wise errors to the one-dimensional Burgers equation. (a) Reference values for the profile of u in function of time computed by using (4.21) using quantization techniques with $M = 500$ grid points; (b) Absolute point-wise error between the approximated and true solution. As in [73], we use $M = 160$ quantized points to compute the numerical solution by means of Algorithm 4.3.2; (c) Absolute point-wise error by using the Algorithm 4.3.3 with $\mathcal{M} = 160$ realizations to the Monte Carlo method; and (d) Absolute point-wise error obtained by Algorithm 4.3.4 using Quantization ($M = 40$) as a control variate variable for Monte Carlo simulation ($\mathcal{M} = 16$ realizations).

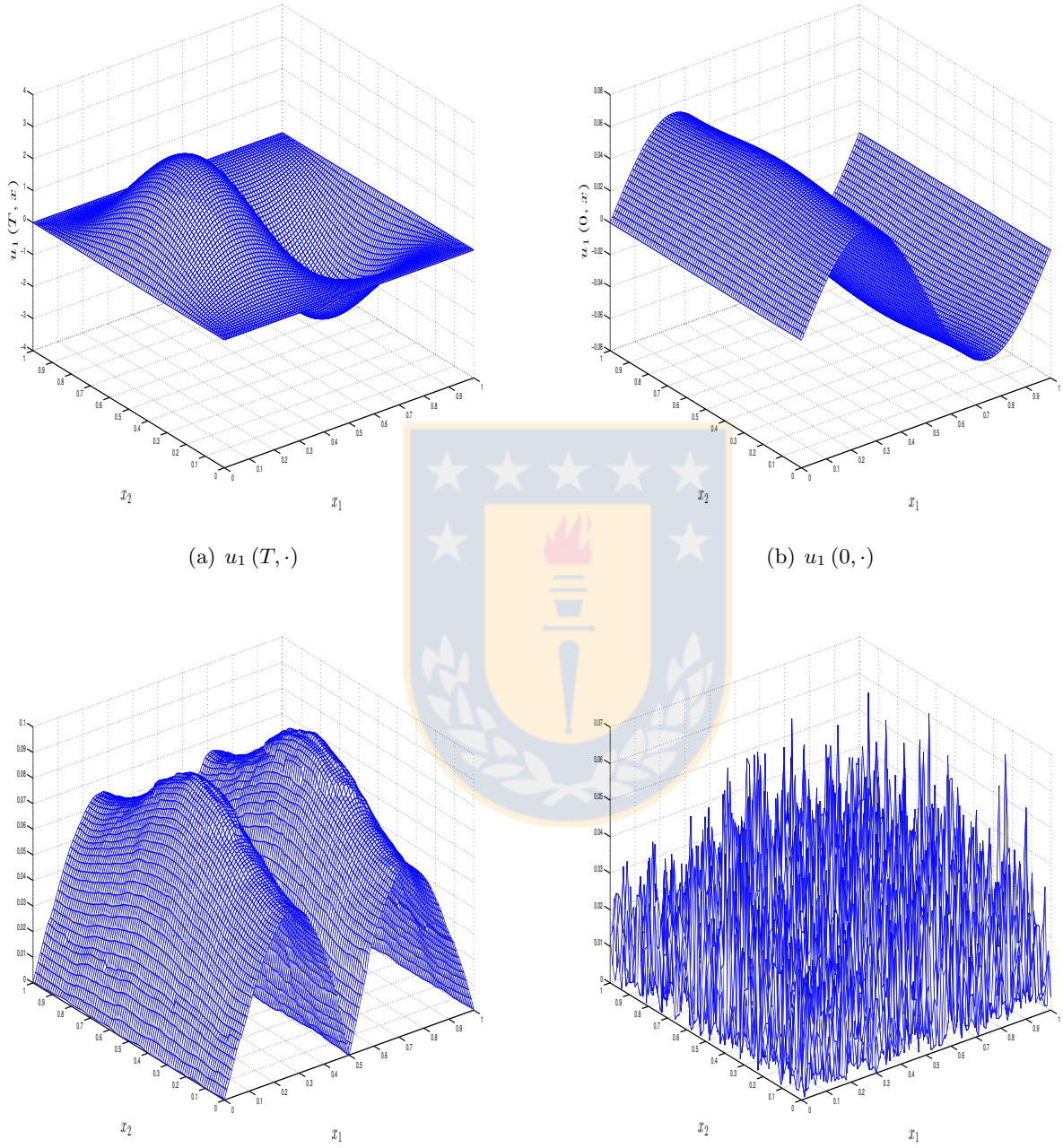

(a) $u_1(T,\cdot)$ (b) $u_1(0,\cdot)$

(c) Algorithm 4.3.2 (d) Algorithm 4.3.4

Figure 4.2: Numerical estimations for the two-dimensional Burgers equation. (a) Terminal condition $u_1(T,\cdot)$; (b) Reference $u_1(0,\cdot)$ via the explicit solution (4.22) using quantization with $M = 600$ points; (c) Absolute point-wise error for $u_1(0,\cdot)$ using Algorithm 4.3.2 with $M = 4$ points for quantization; and (d) Absolute point-wise error for $u_1(0,\cdot)$ by means of Algorithm 4.3.4 using quantization ($M = 4$) as a control variate variable to the Monte-Carlo estimations ($\mathcal{M} = 4$).

4.4 Incompressible Navier-Stokes equations

We consider the Navier-Stokes equations for incompressible fluids in $\mathbb{R}^d$, with $d \in \{2, 3\}$, written in backward form

$$\begin{cases} \dfrac{\partial u}{\partial t} + (u \cdot \nabla)\, u + \dfrac{\nu}{2}\Delta u + \nabla p + f = 0 \quad ; \ 0 \leq t < T, \\ \nabla \cdot u = 0, \quad u\,(T) = g, \end{cases} \tag{4.23}$$

which is equivalent to the classical formulation (4.1) by a time-reversing transformation.

Indeed, let (u, p, f) be the concerning functions of the forward form (4.1) and consider the transformation

$$(u, p, f)\,(t, x) \to (-u, p, -f)\,(T - t, x) =: \left(\tilde{u}, \tilde{p}, \tilde{f}\right)(t, x) \quad \forall\,(t, x) \in [0, T] \times \mathbb{R}^d.$$

Thus the incompressible Navier-Stokes equations system (4.1) is rewritten by

$$\begin{cases} \dfrac{\partial \tilde{u}}{\partial t} + (\tilde{u} \cdot \nabla)\, \tilde{u} = -\nu\Delta\tilde{u} - \nabla\tilde{p} - \tilde{f} \quad ; \ 0 \leq t < T, \\ \nabla \cdot \tilde{u} = 0, \quad \tilde{u}\,(T) = -g. \end{cases}$$

Then defining $\tilde{g} := -g$ and $\tilde{\nu} := 2\nu$, with g and ν as in (4.1), we obtain the backward form

$$\begin{cases} \dfrac{\partial \tilde{u}}{\partial t} + (\tilde{u} \cdot \nabla)\, \tilde{u} + \dfrac{\tilde{\nu}}{2}\Delta\tilde{u} + \nabla\tilde{p} + \tilde{f} = 0 \quad ; \ 0 \leq t \leq T, \\ \nabla \cdot \tilde{u} = 0, \quad \tilde{u}\,(T) = \tilde{g}. \end{cases}$$

The Burgers equation (4.11) can be seen as a simplified version of the incompressible Navier-Stokes equations (4.23). Under regularity assumptions and given a divergence-free external force field f, an approach to incorporate the pressure term ∇p and the incompressibility condition $\nabla \cdot u = 0$ into the Burgers equation (4.11) is be means of the Poisson problem

$$-\Delta p = \operatorname{div}\operatorname{div}(u \otimes u)$$

where $\operatorname{div} := \nabla\cdot$ represents the divergence operator and $\otimes$ the tensor product (see e.g. Chorin (1967) [53], Majda and Bertozzi (2002) [133]). Then the incompressible Navier-Stokes equations (4.23) is equivalent to

$$\begin{cases} \dfrac{\partial u}{\partial t} + (u \cdot \nabla)\, u + \dfrac{\nu}{2}\Delta u + \nabla\,(-\Delta)^{-1} \operatorname{div}\operatorname{div}(u \otimes u) + f = 0 \quad ; \ 0 \leq t < T, \\ u\,(T) = g. \end{cases} \tag{4.24}$$

Recently Delbaen, Qiu and Tang (2015) [76] introduced a coupled FBSDEs system (FBSDS) associated to the backward equation (4.24). Delbaen *et al.* give a probabilistic representation for the nonlocal operator $\nabla\,(-\Delta)^{-1} \operatorname{div}\operatorname{div}$ by means of BSDEs defined on the infinite time interval $(0, \infty)$. Then, incorporating the extra BSDEs in the FBSDEs (4.12), which is associated to the Burgers equation, the authors obtain a new FBSDEs representation to the incompressible Navier-Stokes equations in the whole space. Using their approach, it is possible to numerically approximate the strong solution

u of (4.24) on $(T_0, T]$, with $T_0 < T$ depending on the involved parameters. More precisely, the infinite interval $(0, \infty)$ of the probabilistic representation for the operator $\nabla (-\Delta)^{-1} \operatorname{div} \operatorname{div}$ is truncated by $\left[\frac{1}{N}, N\right]$, for $N \in (1, \infty)$, and the velocity field u is approximated by means of u^N, with $N \in (1, \infty)$, which solves the *truncated* PDE

$$\begin{cases} \dfrac{\partial u^N}{\partial t} + \left(u^N \cdot \nabla\right) u^N + \dfrac{\nu}{2} \Delta u^N + \mathbf{Q}^N \left(u^N \otimes u^N\right) + f = 0 \quad ; \; T_0 \leq t < T, \\ u^N (T) = g. \end{cases} \tag{4.25}$$

Here, for each $N \in (1, \infty)$ is defined

$$\mathbf{Q}^N (\phi \otimes \psi) := \mathbb{E} \int_{\frac{1}{N}}^N \frac{27}{2s^3} \sum_{i,j=1}^d \phi^i \cdot \psi^j (x + B_s) \left(B_s^i - B_{\frac{2s}{3}}^i\right) \left(B_{\frac{2s}{3}}^j - B_{\frac{s}{3}}^j\right) B_{\frac{s}{3}} ds \quad \forall \phi, \psi \in H^m, m > \frac{d}{2} + 1,$$

where B is a d-dimensional Brownian motion. Given $\nu > 0$, $g \in H_\sigma^m$ and $f \in C\left([0, T]; H_\sigma^{m-1}\right)$ with $m > \frac{d}{2} + 1$ we have the estimation

$$\left\| u - u^N \right\|_{C\left([t,T]; C^{k,\alpha}\right)} \leq \frac{C}{N^{\frac{\alpha}{4}}}; \quad \forall t \in (T_0, T], \tag{4.26}$$

for some $T_0 \in (0, T)$, $k \in \mathbb{Z}_+$, $\alpha \in (0, 1)$ and $C > 0$ independent of N. Note that from Morrey's inequality

$$H^m = W^{m,2}\left(\mathbb{R}^d\right) \subset C^{m - \left[\frac{d}{2}\right] - 1, \gamma},$$

where $\gamma = \left[\frac{d}{2}\right] + 1 - \frac{d}{2} = \frac{1}{2}$ when $d = 3$ or any number $\gamma \in (0, 1)$ if $d = 2$ (see e.g. Theorem 6.6 in [76]). Then, the equation (4.25) is associated through the nonlinear Feynman-Kac formula

$$u^N (r, x) = Y_r^{r,x}$$

to the following FBSDS:

$$\begin{cases} dX_s^{t,x} = Y_s \left(s, X_s^{t,x}\right) ds + \sqrt{\nu} dW_s \qquad ; \; s \in [t, T], \\ X_t^{t,x} = x, \\ -dY_s \left(s, X_s^{t,x}\right) = \left[f \left(s, X_s^{t,x}\right) + \mathbf{Q}^N \left(Y_s \otimes Y_s\right) \left(s, X_s^{t,x}\right)\right] ds - \sqrt{\nu} Z_s^{t,x} dW_s, \\ Y_T (T, x) = g (x), \\ \mathbf{Q}^N \left(Y_s \otimes Y_s\right) (s, x) = \displaystyle\sum_{i,j=1}^d \mathbb{E} \int_{\frac{1}{N}}^N \frac{27}{2r^3} Y_s^i \cdot Y_s^j (s, x + B_r) \left(B_r^i - B_{\frac{2r}{3}}^i\right) \left(B_{\frac{2r}{3}}^j - B_{\frac{r}{3}}^j\right) B_{\frac{r}{3}} dr \\ \qquad\qquad = \displaystyle\sum_{i,j=1}^d \mathbb{E} \int_{\frac{1}{3N}}^{\frac{N}{3}} \frac{3}{2r^3} Y_s^i \cdot Y_s^j \left(s, x + \bar{B}_r + \tilde{B}_r + \hat{B}_r\right) \bar{B}_r^i \tilde{B}_r^j \hat{B}_r dr, \end{cases} \tag{4.27}$$

where $W, B, \bar{B}, \tilde{B}$ and $\hat{B}$ are independent d-dimensional Brownian motions and, by abuse of notation, we write $Y_s (t, y) := Y_s^{t,y}$. Moreover, it is worth pointing out that $Y_s^{t,\cdot} = Y_s^{s, X_s^{t,\cdot}}$ (see Theorem 6.4 and Remark 6.2 in [76]).

Following the works of Delarue and Menozzi [73, 74], Delbaen *et al.* [76] introduced a numerical algorithm to approximate the process Y that solves (4.27) and then to simulate the velocity field u of the incompressible Navier-Stokes equations (4.23) in the whole space $\mathbb{R}^d$. Motivated by this, we consider the following numerical algorithm:

Algorithm 4.4.1 *Let $T > 0$. Fix $h = T/N$, with $N \geq 1$, and $\delta > 0$. Define*

$$\bar{u}^N(T, x) = g(x) \quad \forall x \in \mathcal{C}_\delta.$$

Then $\forall k \in \{0, \ldots, N-1\}$, $\forall x \in \mathcal{C}_\delta$,

$$\mathcal{T}(t_k, x) = \bar{u}^N(t_{k+1}, x) \cdot h + \sqrt{\nu} q(\Delta W_k),$$

$$\mathcal{Q}^N(t_k, x) = \mathbb{E} \int_{\frac{1}{3N}}^{\frac{N}{3}} \frac{3}{2r^3} \bar{u}_i^N \cdot \bar{u}_j^N \left(t_{k+1}, \Pi_\delta \left(x + q\left(\bar{B}_r\right) + q\left(\tilde{B}_r\right) + q\left(\hat{B}_r\right)\right)\right) q^i\left(\bar{B}_r\right) q^j\left(\tilde{B}_r\right) q\left(\hat{B}_r\right) dr,$$

$$\bar{u}^N(t_k, x) = \mathbb{E}\left[\bar{u}^N\left(t_{k+1}, \Pi_\delta\left(x + \mathcal{T}(t_k, x)\right)\right)\right] + \left(f(t_{k+1}, x) + \mathcal{Q}^N(t_k, x)\right) \cdot h.$$

Here, the terms $\mathcal{Q}^N(t_k, x)$ involve the Einstein summation convention.

Therefore, the Algorithm 4.4.1 guides us to compute the approximations

$$\bar{u}^N(t_k, x) \approx u^N(t_k, x) \quad \forall k \in \{0, \ldots, N-1\}, \ \forall x \in \mathcal{C}_\delta.$$

Thus a simple piecewise continuous extension of the vector-valued function $\bar{u}^N$ follows from

$$\bar{u}^N(t, x) := \bar{u}^N(t_k, \Pi_\delta(x)) \quad \forall t \in [t_k, t_{k+1}[, \ \forall x \in \mathbb{R}^d.$$

Since the additive noise in the involved SDEs, we approximate $\mathcal{T}(t_k, x)$ by the Euler-Maruyama scheme instead of the stable schemes introduced in Chapters 2 and 3. The drift coefficients correspond to successive numerical approximations $\bar{u}^N$ of the incompressible velocity field u. In some cases, like the Taylor-Green vortices, it is of physical importance to preserve dynamic properties of the random particles moving according to such SDEs. As an alternative to the Euler-Maruyama scheme we refer, for example, to the stochastic splitting method introduced by Pavliotis, Stuart and Zygalakis (2009) [170] for the numerical approximation of particles moving in fluid flows under uncertainties.

To compute expectations of integrals depending on path of Brownian motions introduces an additional source of error in the numerical treatment of the terms $\mathcal{Q}^N$, which approximate the gradient of the pressure. For the local integration of (4.27) we have the approximations

$$\begin{aligned}
\int_{t_k}^{t_{k+1}} \mathbf{Q}^N (Y_s \otimes Y_s)\left(s, X_s^{t_k, x}\right) ds &\approx \int_{t_k}^{t_{k+1}} \mathbf{Q}^N (Y_s \otimes Y_s)\left(s, X_{t_k}^{t_k, x}\right) ds \\
&\approx \int_{t_k}^{t_{k+1}} \mathbb{E} \int_{\frac{1}{3N}}^{\frac{N}{3}} \frac{3}{2r^3} Y_{t_{k+1}}^i \cdot Y_{t_{k+1}}^j \left(t_{k+1}, x + \bar{B}_r + \tilde{B}_r + \hat{B}_r\right) \bar{B}_r^i \tilde{B}_r^j \hat{B}_r dr ds \\
&\approx \mathbb{E} \int_{\frac{1}{3N}}^{\frac{N}{3}} \frac{3}{2r^3} \bar{u}_i^N \cdot \bar{u}_j^N \left(t_{k+1}, \Pi_\delta\left(x + \bar{B}_r + \tilde{B}_r + \hat{B}_r\right)\right) \bar{B}_r^i \tilde{B}_r^j \hat{B}_r dr \cdot h.
\end{aligned}$$

The estimations involve the Einstein notation. Therefore, the key point is to consider an efficient estimation of the term $\mathcal{Q}^N$ which provides us the convergence of $\bar{u}^N$ defined by Algorithm 4.4.1 to the strong solution u^N of (4.25). We use simple Riemann sum approximations to the integrals, together with the quantization to the underlying Gaussian processes. To be clear, we take

$$\mathcal{Q}^N(t_k,x) \approx \sum_{i,j=1}^{d} \mathbb{E} \sum_{l=0}^{N_R-1} \frac{3}{2\left(s_l^N\right)^3} \bar{u}_i^N \cdot \bar{u}_j^N \left(t_{k+1}, \Pi_\delta \left(x + \sqrt{s_l^N}\left[q\left(\bar{\xi}_{s_l^N}\right) + q\left(\tilde{\xi}_{s_l^N}\right) + q\left(\hat{\xi}_{s_l^N}\right)\right]\right)\right)$$
$$\left(\sqrt{s_l^N}\right)^3 q^i\left(\bar{\xi}_{s_l^N}\right) q^j\left(\tilde{\xi}_{s_l^N}\right) q\left(\hat{\xi}_{s_l^N}\right) \cdot \delta_2, \tag{4.28}$$

where $N_R \in \mathbb{Z}_+$, $\delta_2 := \left(\frac{N}{3} - \frac{1}{3N}\right)/N_R$, $s_l^N := \frac{1}{3N} + l \cdot \delta_2$, and

$$\bar{\xi}_r := \frac{\bar{B}_r}{\sqrt{r}}, \tilde{\xi}_r := \frac{\tilde{B}_r}{\sqrt{r}}, \hat{\xi}_r := \frac{\hat{B}_r}{\sqrt{r}}.$$

We highlight some identities in order to deal with the numerical estimation of $\mathcal{Q}^N$ involved in the Algorithm 4.4.1. Since $u(T,x) = u^N(T,x) = Y_T(T,x) = \bar{u}^N(T,x)$, for each $x \in \mathbb{R}^d$

$$\begin{aligned}
\nabla p(T,x) &= \nabla(-\Delta)^{-1} \operatorname{div}\operatorname{div}(u \otimes u)(T,x) \\
&= \sum_{i,j=1}^{d} \nabla(-\Delta)^{-1} \frac{\partial^2}{\partial x_i \partial x_j}\left(u^i \cdot u^j\right)(T,x) \\
&= \mathbb{E}\int_0^\infty \frac{27}{2s^3} \sum_{i,j=1}^{d} u^i \cdot u^j (T, x+B_s)\left(B_s^i - B_{\frac{2s}{3}}^i\right)\left(B_{\frac{2s}{3}}^j - B_{\frac{s}{3}}^j\right) B_{\frac{s}{3}} ds \\
&= \lim_{N\to\infty} \mathbb{E}\int_{\frac{1}{N}}^N \frac{27}{2s^3} \sum_{i,j=1}^{d} u^i \cdot u^j (T, x+B_s)\left(B_s^i - B_{\frac{2s}{3}}^i\right)\left(B_{\frac{2s}{3}}^j - B_{\frac{s}{3}}^j\right) B_{\frac{s}{3}} ds \\
&= \lim_{N\to\infty} \mathbf{Q}^N (u \otimes u)(T,x) \\
&= \lim_{N\to\infty} \sum_{i,j=1}^{d} \mathbb{E}\int_{\frac{1}{3N}}^{\frac{N}{3}} \frac{3}{2r^3} \bar{u}_i^N \cdot \bar{u}_j^N \left(T, x + \bar{B}_r + \tilde{B}_r + \hat{B}_r\right) \bar{B}_r^i \tilde{B}_r^j \hat{B}_r dr.
\end{aligned} \tag{4.29}$$

Hence, we can test the approximation of $\mathcal{Q}^N$ by applying our methodology to the right term of (4.29) and comparing our results directly with the exact values from $\bar{u}^N(T,x) = g(x)$ and $\nabla p(T,\cdot)$.

Moreover, note that

$$\begin{aligned}
&\lim_{N\to\infty}\sum_{i,j=1}^{d}\mathbb{E}\int_{\frac{1}{N}}^{N}\frac{27}{2r^3}\bar{u}_i^N\cdot\bar{u}_j^N\left(T,x+B_r\right)\left(B^i_{\frac{2r}{3}}-B^i_{\frac{r}{3}}\right)\left(B^j_r-B^j_{\frac{2r}{3}}\right)B_{\frac{r}{3}}dr\\
&=\lim_{N\to\infty}\sum_{i,j=1}^{d}\int_{\frac{1}{N}}^{N}\frac{1}{2r}\mathbb{E}\left[\frac{\partial^2}{\partial x_i\partial x_j}\left(\bar{u}_i^N\cdot\bar{u}_j^N\right)\left(T,x+B_r\right)B_r\right]dr\\
&=\lim_{N\to\infty}\sum_{i,j=1}^{d}\int_{\frac{1}{N}}^{N}\frac{1}{2r}\mathbb{E}\left[\frac{\partial^2}{\partial x_i\partial x_j}\left(g_i\cdot g_j\right)\left(x+B_r\right)B_r\right]dr\\
&=\lim_{N\to\infty}\int_{\frac{1}{N}}^{N}\frac{1}{r}\mathbb{E}\left[\left(\frac{\partial g_1}{\partial x_2}\frac{\partial g_2}{\partial x_1}+\left(\frac{\partial g_2}{\partial x_2}\right)^2\right)\left(x+B_r\right)B_r\right]dr,
\end{aligned}$$

which helps to preliminary test the numerical estimation of $Q^N\left(t_k,x\right)$.

Alternative approaches to deal with path-dependent functionals of Brownian motions consider, for example, to use reduction variance techniques based on the Karhunen-Loève expansion of the Brownian motion, the Brownian bridge or well by conditioning the desired expectations by convenient events (see Lejay and Reutenauer (2012) [128], Kolkiewicz (2014) [122]).

4.4.1 Numerical experiments

Taylor-Green Vortex

We begin studying the numerical simulation of the incompressible Navier-Stokes equations by solving the Taylor-Green vortices introduced by Taylor and Green (1937) [201]. It corresponds to a classical turbulence model used to test numerical schemes applied to the Navier-Stokes equations and give us a benchmark to the Algorithm 4.4.1 with respect to finite difference methods (see e.g. Chorin (1968) [55], Frisch, Morf and Orszag (1980) [86], Brachet *et al.* [41, 42], Brachet (1991) [40], Canuto *et al.* (2007) [48]). Let us consider the incompressible Navier-Stokes equations

$$\begin{cases}\dfrac{\partial u}{\partial t}+(u\cdot\nabla)u-\dfrac{\nu}{2}\Delta u+\nabla p=0 \quad ;\ 0<t\leq T,\\ \nabla\cdot u=0,\quad u\left(0\right)=g.\end{cases}\tag{4.30}$$

As we saw this classical formulation is equivalent to the previous one (4.23) with $f\equiv 0$ by a time-reversing transformation, and so we deal with the approximation of the strong solution u of (4.30) by using the Algorithm 4.4.1. From now on, by abuse of notation, we denote in the same way $\bar{u}^N\left(t_k,x\right)$ the estimation of $u\left(t_k,x\right)$ obtained from Algorithm 4.4.1.

We consider the $2d$ Taylor-Green vortex flow that solves (4.30) with initial condition

$$\begin{cases}g_1\left(x\right)=-\cos\left(x_1\right)\sin\left(x_2\right),\\ g_2\left(x\right)=\sin\left(x_1\right)\cos\left(x_2\right).\end{cases}$$

The advantage of this model is that we can directly compare our results with its explicit solution

$$\begin{cases} u_1(t,x) = -\exp(-\nu t)\cos(x_1)\sin(x_2), \\ u_2(t,x) = \exp(-\nu t)\sin(x_1)\cos(x_2), \\ p(t,x) = -\dfrac{1}{4}\exp(-2\nu t)(\cos(2x_1)+\cos(2x_2)), \end{cases} \tag{4.31}$$

for $x = (x_1, x_2)^\top \in [0, 2\pi]^2$. That is,

$$\begin{cases} u_1(t,x) = \exp(-\nu(T-t))\cos(x_1)\sin(x_2), \\ u_2(t,x) = -\exp(-\nu(T-t))\sin(x_1)\cos(x_2), \\ p(t,x) = -\dfrac{1}{4}\exp(-2\nu(T-t))(\cos(2x_1)+\cos(2x_2)) \end{cases}$$

solves the backward incompressible Navier-Stokes equations (4.23).

Chorin [54, 55] approximated this test model by introducing a finite-difference method. Assuming that the discretization steps verify $h = \mathcal{O}(\delta^2)$, for smooth enough spatially periodic solutions and sufficiently small discretization parameters its order of error in the maximum norm is of order δ and $\sqrt{\delta}$ in two and three spatial dimensions, respectively (see Theorem 3 of [56]).

As in [55] we numerically solve the $2d$ Taylor-Green vortex flow (4.31) with viscosity parameter $\nu = 2$ and $h = \mathcal{O}(\delta^2)$. The top plots in Figure 4.3 represent the initial velocity field $u(0,\cdot) = (u_1(0,\cdot), u_2(0,\cdot))^\top$. The left bottom plot shows the reference velocity component $u_1(T,\cdot)$ from (4.31). The right bottom one describes the estimation of the first component $\bar{u}_1^N(T,\cdot)$ obtained from Algorithm 4.4.1 together with the estimation (4.28) by using truncation parameter $N = 6$, time-step $h = 2\delta^2$, space-discretization step $\delta = \pi/39$ and $M = 6$ quantization points, until a final time $T = 20 \cdot h$. We compute the terms Q^N by taking a left Riemann sum approximation of the integral using $N_R = 18$ subintervals of $\left[\frac{1}{3N}, \frac{N}{3}\right]$.

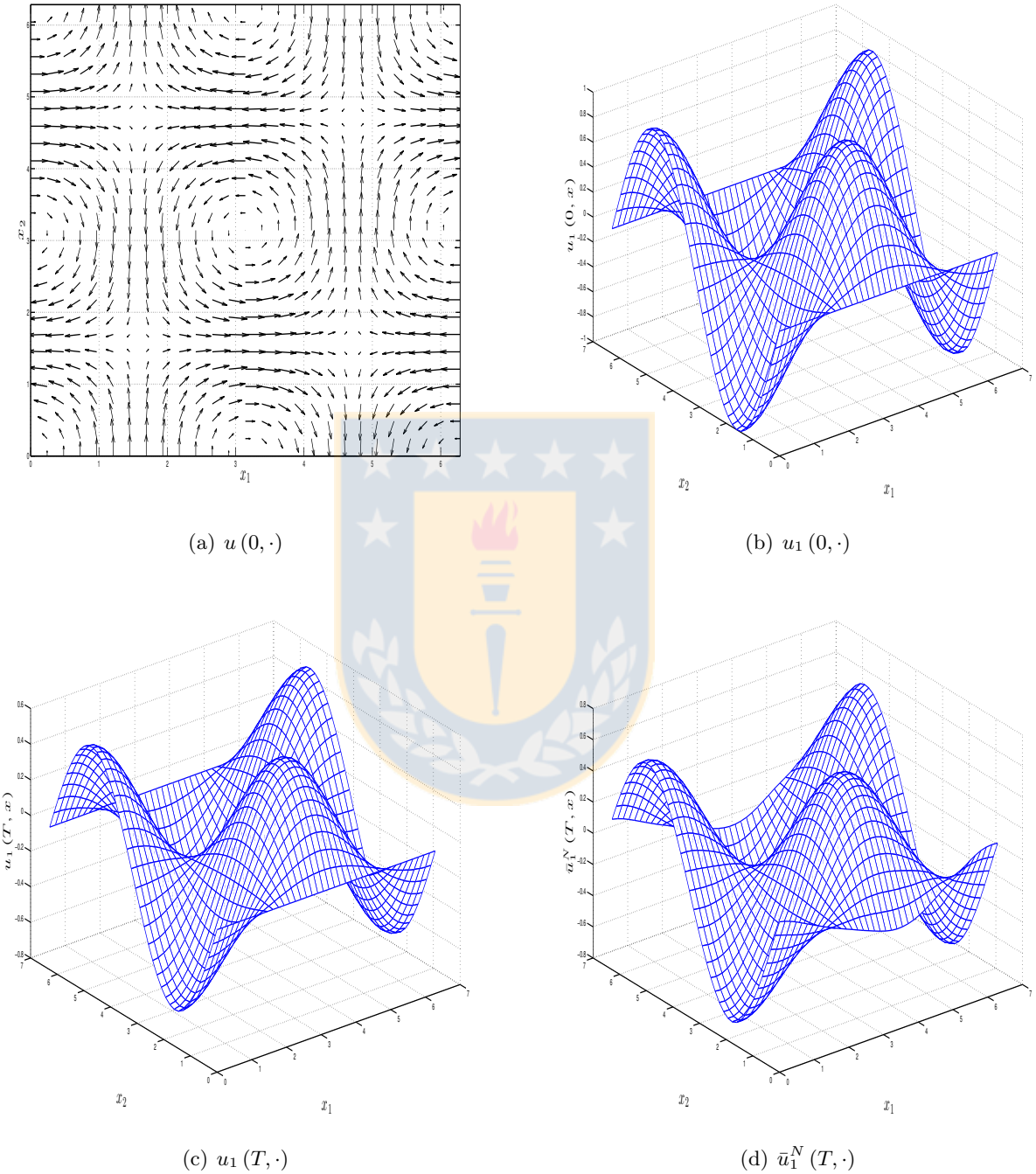

(a) $u\,(0,\cdot)$ (b) $u_1\,(0,\cdot)$

(c) $u_1\,(T,\cdot)$ (d) $\bar{u}_1^N\,(T,\cdot)$

Figure 4.3: Two-dimensional Taylor-Green vortex for $\nu = 2$. Here (a) Initial condition $u\,(0,\cdot)$; (b) First component $u_1\,(0,\cdot)$; (c) Reference $u_1\,(T,\cdot)$ at time $T = 20 \cdot h$; and (d) Estimation $\bar{u}_1^N\,(T,\cdot)$ at time $T = 20 \cdot h$ by means of Algorithm 4.4.1 and the approximation (4.28) ($N = 6$, time-step $h = 2\delta^2$, spatial discretization $\delta = \pi/39$, $M = 6$ quantization points and $N_R = 18$ subintervals).

Table 4.1 shows the estimation errors

$$e_i\left(t_k\right) := \sup_{x \in C_\delta} \left| u_i\left(t_k, x\right) - \bar{u}_i^N\left(t_k, x\right) \right|^2 \qquad ; \; i \in \{1, \ldots, d\}, k \in \{1, \ldots, T/h\}.$$

In comparison with the reported values [55], the results given by Algorithm 4.4.1 are not accurate. This is in part explained because $\delta > h$, i.e. the spatial-step $\delta = \pi/39$ is greater than the time-step $h = 2\delta^2$, and so the "Burgers equation part" estimation is not completely valid.

As in Algorithm 4.3.1, from now on we consider only discretization-steps such that $\delta < h$. Thus, we now take discretization steps $h = 0.025$ and $\delta = \pi/126$. Figure 4.4 and Table 4.2 depict the better new results. Note that the discretization steps are related linearly, instead of the restrictive assumption $h = \mathcal{O}\left(\delta^2\right)$ in case of the finite-difference scheme [56].

Algorithm 4.4.1		
k	$e_1\left(t_k\right)$	$e_2\left(t_k\right)$
1	0.00023	0.00030
2	0.00085	0.00096
3	0.00174	0.00188
4	0.00284	0.00314
5	0.00417	0.00459
6	0.00562	0.00620
7	0.00717	0.00790
8	0.00879	0.00968
9	0.01045	0.01153
10	0.01219	0.01343
20	0.02938	0.03221

Table 4.1: Estimation errors $e_i\left(t_k\right)$ to the two-dimensional Taylor-Green vortex with viscosity parameter $\nu = 2$ obtained from Algorithm 4.4.1 and the estimation (4.28) with $N = 6$, $h = 2\delta^2$, $\delta = \pi/39$, $M = 6$ and $N_R = 18$.

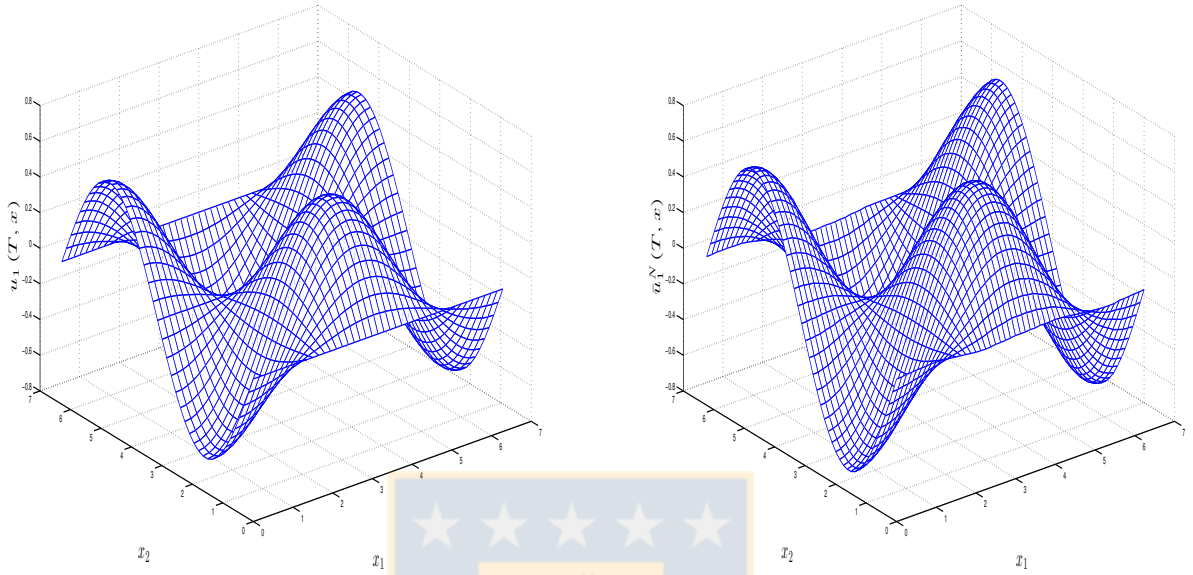

(a) $u_1(T,\cdot)$ (b) $\bar{u}_1^N(T,\cdot)$

Figure 4.4: Two-dimensional Taylor-Green vortex for $\nu = 2$ at time $T = 10 \cdot h$. Here (a) Reference $u_1(T,\cdot)$; and (b) Estimation $\bar{u}_1^N(T,\cdot)$ by means of Algorithm 4.4.1 and the estimation (4.28) ($N = 6$, time-step $h = 0.025$, spatial discretization $\delta = \pi/126$, $M = 6$ quantization points and $N_R = 18$ subintervals).

Algorithm 4.4.1		
k	$e_1(t_k)$	$e_2(t_k)$
1	0.000208	0.000213
2	0.000651	0.000663
3	0.001206	0.001307
4	0.001899	0.002094
5	0.002656	0.002998
6	0.003385	0.003950
7	0.004020	0.004906
8	0.004668	0.005875
9	0.005401	0.006822
10	0.006076	0.007745

Table 4.2: Estimation errors $e_i(t_k)$ to the two-dimensional Taylor-Green vortex with viscosity parameter $\nu = 2$ using Algorithm 4.4.1 and the estimation (4.28) with $N = 6$, $h = 0.025$, $\delta = \pi/126$, $M = 6$ and $N_R = 18$.

Concerning to the computation of $\mathcal{Q}^N(t_k, x)$, from (4.29) and (4.31) we have checked that our above preliminary estimation leads to a simple and reliable way to approximate the pressure terms (see Figure 4.8).

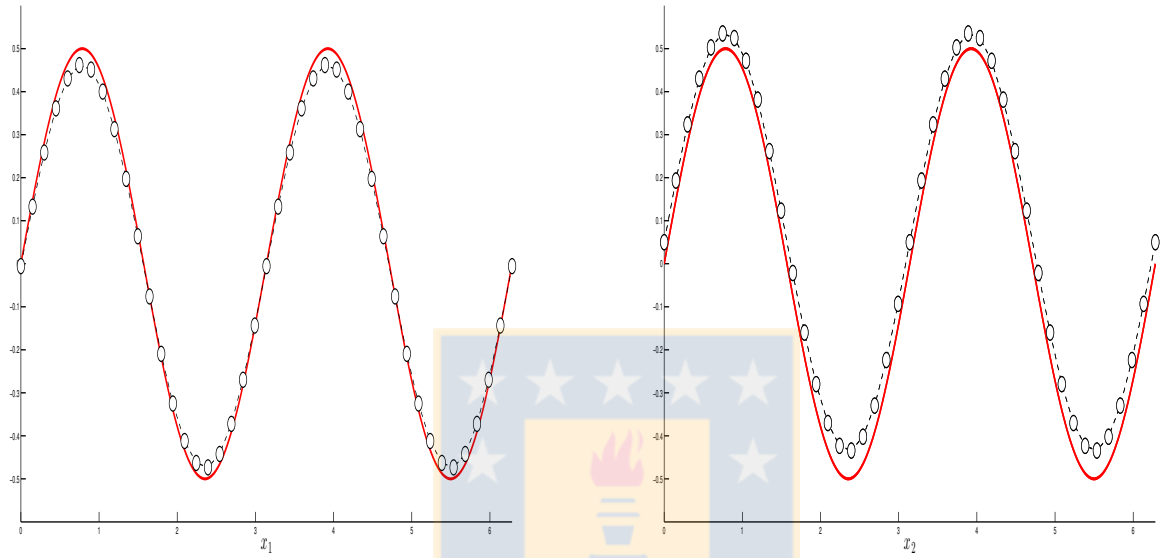

(a) (b)

Figure 4.5: Estimation of pressure terms $\nabla p(t, x)$; $x = (x_1, x_2)^\top$, to the $2d$ Taylor-Green vortex at $t = 0$. The reference values are plotted in solid red lines. Here (a) Estimation of the first component for $x_1 \in [0, 2\pi]$ and $x_2 = 0$; and (b) Estimation of the second component for $x_1 = 0$ and $x_2 \in [0, 2\pi]$. The approximated values have been obtained by means of $\mathcal{Q}^N$ as in Algorithm 4.4.1 and (4.28) ($N = 6$, spatial discretization $\delta = \pi/126$, $M = 6$ quantization points and $N_R = 18$ subintervals).

Beltrami Flow

The Beltrami flows, introduced by E. Beltrami in 1889 [22], are characterized by the property that the vorticity vector $\omega = \operatorname{curl} u$, with rotational operator $\operatorname{curl} := \nabla\times$, satisfies $\omega = \lambda u$ for some parameter λ. That is, the vorticity and the velocity vectors are aligned, or well the vorticity is an eigenvector of the rotational operator. Observing

$$(u \cdot \nabla) u = \nabla \frac{\|u\|^2}{2} - u \times \omega,$$

from the vorticity form of the Navier-Stokes equations is deduced the Bernoulli equation

$$\frac{p(t,x)}{\rho} + \frac{\|u(t,x)\|^2}{2} + \mathrm{g} \cdot \langle (0,0,1), x \rangle = p_s(t),$$

being $p_s(t)$ a constant stagnation pressure at the ground level, $\mathrm{g} > 0$ the acceleration due to gravity and $\rho > 0$ the constant density of the fluid. Then, constructing an explicit velocity field u the pressure term p can be recover from the Bernoulli law.

We study the three-dimensional viscous Beltrami flow

$$\begin{cases} u(t,x) = e^{-\nu\lambda^2 t} g(x), \\ p(t,x) = p_s - \rho \left[\dfrac{\|u(t,x)\|^2}{2} + \mathrm{g} \cdot \langle (0,0,1), x \rangle \right], \end{cases} \tag{4.32}$$

with non-divergence initial velocity field

$$\begin{cases} g_1(x) = -\dfrac{A}{k^2+l^2} \left[\lambda l \cos(kx_1) \sin(lx_2) \sin(mx_3) + mk \sin(kx_1) \cos(lx_2) \cos(mx_3) \right], \\ g_2(x) = \dfrac{A}{k^2+l^2} \left[\lambda k \sin(kx_1) \cos(lx_2) \sin(mx_3) - ml \cos(kx_1) \sin(lx_2) \cos(mx_3) \right], \\ g_3(x) = A \cos(kx_1) \cos(lx_2) \sin(mx_3). \end{cases}$$

Here, $\nu > 0$ is the constant kinematic viscosity, the parameter p_s a time-independent stagnation pressure at ground level, the amplitude constant A of the vertical velocity and Beltrami parameter

$$\lambda = \sqrt{k^2 + l^2 + m^2},$$

with $k, l, m > 0$ (see Shapiro (1993) [187]). The Beltrami flow (4.32) solves the Navier-Stokes equations

$$\begin{cases} \dfrac{\partial u}{\partial t} + (u \cdot \nabla) u = \nu \Delta u - \dfrac{1}{\rho} \nabla p - \mathrm{g} \cdot (0,0,1)^\top & ;\ 0 < t \le T, \\ \nabla \cdot u = 0, \quad u(0) = g(x). \end{cases} \tag{4.33}$$

That is the incompressible Navier-Stokes equations (4.1) with external force $f(t,x) = -\mathrm{g} \cdot (0,0,1)^\top$ and initial divergence-free vector field $g(x)$ as above.

Defining the potential $\phi(t,x) = -\mathrm{g}\cdot\langle(0,0,1),x\rangle$, observe that $f(t,x) = \nabla\phi(t,x)$. Thus, the constant density $\rho > 0$ and the conservative external force field f are considered as part of the pressure term $p(t,x)$. As above, fixing a time scale $T > 0$ and taking a convenient transformation we obtain that

$$\begin{cases} u(t,x) = -e^{-2\nu\lambda^2(T-t)}g(x), \\ p(t,x) = \dfrac{p_s}{\rho} - \left[\dfrac{\|u(T-t,x)\|^2}{2} + \mathrm{g}\cdot\langle(0,0,1),x\rangle + \phi(T-t,x)\right] = \dfrac{p_s}{\rho} - \dfrac{\|u(T-t,x)\|^2}{2}, \end{cases} \tag{4.34}$$

for $t \in [0,T]$ and $x \in \left[0,\frac{2\pi}{k}\right]\times\left[0,\frac{2\pi}{l}\right]\times\left[0,\frac{2\pi}{m}\right]$, is the solution of the backward incompressible Navier-Stokes equations (4.23) with viscosity parameter $\nu > 0$ and without external force field. Observe that the pressure at a given position corresponds to the difference between a constant pressure and the kinetic energy per mass unit of the particle of fluid located at such point. Then, motivated by the previous sections we deal with the numerical approximation of the three-dimensional space-periodic velocity field in (4.34) by means of the Algorithm 4.4.1 and the proposed estimation (4.28).

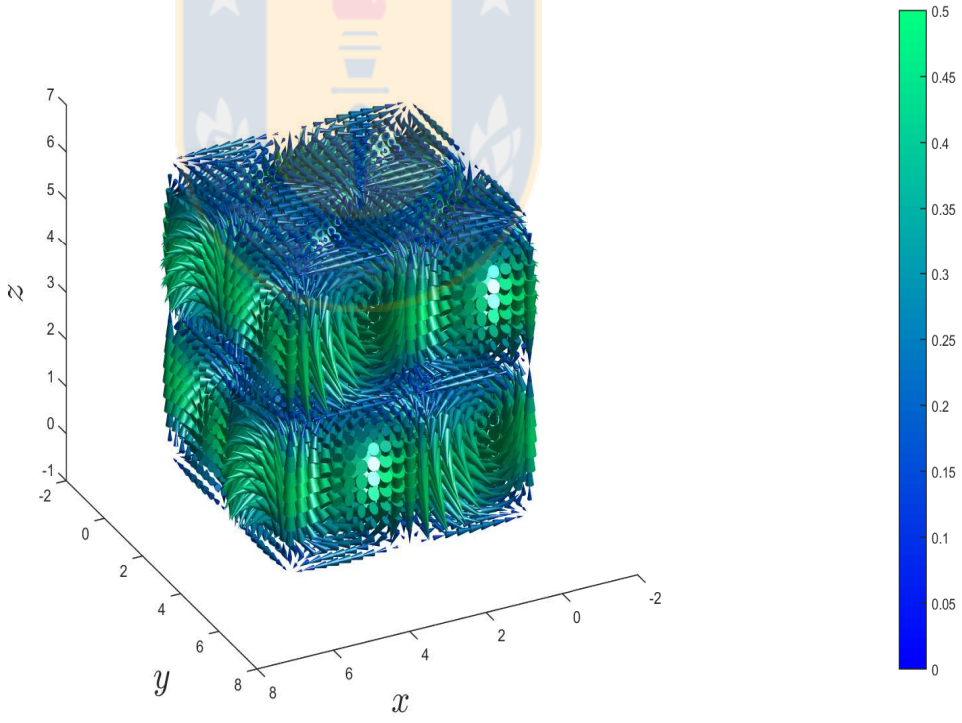

Figure 4.6: Initial spatially-periodic velocity field to the three-dimensional Beltrami flow with parameters $A = 1/2$ and $k = l = m = 1$.

Algorithm 4.4.1										
k	1	2	3	4	5	6	7	8	9	10
$\tilde{e}_1(t_k)$	0.0994	0.2719	0.5046	0.7557	1.0427	1.3278	1.6278	1.8934	2.1408	2.3464
$\tilde{e}_2(t_k)$	0.0762	0.2097	0.3906	0.5483	0.7490	0.8825	1.0559	1.2134	1.3037	1.3780
$\tilde{e}_3(t_k)$	0.0661	0.1944	0.3166	0.4872	0.6616	0.7902	1.0241	1.1166	1.2321	1.3769

Table 4.3: Estimation errors $\tilde{e}_i(t_k) := e_i(t_k) \cdot 10^2$ to the three-dimensional Beltrami flow by using Algorithm 4.4.1 and the approximation (4.28) ($N = 6$, time-step $h = 1/5$, spatial discretization $\delta = \pi/20$, $M = 6$ quantization points and $N_R = 18$ subintervals).

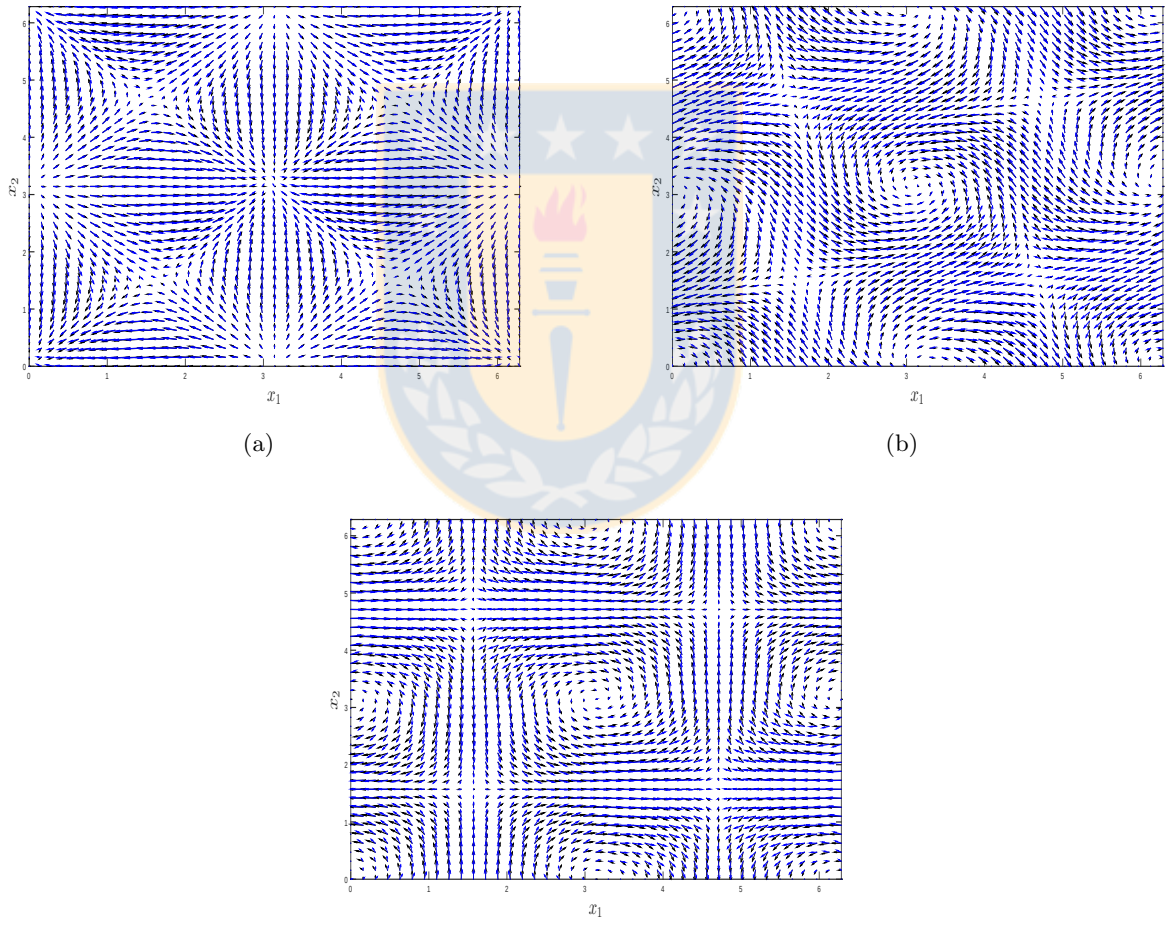

Figure 4.7: Estimation of velocity field $u(t,x)$; $x = (x_1, x_2, x_3)^\top$, to the $3d$ Beltrami flow for $\nu = 0.1$, $A = 1/2$, $k = l = m = 1$ at $T = 10 \cdot h$. The reference values are plotted in solid black lines. Here (a) Estimation of $u(T,\cdot,\cdot,0)$; (b) Estimation of $u(T,\cdot,\cdot,\pi/4)$ and (c) Estimation of $u(T,\cdot,\cdot,\pi/2)$. The approximated values have been obtained by Algorithm 4.4.1 with $\mathcal{Q}^N$ approximated as in (4.28) ($N = 6$, time-step $h = 1/5$, spatial discretization $\delta = \pi/20$, $M = 6$ quantization points and $N_R = 18$ subintervals).

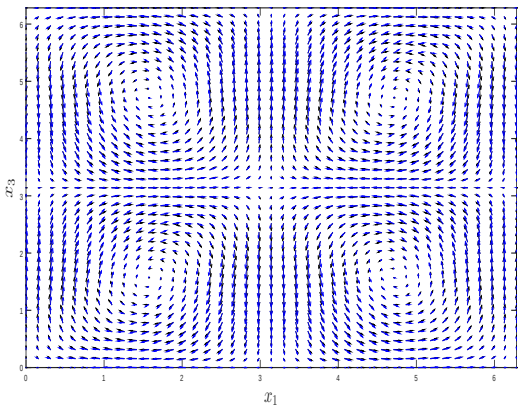

(a)

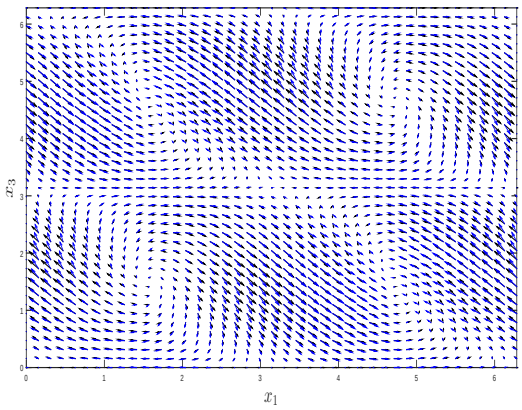

(b)

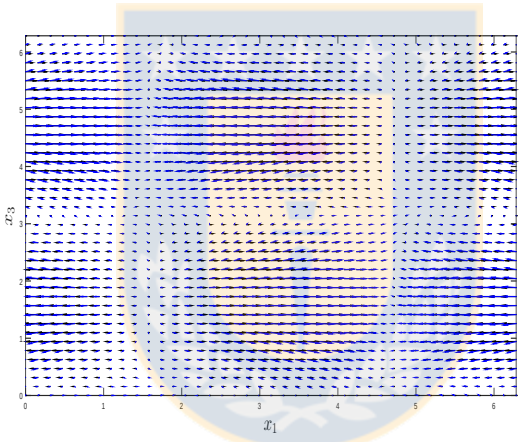

(c)

Figure 4.8: Estimation of velocity field $u(t,x)$; $x=(x_1,x_2,x_3)^\top$, to the $3d$ Beltrami flow for $\nu=0.1$, $A=1/2$, $k=l=m=1$ at $T=10\cdot h$. The reference values are plotted in solid black lines. Here (a) Estimation of $u(T,\cdot,0,\cdot)$; (b) Estimation of $u(T,\cdot,\pi/4,\cdot)$ and (c) Estimation of $u(T,\cdot,\pi/2,\cdot)$. The approximated values have been obtained by Algorithm 4.4.1 with Q^N approximated as in (4.28) ($N=6$, time-step $h=1/5$, spatial discretization $\delta=\pi/20$, $M=6$ quantization points and $N_R=18$ subintervals).

Chapter 5

Conclusions

Among the numerical methods for the approximation of Itô diffusions

$$X_t = X_0 + \int_0^t b\left(X_s\right) ds + \int_0^t \sigma\left(X_s\right) dW_s,$$

the Euler-Maruyama and the implicit Euler methods appear as the usual alternatives. The multiplicative noise intensifies the role of the diffusion term σ on the dynamic of the stochastic process X and various stability criteria have been proposed for solutions of SDEs driven by Brownian motion. The almost sure asymptotic exponential behavior and the sign-preserving ability of the exact solutions bring us a starting point to the design of adequate weak numerical schemes. In general, various numerical schemes converge with some specific order and inherit the dynamical properties of the unknown solutions provided that the step-sizes for time discretizations are small enough. In practice is difficult to choice the best candidate to numerically solve a specific stochastic equation and to identify the maximum time-step to guarantee accurate weak numerical estimations. The convergence and stability properties of traditional Euler methods, and alternative Euler-based schemes, are valid as well as the step size tends to zero. Then it is necessary to reduce the concerned discretization step, increasing the computational effort to the numerical solution of stiff SDEs or in case of the long-time simulation of X.

In some applications the noise structure is represented by means of the Stratonovich integral. Hence, by rewritten it on an appropriate Itô integral we can study stochastic processes governed by Stratonovich SDEs by using the introduced methodologies. Under appropriate assumptions the Itô diffusion process $X = \left(X^1, \ldots, X^d\right)^\top$ can be equivalently expressed by the Stratonovich SDE

$$dX_t^i = \left(b^i\left(X_t\right) - \frac{1}{2} \sum_{k=1}^{m} \left\langle \sigma^k\left(X_t\right), \nabla \sigma^{i,k}\left(X_t\right) \right\rangle \right) dt + \sum_{k=1}^{m} \sigma^{i,k}\left(X_t\right) \circ dW_t^k; \quad \forall i \in \{1, \ldots, d\}.$$

The implicit balanced Euler method is well-known to improve the stability properties of the Euler-Maruyama method, at cost of to identify appropriate weight functions to capture the correct dynamical behavior of the exact solutions. By incorporating such additional terms, the order of convergence of the Euler method is affected and additional time is needed to solve of implicit equations at each time

step. To the best of our knowledge, the balanced schemes presented in specialized literature involves stabilizing functions that depend on the drift term, the diffusion coefficient and the Brownian motion. The incorporation of the Wiener process on implicitness reduce the order of weak convergence of the original Euler scheme. Concerning to the weak numerical estimation of SDEs, it is well-known that the Brownian increments can be replaced by discrete random variables having similar moment properties. This permits us to introduce first-order weak methods by studying the explicit stability region and the sign-preserving ability of the presented schemes.

In case of the linear scalar pure diffusion

$$X_t = X_0 + \int_0^t \sigma X_s dW_s$$

we introduce the balanced Euler scheme

$$Z_{n+1} = Z_n + \sigma Z_n \sqrt{\Delta}\xi_n - \alpha(\Delta)\sigma\sigma^\top (Z_{n+1} - Z_n)\Delta,$$

with bounded weight $\alpha(\Delta) > 1/4$ for all $\Delta > 0$ and ξ_n a two-point estimation of the Gaussian increment $(W_{n+1} - W_n)/\sqrt{\Delta}$, i.e. $\mathbb{P}(\xi_n = \pm 1) = 1/2$ for each $n \in \mathbb{N}$. In the same direction, we construct the stabilized trapezoidal scheme

$$Y_{n+1} = Y_n + \frac{\sigma}{2}(Y_{n+1} + Y_n)\sqrt{\Delta}\xi_n - \frac{\sigma\sigma^\top}{4}(Y_{n+1} + Y_n)\Delta + \beta(\Delta)(Y_{n+1} - Y_n)\Delta,$$

where $\beta(\Delta) \in \left]-\infty, -\frac{5}{16}\sigma\sigma^\top\right[$. Observe that the weight functions $\alpha, \beta :]0, +\infty[\to \mathbb{R}$ do not involve random variables. The novel stabilized schemes Z and Y are almost sure asymptotically stable and preserves the sign of the initial data for any discretization step $\Delta > 0$. Moreover, the first order of weak convergence of the balanced Euler scheme Z is inherited from the classical Euler-Maruyama method.

In general, we study the weak balanced Euler method

$$Z_{n+1} = Z_n + b(Z_n)\Delta + \sigma(Z_n)\sqrt{\Delta}\xi_n + c(\Delta, Z_n)(Z_{n+1} - Z_n)\Delta,$$

for which is needed to identify adequate weights $c(\Delta, x)$ for each $x \in \mathbb{R}^d$, and ξ_n^k a convenient two-point discretization of the Gaussian variable $\left(W_{n+1}^k - W_n^k\right)/\sqrt{\Delta}$ for each $k \in \{1, \ldots, m\}$, for all $n \in \mathbb{N}$ and any given $\Delta > 0$. Motivated by the above successful equation test, we propose two methodologies for constructing weight terms. The first one, inspired by the linear scalar test, involves the closed formula

$$c(\Delta, x) = \nabla b(x) - \sum_{k=1}^{m} \alpha_k(\Delta)\nabla\sigma^k(x)\left(\nabla\sigma^k(x)\right)^\top; \quad \forall x \in \mathbb{R},$$

where $\alpha_k(\Delta) > 1/4$ are bounded for each $k \in \{1, \ldots, m\}$ and for all $\Delta > 0$. At cost of to invert a $d \times d$ matrix, under appropriate assumptions on the drift and diffusion coefficients we obtain explicit first order weak balanced Euler schemes that reproduce the stability properties of the exact solution

as well as Δ tends to zero. Second, given a time-step $\Delta > 0$ we suggest an optimization procedure to construct the stabilizing function $c(\Delta, \cdot)$. Basically, we study the maximum asymptotic exponential rate of the resulting balanced scheme and choose its weight function in order to have upper bounds as close as possible to the exact unknown solution.

In the context of systems of linear SDEs

$$X_t = X_0 + \int_0^t BX_s ds + \sum_{k=1}^m \int_0^t \sigma^k X_s dW_s^k,$$

with real matrices $B \in \mathbb{R}^{d\times d}$ and $\sigma^1, \ldots, \sigma^m \in \mathbb{R}^{d\times d}$, it is well-known that

$$\limsup_{t\to+\infty} \frac{1}{t} \log \|X_t\| \leq \ell := \sup_{x\in\mathbb{R}^d, \|x\|=1} \left(\langle x, Bx\rangle + \sum_{k=1}^m \left(\frac{1}{2} \left\|\sigma^k x\right\|^2 - \langle x, \sigma^k x\rangle^2 \right) \right) \quad a.s.$$

That is, the $a.s.$ asymptotic long-time behavior of X depends on the top Lyapunov coefficient ℓ. Then, in order to avoid time-steps restrictions and additional computational efforts we propose to design stabilized weak Euler schemes of the form

$$V_{n+1} = V_n + (I + \Delta M(\Delta)) \left(B\Delta + \sum_{k=1}^m \sigma^k \sqrt{\Delta} \xi_n^k \right) V_n,$$

with weight function $M :]0, \infty[\to \mathbb{R}^{d\times d}$. For any given time step $\Delta > 0$ the stabilizing factor $M(\Delta)$ is obtained previously to each simulation by means of the solution of an auxiliary optimization problem. More precisely, we find the stabilizing factor $M(\Delta)$ by taking the upper bound of

$$\limsup_{n\to+\infty} \frac{1}{n\Delta} \log \|V_n\|$$

as close as possible to the top Lyapunov exponent ℓ. An optimization algorithm is then demanded to construct optimal weak balanced schemes.

In the general case of multidimensional nonlinear SDEs with multiplicative noise, the optimal weight function $\Delta \to M(\Delta, \cdot)$ is difficult to obtain. We consider weak Euler schemes of type

$$V_{n+1} = V_n + (I + \Delta M(\Delta, V_n)) \left(b(V_n)\Delta + \sum_{k=1}^m \sigma^k(V_n) \sqrt{\Delta} \xi_n^k \right),$$

with $M :]0, \infty[\times \mathbb{R}^d \to \mathbb{R}^{d\times d}$. Under smoothness, growth bounds and Lipschitz assumptions on the drift and diffusion terms, first-order stabilized weak Euler schemes are obtained under appropriate restrictions on the stabilizing terms. Moreover, it is possible to improve the order of convergence by using Romberg extrapolation techniques.

Finally, we highlight some methodologies to construct stabilizing functions in general contexts. First, consider the stochastic Duffing-Van der Pol equation

$$\ddot{x} = \alpha x + \beta \dot{x} - ax^3 - bx^2\dot{x} + \sigma x \dot{W}_t^1,$$

with given parameters $\alpha, \beta, a, b \in \mathbb{R}$. Defining $X^1 := x$ and $X^2 := \dot{x}$, we obtain the 2-dimensional nonlinear system

$$dX_t = \begin{pmatrix} X_t^2 \\ \alpha X_t^1 + \beta X_t^2 - a\left(X_t^1\right)^3 - b\left(X_t^1\right)^2 X_t^2 \end{pmatrix} dt + \begin{pmatrix} 0 & 0 \\ \sigma & 0 \end{pmatrix} X_t dW_t^1,$$

where $X_t = \left(X^1, X^2\right)^\top$ (see e.g. [10, 12, 20, 21, 105], additionaly [94] in the deterministic context). Then the linearized Duffing-Van der Pol system around the zero solution results

$$Y_t = X_0 + \int_0^t \begin{pmatrix} 0 & 1 \\ \alpha & \beta \end{pmatrix} Y_s ds + \sum_{k=1}^m \int_0^t \begin{pmatrix} 0 & 0 \\ \sigma & 0 \end{pmatrix} Y_s dW_s^1. \tag{5.1}$$

Motivated by Remark 2.3.2 we consider the weak numerical scheme $V = \left(V^1, V^2\right)^\top$ defined by

$$V_{n+1} = V_n + \left(I + \Delta M\left(\Delta\right)\right) \begin{pmatrix} V_n^2 \Delta \\ \left(\alpha V_n^1 + \beta V_n^2 - a\left(V_n^1\right)^3 - b\left(V_n^1\right)^2 V_n^2\right)\Delta + \sigma V_n^1 \sqrt{\Delta}\xi_n^1 \end{pmatrix}, \tag{5.2}$$

where the weight function $M\left(\Delta\right)$ is constructed according to the linearized solution Y.

The local linearization technique permits us to introduce novel numerical schemes incorporating general stabilizing forms. As in Biscay *et al.* (1996) [30], we locally approximate a nonlinear SDE as

$$\begin{aligned} X_t &\approx X_{T_n} + \int_{T_n}^t \left(\nabla b\left(X_{T_n}\right)\left(X_s - X_{T_n}\right) + b\left(X_{T_n}\right)\right) ds \\ &\quad + \sum_{k=1}^m \int_{T_n}^t \left(\nabla \sigma^k\left(X_{T_n}\right)\left(X_s - X_{T_n}\right) + \sigma^k\left(X_{T_n}\right)\right) dW_s^k \end{aligned}$$

for each $t \in [T_n, T_{n+1}]$, and so $X_{T_{n+1}}$ can be weakly approximated by

$$\begin{aligned} U_{n+1} &= U_n + b\left(U_n\right)\Delta + \sum_{k=1}^m \sigma^k\left(U_n\right)\sqrt{\Delta}\xi_n^k \\ &\quad + \Delta M\left(\Delta, U_n\right)\left(\nabla b\left(U_n\right)\Delta + \sum_{k=1}^m \nabla \sigma^k\left(U_n\right)\sqrt{\Delta}\xi_n^k\right) U_n, \end{aligned}$$

with correction factor $M :]0, \infty[\times \mathbb{R}^d \to \mathbb{R}^{d \times d}$. The numerical method U_n generalizes the above weak scheme V_n introduced in (2.14) for bilinear systems of SDEs .

The usage of modifying factors to deal with stability issues is not only associated to the balanced Euler method. We mention, for example, the θ-method, the Runge-Kutta method, the S-ROCK method, Row-type methods and the tamed Euler method. Additional stabilizing techniques involves the local linearization techniques, splitting procedures, predictor-corrector schemes, composite methods and adaptive-step schemes. A key point is to propose a procedure to obtain stabilizing terms. From a mathematical point of view, additional work is spent to prove the rate of convergence and the

dynamic properties of the introduced numerical methods. On the basis of the theoretical results, we identified at least two ways to design weight functions used with successful in various classical test equations. Our computational tests motivate the extension of the stabilizing techniques for the numerical solution of general SDEs. The ongoing researches on the numerical solution of SDEs motivate future works in this way. A manuscript with some advances has been recently submitted (Mardones and Mora (2017) [139]).

The second part of the PhD thesis work introduces explicit stable schemes for SDEs with multiplicative noise. At a first step, we study the linear scalar SDE

$$X_t = X_0 + \int_0^t \mu X_s ds + \int_0^t \sigma X_s dW_s$$

and consider its unique adapted closed solution

$$X_t = e^{\left(\mu - \frac{1}{2}\sigma\sigma^\top\right)t + \sigma W_t} X_0.$$

Then we have the weak exponential scheme

$$\bar{X}_{n+1} = e^{\left(\mu - \frac{1}{2}\sigma\sigma^\top\right)\Delta + \sigma\sqrt{\Delta}\widehat{W}_n} \bar{X}_n,$$

with independent and identically distributed random variables $\widehat{W}_n$ with symmetric law and unit variance. In the same direction, the approximation of nonlinear scalar SDEs by linear equations ones provides us to take advantage of the above closed exponential solution. Indeed, we introduce first-order weak explicit exponential schemes inheriting the sign-preserving ability and asymptotic exponential behavior of the unknown exact solutions for any discretization step $\Delta > 0$.

The work presented in Chapter 3 and introduced in earlier manuscripts [156] began the collaboration research with Dr. Juan Carlos Jiménez, Dra. Mónica Selva and Dr. Rolando Biscay, and the introduced methodology have been extended to nonlinear SDEs. In general, the diffusion process X is decomposed by means of

$$X_t = \|X_t\| \cdot \frac{X_t}{\|X_t\|}.$$

Hence we consider a coupled system of SDEs governing the stochastic processes $\|X_t\|$ and $X_t/\|X_t\|$ in order to estimate the exact solution X. We named to this approach direction and norm decomposition method (DND method for short). That is, the norm process involves

$$\begin{aligned}\|X_t\| = \|X_0\| &+ \int_0^t \left(\frac{\langle X_s, b(X_s)\rangle + \frac{1}{2}\sum_{k=1}^m \left\|\sigma^k(X_s)\right\|^2}{\|X_s\|^2} - \frac{1}{2}\sum_{k=1}^m \frac{\langle X_s, \sigma^k(X_s)\rangle^2}{\|X_s\|^4} \right) \cdot \|X_s\| \; ds \\ &+ \sum_{k=1}^m \int_0^t \frac{\langle X_s, \sigma^k(X_s)\rangle}{\|X_s\|^2} \cdot \|X_s\| \; dW_s^k\end{aligned}$$

and the direction process drives us to

$$\begin{aligned}\frac{X_t}{\|X_t\|} = \frac{X_0}{\|X_0\|} &+ \int_0^t \left(\frac{b\left(X_s\right)}{\|X_s\|} - \left\langle \frac{X_s}{\|X_s\|}, \frac{b\left(X_s\right)}{\|X_s\|} \right\rangle \frac{X_s}{\|X_s\|} \right) ds \\ &+ \frac{1}{2} \sum_{k=1}^{m} \int_0^t \left(3 \left\langle \frac{X_s}{\|X_s\|}, \frac{\sigma^k\left(X_s\right)}{\|X_s\|} \right\rangle^2 - \left\langle \frac{\sigma^k\left(X_s\right)}{\|X_s\|}, \frac{\sigma^k\left(X_s\right)}{\|X_s\|} \right\rangle \right) \frac{X_s}{\|X_s\|} \, ds \\ &- \sum_{k=1}^{m} \int_0^t \left\langle \frac{X_s}{\|X_s\|}, \frac{\sigma^k\left(X_s\right)}{\|X_s\|} \right\rangle \frac{\sigma^k\left(X_s\right)}{\|X_s\|} ds \\ &+ \sum_{k=1}^{m} \int_0^t \left(\frac{\sigma^k\left(X_s\right)}{\|X_s\|} - \left\langle \frac{X_s}{\|X_s\|}, \frac{\sigma^k\left(X_s\right)}{\|X_s\|} \right\rangle \frac{X_s}{\|X_s\|} \right) \, dW_s^k.\end{aligned}$$

Then the coupled system of SDEs can be accurately solved be taking advantage of the underlying properties of each SDE. Indeed, the norm process $\|X_t\|$ is governed by a scalar SDE with multiplicative noise, then locally rewriting its SDE on $[T_n, T_{n+1}]$ and freezing the coefficients at the time node T_n we can compute the estimation of $\left\|X_{T_{n+1}}\right\|$ by explicitly solving the resulting linear scalar SDE with initial data $\|X_{T_n}\|$. The key idea is to approximate the drift and diffusion coefficients by linear ones. This novel scalar scheme shows a notable performance solving various numerical tests. On the other hand, the stochastic process $X_t / \|X_t\|$ belongs to the unit sphere at each time and hence preserves its norm. Our first approximation for the direction process is obtained by applying the Euler-Maruyama scheme to its SDE together with a projection technique to guarantee the unit norm property. In case of multidimensional linear SDEs, we conveniently rewrite the concerned SDEs for the direction and norm processes in order to construct specific numerical schemes. Moreover, the numerical solution of systems of bilinear SDEs is studied by taking into account the cases of well and ill-conditioned drift matrices. In both cases, we modify the Euler-Maruyama scheme applied to the angle process improving the performance of our preliminary proposed schemes.

Given the drift coefficient b and a diffusion matrix $\sigma\sigma^\top$, the infinitesimal Itô generator $\mathcal{L}$ of the diffusion process X is defined by the second-order differential operator

$$\mathcal{L}u = \langle b, \nabla u \rangle + \frac{1}{2} \operatorname{tr}\left\{ \sigma\sigma^\top H u \right\}.$$

Here, ∇u and Hu represent the gradient vector and Hessian matrix of the scalar field $u : \mathbb{R}^d \to \mathbb{R}$, respectively. Fix $T > 0$ and let

$$u\left(t,x\right) = \mathbb{E}\left(f\left(X_T\right) \diagup X_t = x\right) = \mathbb{E}\left(f\left(X_T^{t,x}\right)\right)$$

be the transition probabilities of the Itô diffusion. Moreover, let $p\left(t,x,\cdot\right) = \mathbb{P} \circ \left(X_T^{t,x}\right)^{-1}(\cdot)$ be the transition density of the process $X^{t,x}$. Under certain hypotheses on the terminal condition f we have

$$u\left(t,x\right) = \int_{\mathbb{R}^d} f\left(y\right) p\left(t,x,dy\right); \quad \forall t \in [0,T).$$

Here, the stochastic process $X^{t,x}$ is given by

$$X_T^{t,x} = x + \int_t^T b\left(X_s^{t,x}\right) ds + \int_t^T \sigma\left(X_s^{t,x}\right) dW_s.$$

Then $u : [0,T] \times \mathbb{R}^d \to \mathbb{R}$ is governed by the backward Kolmogorov equation

$$\begin{cases} \dfrac{\partial}{\partial t} u\left(t,x\right) = -\mathcal{L}u\left(t,x\right) & ;\ \forall\left(t,x\right) \in [0,T) \times \mathbb{R}^d, \\ u\left(T,x\right) = f\left(x\right) & ;\ \forall x \in \mathbb{R}^d. \end{cases}$$

By a time-reversing transformation we can rewrite the Kolmogorov PDE in the forward equivalent form

$$\frac{\partial}{\partial t} u = \mathcal{L}u.$$

In general, to prove the weak convergence of numerical methods applied to Itô SDEs needed the regularity of the Kolmogorov equation. In this PhD thesis work we deal with SDEs on a classical theoretical setting where the desired regularity holds. More generally, we highlight some methodologies to study the regularity of the Kolmogorov equation. First, we have the seminal Kolmogorov's work (1934) [123] on which is demonstrated the hypoellipticity of a non-elliptic operator, and then the regularity of the involved solutions. Then the celebrated Hörmander's theorem (1967) [103] permits us to study the hypoellipticity of differential operators and thus the regularity of solutions. By its way, the theory of stochastic flows studies the differentiability of $X^{t,x}$ with respect to the initial data $x \in \mathbb{R}^d$ and $t \in \mathbb{R}$ and hence, by means of the Itô formula, to study the regularity of the Kolmogorov equation (see Gihman and Skorohod (1972) [87]). On another hand, the theory of Malliavin calculus helps us to determine the hypoellipticity of differential operators at cost of additional boundedness assumptions on the coefficients (see e.g. Malliavin (1997) [135]). Finally, the regularity of transition densities for diffusion processes governed by SDEs establishes another direction to study the smoothness of solutions for PDEs (see e.g. Delarue and Menozzi [75]). To the best of our knowledge, necessary and sufficient conditions to the existence and smoothness of solutions of the Kolmogorov equation is an open problem (see e.g. Hairer, Hutzenthaler and Jentzen (2015) [95] and references therein).

The DND method provides us the introduction of first-order weak numerical schemes with a promising performance in a broad class of numerical tests. From a theoretical point of view, the almost sure asymptotic exponential behavior of the exact solution is studied be means of the norm process. Hence, the new stable scalar exponential schemes permit us to reproduce the *a.s.* asymptotic exponential behavior of the unknown exact solutions for any discretization step. The sign-preserving ability of the scalar schemes holds because their exponential-type formulation. The introduced weak numerical schemes are explicitly given by *derivative-free* formulas, up to evaluation at zero.

Recently, the DND method have been extended to systems of nonlinear SDEs (see Mora, Mardones, Jiménez, Selva and Biscay (2017) [157]). The dynamical properties of exact solutions are recovered by the numerical schemes for any time-step, new test equations have been performed and additional references included. The introduced stable schemes converges weakly with order one and strongly a half under smoothness and growth assumptions on the globally Lipschitz assumptions. The same rate of convergences hold for non-globally Lipschitz drift coefficients under the hypotheses of existence and

smoothness of solutions of the associated Kolmogorov equation. The manuscript versions of the work can be found in [158].

The last part of the PhD thesis work is devoted the numerical simulation of the Navier-Stokes equations for incompressible fluids in $\mathbb{R}^d$, for space dimension $d \in \{2, 3\}$,

$$\begin{cases} \frac{\partial u}{\partial t} + (u \cdot \nabla) u = \nu \triangle u - \nabla p + f; \quad 0 < t \leq T, \\ \nabla \cdot u = 0, \quad u(0) = g, \end{cases} \tag{5.3}$$

where $T > 0$ is a fixed time, $\nu > 0$ is the kinematic viscosity, f is the external force field and g is a given initial divergence-free vector field.

Among different probabilistic representations, the FBSDEs associated to the unsteady Navier-Stokes equations is a novel approach. Assuming that the solution is known on a time interval $[0, T]$ and taking a convenient time-reversing transformation, a d-dimensional diffusion process X is associated to the differential operator $u \cdot \nabla - \nu \triangle$ part. Then, defining

$$Y_s := -u(T - s, X_s), \quad Z_s := -Du(T - s, X_s),$$

the process (X, Y, Z) is governed by the FBSDEs system

$$\begin{cases} X_s = x + \int_t^s Y_r dr + \int_t^s \sqrt{2\nu} dW_r, \\ Y_s = -g(X_T) + \int_s^T [\nabla p(T - r, X_r) - f(T - r, X_r)] dr - \int_s^T \sqrt{2\nu} Z_r dW_r, \end{cases} \tag{5.4}$$

where W is a d-dimensional standard Brownian motion. The simplified model obtained by removing the pressure term ∇p from the FBSDEs is associated to the Burgers equation [45], which remains a non-linear equation due to the term $u \cdot \nabla u$. Under appropriate conditions, the pressure term p can be recovered by solving a Poisson problem

$$\triangle p = \mathcal{P}(u)$$

for a given functional $\mathcal{P}$ of the solution. The numerical solution of the system of incompressible Navier-Stokes equations involves various difficulties due to the presence of a nonlinear term, the incompressibility condition as well as the computation of the pressure term.

Recently Delbaen, Qiu and Tang (2015) introduced in [76] a new class of coupled FBSDEs associated to the incompressible Navier-Stokes equations. Since their probabilistic approach involves a BSDE defined on an infinite time interval for the stochastic representation of the pressure term, Delbaen *et al.* deduced an approximated solution to the velocity field by truncating the infinite time interval of the associated FBSDEs system. Hence it is proposed a numerical simulation algorithm to simulate the incompressible Navier-Stokes equations in the whole space that follows from a classical methodology of Delarue and Menozzi [73, 74] for FBSDEs.

The passive tracers model considers the diffusion process X representing the position of a particle moving over a fluid flow subject to molecular diffusion

$$X_t = X_0 + \int_0^t u(s, X_s) ds + \sum_{k=1}^{d} \int_0^t \sigma dW_s^k, \tag{5.5}$$

where $u : [0, \infty[\times \mathbb{R}^d \to \mathbb{R}^d$ is an incompressible fluid velocity field (i.e. $\nabla \cdot u := \sum_{i=1}^{d} \frac{\partial u}{\partial x_i} = 0$), $W = \left(W^1, \ldots, W^d\right)^\top$ a d-dimensional Brownian motion, σ the molecular diffusivity and X_0 the initial position of the particle. The additive noise changes the nature of the noise concerned on this PhD thesis work. The banishing viscosity phenomenon, i.e. low viscosity parameter or high Reynolds number, becomes the fluid on a turbulent flow and numerical instabilities appears. In the new FBSDEs system representation for the incompressible Navier-Stokes equations [76], we apply the Euler-Maruyama method to approximate the *forward* SDE with additive noise. In our numerical tests we do not see the necessity to modify such scheme. The presented work deals with the numerical simulation of non-turbulent flows.

The approximation of expectations of integrals involving path of Brownian motions appears as an additional source of error in order to deal with the pressure gradient estimation, because the Poisson problem and the additional BSDE representation of the concerned nonlocal operator. In the Burgers equation case, we consider quantization as control variate variable for the Monte-Carlo method in the computation of conditional expectations, reducing the approximation error or improving the computational effort of the algorithms. We do not recommend such technique to the Navier-Stokes context because the increasing computational costs especially in the three dimensional space. In our numerical tests, the quantization of the underlying Gaussian processes together with the Riemann sum estimation of integrals appear as a first approach to deal with this problem. The implementation of these algorithms involves the optimality of quantization parameters to the underlying Gaussian random variables. Moreover, adequate reduction variance methods to compute conditional expectations appearing in the FBSDEs is demanded. We mention the usage of the Karhumen-Loève expansion for the Brownian motion and the Brownian bridge as potential alternatives.

In this PhD thesis work we do not consider the theoretical analysis of the proposed numerical algorithms for the estimation of systems of *forward-backward* SDEs. In the Navier-Stokes equations context, a detailed error analysis of the probabilistic algorithms in terms of the regularity of the external force field f, the given data g, the kinematic viscosity $\nu > 0$ and the discretization parameters is desired. On the current *state of arts* on weak numerical methods for FBSDEs we are not in position to demonstrate the convergence and to present a detailed numerical analysis of the involved algorithms. Our computational results motivate us to the theoretical study of convergence of the probabilistic numerical algorithms associated to the incompressible Navier-Stokes equations.

Information says a lot about phenomena, helps us understand and improve our comprehension only if it can be quantified. Dealing with the solution of real world applications involves the knowledge of quantities associated to diffusion processes hence the simulation of systems of stochastic differential equations. Randomness appears, then data analysis must be appropriate and the scientific study can be confusing with respect to our sense of intuition. The expectation parameters are important in any application and can be approximated by the simulation of mathematical models, where the precision of the results must be considered. Last but not least, the distribution of the diffusion processes is relevant and essential for the correct interpretation of data.

The computational effort must be considered before any numerical computation and the complexity and estimation of the computer work is necessary. The error analysis of the numerical schemes helps us choose an appropriate discretization setting for computational estimations. The appropriate implementation of computable operations together with the accuracy of the computer machine are very important. The application of adequate numerical methodologies is a key element to the simulation of SDEs. The sample paths are of stochastic nature, the regularity assumptions and hypotheses on parameters are crucial to the correct usage of the mathematical models. A notable example is the context of stable SDEs:

We can initialize all the sample paths in the same state knowing that their continuous trajectories will never touch again, and in fact they will tend to the same place as well as time goes to infinity.

Bibliography

[1] A. Abdulle and S. Cirilli, *S-ROCK: Chebyshev methods for stiff stochastic differential equations*, SIAM J. Sci. Comput., 30 (2008), pp. 997–1014.

[2] J. A. Acebrón, Á. Rodríguez-Rozas, and R. Spigler, *Domain decomposition solution of nonlinear two-dimensional parabolic problems by random trees*, J. Comput. Phys., 228 (2009), pp. 5574–5591.

[3] ——, *Efficient parallel solution of nonlinear parabolic partial differential equations by a probabilistic domain decomposition*, J. Sci. Comput., 43 (2010), pp. 135–157.

[4] J. Alcock and K. Burrage, *A note on the Balanced method*, BIT, 46 (2006), pp. 689–710.

[5] ——, *Stable strong order 1.0 schemes for solving stochastic ordinary differential equations*, BIT, 52 (2012), pp. 539–557.

[6] D. F. Anderson and J. C. Mattingly, *A weak trapezoidal method for a class of stochastic differential equations*, Commun. Math. Sci., 9 (2011), pp. 301–318.

[7] F. Antonelli, *Backward-forward stochastic differential equations*, Ann. Appl. Probab., 3 (1993), pp. 777–793.

[8] X. Appleby, J. A. D. Mao and A. Rodkina, *Stabilization and destabilization of nonlinear differential equations by noise*, IEEE Trans. Automat. Control, 53 (2008), pp. 683–691.

[9] L. Arnold, *Stochastic differential equations: Theory and applications*, Wiley, New York, 1974.

[10] ——, *Random dynamical systems*, Springer-Verlag, Berlin-Heidelberg, 1998.

[11] L. Arnold and W. Kliemann, *Large deviations of linear stochastic differential equations*, in Stochastic Differential Systems, H. J. Engelbert and W. Schmidt, eds., vol. 96 of Lecture Notes in Control and Information Sciences, Berlin, 1987, Springer-Verlag, pp. 115–151.

[12] L. Arnold, N. Sri Namachchivaya, and K. R. Schenk-Hoppé, *Toward an understanding of stochastic Hopf bifurcation: a case study*, IJBC, 6 (1996), pp. 1947–1975.

[13] V. I. Arnol'd, *Ordinary differential equations*, The MIT Press, Cambridge, 1973.

[14] Y. Bakhtin and C. Mueller, *Solutions of semilinear wave equation via stochastic cascades*, Commun. Stoch. Anal., 4 (2010), pp. 425–431.

[15] V. Bally and G. Pagès, *A quantization algorithm for solving multi-dimensional discrete-time optimal stopping problems*, Bernoulli, 9 (2003), pp. 1003–1049.

[16] L. Banäs, Z. Brzézniak, and A. Prohl, *Computational studies for the stochastic Landau-Lifshitz-Gilbert equation*, SIAM J. Sci. Comput., 35 (2013), pp. 62–81.

[17] P. H. Baxendale, *Moment stability and large deviations for linear stochastic differential equations*, in Probabilistic Methods in Mathematical Physics, Proc. 1985 Katata/Kyoto conf., K. Itô and N. Ikeda, eds., Academic Press, Boston, 1987, pp. 31–54.

[18] ——, *Invariant measures for nonlinear stochastic differential equations*, in Lyapunov Exponents, Proc. Oberwolfach 1990, L. Arnold, H. Crauel, and J.P. Eckmann, eds., Lect. Notes Math. 1486, Springer, Berlin, 1991, pp. 123–140.

[19] ——, *A stochastic Hopf bifurcation*, Probab. Theory Relat. Fields, 99 (1994), pp. 581–616.

[20] ——, *Stochastic averaging and asymptotic behavior of the stochastic Duffing-Van der Pol equation*, Stoch. Proc. Appl., 113 (2004), pp. 235–272.

[21] P. H. Baxendale and L. Goukasian, *Lyapunov exponents for small random perturbations of Hamiltonian systems*, Ann. Probab., 30 (2002), pp. 101–134.

[22] Eugenio Beltrami, *Considerations on Hydrodynamics*, Int. J. Fusion Energy, 3 (1985), pp. 53–57. Translated by Dr. Giuseppe Filipponi from original paper appeared in 1889 in Rendiconti del Reale Instítuto Lombardo, Series II, Vol. 22.

[23] S. Benachour, B. Roynette, and P. Vallois, *Branching process associated with 2d-Navier Stokes equation*, Rev. Mat. Iberoam., 17 (2001), pp. 331–373.

[24] C. Bender and J. Zhang, *Time discretization and Markovian iteration for coupled FBSDEs*, Ann. Appl. Probab., 18 (2008), pp. 143–177.

[25] A. Berkaoui, M. Bossy, and A. Diop, *Euler scheme for SDEs with non-Lipschitz diffusion coefficient: strong convergence*, ESAIM Probab. Stat., 12 (2008), pp. 1–11.

[26] G. Berkolaiko, E. Buckwar, C. Kelly, and A. Rodkina, *Almost sure asymptotic stability analysis of the Euler-Maruyama method applied to a test system with stabilising and destabilising stochastic perturbations*, LMS J. Comput. Math., 15 (2012), pp. 71–83.

[27] F. Bernardin, M. Bossy, C. Claire, J. F. Jabir, and A. Rousseau, *Stochastic Lagrangian method for downscaling problems in computational fluid dynamics*, ESAIM Math. Model. Numer. Anal., 44 (2010), pp. 885–920.

[28] W.-J. Beyn, E. Isaak, and R. Kruse, *Stochastic C-stability and B-consistency of explicit and implicit Euler-type schemes*, J. Sci. Comput., 67 (2016), pp. 955–987.

[29] R. N. Bhattacharya, L. Chen, S. Dobson, R. B. Guenther, C. Orum, M. Ossiander, E. Thomann, and E. C. Waymire, *Majorizing kernels and stochastic cascades with applications to incompressible Navier-Stokes equations*, Trans. Amer. Math. Soc., 355 (2003), pp. 5003–5040.

[30] R. Biscay, J. C. Jiménez, J. J. Riera, and P. A. Valdes, *Local linearization method for the numerical solution of stochastic differential equations*, Ann. Inst. Statist. Math., 48 (1996), pp. 631–644.

[31] D. Blömker, M. Romito, and R. Tribe, *A probabilistic representation for the solutions to some non-linear PDEs using pruned branching trees*, Ann. Inst. H. Poincaré, 43 (2007), pp. 175–192.

[32] M. Bossy, *Some stochastic particle methods for nonlinear parabolic PDEs*, ESAIM Proc., 15 (2005), pp. 18–57.

[33] M. Bossy and A. Diop, *Weak convergence analysis of the symmetrized Euler scheme for one dimensional SDEs with diffusion coefficient* $|x|^\alpha$, $\alpha \in [1/2, 1)$, arXiv:1508.04573v1, (2010).

[34] M. Bossy, J.-F. Jabir, and D. Talay, *On conditional McKean Lagrangian stochastic models*, Probab. Theory Relat. Fields, 151 (2011), pp. 319–351.

[35] M. Bossy and B. Jourdain, *Rate of convergence of a particle method for the solution of a* 1*d viscous scalar conservation law in a bounded interval*, Ann. Probab., 30 (2002), pp. 1797–1832.

[36] M. Bossy and D. Talay, *Convergence rate for the approximation of the limit law of weakly interacting particles: Application to the Burgers equation*, Ann. Appl. Probab., 6 (1996), pp. 818–861.

[37] ——, *A stochastic particle method for the McKean-Vlasov and the Burgers equation*, Math. Comp., 66 (1997), pp. 157–192.

[38] B. Bouchard and S. Menozzi, *Strong approximations of BSDEs in a domain*, Bernoulli, 15 (2009), pp. 1117–1147.

[39] B. Bouchard and N. Touzi, *Discrete-time approximation and Monte-Carlo simulation of backward stochastic differential equations*, Stoch. Proc. Appl., 111 (2004), pp. 175–206.

[40] M. E. Brachet, *Direct simulation of the three-dimensional turbulence in the Taylor-Green vortex*, Fluid Dyn. Res., 8 (1991), pp. 1–8.

[41] M. E. Brachet, U. Frisch, D. Meiron, R. Morf, B. Nickel, and S. Orszag, *The Taylor-Green vortex and fully developed turbulence*, J. Stat. Phys., 34 (1984), pp. 1049–1063.

[42] M. E. Brachet, U. Frisch, D. I. Meiron, R. H. Morf, B. G. Nickel, and S. A. Orszag, *Small-scale structure of the Taylor-Green vortex*, J. Fluid Mech., 130 (1983), pp. 411–452.

[43] E. Buckwar and C. Kelly, *Towards a systematic linear stability analysis of numerical methods for systems of stochastic differential equations*, SIAM J. Numer. Anal., 48 (2010), pp. 298–321.

[44] ——, *Non-normal drift structures and linear stability analysis of numerical methods for systems of stochastic differential equations*, Comput. Math. Appl., 64 (2012), pp. 2282–2293.

[45] J. M. Burgers, *A mathematical model illustrating the theory of turbulence*, Adv. Appl. Mech., 1 (1948), pp. 171–199.

[46] K. Burrage and T. Tian, *Implicit Taylor methods for stiff stochastic differential equations*, Appl. Numer. Math., 38 (2001), pp. 167–185.

[47] ——, *Predictor-corrector methods of Runge-Kutta type for stochastic differential equations*, SIAM J. Numer. Anal., 40 (2002), pp. 1516–1537.

[48] C. Canuto, M. Y. Hussaini, A. Quarteroni, and T. A. Zang, *Spectral Methods: Evolution to Complex Geometries and Applications to Fluid Dynamics*, Springer-Verlag, Berlin-Heidelberg, 2007.

[49] F. Carbonell, J. C. Jiménez, and R. J. Biscay, *Weak local linear discretizations for stochastic differential equations: convergence and numerical schemes*, J. Comput. Appl. Math., 197 (2006), pp. 578–596.

[50] J.-F. Chassagneux, A. Jacquier, and I. Mihaylov, *An explicit Euler scheme with strong rate of convergence for financial SDEs with non-Lipschitz coefficients*, SIAM J. Financial Math, 7 (2016), pp. 993–1021.

[51] P. Cheridito, H. M. Soner, N. Touzi, and N. Victoir, *Second-order backward stochastic differential equations and fully nonlinear parabolic PDEs*, Comm. Pure Appl. Math., 60 (2007), pp. 1081–1110.

[52] D. Chevance, *Résolution numérique des équations différentielles stochastiques rétrogrades*, PhD thesis, Université de Provence, 1997.

[53] A. J. Chorin, *A numerical method for solving incompressible viscous flow problems*, J. Comput. Phys., 2 (1967), pp. 12–26.

[54] ——, *The numerical solution of the Navier-Stokes equations for an incompressible fluid*, Bull. Amer. Math. Soc., 73 (1967), pp. 928–931.

[55] ——, *Numerical solution of the Navier-Stokes equations*, Math. Comp., 22 (1968), pp. 745–762.

[56] ——, *On the convergence of discrete approximations to the Navier-Stokes equations*, Math. Comp., 23 (1969), pp. 341–353.

[57] ——, *Numerical study of slightly viscous flow*, J. Fluid Mech., 57 (1973), pp. 785–796.

[58] ——, *A vortex method for the study of rapid flow*, in Proceedings of the Third International Conference on Numerical Methods in Fluid Mechanics, H. Cabannes and R. Temam, eds., vol. 19 of Lecture Notes in Physics, Berlin-Heidelberg-New York, 1973, Springer-Verlag, pp. 100–104.

[59] ——, *Random vortices and random vortex sheets*, in Computational fluid dynamics, H. B. Keller, ed., vol. 11 of SIAM-AMS Proceedings, Providence, R.I., 1978, Amer. Math. Soc., pp. 19–31.

[60] ——, *Vorticity and turbulence*, Springer-Verlag, New York, corrected second printing ed., 1998.

[61] A. J. Chorin and J. E. Marsden, *A mathematical introduction to fluid mechanics*, Springer-Verlag, New York, 1979.

[62] J. E. Cohen and C. M. Newman, *The stability of large random matrices and their products*, Ann. Probab., 12 (1984), pp. 283–310.

[63] P. Constantin and G. Iyer, *A stochastic Lagrangian representation of the three-dimensional incompressible Navier-Stokes equations*, Comm. Pure Appl. Math., 61 (2008), pp. 330–345.

[64] ——, *A stochastic-Lagrangian approach to the Navier-Stokes equations in domains with boundary*, Ann. Appl. Probab., 21 (2011), pp. 1466–1492.

[65] S. Corlay and G. Pagès, *Functional quantization-based stratified sampling methods*, Monte Carlo Methods Appl., 21 (2015), pp. 1–32.

[66] S. Corlay, G. Pagès, and J. Printems, *The optimal quantization website*, 2005.

[67] M. G. Crandall, I. Hitoshi, and P.-L. Lions, *User's guide to viscosity solutions of second order partial differential equations*, Bull. Amer. Math. Soc., 27 (1992), pp. 1–67.

[68] A. B. Cruzeiro and E. Shamarova, *Navier-Stokes equations and forward-backward SDEs on the group of diffeomorphisms of a torus*, Stoch. Proc. Appl., 119 (2009), pp. 4034–4060.

[69] ——, *On a forward-backward stochastic system associated to the Burgers equation*, in Stochastic Analysis with Financial Applications, A. Kohatsu-Higa, N. Privault, and S. J. Sheu, eds., vol. 65 of Progress in Probability, Birkhäuser, 2011, pp. 43–59.

[70] D. Dacunha-Castelle and M. Duflo, *Probabilités et statistiques 2. Problèmes à temps mobile*, Masson, Paris, 1983.

[71] H. De la Cruz Cancino, R. J. Biscay, J. C. Jiménez, F. Carbonell, and T. Ozaki, *High order local linearization methods: an approach for constructing A-stable explicit schemes for stochastic differential equations with additive noise*, BIT, 50 (2010), pp. 509–539.

[72] F. Delarue, *On the existence and uniqueness of solutions to FBSDEs in a non-degenerate case*, Stoch. Proc. Appl., 99 (2002), pp. 209–286.

[73] F. Delarue and S. Menozzi, *A forward-backward stochastic algorithm for quasi-linear PDEs*, Ann. Appl. Probab., 16 (2006), pp. 140–184.

[74] ——, *An interpolated stochastic algorithm for quasi-linear PDEs*, Math. Comp., 77 (2008), pp. 125–158.

[75] ——, *Density estimates for a random noise propagating through a chain of differential equations*, J. Funct. Anal., 259 (2010), pp. 1577–1630.

[76] F. Delbaen, J. Qiu, and S. Tang, *Forward-backward stochastic differential systems associated to Navier-Stokes equations in the whole space*, Stoch. Proc. Appl., 125 (2015), pp. 2516–2561.

[77] Y. Desheng, *The asymptotic behavior of the stochastic Ginzburg-Landau equation with multiplicative noise*, J. Math. Phys., 45 (2004), pp. 4064–4076.

[78] J. Douglas, J. Ma, and P. Protter, *Numerical methods for forward-backward stochastic differential equations*, Ann. Appl. Probab., 6 (1996), pp. 940–968.

[79] Euler, *Principes généraux du mouvement des fluides*, Mém. Acad. Roy. Sci. Berlin, 11 (1757), pp. 274–315.

[80] C. L. Fefferman, *Existence and smoothness of the Navier-Stokes equation*. http://www.claymath.org/, 2000.

[81] W. Feller, *An introduction to probability theory and its applications*, vol. 2, Wiley, New York, second ed., 1971.

[82] R. P. Feynman, *Space-time approach to non-relativistic quantum mechanics*, Rev. Mod. Phys., 20 (1948), pp. 367–387.

[83] George S. Fishman, *A first course in Monte Carlo*, Duxbury Press, 2005.

[84] E. Floriani and R. Vilela Mendes, *A stochastic approach to the solution of magnetohydrodynamic equations*, J. Comput. Phys., 242 (2013), pp. 777–789.

[85] J. Fontbona, *A probabilistic interpretation and stochastic particle approximations of the 3-dimensional Navier-Stokes equations*, Probab. Theory Relat. Fields, 136 (2006), pp. 102–156.

[86] U. Frisch, R. H. Morf, and S. A. Orszag, *Spontaneous singularity in three-dimensional, inviscid, incompressible flow*, Phys. Rev. Lett., 44 (1980), pp. 572–575.

[87] I. I. Gihman and A. V. Skorohod, *Stochastic differential equations*, Springer-Verlag, Berlin-Heidelberg, 1972.

[88] P. Glasserman, *Monte Carlo methods in financial engineering*, vol. 53 of Stochastic Modelling and Applied Probability, Springer-Verlag, New York-Berlin-Heidelberg, 2000.

[89] E. Gobet, J.-P. Lemor, and X. Warin, *A regression-based Monte Carlo method to solve backward stochastic differential equations*, Ann. Appl. Probab., 15 (2005), pp. 2172–2202.

[90] Siegfried Graf and Harald Luschgy, *Foundations of quantization for probability distributions*, vol. 1730 of Lecture Notes in Mathematics, Springer-Verlag, Berlin, 2000.

[91] C. Graham and D. Talay, *Stochastic simulation and Monte Carlo methods. Mathematical foundations of stochastic simulation*, Springer-Verlag, Berlin-Heidelberg, 2013.

[92] A. Grorud and D. Talay, *Approximation of Lyapunov exponents of nonlinear stochastic differential equations*, SIAM J. Numer. Anal., 56 (1996), pp. 627–650.

[93] I. Gyöngy, *Approximations of stochastic partial differential equations*, in Stochastic Partial Differential Equations, G. Da Prato and L. Tubaro, eds., vol. 227 of Lecture Notes in Pure and Appl. Math., New York, 2002, Deker, pp. 287–307.

[94] E. Hairer and G. Wanner, *Solving ordinary differential equations II. Stiff and differential-algebraic problems*, Springer-Verlag, Berlin-Heidelberg, 1991.

[95] M. Hairer, M. Hutzenthaler, and A. Jentzen, *Loss of regularity of Kolmogorov equations*, Ann. Prob., 43 (2015), pp. 468–527.

[96] T. E. Harris, *The theory of branching processes*, Springer-Verlag, Berlin-Gottingen-Heidelberg, 1996.

[97] P. Henry-Labordère, X. Tan, and N. Touzi, *A numerical algorithm for a class of BSDEs via the branching process*, Stoch. Proc. Appl., 124 (2014), pp. 1112–1140.

[98] D.J. Higham, *Stochastic ordinary differential equations in applied and computational mathematics*, IMA J. Appl. Math., 76 (2011), pp. 449–474.

[99] D. J. Higham, *Mean-square and asymptotic stability of the stochastic theta method*, SIAM J. Numer. Anal., 38 (2000), pp. 753–769.

[100] D. J. Higham and X. Mao, *Nonnormality and stochastic differential equations*, BIT, 46 (2006), pp. 525–532.

[101] D. J. Higham, X. Mao, and A. M. Stuart, *Strong convergence of Euler-type methods for nonlinear stochastic differential equations*, SIAM J. Numer. Anal., 40 (2002), pp. 1041–1063.

[102] D. J. Higham, X. Mao, and C. Yuan, *Almost sure and moment exponential stability in the numerical simulation of stochastic differential equations*, SIAM J. Numer. Anal., 45 (2007), pp. 592–609.

[103] L. Hörmander, *Hypoelliptic second order differential equations*, Acta Math., 119 (1967), pp. 147–161.

[104] W. Horsthemke and R. Lefever, *Noise-induced transitions. Theory and applications in Physics, Chemistry, and Biology*, Springer-Verlag, Berlin, 1984.

[105] M. Hutzenthaler and A. Jentzen, *Numerical approximations of stochastic differential equations with non-globally Lipschitz continuous coefficients*, Mem. Amer. Math. Soc., 236 (2013).

[106] M. Hutzenthaler, A. Jentzen, and P. E. Kloeden, *Strong and weak divergence in finite time of Euler's method for stochastic differential equations with non-globally Lipschitz continuous coefficients*, Proc. R. Soc. Lond. Ser. A, 467 (2011), pp. 1563–1576.

[107] ——, *Strong convergence of an explicit numerical method for SDEs with nonglobally Lipschitz continuous coefficients*, Ann. Appl. Probab., 22 (2012), pp. 1611–1641.

[108] N. Ikeda and S. Watanabe, *Stochastic differential equations and diffusion processes*, North-Holland, Amsterdam, second ed., 1989.

[109] P. Imkeller and C. Lederer, *An explicit description of the Lyapunov exponents of the noisy driven harmonic oscillator*, Dynam. Stabil. Syst., 14 (1999), pp. 385–405.

[110] ——, *Some formulas for Lyapunov exponents and rotation numbers in two dimensions and the stability of the harmonic oscillator and the inverted pendulum*, Dyn. Syst., 16 (2001), pp. 29–61.

[111] K. Itô, *Stochastic integral*, Proc. Imp. Acad. Tokyo, 20 (1944), pp. 519–524.

[112] ——, *On a stochastic integral equation*, Proc. Japan Acad., 22 (1946), pp. 32–35.

[113] G. Iyer and J. Mattingly, *A stochastic-Lagrangian particle system for the Navier-stokes equations*, Nonlinearity, 21 (2008), pp. 2537–2553.

[114] A. Jentzen and P. Kloeden, *Taylor approximations for stochastic partial differential equations*, SIAM, Philadelphia, 2011.

[115] M. Kac, *On distributions of certain Wiener functionals*, Trans. Amer. Math. Soc., 65 (1949), pp. 1–13.

[116] C. Kahl and H. Schurz, *Balanced Milstein methods for ordinary SDEs*, Monte Carlo Methods Appl., 12 (2006), pp. 143–170.

[117] I. Karatzas and S. E. Shreve, *Brownian motion and stochastic calculus*, Springer-Verlag, New York, 1988.

[118] R. Khasminskii, *Stochastic stability for differential equations*, Springer-Verlag, Berlin-Heidelberg, second ed., 2012.

[119] R. Z. Khas'minskii, *Necessary and sufficient conditions for the asymptotic stability of linear stochastic systems*, Theory Probab. Appl., 12 (1967), pp. 144–147.

[120] P. E. Kloeden and E. Platen, *Numerical solution of stochastic differential equations*, Springer-Verlag, Berlin, 1992.

[121] P. E. Kloeden, E. Platen, and H. Schurz, *Numerical solution of SDE through computer experiments*, Springer-Verlag, Berlin-Heidelberg, 1994.

[122] A. W. Kolkiewicz, *Efficient Monte Carlo simulation for integral functionals of Brownian motion*, J. Complexity, 30 (2014), pp. 255–278.

[123] A. Kolmogoroff, *Zufallige bewegungen (zur theorie der Brownschen bewegung)*, Annals of Mathematics, 35 (1934), pp. 116–117.

[124] F. Kozin and S. Prodromou, *Necessary and sufficient conditions for almost sure sample stability of linear Itô equations*, SIAM J. Appl. Math., 21 (1971), pp. 413–424.

[125] H. Kunita, *Stochastic flows and stochastic differential equations*, Cambridge University Press, Cambridge, 1990.

[126] Y. Le Jan and A. S. Sznitman, *Stochastic cascades and 3-dimensional Navier-Stokes equations*, Probab. Theory Relat. Fields, 109 (1997), pp. 343–366.

[127] A. Lejay, *A probabilistic representation of the solution of some quasi-linear PDE with a divergence form operator. application to existence of weak solutions of FBSDE*, Stoch. Proc. Appl., 110 (2004), pp. 145–176.

[128] A. Lejay and V. Reutenauer, *A variance reduction technique using a quantized brownian motion as a control variate*, J. Comput. Finance, 14 (2012), pp. 61–84.

[129] J. Ma, P. Protter, J. San Martín, and S. Torres, *Numerical method for backward stochastic differential equations*, Ann. Appl. Probab., 12 (2002), pp. 302–316.

[130] J. Ma, P. Protter, and J. Yong, *Solving forward-backward stochastic differential equations explicitly - a four step scheme*, Probab. Theory Relat. Fields, 98 (1994), pp. 339–359.

[131] J. Ma and J. Yong, *Forward-backward stochastic differential equations and their applications*, vol. 1702 of Lecture Notes in Mathematics, Springer-Verlag, Berlin-Heidelberg, 1999.

[132] J. Ma and J. Zhang, *Path regularity for solutions of backward stochastic differential equations*, Probab. Theory Relat. Fields, 122 (2002), pp. 163–190.

[133] A. J. Majda and A. L. Bertozzi, *Vorticity and Incompressible Flow*, Cambridge University Press, Cambridge, 2002.

[134] G. Malara and F. Arena, *Analytical modelling of an U-Oscillating Water Column and performance in random waves*, Renew. Energ., 60 (2013), pp. 116–126.

[135] P. Malliavin, *Stochastic analysis*, Springer-Verlag, Berlin-Heidelberg, first reprint ed., 2002.

[136] X. Mao, *Exponential stability of stochastic differential equations*, Deker, New York, 1994.

[137] ——, *Backward stochastic differential equations and quasilinear partial differential equations*, in Stochastic Partial Differential Equations, A. Etheridge, ed., vol. 216 of London Mathematical Society Lecture Note Series, Cambridge, 1995, Cambridge University Press, pp. 189–208.

[138] ——, *Stochastic differential equations and applications*, Woodhead Publishing, Chichester, second ed., 2007.

[139] H. A. Mardones and C. M. Mora, *First-order weak balanced schemes for stochastic differential equations*, Submitted, (2017).

[140] G. Maruyama, *Continuous markov processes and stochastic equations*, Rend. Circ. Mat. Palermo, 4 (1955), pp. 48–90.

[141] H. P. McKean, *Application of Brownian motion to the equation of Kolmogorov-Petrovskii-Piskunov*, Comm. Pure Appl. Math., 28 (1975), pp. 323–331.

[142] S. Méléard, *A trajectorial proof of the vortex method for the two-dimensional Navier-Stokes equation*, Ann. Appl. Probab., 10 (2000), pp. 1197–1211.

[143] ——, *Monte-Carlo approximations for 2d Navier-Stokes equations with measure initial data*, Probab. Theory Relat. Fields, 121 (2001), pp. 367–388.

[144] ——, *Stochastic particle approximations for two-dimensional Navier-Stokes equations*, in Dynamics and randomness II, A. Maass, S. Martínez, and J. San Martín, eds., vol. 10 of Nonlinear Phenomena and Complex Systems, Kluwer Acad. Publ., Dordrecht, 2004, pp. 147–197.

[145] R. Mikulevicius and E. Platen, *Rate of convergence of the Euler approximation for diffusion processes*, Math. Nachr., 151 (1991), pp. 233–239.

[146] G. N. Milstein, *Weak approximation of solutions of systems of stochastic differential equations*, Theor. Probability Appl., 30 (1985), pp. 750–766.

[147] ——, *Numerical Integration of Stochastic Differential Equations*, Kluwer Academic Publishers, Dordrecht, 1995.

[148] G. N. Milstein, E. Platen, and H. Schurz, *Balanced implicit methods for stiff stochastic systems*, SIAM J. Num. Anal., 35 (1998), pp. 1010–1019.

[149] G. N. Milstein, Yu M. Repin, and M. V. Tretyakov, *Numerical methods for stochastic systems preserving symplectic structure*, SIAM J. Numer. Anal., 40 (2002), pp. 1583–1604.

[150] G. N. Milstein and M. V. Tretyakov, *Stochastic numerics for mathematical physics*, Springer-Verlag, Berlin-Heidelberg, 2004.

[151] ——, *Solving the Dirichlet problem for Navier-Stokes equations by probabilistic approach*, BIT Numer. Math., 52 (2012), pp. 141–153.

[152] T. Mitsui and Y. Saito, *Stability analysis of numerical schemes for stochastic differential equations*, SIAM J. Numer. Anal., 33 (1996), pp. 2254–2267.

[153] C. Mora, *Numerical solution of conservative finite-dimensional stochastic Schrödinger equations*, Ann. Appl. Probab., 15 (2005), pp. 2144–2171.

[154] ——, *Weak exponential schemes for stochastic differential equations with additive noise*, IMA J. Numer. Anal., 25 (2005), pp. 486–506.

[155] C. M. Mora and H. A. Mardones, *First-order weak balanced schemes for bilinear stochastic differential equations*, arXiv:1403.6142v2, (2014).

[156] ——, *Stable numerical methods for two classes of SDEs with multiplicative noise: bilinear and scalar*, arXiv:1303.6316v2, (2014).

[157] C. M. Mora, H. A. Mardones, J. C. Jiménez, M. Selva, and R. Biscay, *A stable numerical scheme for stochastic differential equations with multiplicative noise*, SIAM J. Numer. Anal., 55 (2017), pp. 1614–1649.

[158] ——, *A stable numerical scheme for stochastic differential equations with multiplicative noise*, arXiv:1303.6316v3, (2017).

[159] E. Moro and H. Schurz, *Boundary preserving semianalytic numerical algorithms for stochastic differential equations*, SIAM J. Sci. Comput., 29 (2007), pp. 1525–1549.

[160] C. Navier, *Mémoire sur les lois du mouvement des fluides*, Mem. Acad. Sci. Inst. France, 6 (1822), pp. 389–440.

[161] B. Øksendal, *Stochastic differential equations. An introduction with applications*, Springer-Verlag, Berlin-Heidelberg, 1985.

[162] D. Olbers, J. Willebrand, and C. Eden, *Ocean Dynamics*, Springer-Verlag, Berlin-Heidelberg, 2012.

[163] M. Ossiander, *A probabilistic representation of solutions of the incompressible Navier-Stokes equations in* $\mathbb{R}^3$, Probab. Theory Relat. Fields, 133 (2005), pp. 267–298.

[164] G. Pagès and J. Printems, *Optimal quadratic quantization for numerics: the Gaussian case*, Monte Carlo Methods Appl., 9 (2003), pp. 135–165.

[165] ——, *Functional quantization for numerics with an application to option pricing*, Monte Carlo Methods Appl., 11 (2005), pp. 407–446.

[166] É. Pardoux, *Backward stochastic differential equations and viscosity solutions of systems of semilinear parabolic and elliptic PDEs of second order*, in Stochastic Analysis and Related Topics VI, L. Decreusefond, Jon Gjerde, B. Øksendal, and A. S. Üstünel, eds., vol. 42 of Progress in Probability, Boston, 1998, Birkhäuser, pp. 79–127.

[167] É. Pardoux and S. Peng, *Backward stochastic differential equations and quasilinear parabolic partial differential equations*, in Stochastic Partial Differential Equations and Their Applications, B. L. Rozovskii and R. B. Sowers, eds., vol. 176 of Lect. Notes Control Inf. Sci., Berlin-Heidelberg-New York, 1992, Springer-Verlag, pp. 200–217.

[168] É. Pardoux and S. G. Peng, *Adapted solution of a backward stochastic differential equation*, Syst. Control Lett., 14 (1990), pp. 55–61.

[169] É. Pardoux and S. Tang, *Forward-backward stochastic differential equations and quasilinear parabolic PDEs*, Probab. Theory Relat. Fields, 114 (1999), pp. 123–150.

[170] G. A. Pavliotis, A. M. Stuart, and K. C. Zygalakis, *Calculating effective diffusivities in the limit of vanishing molecular diffusion*, J. Comput Phys., 228 (2009), pp. 1030–1055.

[171] S. Peng, *Backward stochastic differential equation, nonlinear expectation and their applications*, in Proceedings of the International Congress of Mathematicians, R. Bhatia, ed., vol. I, New Delhi, 2010, Hindustan Book Agency, pp. 393–432.

[172] S. Peng and M. Xu, *Numerical algorithms for backward stochastic differential equations with 1-d Brownian motion: convergence and simulation*, ESAIM Math. Model. Numer. Anal., 45 (2011), pp. 335–360.

[173] I. C. Percival, *Quantum state diffusion*, Cambridge University Press, 1998.

[174] N. Perrin, *Probabilistic interpretation for the nonlinear Poisson-Boltzmann equation in molecular dynamics*, ESAIM Proc., 35 (2012), pp. 174–183.

[175] W. P. Petersen, *A general implicit splitting for stabilizing numerical simulations of Itô stochastic differential equations*, SIAM J. Numer. Anal., 35 (1998), pp. 1439–1451.

[176] E. Platen, *On weak implicit and predictor-corrector methods*, Math. Comput. Simulation, 38 (1995), pp. 69–76.

[177] S. B. Pope, *Turbulent Flows*, Cambridge University Press, London, 2003.

[178] P. E. Protter, *Stochastic integration and differential equations*, Springer-Verlag, Berlin-Heidelberg, second ed., 2005.

[179] J. M. Ramirez, *Multiplicative cascades applied to PDEs (two numerical examples)*, J. Comput. Phys., 214 (2006), pp. 122–136.

[180] A. Rasulov, G. Raimova, and M. Mascagni, *Monte Carlo solution of Cauchy problem for a nonlinear parabolic equation*, Math. Comput. Simulation, 80 (2010), pp. 1118–1123.

[181] L. C. G. Rogers and D. Williams, *Diffusions, Markov processes and Martingales*, vol. 2, Cambridge University Press, Cambridge, second ed., 2000.

[182] W. Rümelin, *Numerical treatment of stochastic differential equations*, SIAM J. Numer. Anal., 19 (1982), pp. 604–613.

[183] H. Schurz, *General theorems for numerical approximation of stochastic processes on the Hilbert space $H_2\left([0,T],\mu,\mathbb{R}^d\right)$*, Electron. Trans. Numer. Anal., 16 (2003), pp. 50–59.

[184] ——, *Convergence and stability of balanced implicit methods for systems of SDEs*, Int. J. Numer. Anal. Model., 2 (2005), pp. 197–220.

[185] ——, *An axiomatic approach to numerical approximations of stochastic processes*, Int. J. Numer. Anal. Model., 3 (2006), pp. 459–480.

[186] ——, *Basic concepts of numerical analysis of stochastic differential equations explained by balanced implicit theta methods*, in Stochastic Differential Equations and Processes, Z. Mounir and D. V. Filatova, eds., New York, 2012, Springer, pp. 1–139.

[187] A. Shapiro, *The use of an exact solution of the Navier-Stokes equations in a validation test of a three-dimensional nonhydrostatic numerical model*, Mon. Weather Rev., 121 (1993), pp. 2420–2425.

[188] I. Shoji, *Approximation of continuous time stochastic processes by a local linearization method*, Math. Comp., 67 (1998), pp. 287–298.

[189] N. A. Simonov, *Stochastic iterative methods for solving parabolic equations*, Siberian Math. J., 38 (1997), pp. 993–1007.

[190] ——, *Monte Carlo solution to three-dimensional vorticity equation*, Math. Comput. Simulation, 47 (1998), pp. 455–459.

[191] A. V. Skorokhod and I. I. Gikhman, *Introduction to the theory of random processes*, Saunders, Philadelphia, 1969.

[192] N. Soontiens, M. Stastna, and M. L. Waite, *Trapped internal waves over topography: Non-Boussinesq effects, symmetry breaking and downstream recovery jumps*, Phys. Fluids, 25 (2013), p. 066602.

[193] G. G. Stokes, *On the theories of the internal friction of fluids in motion, and of the equilibrium and motion of elastic solids*, Trans. Camb. Phil. Soc., 8 (1849), pp. 287–319.

[194] Y. Sui, W. Zhao, and T. Zhou, *Numerical method for hyperbolic conservation laws via forward backward SDEs*, arXiv:1311.0364v2, (2014).

[195] A. S. Sznitman, *Topics in propagation of chaos*, in Ecole d'Eté de Probabilités de Saint-Flour XIX - 1989, A. Dold, B. Eckmann, and F. Takens, eds., Lect. Notes Math. 1464, Springer, Berlin, 1991, pp. 165–251.

[196] D. Talay, *Efficient numerical schemes for the approximation of expectations of functionals of S.D.E.*, in Filtering and Control of Random Processes, H. Korezlioglu, G. Mazziotto, and J. Szpirglas, eds., vol. 61 of Lecture Notes in Control and Information Science, Springer-Verlag, Berlin, 1984, pp. 294–313.

[197] ——, *Discrétisation d'une E.D.S. et calcul approché d'espérances de fonctionnelles de la solution*, Math. Model. Numer. Anal., 20 (1986), pp. 141–179.

[198] ——, *Approximation of upper Lyapunov exponents of bilinear stochastic differential systems*, SIAM J. Numer. Anal., 28 (1991), pp. 1141–1164.

[199] ——, *Probabilistic numerical methods for partial differential equations: elements of analysis*, in Probabilistic models for nonlinear partial differential equations (Montecatini Terme, 1995), Denis Talay and Luciano Tubaro, eds., vol. 1627 of Lecture Notes in Mathematics, Berlin, 1996, Springer-Verlag, pp. 148–196.

[200] D. Talay and O. Vaillant, *A stochastic particle method with random weights for the computation of statistical solutions of McKean-Vlasov equations*, Ann. Appl. Probab., 13 (2003), pp. 140–180.

[201] G. I. Taylor and A. E. Green, *Mechanism of the production of small eddies from large ones*, Proc. R. Soc. Lond. A, 158 (1937), pp. 499–521.

[202] M. V. Tretyakov and Z. Zhang, *A fundamental mean-square convergence theorem for SDEs with locally Lipschitz coefficients and its applications*, SIAM J. Numer. Anal., 51 (2013), pp. 3135–3162.

[203] S. Watanabe, *On the branching process for Brownian particles with an absorbing boundary*, J. Math. Kyoto Univ., 4 (1965), pp. 385–398.

[204] E. C. Waymire, *Probability & incompressible Navier-Stokes equations: An overview of some recent developments*, Probab. Surv., 2 (2005), pp. 1–32.

[205] J. Zhang, *A numerical scheme for BSDEs*, Ann. Appl. Probab., 14 (2004), pp. 459–488.

[206] X. Zhang, *A stochastic representation for backward incompressible Navier-Stokes equations*, Probab. Theory Relat. Fields, 148 (2010), pp. 305–332.

[207] W. Zhao, L. Chen, and S. Peng, *A new kind of accurate numerical method for backward stochastic differential equations*, SIAM J. Sci. Comput., 28 (2006), pp. 1563–1581.